1993

Engine dynamic signal monitoring and diagnostics.

Jimi Sauw-Yoeng. Tjong
University of Windsor

Recommended Citation

NOTICE

AVIS

The quality of this microform is heavily dependent upon the quality of the original thesis submitted for microfilming. Every effort has been made to ensure the highest quality of reproduction possible.

La qualité de cette microforme dépend grandement de la qualité de la thèse soumise au microfilmage. Nous avons tout fait pour assurer une qualité supérieure de reproduction.

If pages are missing, contact the university which granted the degree.

S'il manque des pages, veuillez communiquer avec l'université qui a conféré le grade.

Some pages may have indistinct print especially if the original pages were typed with a poor typewriter ribbon or if the university sent us an inferior photocopy.

La qualité d'impression de certaines pages peut laisser à désirer, surtout si les pages originales ont été dactylographiées à l'aide d'un ruban usé ou si l'université nous a fait parvenir une photocopie de qualité inférieure.

Canada

ENGINE DYNAMIC SIGNAL MONITORING AND DIAGNOSTICS

by

JIMI SAUW-YOENG TJONG

A Dissertation
submitted to the
Faculty of Graduate Studies and Research
through Department of Mechanical Engineering in
Partial Fulfillment of the Requirements for the
Degree of Doctor of Philosophy
at the University of Windsor

Windsor, Ontario, Canada
1992

The author has granted an irrevocable non-exclusive licence allowing the National Library of Canada to reproduce, loan, distribute or sell copies of his/her thesis by any means and in any form or format, making this thesis available to interested persons.

L'auteur a accordé une licence irrévocable et non exclusive permettant à la Bibliothèque nationale du Canada de reproduire, prêter, distribuer ou vendre des copies de sa thèse de quelque manière et sous quelque forme que ce soit pour mettre des exemplaires de cette thèse à la disposition des personnes intéressées.

The author retains ownership of the copyright in his/her thesis. Neither the thesis nor substantial extracts from it may be printed or otherwise reproduced without his/her permission.

L'auteur conserve la propriété du droit d'auteur qui protège sa thèse. Ni la thèse ni des extraits substantiels de celle-ci ne doivent être imprimés ou autrement reproduits sans son autorisation.

Canada

Name __JIMI SAVW·YOENG TJONG__

Dissertation Abstracts International is arranged by broad, general subject categories. Please select the one subject which most nearly describes the content of your dissertation. Enter the corresponding four-digit code in the spaces provided.

__AUTUMOTIVE__

SUBJECT TERM

`0 5 4 0` **U·M·I**

SUBJECT CODE

Subject Categories

THE HUMANITIES AND SOCIAL SCIENCES

COMMUNICATIONS AND THE ARTS
Architecture	0729
Art History	0377
Cinema	0900
Dance	0378
Fine Arts	0357
Information Science	0723
Journalism	0391
Library Science	0399
Mass Communications	0708
Music	0413
Speech Communication	0459
Theater	0465

EDUCATION
General	0515
Administration	0514
Adult and Continuing	0516
Agricultural	0517
Art	0273
Bilingual and Multicultural	0282
Business	0688
Community College	0275
Curriculum and Instruction	0727
Early Childhood	0518
Elementary	0524
Finance	0277
Guidance and Counseling	0519
Health	0680
Higher	0745
History of	0520
Home Economics	0278
Industrial	0521
Language and Literature	0279
Mathematics	0280
Music	0522
Philosophy of	0998
Physical	0523

Psychology	0525
Reading	0535
Religious	0527
Sciences	0714
Secondary	0533
Social Sciences	0534
Sociology of	0340
Special	0529
Teacher Training	0530
Technology	0710
Tests and Measurements	0288
Vocational	0747

LANGUAGE, LITERATURE AND LINGUISTICS
Language	
General	0679
Ancient	0289
Linguistics	0290
Modern	0291
Literature	
General	0401
Classical	0294
Comparative	0295
Medieval	0297
Modern	0298
African	0316
American	0591
Asian	0305
Canadian (English)	0352
Canadian (French)	0355
English	0593
Germanic	0311
Latin American	0312
Middle Eastern	0315
Romance	0313
Slavic and East European	0314

PHILOSOPHY, RELIGION AND THEOLOGY
Philosophy	0422
Religion	
General	0318
Biblical Studies	0321
Clergy	0319
History of	0320
Philosophy of	0322
Theology	0469

SOCIAL SCIENCES
American Studies	0323
Anthropology	
Archaeology	0324
Cultural	0326
Physical	0327
Business Administration	
General	0310
Accounting	0272
Banking	0770
Management	0454
Marketing	0338
Canadian Studies	0385
Economics	
General	0501
Agricultural	0503
Commerce-Business	0505
Finance	0508
History	0509
Labor	0510
Theory	0511
Folklore	0358
Geography	0366
Gerontology	0351
History	
General	0578

Ancient	0579
Medieval	0581
Modern	0582
Black	0328
African	0331
Asia, Australia and Oceania	0332
Canadian	0334
European	0335
Latin American	0336
Middle Eastern	0333
United States	0337
History of Science	0585
Law	0398
Political Science	
General	0615
International Law and Relations	0616
Public Administration	0617
Recreation	0814
Social Work	0452
Sociology	
General	0626
Criminology and Penology	0627
Demography	0938
Ethnic and Racial Studies	0631
Individual and Family Studies	0628
Industrial and Labor Relations	0629
Public and Social Welfare	0630
Social Structure and Development	0700
Theory and Methods	0344
Transportation	0709
Urban and Regional Planning	0999
Women's Studies	0453

THE SCIENCES AND ENGINEERING

BIOLOGICAL SCIENCES
Agriculture	
General	0473
Agronomy	0285
Animal Culture and Nutrition	0475
Animal Pathology	0476
Food Science and Technology	0359
Forestry and Wildlife	0478
Plant Culture	0479
Plant Pathology	0480
Plant Physiology	0817
Range Management	0777
Wood Technology	0746
Biology	
General	0306
Anatomy	0287
Biostatistics	0308
Botany	0309
Cell	0379
Ecology	0329
Entomology	0353
Genetics	0369
Limnology	0793
Microbiology	0410
Molecular	0307
Neuroscience	0317
Oceanography	0416
Physiology	0433
Radiation	0821
Veterinary Science	0778
Zoology	0472
Biophysics	
General	0786
Medical	0760

EARTH SCIENCES
Biogeochemistry	0425
Geochemistry	0996

Geodesy	0370
Geology	0372
Geophysics	0373
Hydrology	0388
Mineralogy	0411
Paleobotany	0345
Paleoecology	0426
Paleontology	0418
Paleozoology	0985
Palynology	0427
Physical Geography	0368
Physical Oceanography	0415

HEALTH AND ENVIRONMENTAL SCIENCES
Environmental Sciences	0768
Health Sciences	
General	0566
Audiology	0300
Chemotherapy	0992
Dentistry	0567
Education	0350
Hospital Management	0769
Human Development	0758
Immunology	0982
Medicine and Surgery	0564
Mental Health	0347
Nursing	0569
Nutrition	0570
Obstetrics and Gynecology	0380
Occupational Health and Therapy	0354
Ophthalmology	0381
Pathology	0571
Pharmacology	0419
Pharmacy	0572
Physical Therapy	0382
Public Health	0573
Radiology	0574
Recreation	0575

Speech Pathology	0460
Toxicology	0383
Home Economics	0386

PHYSICAL SCIENCES

Pure Sciences
Chemistry	
General	0485
Agricultural	0749
Analytical	0486
Biochemistry	0487
Inorganic	0488
Nuclear	0738
Organic	0490
Pharmaceutical	0491
Physical	0494
Polymer	0495
Radiation	0754
Mathematics	0405
Physics	
General	0605
Acoustics	0986
Astronomy and Astrophysics	0606
Atmospheric Science	0608
Atomic	0748
Electronics and Electricity	0607
Elementary Particles and High Energy	0798
Fluid and Plasma	0759
Molecular	0609
Nuclear	0610
Optics	0752
Radiation	0756
Solid State	0611
Statistics	0463

Applied Sciences
Applied Mechanics	0346
Computer Science	0984

Engineering	
General	0537
Aerospace	0538
Agricultural	0539
Automotive	0540
Biomedical	0541
Chemical	0542
Civil	0543
Electronics and Electrical	0544
Heat and Thermodynamics	0348
Hydraulic	0545
Industrial	0546
Marine	0547
Materials Science	0794
Mechanical	0548
Metallurgy	0743
Mining	0551
Nuclear	0552
Packaging	0549
Petroleum	0765
Sanitary and Municipal	0554
System Science	0790
Geotechnology	0428
Operations Research	0796
Plastics Technology	0795
Textile Technology	0994

PSYCHOLOGY
General	0621
Behavioral	0384
Clinical	0622
Developmental	0620
Experimental	0623
Industrial	0624
Personality	0625
Physiological	0989
Psychobiology	0349
Psychometrics	0632
Social	0451

ABSTRACT

A study was undertaken to determine the feasibility of developing an engine dynamic signal monitoring and diagnostic system for use on-line in a high volume engine manufacturing plant as well as in a research environment for the development of new engine components. The system will enable rapid and precise diagnostics of the production engine for identifying and locating manufacturing or assembly defects which do not include thermodynamics, combustion / or emission related defects.

Recently published literature on engine noise and vibration monitoring and diagnostic systems is reviewed with special emphasis on the use of noise and vibration for on-line monitoring and diagnosing. A complete bibliography of 175 references is appended, together with the summary chart outlining the subject classified by topics.

The feasibility of using noise and vibration for the detection of engine manufacturing and assembly defects as well as evaluating the effectiveness of component design changes, was originally carried out in the dynamometer laboratory. Here, customer returned engines were evaluated for noise and vibration using three different monitoring systems developed for the same purposes. In these systems accelerometers, microphones and pressure transducers were used in conjunction with both a conventional dynamic signal analyzer and a specially designed eight channel data acquisition system coupled with custom designed computer programs. All these systems are capable of detecting defects in customer returned engines. Detail reviews were carried out emphasizing the advantages and disadvantages of each system. The noise and vibration measurements were then correlated with actual manufacturing and assembly defects. The systems were also tested for evaluating the noise and vibration characteristics of changes in piston design.

With the success in diagnosing customer returned engines, a field study was

undertaken to determine the feasibility of using noise and vibration for detecting missing connecting rod bearings, loose connecting rod nuts, and other related manufacturing/ assembly defects. A modified monitoring system which includes accelerometers and microphones together with a uniquely designed data acquisition system was used to obtain the noise and vibration data. In the initial phase, data was collected from fifteen partially completed engines having different defects. These were then analyzed to set the vibration limits for rejection. The on-line engine monitoring and diagnostic system was implemented and it was observed that in the test of more than 120,000 engines, the success rate in reduction of defective engines was 100 percent.

Thus it was concluded that the monitoring system with a specially designed data acquisition system is capable of on-line monitoring and rapid and precise diagnosing of production engines with manufacturing and / or assembly defects. The system is also well suited for use in evaluating the noise and vibration characteristics of any engine when one or more of its components has undergone design changes.

DEDICATION

This work is dedicated to my wife, JASMIN and our daughter, VEHNIAH.

ACKNOWLEDGEMENTS

TABLE OF CONTENTS

LIST OF TABLES

TABLE

LIST OF FIGURES

FIGURE

NOMENCLATURE

a	distance from piston pin to top of piston skirt
A	acceleration
(A_1)	lateral component of the pin force
(A_2)	the axial component of the pin force
ADC	Analog to Digital Converter
AV	average
b	distance from piston pin to bottom of piston skirt
BDC	Bottom Dead Center
c	distance from piston pin to C.G.
CID	Cylinder Identification
CPU	Central Processing Unit
Dalisp	Data Analysis and Display Software by DSP Development Corporation.
dB	decibel
d_p	piston pin diameter
e	distance from piston center line to piston C.G.
f	distance from piston pin to top ring
F	represents the failure of fault detection
F_1	piston/bore reaction force at top of skirt
F_2	piston/bore reaction force at bottom of skirt
FFT	Fast Fourier Transform
g	acceleration of gravity
HPIB	Hewlett Packard Interface Bus
H_a'	the angular momentum after impact
H(s)	system transfer function
i	the index for vector data points
$\overline{I}$	sound intensity vector
I_3	mass moment of inertia of piston about piston C.G.
I_{rod}	mass moment of inertia of connecting rod about rod C.G.
ICP	Integral Circuit Piezoelectric
I/O	Input/ Output
ISR	Interrupt Service Routine
J_B	sign coefficient accounting for piston velocity direction and thrust or antithrust contact with the bore at the bottom of skirt
J_p	sign coefficient accounting for relative angular
J_{SB}	sign coefficient accounting for piston contact with thrust or antithrust side of bore at bottom of skirt
J_{ST}	sign coefficient accounting for piston contact with thrust or antithrust side of bore at top of skirt
J_T	sign coefficient accounting for piston velocity direction and thrust or antithrust contact with the bore at the bottom of skirt

J_V	sign coefficient accounting for velocity direction of piston
k	k^{th} mode of the system
KE	Kinetic Energy
kHz	kilo Hertz
m	the number of traces collected
M	moment developed between piston pin and piston due to friction
m_2	mass of piston pin
m_3	mass of piston
m_{eq}	the mass at point 2 of piston pin location
$m_2 eq$	the equivalent connecting rod mass located at point 2
m_{rod}	mass of connecting rod
P_H	lateral component of gas pressure load
P_V	axial component of gas pressure load
p	instantaneous pressure
Pa	Pascal
P_k	pole location for the kth mode $= \sigma_k + j\omega_k$
PIP	Profile Ignition Pickup
Q	the offset distance between the piston and crank shaft axis
Q_k	arbitrary scaling constant
r	the index of a particular trace
R	radius of bore
RAM	Random Access Memory
re	References
RPM	Revolution Per Minute
s	distance from crank pin (point 1) to rod C.G.
$s_{1,2}$	the roots of the characteristic equation
S	represents the satisfied fault detection at both TDC and BDC
SB	represents the satisfied fault detection only at BDC
SDOF	Single Degree of Freedom
SPL	Sound Pressure Level
ST	represents the satisfied fault detection only at TDC
T	transpose of the vector
t_d	time delay
t_w	time windows
TDA	Time Domain Averaging
TDC	Top Dead Center
TTL	Transistor-Transistor Logic
u	distance from piston center line to piston pin
$\{U_k\}$	mode shape vector
US	represents the unsatisfied fault detection
v	distance from bore center line to crankshaft axis
v_r	the instantaneous particle velocity
VAR	variance
W	the acoustic power passing through a surface, S
x_2	lateral displacement of piston pin

$\dot{x}_2$	velocity of the mass m_{eq}
$\dot{x}_3$	horizontal velocity of the piston
$\ddot{x}_2$	lateral acceleration of piston pin
$\ddot{x}_3$	lateral acceleration of piston C.G.
$X(i)$	the ith component of a vector X
$\ddot{y}_2$	axial acceleration of piston pin
$\ddot{y}_3$	axial acceleration of piston C.G.
$Y(i)$	the average vector for all traces X
z	damping ratio
$Z(i)$	the ith component of the variance vector
$\dot{\beta}$	the angular velocity of the piston
$\dot{\beta}'$	the new angular velocity
$\ddot{\beta}$	angular acceleration of piston
δ	r differential length
η	loss factor
θ	crank angle
μ	coefficient of friction between piston skirt and bore
μ_p	coefficient of friction between the piston and pin
ρ_o	the density of air
σ	damping factor
$\dot{\phi}$	relative angular velocity of the connecting rod
ϕ_o	the angle of the connecting rod to the bore center line at TDC
$\ddot{\phi}$	angular acceleration of connecting rod
ω	angular velocity
ω_d	damped natural frequency
ω_n	underdamped natural frequency

CHAPTER 1.

INTRODUCTION

Today, achieving higher productivity at the minimal cost is one of the key goals of engine manufacturers. This, coupled with higher standards of customer satisfaction, requires not only innovative concepts in engine design, manufacturing and assembly processes but also the integration of on-line engine monitoring and a diagnostic system which is capable of detecting manufacturing and assembly defects. The implementation of such a system would greatly increase productivity, customer satisfaction and reduce scrap costs.

Hence, it is necessary for engine manufacturers who wish to succeed in the highly competitive market of the future to plan immediately for integration of on-line engine monitoring and diagnostic systems.

A typical engine manufacturer is capable of producing 2000 engines per day which is equivalent to about 3 million dollars daily output. One such manufacturer listens to the voice of the customers through participations in dealer visitations and vehicle assembly plants to better understand its customer needs and concerns. The statistical data of one representative manufacturer indicates that it exchanges 0.05 percent of engine production to its customers. The majority (60 percent) of the engine exchanges are related to excessive engine noise and vibration. Upon examination of the customer return engines, the main concerns involve engine manufacturing and assembly defects.

Thus, one concerned engine manufacturer who is aware of the high cost incurred by these defective engines being received by the customers, decided to develop and implement non-destructive techniques for the on-line detection of manufacturing and assembly defects.

At present, an engine assembly requires the engine to be tested at several stages

of the assembly process. However, it is desirable to detect all the defects in the engine at the earliest possible stage in order to prevent major damage and hence additional repair and assembly cost due to further operation with the defective engine.

A conventional method to detect a missing connecting rod bearing, referred to as the cold test, is to measure the deck height of the piston at top dead center from the cylinder block bank face. However, this method needs to be improved due to its inconsistency in results, long set-up time, prolonged calibration time and problems with maintainability and durability of the gage. Replacement of this dimensional gage with vibration measurement is necessary and an investigation was initiated for this purpose.

One other engine diagnostic method in the automotive industry is auditory assessment by an operator who can infer the mechanical defects causing a particular engine noise. However, the reliability of the judgements is sometimes questionable due to the effect of inconsistency of the physiological condition of the inspector and ambient conditions. Most important of all, the operator's judgment is subjective, especially in the case of defects that are on the borderline of acceptability.

The goal of this research is to develop a viable and cost effective method of diagnosing manufacturing and assembly defects in internal combustion engines using noise and vibration signals.

In view of the above considerations, the following objectives were set for this dissertation:

1. To review the recently published literature on engine signal monitoring and diagnostic methods with an emphasis on various mechanical signature analysis techniques.

2. To determine appropriate transducers for the on-line detection of manufacturing and assembly defects.

3. To develop and implement a viable and cost effective on-line monitoring and diagnostic system for identifying and locating engine manufacturing and

assembly defects by means of vibration and noise measurement and analysis.

4. To develop a practical and cost effective system for use in evaluating the noise and vibration characteristics of an engine component before and after design changes.

5. To recommend areas for future research and development.

CHAPTER 2.

LITERATURE SURVEY

In this chapter, a literature survey was conducted in the area of engine dynamic signal monitoring and diagnostic procedures for use in the dynamometer laboratory as well as in the production cold and hot test stands. First, a review of fault diagnosis for internal combustion engine is presented. It is followed by a summary of the past work on data processing techniques. Finally, different methods of diagnosing engine faults are presented.

2.1 Fault Diagnosis in Internal Combustion Engines

One of the most common procedures followed by the automotive industry to evaluate engine noise during inspection consists of operating the engine on a test stand. Noise level evaluation is based on an auditory assessment by an inspector/operator who, from sound level and frequency variations, can infer the mechanical defects causing the particular noise. Though this method is often simple and fast, the difficulties involved are obvious. The operator judgment is affected by ambient conditions (e.g. noise in the test areas) and by alterations of his physiological condition (fatigue, inurement, etc.). Most important of all, the operator's judgment is subjective and does not necessarily agree with the judgment of another operator, especially in the case of defects on the borderline of acceptability. These considerations show the need for a proper measurement apparatus in order to maintain a constant quality standard.

The main objective of this study is to develop techniques of diagnosing defects in various internal combustion engines. These techniques use the measurement of engine noise and vibration as the primary source of parameters coupled with other data such as pressure, temperature, torque, etc.. Besides being able to detect the presence of a fault,

4

the techniques must also be capable of diagnosing the types of defect so that cost effective remedial measures may be applied. Virtually all operating conditions of engine produce vibration, and therefore, noise. Hence abnormal operation can be detected from the noise and vibration produced. The use of noise or vibration measurement has great advantages because it is fundamentally non-destructive and non-invasive.

Most of the published technical papers are concentrated on the techniques for condition monitoring of rotating machinery. They include the analysis of vibration data, metallic debris detection and spectrographic oil analysis.

Presently, engine diagnostic equipment is available and is used in automotive industries for on-line testing of internal combustion engines. The systems generally rely upon measurement of parameters from the electrical system and an analysis of small fluctuations in the power output and crankshaft rotation. The fault conditions are deduced from the power output characteristics of each cylinder. This method of detection is not specific. The use of engine noise and vibration measurements generally provide a more specific indication of engine defects such as excessive bearing clearances, piston slap or scuffing, crankshaft imbalance and various assembly defects.

Generally, the current techniques of applying noise and vibration for detecting faults are mainly developed for monitoring and diagnosis of machinery rotating at a constant speed. Rotating machines mainly produce repetitive signals of a more or less periodic nature. Most techniques are oriented toward the description or extraction of such type of signals. Spectral analysis is commonly used because it is based on a decomposition of this class of signal. Another method is the time domain averaging which filters out periodic signals time-locked to such a period.

The dynamic signals of an internal combustion engine can be characterized as "almost periodic" in nature. They are often produced by mechanical systems incorporating some periodic movement, but may also be generated by random effects accompanying friction, fluid flow, impact, etc... Thus, conventional methods of analysis are generally not

5

effective for reliably detecting faults in internal combustion engines.

The majority of the applications of noise and vibration measurement for fault diagnosis have been concentrated in the areas of gears and bearings [162] . The techniques range from simple measurement of noise and vibration signal levels to more detailed evaluation in the time and frequency domains.

2.2 Analysis Techniques

Applications in the diagnosis of internal combustion engine faults are described by Braun and Seth [22, 23]. The main interest in this project is not the specific methods of measurement, but the way in which the results are processed in order to extract the relevant data and identify the fault. The analysis techniques that need to be applied for the diagnosis of internal combustion engine can be divided into three main sections:

1. Data acquisition

2. Data reduction and processing

3. Algorithms for the diagnosis of engine faults.

The objective of this study is to develop methods of recognizing engine faults applicable in a production cold or hot test environment.

2.2.1 Data Acquisition

The following points must be considered together with the knowledge of the analysis, the diagnostic procedures and the environment:

1. Vibration is strongly related to the distance from the point of measurement to the ultimate source.

2. Vibration is more related to engine operating condition than to noise.

3. Depending upon the microphone position, a measurement of noise will be less biased to a particular part of the machine and the information relating to a particular

aspect of the machine's performance is likely to be scrambled. Noise is also capable of being modified by the acoustic environment.

In production line testing (cold or hot test) the main consideration is to keep the number of connections to the engine to a bare minimum. Hence the relative merits of noise or vibration measurement are listed below:

2.2.2 Noise

Noise is:

1. Capable of providing data on the condition of an engine from a single measurement.

2. A non-contact measurement.

3. The data analysis procedures are generally more complex.

4. Enclosures are sometimes necessary for testing in a production environment.

2.2.3 Vibration

Vibration is:

1. Capable of providing condition data on individual components of the engine.

2. No special enclosures are required in a production environment.

3. Vibration is directly related to mechanical operations within the engine.

4. A large number of transducers may be required, thus generating a lot of data for processing.

2.2.4 Transducers

The most commonly used transducers to measure noise and vibration are discussed in the following sections.

2.2.4.1 Noise

The choice of microphone depends on the required frequency response, durability and cost. Bruel and Kjaer [24] describe in detail the frequency response of different microphone designs.

2.2.4.2 Vibration

The piezoelectric accelerometer is the most commonly used transducer for vibration measurements because of its relatively small size, low cost and measuring stability with a wide frequency range. The use of a scanning laser interferometer is useful when considering the large number of measurement positions on the engine. It is a non-contact device that can be placed alongside the engine. It is even capable of directing the beam onto both sides of the engine using mirrors. At present, the use of a laser interferometer is limited because of its high capital cost. Anderton [5] described the use of a laser doppler velocimeter for measuring surface vibration.

2.3 Data Processing Techniques

The generation of noise and vibration by a faulty engine can be categorized into three areas:

1. Impacts between components associated with incorrect clearance (valve train, gears, connecting rods, pistons and bearings). This results in an impulse generated vibration which occurs at a fixed point in the engine cycle.

2. Imbalance in rotating components (crankshaft, camshaft, gears, balance shafts). The resulting vibration is harmonic at low orders of engine rotation.

3. Abnormal combustion (incorrect ignition timing, incorrect valve opening). The resulting vibration generally causes an increase in the energy above approximately 2 kHz in the firing pulse of the cylinder.

Thus, the noise and vibration generated by a faulty engine are complex in nature. The analysis must decompose the data in such a way that the fault recognition process can be concentrated on those attributes of the signal which are most representative of the faults to be diagnosed, avoiding the inclusion of a contaminated signals.

2.3.1 Frequency Domain Signal Analysis

In general, the harmonic nature of vibration caused by an out of balance crankshaft in an engine can be diagnosed using a narrow band frequency analysis. However, most engine faults such as piston slap, valve knock, are characterized by impulses which contain a particular frequency spectrum. Therefore, it is possible to diagnose some engine faults by identifying their associated frequency components. Both narrow band and 1/3 octave band procedures can be applied on the raw signal, time averaged signal and the signal envelope.

Wallace and Darlow [166] formulated an efficient approach to recovering transient shaft speed information using Fourier Transform techniques. In a similar work, Pischinger [117] described a method of time frequency windows for direct determination of the combustion noise from the airborne noise of a diesel engine. This method shows influences on the combustion noise, particularly where the mechanical noise is predominant. Meier [94-99] used frequency domain signal analysis in detecting engine faults in production test cells. Chung [32], on the other hand, discussed the application of Digital Fourier Transform methods (i.e., coherence and transfer function techniques) to investigate noise generated by an engine. The transfer functions, in these cases, were determined empirically for pinpointing the noise generation of an engine as well as to predict the effect on engine noise of various assumed cylinder pressure wave forms. Bianchi [17] utilized Fast Fourier Transform waveform analysis techniques on engine pressure signals to determine the diagnostic viability.

9

2.3.2 Power Cepstrum

Power cepstrum is the even or cosine transform of the logarithm of a power spectrum. It is the detection of periodicity within the spectrum of a given signal. Thus, it is commonly used to identify the harmonic and sideband components within a signal, such as that of a gearbox [24, 90]. However, the use of time domain methods in diagnosing engine faults is preferred over power cepstrum because of cost and effectiveness.

2.3.3 Acoustic Intensity Techniques

In recent engine work on acoustic intensity, Thompson [157] described the finite difference approximation errors in acoustic intensity measurements. Pope [118], in a similar work, stated that the cross-spectral method can provide diagnostic data from noise sources that were not previously obtainable. The same method can be used to measure sound power without requiring a special acoustical facility. By using the lead wrapping approach, Crocker [43] measured the sound power radiated from major surfaces of a diesel engine in order to identify the generating noise source. In this work, surface intensity and acoustic intensity were used to measure the sound power.

Acoustic intensity measurements are also used for determining noise sources in engines [40]. Chung [31] developed a cross-spectral method of measuring acoustic intensity at General Motors Research Laboratories. He demonstrated a rapid space time averaging technique, a detailed mapping of noise emission, a noise source ranking and a calculation for total engine sound power. Furthermore, he proved the reasonable accuracy and the effectiveness of the acoustic intensity method. Abe [1], on the other hand, developed digital acoustic intensity techniques in engine noise studies. Using a phased-locked data acquisition, an acoustic power balance was constructed for an engine. These results were shown to correlate well with other methods such as lead covering, average surface vibration level and close microphone.

10

2.3.4 Time Domain Analysis and Variance Techniques

Braun and Seth [22, 23, 139, 140, 142, 143], in their various work in engine diagnostics, formulated techniques for the decomposition of signals obtained from transducers. The authors proposed that a raw signal from a transducer can be decomposed into three distinct components:

1. A periodic signal
2. A random repetitive signal
3. A residual non-synchronous signal.

A variance analysis technique was developed in which cycle to cycle variability at each point in the engine cycle is calculated. This technique was demonstrated to be particularly useful for detecting faults in both manufacturing and assembly processes. This technique was later extended for evaluating engine noise by changing the piston profile [161].

2.3.5 Finite Element Analysis

As inexpensive computing power is readily available, the finite element method can now be used in an engine noise analysis which is considered to be very computing intensive.

Crocker [44] used an engine structure analysis which involved the finite element method and modal analysis to design a low noise engine. Crocker and Lalor [41], later on, extended the use of the finite element technique to predict engine structure noise and vibration with the objective of optimizing engine structure design for low noise. Challen [28] reviewed the progress in diesel engine noise reduction with emphasis on finite element modelling techniques of engine structures. Finite element analysis can be used in conjunction with experimental modal analysis for predicting the effect of design changes on the structural behaviour of the engine block [21].

2.3.6 Other Techniques

Otte [113], in his recent work, discussed a signal processing technique for verifying the correlation between multiple vibration and acoustical signals. It is based on the principal component analysis, a multivariate statistical analysis technique, and utilizes an eigenvalue decomposition of a covariance matrix. Various forms of spectral density functions (power spectral density, cross spectral density, transfer and coherence functions) and time domain functions (cross-correlation, impulse response, and inverse complex coherence function) can be used in the signal analysis to detect machine defects [49]. The time domain functions are useful for noise source identification (such as determining time delays associated with multiple potential noise sources), to identify important sources and relate the delays to the geometry of structures in order to determine the transmission paths.

Another approach for engine analysis is the pattern recognition techniques which were introduced by Cortina [35]. These techniques were used to reduce complexity and to permit the implementation of Bayes' procedures in a practical field portable equipment. This results in the design of pre-detection filters which can simplify and reduce the measurement equipment required to detect faults in real time. While Carr and Lalor [26] proposed the use of energy methods for predicting and reducing noise from engine covers, Alfredson [3] described the partial coherence technique for source identification on a diesel engine.

2.4 Diagnosis of Engine Faults

The process of engine diagnosis is one of data reduction which results in discrete classification in terms of engine faults. The data is generally reduced in order to extract the characteristics of the engine conditions. The extraction of characteristics permits concentration on those components which are directly related to the specific condition of

the engine. A common method of characteristics extraction is to compare the measured data set with a reference and compute the degree of deviation from the reference. Seth, Stuart and Field [140, 142, 143] formulated the strategy for engine diagnostic algorithms used in production cold test and hot test stands. The use of a selected number of engine characteristics to make a logic based decision was included. The complexity of the logic structure sometimes necessitates a diagnostics program development on the basis of a hierarchy approach.

Although the primary purpose of this study is concerned with the development of analysis techniques for engine fault detection, we need to understand the basic mechanism by which engine faults lead to noise and vibration. Many technical papers have been published on the subject of engine noise and vibration, and a selection of those which are particularly relevant to this study is referenced under the topics of piston noise, gear noise and valvetrain noise in Appendix A. The following describes the common faults associated with different components in an engine. Discussion on detection techniques and noise reduction are reviewed briefly.

2.4.1 Fuel Injector and Fuel Pump Noise

The present stringent legislation restricting gaseous emission in passenger cars creates an increase in world demand for electronically controlled, multiport injection systems for spark ignition engines. These systems are part of an engine that produced objectionable noise in the passenger compartment of a vehicle. Young [175] described the Lucas designed fuel injector which has reduced injector noise emission. Sound power measurements were made to quantify this reduction. The fuel pump is another noise source that needs to be eliminated. Kemmer [78] stated the methods for reducing noise in electrical fuel pump. As a remedy, he recommended having a fairly continuous flow and smooth pressure variations in the pump.

13

2.4.2 Valve Train Noise

There are many factors which cause valve noise in an engine. They include valve lift, valve bounce, valve tilt , valve seat distortion (mechanical or thermal), and valve insert rigidity [70]. Hanaoka [65] developed a new method of cam design that reduces valve train noise which occurs at the instant the valve opens and closes, and also when the follower is on the cam lobe. Generally, valve noises are caused by impacts, and their sound intensity is proportional to the impact speed. Follower noises are caused by frictional vibrations due to metal to metal contact at points where the oil film thickness becomes zero. Irregular contact surfaces increase these noises, and valve train noises at high speeds are caused by irregular valve dynamic behaviour.

2.4.3 Noise Cancellation Techniques

There are two ways of reducing high levels of structure-borne noise generated, at the engine second order frequency, by the reciprocating imbalance forces. One is a design approach to reduce the magnitude of the vibration generated mechanism, another applies cancellation techniques to reduce the resultant interior vehicle noise. For example, Wood [174] proposed a noise regulator device to achieve cancellation of structure-borne noise in four cylinder vehicles. Cancellation techniques can achieve, in principle, very significant noise reduction, but being essentially 'add-on' methods, they incur a mass penalty.

2.4.4 Passenger Car Interior Noise

Winklhofer [173] described the engine noise contribution towards the interior noise of the car and also gave ways of reducing engine noise in general.

14

2.4.5 Diesel Engine Noise Reduction

To improve passengers' comfort, various attempts are made by commercial vehicle manufacturers to reduce the dominant vehicle noise which is the engine. This is particularly true with diesel engines as they are much noisier than the gasoline counterpart. Windett [172] described various methods of improving diesel engine noise which could be carried out in a production process without major re-design of the basic engine. Watanabe [168], in a similar work, analyzed the transient noise characteristics of diesel engines and proposed methods of measurements. Russell [128-134] offered three approaches to control diesel engine noise. This is achieved by:

1. Control at source, of all major sources:

    i) Smooth cylinder pressure development

    ii) Elimination of timing drive impacts

    iii) Minimum piston slap impacts.

2. Quiet structures, either:

    a. Vibration isolation of external surfaces from all sources.

    b. Combination of treatments of thin section surface areas of structures:

    i) Crankcase/cylinder block resonances tuned to frequencies at which excitation is minimum.

    ii) Vibration damping treatments to sump, valve gear covers, etc., when made of flexible sheet materials.

    iii) Vibration isolation of sump, valve gear covers, pulleys, etc., when made of flexural stiff.

3. Enclosures, either:

    a. Closely fitting enclosures made from flexible, damped, material which does not radiate sound efficiently, supported from the engine via vibration-isolating mounts. Little or no acoustic absorbent in the small gap between the engine and enclosure,

15

or

b. Ventilated sound-proof "tunnel" around the engine and gear box, lined with acoustic absorbent.

2.4.6 Gear Noise

Gear noise is one of the major concerns for engine manufacturers. Substantial research in the areas of gear noise was carried out by Welbourn [171]. He described the causes of gear noise and provided references on various topics related to gear noise. In a similar work, Watanabe [168] identified gear tooth characteristics that minimize noise generation (excitation). A new "maximum-conjugacy" tooth form employed these characteristics to reduce gear noise to about 15% of that of conventional gear quality class 9 or better, including all automotive gearing.

Externally measured vibrations can be associated with dynamic loads due to wear [159]. Thus the degree of vibration can provide an indication of wear and useful life. Shmuter [146, 147] described a method of identification of gear noise associated with conjugate errors and nicks. He also presented an original and practical method applicable to torsional and gear related systems. There is a potential of 10-20 dB reduction in gear noise by using coated gears [126] even at relatively low rpm. Nivi [105], in his work, indicated that the presence of gear nicks on the rear axle carrier may be detected by measuring its torsional vibration. This detection method was incorporated in an in-process rear axle test stand with reasonable success. Galotto (59) described a gear noise control device for quality inspection (detection of gear defects) in a production line.

2.4.7 Combustion Noise

Another major source of engine noise is the combustion process. Warren and Hanley [170] outlined a study on combustion and diesel engine noise. They concluded

16

that the diesel engine cylinder pressure spectrum was dominated by cycle to cycle variations in the cylinder pressure, not by repeatable, periodic process. Volkswagenwerk [165] published several technical papers which detailed the combustion processes that generate noise and vibration in engines. Various methods for detecting knocks due to combustion were also mentioned. The quantitative measurement of spark knock, the relationship with composition and knock resistance of gasoline and the detection of knock, are described in detail in references [10, 11, 14]. Anderton [6] showed that for a given engine speed and bore, there is a very large variation in the overall noise, of the order of 25-30 dBA, and that this variation is associated with a particular combustion system. Furthermore, he clarified that it is possible to design lower noise engines, even using conventional structures, provided that the maximum speed is limited and an intrinsically quieter combustion system is used.

2.4.8 Engine Balance

Balancing the automotive engine is one of the best ways of reducing noise and vibration in an engine. Various balancing methods are discussed in detail by Thomson [160] and in the General Motors Corporation Manual [60].

2.4.9 Piston Noise

Ross and Ungar [127] showed that piston slap is initiated when the side thrust changes direction. This occurs under two conditions: when the force in the connecting rod changes from tension to compression and vice versa, or when the component of the connecting rod force normal to the cylinder axis changes direction as a result of changes in the sign of the angle between the connecting rod and the cylinder axis. The latter condition always occurs at the top and bottom dead center; the former condition is realized when the total inertia force contribution to the side thrust just balances the resulting force from the

17

gas pressure. In practical engines, one always encounters piston slap at the top and bottom dead center, but mid-stroke slaps may be suppressed at low speed operating conditions where the aforementioned force balance cannot be attained.

Takiguchi [156] stated that an optimum piston design for noise reduction includes changing the piston profile to reduce friction and increase lubrication. Under most running conditions, there are six slaps per combustion cycle, the first and by far the largest of which occurs around TDC firing, when the piston moves rapidly from the non thrust to the thrust face of the bore [124]. For the conditions under which piston slap in gasoline engines is particularly intrusive, that is at low to medium speeds and loads, there are invariably six slaps per cycle. In this mode, the excitation given to the block by the primary slap is much greater than by the other five so that, it has been found possible to concentrate only upon the effects of this impact when assessing piston slap noise.

By measuring the cylinder wall strain, a block vibration or radiated noise from an engine, Richmond and Parker [125] were able to assess piston slap noise. A knowledge of the relative movement of the piston in the cylinder is important in understanding piston slap noise. A simulation model [103, 109] was created for this purpose. In his paper, Lalor [88] made three conclusions:

(a) speed is the most important parameter controlling the mechanical noise of all sizes of engine throughout their speed range,

(b) mechanical clearance is also an important parameter for small engines at low speed, and throughout the speed range for large engines,

(c) reciprocating mass is also an important parameter for small engines at high speed.

A further improvement in piston design can also be made to reduce noise. This can be accomplished by reducing the impact of the top land and skirt [76].
The maximum influence on piston design manifests itself in the structural vibration signals, measured on the cylinder liner, in the frequency range between 4 and 8 kHz. Haddad and Pullen [64] stated that piston slap appears to be of major importance in producing the

resultant engine vibration and noise, especially at lower engine speeds. Hodgett and McDonald [71] proved both experimentally and theoretically that the piston forces transmitted to the main bearings and to the engine mounts are increased by the resonances of crankshaft vibrations. In his paper, Fujimoto [58] concluded that the effect of oil film on the motion of the piston within the clearance is considerable, particularly on the lower part of the piston skirt.

2.4.10 Combustion Knock

Combustion knock is caused by irregular combustion which generates pressure oscillations in the cylinder. It is controlled in the early stage of engine design and by proper fuel selection. The placement and design of valves, spark plugs, fuel injection ports and the additive contents in engine fuel are factors causing the existence of combustion knock.

Ferraro [52] developed a knock intensity meter based on a criterion correlating knock intensity and kinetic energy associated with knock-typical pressure oscillations.

2.4.11 Engine Valve Cover, Sumps, Shields, and Enclosures

Sung and Lalor [154] discussed the use of shields and partial enclosures for engine noise reduction. Carr and Lalor [26] showed that the vibrational energy of a valve cover was usually lower when center fixing rather than when edge bolting is used. Using a damped steel sump reduced sump vibrational energy by increasing the damping without significantly affecting the energy transfer. Using a damped steel sump generally reduced crankcase vibrational energy. They also showed that the energy transfer was highest when the modal characteristics of the cover flange were similar to that of the engine component to which the flange was attached.

2.4.12 Engine Sound Quality

Quietness and better sound quality bring a more comfortable feeling to driver/passengers, as well as better handling and performance. Kuroda and Fujii [87] indicated that superior engine sound quality can be achieved by increasing the counterweights and stiffness of a crankshaft and, also, by optimizing the spark advance and improving the vibration characteristics of various engine parts. Crocker [39] described the use of digital signal processing techniques used to assess engine noise quality for a variety of engine types and conditions. Furthermore, he identified the causes and solutions for subjective unpleasantness.

2.4.13 General Vehicle Noise and Vibration

Flower and Ford [54, 55] described the optimization of engine mount design for improving vehicle noise, vibration and ride qualities.

CHAPTER 3.

THEORY

Different aspects of engine behaviour are governed greatly by the transverse and rotational movement of a reciprocating piston within the cylinder bore. As the horsepower and torque rating of an engine increase, the piston skirts become shorter thereby permitting a greater angle of piston to bore inclination. Hence, in this chapter, these influences are discussed in detail and potential engine design improvements are taken into consideration.

3.1 Dynamics of Piston- Crank Mechanism

During one cycle of engine running, the piston, connecting rod and crankshaft mechanism are exposed to three different categories of primary exciting forces, namely: a) combustion force, b) inertia force and c) a combination of both combustion and inertia forces. The separation of vibration signals between the contribution of these exciting forces is one of the main problems in this study.

When one or a combination of these forces move the piston and crankshaft with respect to their bearings, the mechanical clearances between components cause excitation upon impact. Especially when the piston is moving from compression to the expansion stroke, side force reversal causes the greatest impact to the respective components.

In this section, kinematic and dynamic relationships of the piston are derived to understand the mechanism of the engine vibration generation. These are compared to the vibration signals which are obtained during both cold and hot test of the engines.

3.1.1 Piston Kinematics

For the piston-slider crank mechanism shown in Figure 3.1, the displacement of piston can be derived using kinematics as follows:

$$y = Y_o + r(1 - \cos\theta) + L\left[1 - \sqrt{1 - \left(\frac{r}{L}\right)^2 \sin^2\theta}\right] \qquad (3.1)$$

where

y = location of the piston from the top dead center

Y_o = the distance from the top of block deck to top of piston at TDC

r = radius of the crank

θ = crank angle

L = length of the connecting rod.

If λ is defined as the ratio of radius of the crank to the length of the connecting rod, i.e.,

$$\lambda = \frac{r}{L}$$

and Φ is defined as

$$\Phi = \sqrt{1 - \left(\frac{r}{L}\right)^2 \sin^2\theta} = \sqrt{1 - \lambda^2 \sin^2\theta} \qquad (3.2)$$

then, by substituting these relationships into Equation (3.1), the piston location becomes

$$y = Y_o + r(1 - \cos\theta) + L(1 - \Phi) \qquad (3.3)$$

Now the velocity, V, and acceleration, A, of the piston are the first and second time derivatives of the piston displacement, i.e.,

22

Top of Engine Block Deck
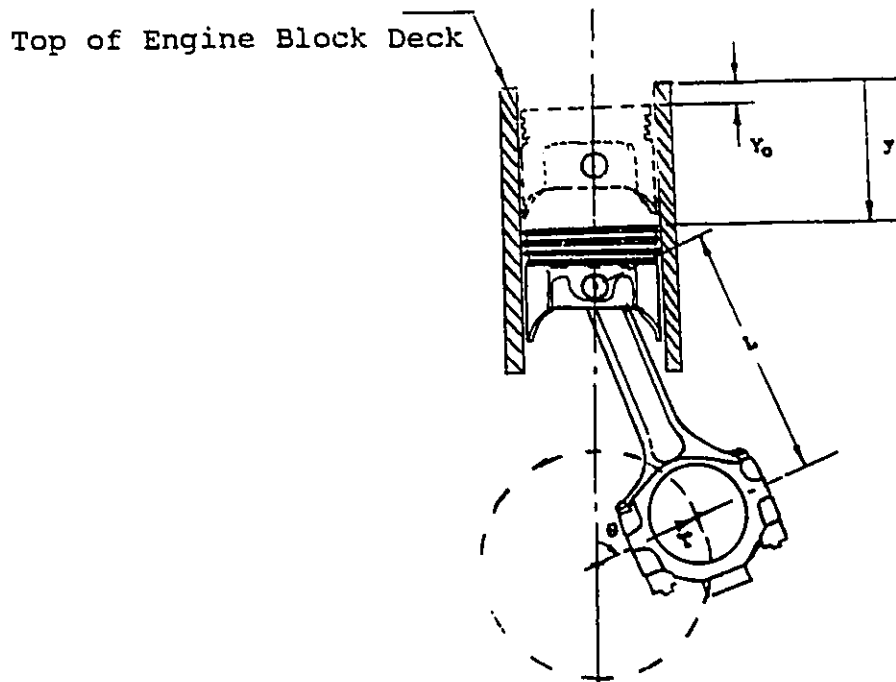
Figure 3.1 : Piston Slider Crank Mechanism without Offsets

Top of Engine Block Deck
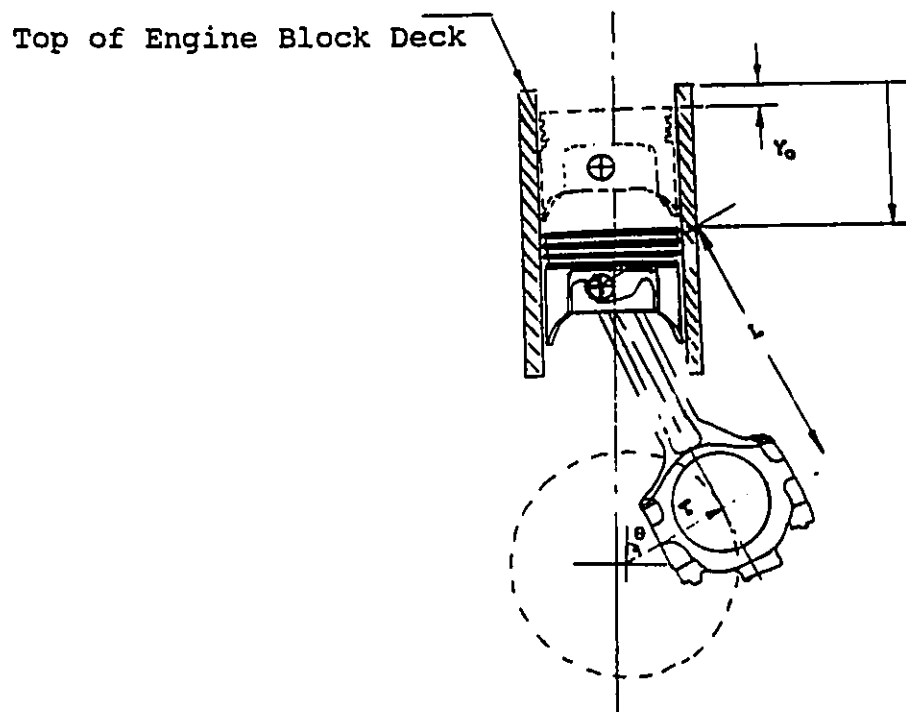
Figure 3.2 : Piston Slider Crank Mechanism with Offsets

23

$$V = y' = r\omega \sin\theta \left(1 + \frac{\lambda\cos\theta}{\phi} \right) \qquad (3.4)$$

and

$$A = y'' = r\omega^2 \left[\cos\theta + \frac{\lambda(\cos 2\theta + \lambda^2 \sin^4\theta)}{\phi^3} \right] \qquad (3.5)$$

In a practical engine design, the piston pin and/or crank shaft axis are offset from the bore center line as shown in Figure 3.2 and this offset must be taken into account in the analysis. The geometry of the connecting rod system with offset is shown in Figure 3.3.

In Figure 3.3, the piston displacement from the top deck to the top of piston at any crank angle, θ, is given by

$$y = Y_o + (r + L)\cos\phi_o - L\cos\phi - r\cos\theta \qquad (3.6)$$

where ϕ_o is the angle of the connecting rod to the bore center line at TDC.
Furthermore

$$\cos\phi_o = \frac{\sqrt{(r + L)^2 - Q^2}}{r + L} \qquad (3.7)$$

and

$$\cos\phi = \sqrt{1 - \left(\frac{r}{L}\sin\theta - \frac{Q}{L} \right)^2} \qquad (3.8)$$

If γ is the ratio of the offset distance between the piston and crank shaft axis to the length of the connecting rod, i.e.,

Piston TDC

Top of Engine Block Deck

Q

Y_0

Y

$(r+L)\cos\phi_0$

ϕ_0

ϕ

L

θ

r

$\sin\phi_0 = \dfrac{-Q}{L+r}$
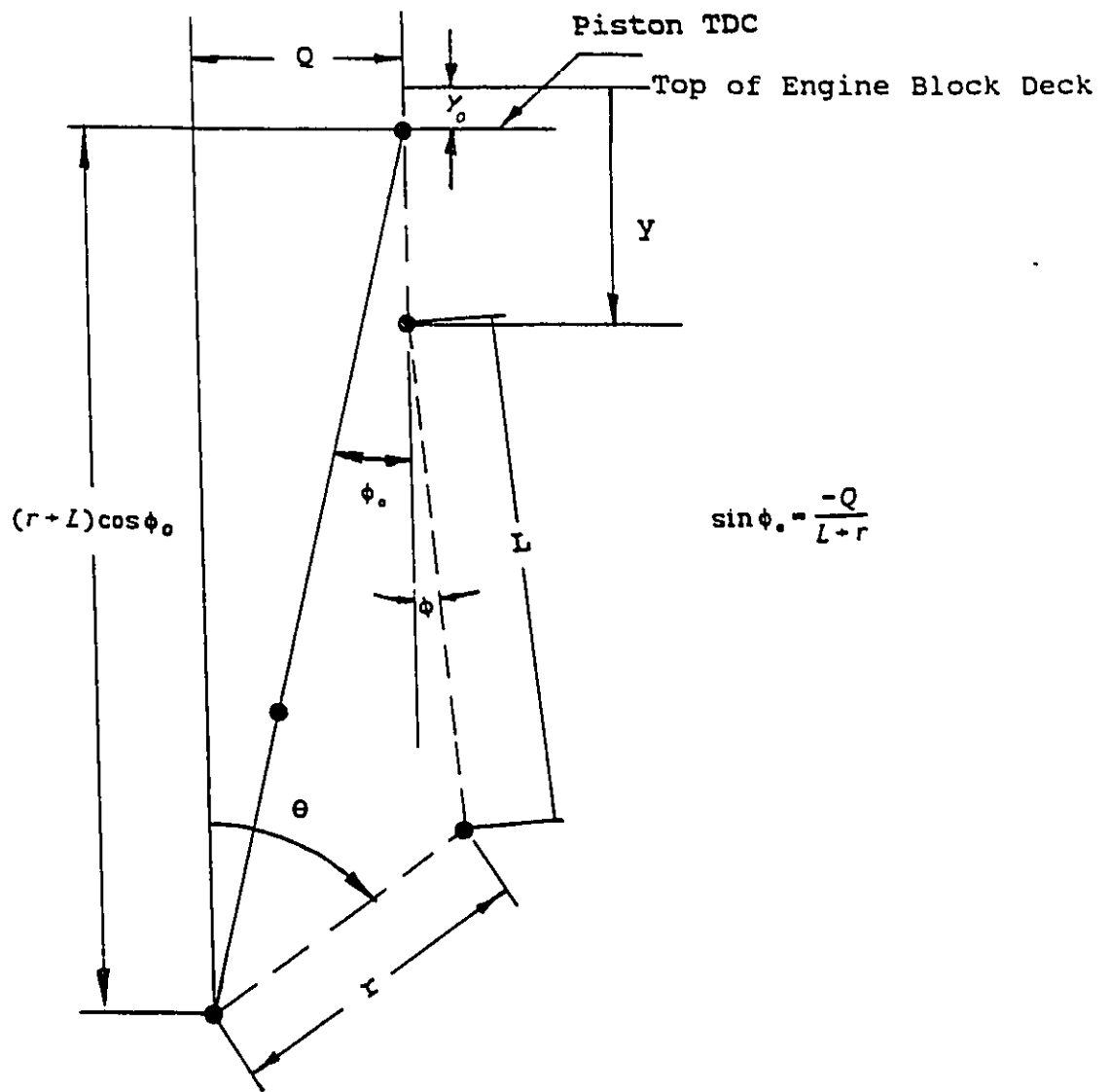
Figure 3.3 : Connecting Rod System with Offset.

$$\gamma = \frac{Q}{L} \qquad (3.9)$$

and Φ is defined as

$$\Phi = \cos\phi = \sqrt{1 - (\lambda\sin\theta - \gamma)^2} \qquad (3.10)$$

where Q is the offset distance between the piston and crank shaft axis.

The velocity and acceleration expressions now become:

$$V = y' = r\omega\sin\theta\left(1 + \frac{\lambda\cos\theta}{\Phi}\right) - \frac{r\omega\gamma\cos\theta}{\Phi} \qquad (3.11)$$

and

$$A = y'' = r\omega^2\cos\theta + \frac{L\omega^2}{\Phi^3}[\Phi^2\left(\cos^2\theta - \sin^2\theta + \frac{\gamma}{\lambda}\sin\theta\right)$$

$$+ (\gamma\cos\theta - \lambda\sin\theta\cos\theta)^2] \qquad (3.12)$$

For the special case of zero offset, i.e., $\gamma = 0$ and Equations (3.11) and (3.12) reduce to Equations (3.4) and (3.5).

3.1.2 Connecting Rod Dynamics

The types of piston motion which affect the piston slap impulse are:

1) piston translation with friction in the cylinder space, and

2) angular moti n of the piston.

As it is difficult to calculate the impact to the cylinder wall due to the piston motion, an

approximate method which replaces the distributed mass of the connecting rod with an equivalent two-mass system is used for piston dynamics calculations. The dynamics of the connecting rod are formulated in a similar manner.

For the rigid connecting rod shown in Figure 3.4, its equivalent two mass system is illustrated in Figure 3.5. For this system to be dynamically similar to the original system the following conditions need to be satisfied:

a) inertial equivalent,

$$I_{rod} = m_1 s^2 + m_2 (L - s)^2 \qquad (3.13)$$

b) mass equivalent,

$$m_{rod} = m_{1eq} + m_{2eq} \qquad (3.14)$$

c) moment equivalent,

$$m_{2eq}(L - s) - m_{1eq} s = 0 \qquad (3.15)$$

where

m_1 is the big-end mass of the connecting rod,

m_2 is the small-end mass of the connecting rod

I_{rod} is the mass moment inertia of the original connecting rod

The moment of inertia of the equivalent connecting rod is calculated as:

$$I_{eq} = m_{1eq} s^2 + m_{2eq}(L - s)^2 = m_{rod} s(L - s) \qquad (3.16)$$

Using this approximation, there is an error in estimating the inertia of the rod. This error is $I_{rod} - m_{rod} s(L - s)$. Therefore, in order for the two mass system to be dynamically equivalent to the original connecting rod, a corrective torque T must be applied about the big end. This torque is

$$T = I_c \ddot{\phi} \qquad (3.17)$$
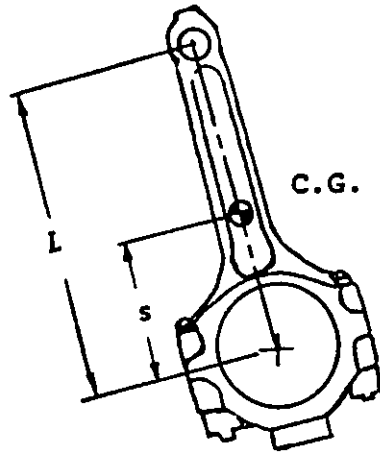
Figure 3.4 : Connecting Rod Geometry.
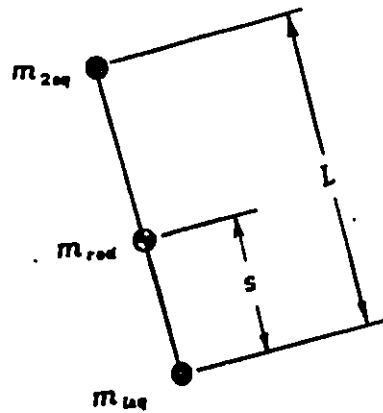
Figure 3.5 : Equivalent Connecting Rod.

28

where

$$I_c = I_{rod} - m_{rod}s(L - s)$$ (3.18)

and $\ddot{\phi}$ = the rotational acceleration of the connecting rod.

The angular velocity of the connecting rod is,

$$\dot{\phi} = \frac{d\phi}{dt} = \frac{r\omega\cos\theta}{L\cos\phi}$$ (3.19)

where $\omega = \dot{\theta}$ = angular velocity of the crank shaft.

Differentiating the velocity with respect to time gives the angular acceleration

$$\ddot{\phi} = \frac{-rL\omega^2\sin\theta\cos\phi + rL\dot{\phi}\omega\cos\theta\sin\phi}{(L\cos\phi)^2}$$ (3.20)

$$\ddot{\phi} = \frac{L\dot{\phi}^2\sin\phi - r\omega^2\sin\theta}{L\cos\phi}$$ (3.20a)

3.1.3 Piston Dynamics

As stated in the previous section, the mass and moment of inertia of the piston are the most important factors which control the dynamic behaviour of the systems. However, the dynamics of the connecting rod has to be considered due to its large share of the total mass in the piston mechanism. A typical percentage of the total mass distribution of the piston and the connecting rod is shown in Figure 3.6. For the piston/rod assembly geometry shown in Figure 3.7, the coordinate system and the sign convention are as shown. The following is a description of the notation:

1) The positive x-coordinate is directed to the right from the piston (and bore) center line.

2) The positive y-coordinate is directed downward from the top of the piston skirt.

3) The rotation of the piston (β) is positive clockwise.

4) The crank rotation (θ) is also positive clockwise.

29

Total Oscillating Mass = 100%

Piston = 38.2%

Rings = 2.3%

Pin = 10.3%
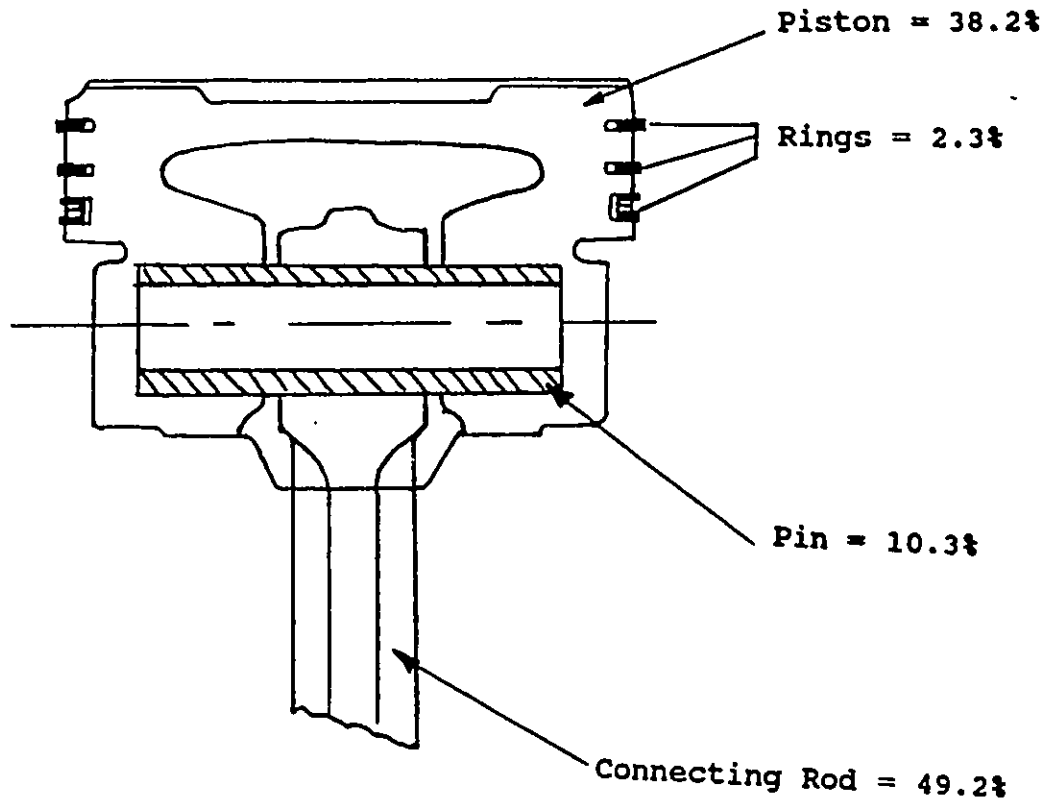
Connecting Rod = 49.2%

Figure 3.6 : Distribution of the Oscillating Masses.
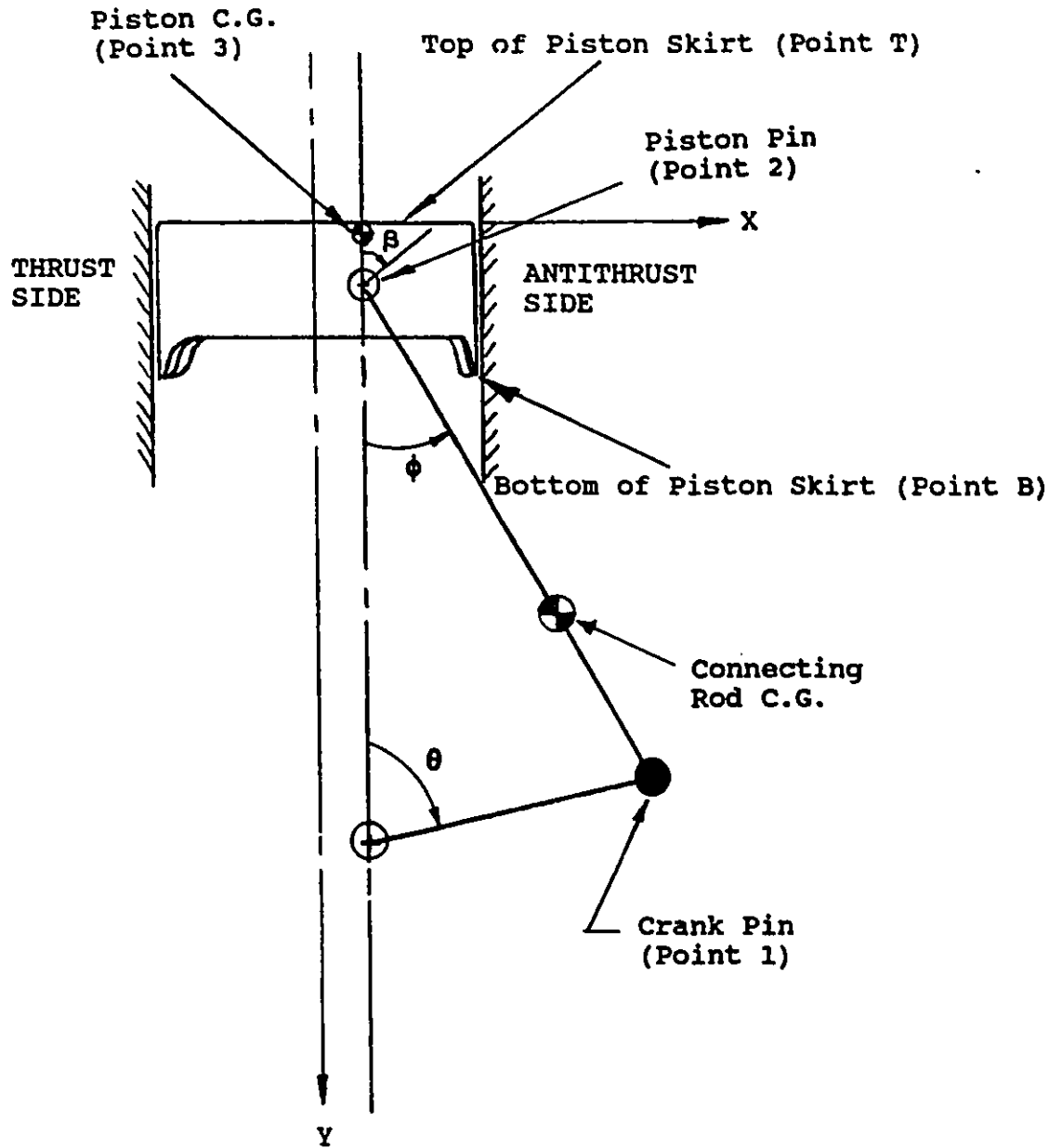
Figure 3.7 : Piston Sign Convention.

5) The connecting rod rotation (ϕ) is positive counterclockwise.

6) The thrust side of the piston is on the left and the antithrust side is on the right.

7) The location of the piston pin, crank axis, piston C.G., etc. are defined in the x-y coordinate system.

The piston lateral displacement (x) is zero when the center of the piston is located at the center of the bore. The piston axial location (y) is zero when the piston is at its highest point (TDC). The piston rotation (β) is zero when the piston position is vertical. Crank rotation is zero ($360°$ and $720°$) when the crank position is vertically upward. A crank angle of $0°$ corresponds to the top of the power stroke. The connecting rod rotation (ϕ) is also zero when the rod is vertical. Points 1, 2, 3, T and B are denoted as the center of the crank pin, the center of the piston pin, the piston C.G., the top of the piston skirt and the bottom of the piston skirt, respectively. The point designations are used as subscripts in specifying the piston motion and its properties. For example, the mass of the piston is denoted as m_3 and the mass moment of inertia of the piston about the piston C.G. is denoted as I_3. The lateral acceleration of the piston pin is denoted as $\ddot{x}_2$ and axial acceleration of the piston C.G. is $\ddot{y}_3$.

The geometry of the piston and the forces acting on it are shown in Figure 3.8. Taking moments about the crank pin (point 1) for the piston and connecting rod loads gives

$$
\begin{aligned}
& -P_V(L_2 + u) + P_H(L_1 + f) + F_1(L_1 + a) + F_2(L_1 - b) \\
& + J_T\mu F_1(L_2 + u + x_2 + J_{ST}R) + J_B\mu F_2(L_2 + u + x_2 + J_{SB}R) \\
& - m_3g(L_2 - e + u) + m_3\ddot{y}_3(L_2 - e + u) - m_3\ddot{x}_3(L_1 + c) \\
& - m_2\ddot{x}_2L_1 + m_2\ddot{y}_2L_2 + m_{rod}s^2\ddot{\phi} \\
& - I_3\ddot{\beta} + I_{rod}\ddot{\phi} = 0
\end{aligned}
\tag{3.21}
$$
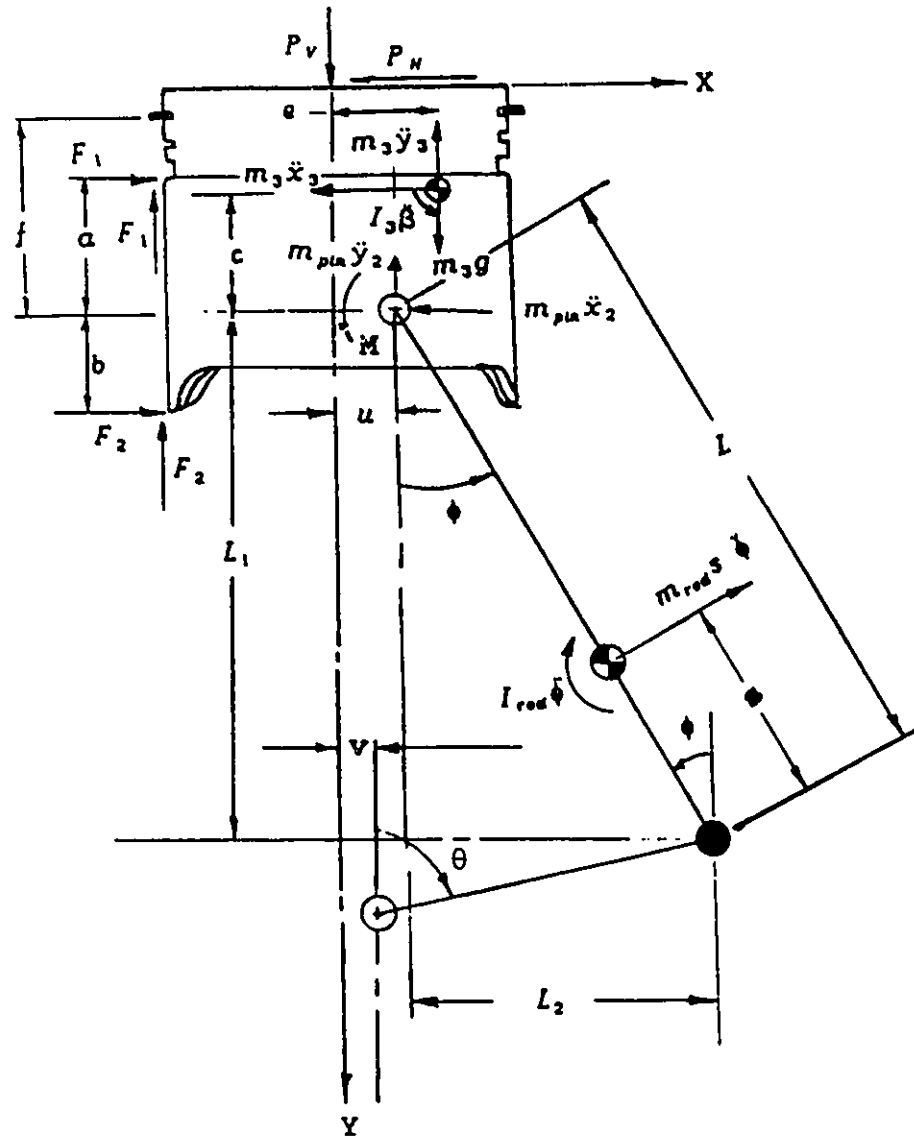
Figure 3.8 : Piston Geometry and the Associated Forces.

33

Summing moments about the piston pin (point 2) for the piston loads gives

$$-P_V(u) - P_H(f) + F_1(a) - F_2(b)$$

$$+ J_T\mu F_1(u + x_2 + J_{ST}R) + J_B\mu F_2(L_2 + u + x_2 + J_{SB}R)$$

$$+ m_3 g(e - u) - m_3 \ddot{y}_3(e - u)$$

$$- m_3 \ddot{x}_3(c) - M - I_3\ddot{\beta} = 0 \qquad\qquad (3.22)$$

The terms used in Equations (3.21) and (3.22) are defined as follows:

a = distance from piston pin to top of piston skirt.

b = distance from piston pin to bottom of piston skirt.

c = distance from piston pin to C.G.

e = distance from piston center line to piston C.G.

f = distance from piston pin to top ring.

g = acceleration of gravity.

m_2 = mass of piston pin.

m_3 = mass of piston.

m_{rod} = mass of connecting rod.

s = distance from crank pin (point 1) to rod C.G.

u = distance from piston center line to piston pin.

v = distance from bore center line to crankshaft axis.

x_2 = lateral displacement of piston pin.

$\ddot{x}_2$ = lateral acceleration of piston pin.

$\ddot{x}_3$ = lateral acceleration of piston C.G.

$\ddot{y}_2$ = axial acceleration of piston pin.

$\ddot{y}_3$ = axial acceleration of piston C.G.

F_1 = piston/bore reaction force at top of skirt.

34

F_2 = piston/bore reaction force at bottom of skirt.

I_3 = mass moment of inertia of piston about piston C.G.

I_{rod} = mass moment of inertia of connecting rod about rod C.G.

J_B = sign coefficient accounting for piston velocity direction and thrust or antithrust contact with the bore at the bottom of skirt.

J_T = sign coefficient accounting for piston velocity direction and thrust or antithrust contact with the bore at the bottom of skirt.

J_{SB} = sign coefficient accounting for piston contact with thrust or antithrust side of bore at bottom of skirt.

J_{ST} = sign coefficient accounting for piston contact with thrust or antithrust side of bore at top of skirt.

$L_1 = L \cos \phi$

$L_2 = L \sin \phi$

M = moment developed between piston pin and piston due to friction.

P_H = lateral component of gas pressure load.

P_V = axial component of gas pressure load.

R = radius of bore.

μ = coefficient of friction between piston skirt and bore.

$\ddot{\beta}$ = angular acceleration of piston.

$\ddot{\phi}$ = angular acceleration of connecting rod.

The motion of the piston C.G. $(x_3, \dot{x}_3, \ddot{x}_3, y_3, \dot{y}_3, \ddot{y}_3)$ is related to the motion of the piston pin $(x_2, \dot{x}_2, \ddot{x}_2, y_2, \dot{y}_2, \ddot{y}_2)$ and to the piston rotation $(\beta, \dot{\beta}, \ddot{\beta})$ in the following manner

$$x_3 = x_2 + c\beta \tag{3.23}$$

$$\dot{x}_3 = \dot{x}_2 + c\dot{\beta} \tag{3.24}$$

$$\ddot{x}_3 = \ddot{x}_2 + c\ddot{\beta} \tag{3.25}$$

$$y_3 = y_2 + (e - u)\beta \tag{3.26}$$

$$\dot{y}_3 = \dot{y}_2 + (e - u)\dot{\beta} \tag{3.27}$$

$$\ddot{y}_3 = \ddot{y}_2 + (e - u)\ddot{\beta} \tag{3.28}$$

Substituting Equations (3.25) and (3.28) into Equation (3.21) and rearranging terms gives

$$H_1 F_1 + H_2 F_2 + H_3 \ddot{x}_2 + H_4 \ddot{\beta} + H_5 = 0 \tag{3.29}$$

where

$$H_1 = L_1 + a + J_T \mu (L_2 + u + x_2 + J_{ST} R) \tag{3.30}$$

$$H_2 = L_1 - b + J_B \mu (L_2 + u + x_2 + J_{SB} R) \tag{3.31}$$

$$H_3 = -m_3 (L_1 + c) - m_2 L_1 \tag{3.32}$$

$$H_4 = m_3 (L_2 - e + u)(e - u) - m_3 (L_1 + c)(c) - I_3 \tag{3.33}$$

$$H_5 = (I_{rod} + m_{rod} s^2)\ddot{\phi} - P_V (L_2 + u) - P_H (L_1 + f) \tag{3.34}$$

$$-m_3 g (L_2 - e + u) + m_3 \ddot{y}_2 (L_2 - e + u)$$

$$+ m_2 \ddot{y}_2 L_2$$

Substituting Equations (3.25) and (3.28) into Equation (3.22) and rearranging terms gives

$$H_6 F_1 + H_7 F_2 + H_8 \ddot{x}_2 + H_9 \ddot{\beta} + H_{10} = 0 \tag{3.35}$$

where

$$H_6 = a + J_T \mu(u + x_2 + J_{ST} \, R) \tag{3.36}$$

$$H_7 = -b + J_B \mu(u + x_2 + J_{SB} R) \tag{3.37}$$

$$H_8 = -m_3(c) \tag{3.38}$$

$$H_9 = -m_3(e - u)^2 - m_3(c^2) - I_3 \tag{3.39}$$

$$H_{10} = -P_V(u) - P_H(f) + m_3 g(e - u)$$
$$-m_3 \ddot{y}_2(e - u) - M \tag{3.40}$$

Equations (3.29) and (3.35) are two of the equations required to solve for the four unknowns $(F_1, F_2, \ddot{x}_2, \ddot{\beta})$. The other two equations can be developed once the mode of the piston motion is specified.

The four modes of the piston motion (relative to the cylinder) which are used to describe the behavior of the piston are shown in Figure 3.9. They are as follows:

Mode 1. No horizontal movement is present. Both the top and the bottom of the skirt are in contact with the bore, either diagonally or vertically.

Mode 2. Piston is rotating about the top of the skirt.

Mode 3. Piston is rotating about the bottom of the skirt.

Mode 4. Piston is free in the bore, translating and rotating according to the net transverse force and turning moment applied to it.

Each type of motion can be defined by a particular set of equations from which the subsequent behavior of the piston may be determined. In order to derive these equations the following simplifying assumptions are made:

1. The angular acceleration of the crankshaft is zero.

2. The angular velocity of the connecting rod is independent of the transverse motion of the piston.

Assumption 2 simplifies the calculations by eliminating the coupling of the

Mode 1 : Both top and bottom of piston skirt are in contact with
          the cylinder bore, either vertically or diagonally.

Mode 2 : Top of piston skirt in contact with one side of
          cylinder bore.
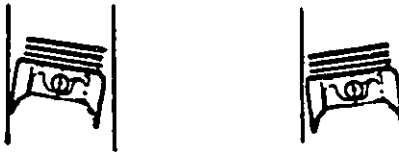
Mode 3 : Bottom of piston skirt in contact with one side of
          cylinder bore.

Mode 4 : Piston free in cylinder bore.

Figure 3.9 : Basic Modes of Piston Motion.

differential equations. The justification here is that, although the transverse piston motion may alter the angular acceleration of the connecting rod, the time for which such acceleration occurs is too short to influence the angular velocity significantly.

The equations of motion for each regime are derived below:

a) In Mode 1, where there is no lateral movement of the piston, we have

$$\ddot{x}_2 = 0 \tag{3.41}$$

$$\ddot{\beta} = 0 \tag{3.42}$$

and therefore,

$$H_1 F_1 + H_2 F_2 = -H_5 \tag{3.43}$$

and

$$H_6 F_1 + H_7 F_2 = -H_{10} \tag{3.44}$$

from which we obtain

$$F_1 = \frac{-H_5 H_7 + H_2 H_{10}}{H_1 H_7 - H_2 H_6} \tag{3.45}$$

$$F_2 = \frac{-H_1 H_{10} + H_5 H_6}{H_1 H_7 - H_2 H_6} \tag{3.46}$$

b) In Mode 4, where there is no piston contact with the bore, we have

39

$$F_1 = 0 \qquad\qquad (3.47)$$

$$F_2 = 0 \qquad\qquad (3.48)$$

and therefore,

$$H_3\ddot{x}_2 + H_4\ddot{\beta} = -H_5 \qquad\qquad (3.49)$$

and

$$H_8\ddot{x}_2 + H_9\ddot{\beta} = -H_{10} \qquad\qquad (3.50)$$

from which we obtain

$$\ddot{x}_2 = \frac{-H_5 H_9 + H_4 H_{10}}{H_3 H_9 - H_4 H_8} \qquad\qquad (3.51)$$

$$\ddot{\beta} = \frac{-H_3 H_{10} + H_5 H_8}{H_3 H_9 - H_4 H_8} \qquad\qquad (3.52)$$

c) In mode 2, where the piston rotates about the top of the skirt as shown in Figure 3.9, we
   have

$$F_2 = 0 \qquad\qquad (3.53)$$

$$\ddot{x}_2 = -\alpha\ddot{\beta} \qquad\qquad (3.54)$$

and therefore,

$$H_1 F_1 + (-H_3\alpha + H_4)\ddot{\beta} = -H_5 \qquad\qquad (3.55)$$

and

$$H_6F_1 + (-H_8\alpha + H_9)\ddot{\beta} = -H_{10} \qquad (3.56)$$

from which we obtain

$$F_1 = \frac{-H_5(-H_8\alpha + H_9) + (-H_3\alpha + H_4)H_{10}}{H_1(-H_8\alpha + H_9) - (-H_3\alpha + H_4)H_6} \qquad (3.57)$$

$$\ddot{\beta} = \frac{-H_1\ddot{H}_{10} + H_5H_6}{H_1(-H_8\alpha + H_9) - (-H_3\alpha + H_4)H_6} \qquad (3.58)$$

d) In Mode 3, where the piston rotates about the bottom of the skirt as shown in Figure 3.9, we have

$$F_1 = 0 \qquad (3.59)$$

$$\ddot{x}_2 = b\ddot{\beta} \qquad (3.60)$$

and therefore,

$$H_2F_2 + (H_3b + H_4)\ddot{\beta} = -H_5 \qquad (3.61)$$

and

$$H_7F_2 + (H_8b + H_9)\ddot{\beta} = -H_{10} \qquad (3.62)$$

from which we obtain

$$F_2 = \frac{-H_5(H_8b + H_9) + (H_3b + H_4)H_{10}}{H_2(H_8b + H_9) - (H_3b + H_4)H_7} \qquad (3.63)$$

and

41

$$\ddot{\beta} = \frac{-H_2 H_{10} + H_5 H_7}{H_2(H_8 b + H_9) - (H_3 b + H_4)H_7} \qquad (3.64)$$

3.1.4 Piston/Piston Pin Friction Forces

The moment (M) developed between the piston and the piston pin cannot be determined until the pin force (A) is known. The direction of the moment depends on the relative angular velocity of the piston $(\dot{\beta})$ and of the connecting rod $(\dot{\phi})$. An iterative approach is used to determine the lateral component of the pin force (A_1) and the axial component (A_2).

The piston contact forces $(F_1$ and $F_2)$ and the piston accelerations $(\ddot{x}_2$ and $\ddot{\beta})$ are determined from the moment relationships derived in the previous section by initially setting the friction moment (M) equal to zero. Then, summing the piston forces in the lateral (x) direction and axial (y) direction provides the two equations necessary to solve for A_1 and A_2. From the free body diagram of the piston, Figure 3.10, we can derive :

$$A_1 + J_p \mu_p A_2 - F_1 - F_2 + m_3 \ddot{x}_3 + P_H = 0 \qquad (3.65)$$

$$A_2 - J_p \mu_p A_1 + J_v \mu(F_1 + F_2) + m_3 \ddot{y}_3 - P_v - m_3 g = 0 \qquad (3.66)$$

where

μ_p = coefficient of friction between the piston and pin.

J_p = sign coefficient accounting for relative angular velocity of piston and connecting rod.

J_v = sign coefficient accounting for velocity direction of piston.

Rearranging terms in Equation (3.65) and (3.66), one obtains
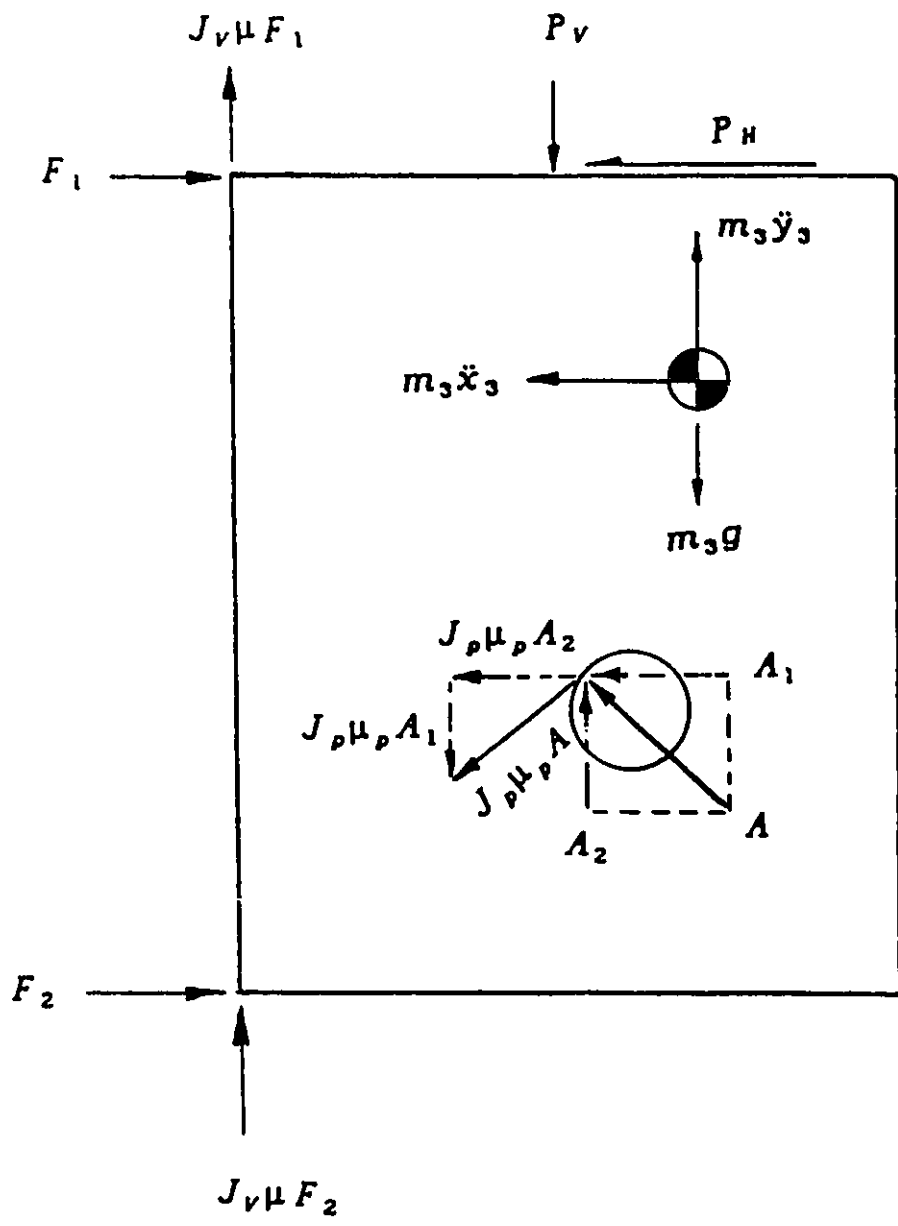
Figure 3.10 : Pin Forces Acting on Piston.

$$A_1 + C_1 A_2 = C_2 \tag{3.67}$$

$$C_3 A_1 + A_2 = C_4 \tag{3.68}$$

where

$$C_1 = J_p \mu_p \tag{3.69}$$

$$C_2 = F_1 + F_2 - m_3 \ddot{x}_3 - P_H \tag{3.70}$$

$$C_3 = -J_p \mu_p \tag{3.71}$$

$$C_4 = -J_V \mu (F_1 + F_2) - m_3 \ddot{y}_3 + P_V + m_3 g \tag{3.72}$$

Solving for A_1 and A_2 gives

$$A_1 = \frac{C_1 C_4 - C_2}{C_1 C_3 - 1} \tag{3.73}$$

$$A_2 = \frac{C_2 C_3 - C_4}{C_1 C_3 - 1} \tag{3.74}$$

The friction moment M can be determined from A_1 and A_2 as follows:

$$M = J_p \frac{\mu_p d_p}{2} \sqrt{A_1^2 + A_2^2} = J_p \frac{\mu_p d_p}{2} A \tag{3.75}$$

where d_p = piston pin diameter.

This moment is now used to determine new contact forces and piston accelerations. New values for A_1 and A_2 are determined from Equations (3.73) and (3.74). The process is repeated until convergence of M is achieved. In all tested cases convergence was achieved.

3.1.5 Piston Motion and Impacts

The piston accelerations $(\ddot{x}_2$ and $\ddot{\beta})$ can be determined at every crank angle throughout a four stroke cycle. The lateral velocity and location of the piston are calculated by integrating $\ddot{x}$ and $\ddot{\beta}$ over a specified range using the appropriate time step.

The location of the top and bottom of the piston skirt is continually monitored so that the mode of the piston motion can be determined at each crank angle. In the case when the piston impacts the cylinder bore, the kinetic energy of the piston at impact is determined for that location.

To model the impact between the piston skirt and the cylinder bore the following assumptions are made:

1) The velocity of a point on the piston at which impact occurs is reduced to zero, i.e., rebound does not occur.

2) If the piston is free in the bore prior to impact, then the angular velocity of the piston after impact is determined according to the principle of conservation of angular momentum.

The piston angular velocity after impact may be determined as follows. Consider a system consisting of piston and cylinder (Figure 3.11) just prior to impact, with the piston having a horizontal velocity $\dot{x}_3$ and angular velocity $\dot{\beta}$. The equivalent mass at point 2 (piston pin location) m_{eq} is :

$$m_{eq} = m_2 + m_{2eq}$$

where m_2 = mass of piston pin, and

m_{2eq} = the equivalent mass of connecting rod.

The mass m_{eq} has a velocity $\dot{x}_2$. The angular momentum just before impact with respect to the contact point P (see Figure 3.11) is given by

$$H_a = m_3\dot{x}_3(b + c) + I_3\dot{\beta} + m_{eq}\dot{x}_2 b \tag{3.76}$$
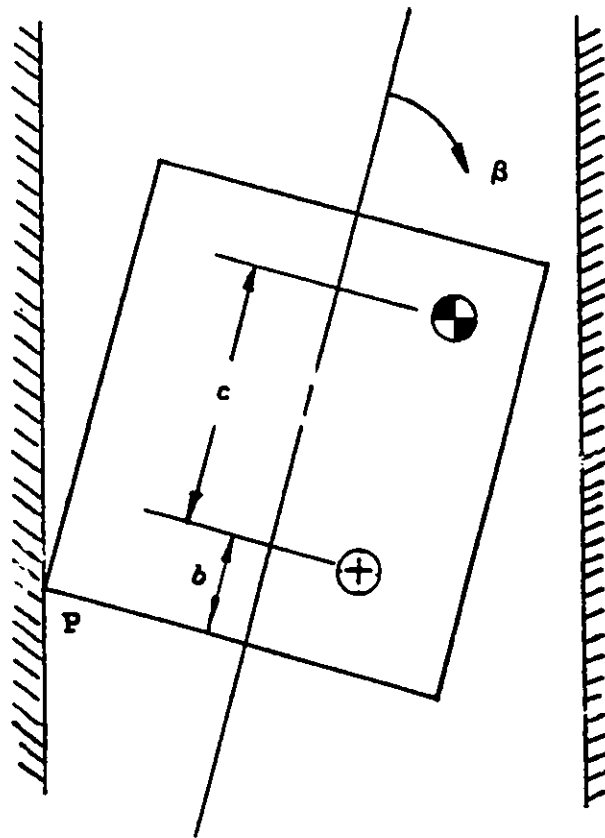
Figure 3.11 :   Piston Impact with Cylinder Bore.

After impact the velocity of the impact at P is zero and the piston rotates about the point of contact at the new angular velocity $\dot{\beta}'$. Thus the angular momentum after impact is given by

$$H_{\alpha}' = m_3 \dot{x}_3'(b + c) + I_3 \dot{\beta}' + m_{eq} \dot{x}_2' b \qquad (3.77)$$

but, from Figure 3.11, we have

$$\dot{x}_2' = b \dot{\beta}' \quad \text{and} \quad \dot{x}_3' = (b + c)\dot{\beta}' \qquad (3.78)$$

Then

$$H_{\alpha}' = I_3 \dot{\beta}' + m_{eq} b^2 \dot{\beta}' + m_3(b + c)^2 \dot{\beta}' \qquad (3.79)$$

Applying the principle of conservation of angular momentum,

$$H_{\alpha} = H_{\alpha}' \qquad (3.80)$$

and

$$\dot{\beta}' = \frac{m_3 \dot{x}_3(b + c) + I_3 \dot{\beta} + m_{eq} \dot{x}_2 b}{I_3 + m_3(b + c)^2 + m_{eq} b^2} \qquad (3.81)$$

Equation (3.81) defines the angular velocity of the piston after impact.

To quantify the impact, the change in kinetic energy of the piston during impact is calculated as follows:

47

Kinetic Energy lost $= KE_1 - KE_2$

where

$$KE_1 = 0.5[m_3\dot{x}_3^2 + m_3\dot{y}_3^2 + m_{eq}\dot{x}_2^2 + I_3\dot{\beta}^2] \qquad (3.82)$$

= kinetic energy of piston before impact

$$KE_2 = 0.5[m_3\dot{x}_{3a}^2 + m_3\dot{y}_{3a}^2 + m_{eq}\dot{x}_{2a}^2 + I_3\dot{\beta}_a^2] \qquad (3.83)$$

= kinetic energy of piston after impact

where the subscript "a" refers to the velocities after impact.

A computer program was used to predict the piston motion (lateral and rotational). Figure 3.12 shows the typical specifications of an engine used in the experiments.

Initially, the locations of the piston pins with respect to crank angles were calculated. Sudden alternations of piston pin locations in the lateral direction which might cause piston slaps were observed as illustrated in Figure 3.13. The cyclic change in displacement of the piston pin with respect to the crank angle was also seen in the axial direction, as indicated in Figure 3.14.

The velocity and acceleration of the piston pin were obtained by the first and second derivatives of the piston pin displacement equations. Figures 3.15 to 3.18 illustrate the plotted output.

By taking moments about the piston pin, as depicted in Equation 3.22, the piston / bore reaction forces were calculated and plotted as shown in Figures 3.21 to 3.26. Finally, the kinetic energy loss at impact was calculated and it is illustrated in Figure 3.27.

```
ENGINE CHARACTERISTICS :


     ENGINE SPEED........................2000 RPM
     BORE DIAMETER.......................96.841 mm
     STROKE..............................86.106 mm
     CRANK OFFSET........................ 0.000 mm


CONNECTING ROD CHARACTERISTICS :


     CONNECTING ROD LENGTH..............150.19 mm
     CONNECTING ROD CG..................35.052 mm
     CONNECTING ROD WEIGHT..............672 g


PISTON CHARACTERISTICS :


     PISTON HEIGHT......................69.088 mm
     SKIRT HEIGHT.......................43.942 mm
     PISTON PIN (X-COORD.)..............-0.762 mm
     PISTON PIN (Y-COORD.)..............41.402 mm
     PISTON CG (X-COORD.)...............0.101 mm
     PISTON CG (Y-COORD.)...............18.440 mm
     PISTON PIN WEIGHT..................143.01 g
     PISTON WEIGHT......................522 g


PISTON/BORE CLEARANCES :


     SKIRT TOP CLEARANCE................0.051 mm
     SKIRT BOTTOM CLEARANCE.............0.025 mm


FRICTION COEFFICIENTS AND PIN DIAMETER :


     PISTON/BORE FRICTION COEFF.........0.100
     PISTON PIN FRICTION COEFF..........0.100
     PISTON PIN DIAMETER................23.165 mm
```

Figure 3.12 : A Typical Specification of a 4-stroke Engine.

PISTON PIN LOCATION
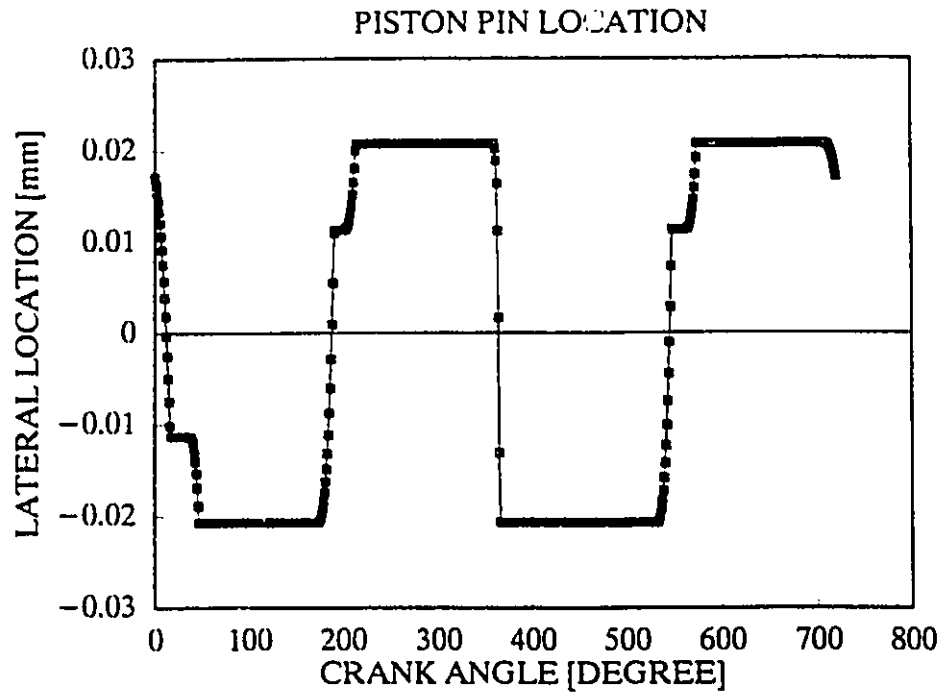
Figure 3.13 : Lateral Piston Pin Location Versus Crank Angle.

PISTON PIN LOCATION
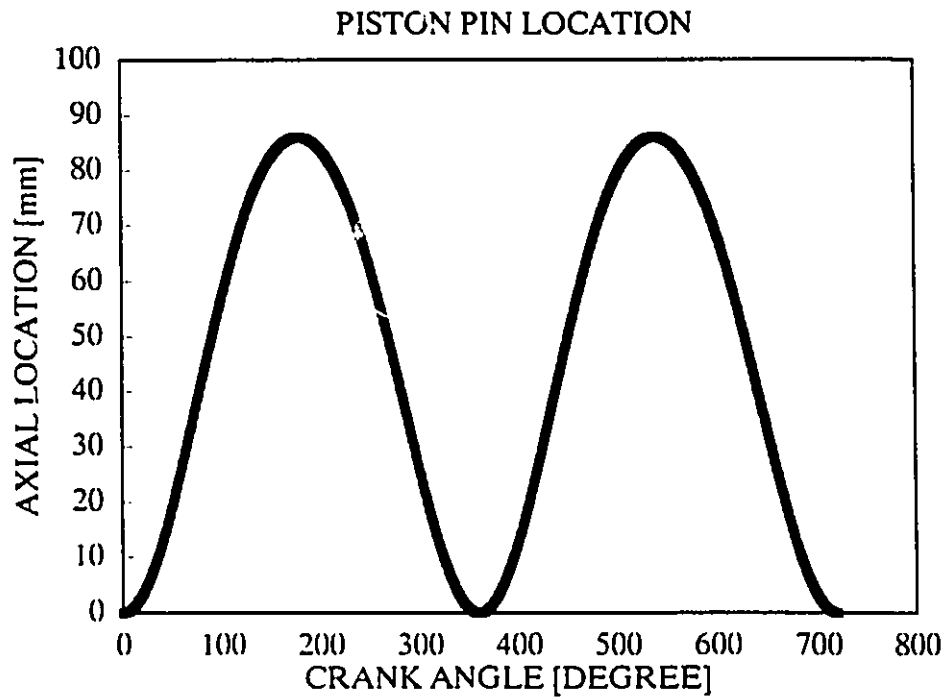
Figure 3.14 : Axial Piston Pin Location Versus Crank Angle.

PISTON PIN VELOCITY
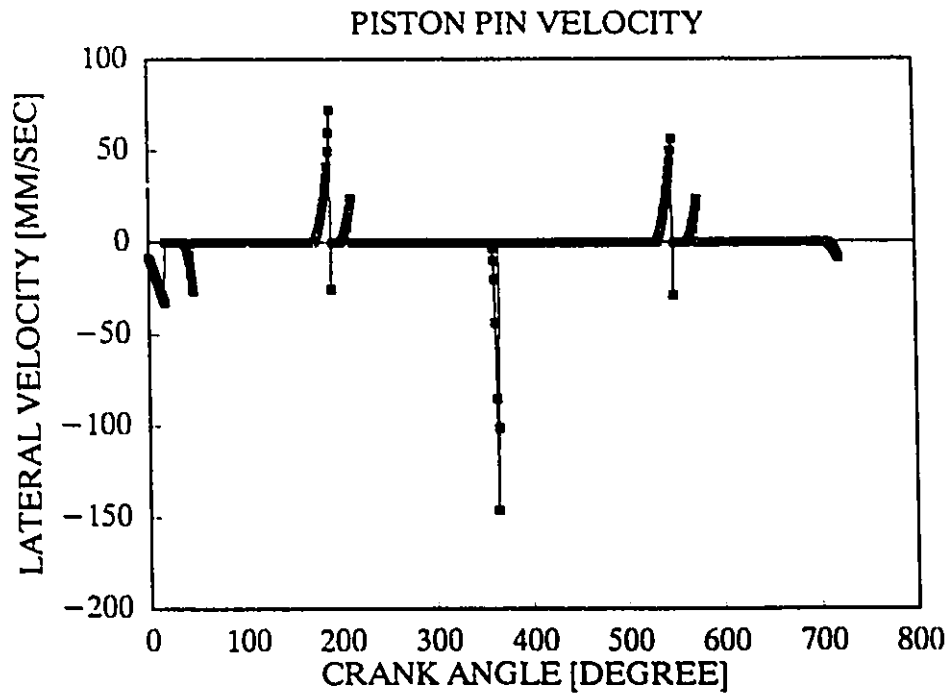
Figure 3.15 : Lateral Piston Pin Velocity Versus Crank Angle.

PISTON PIN VELOCITY
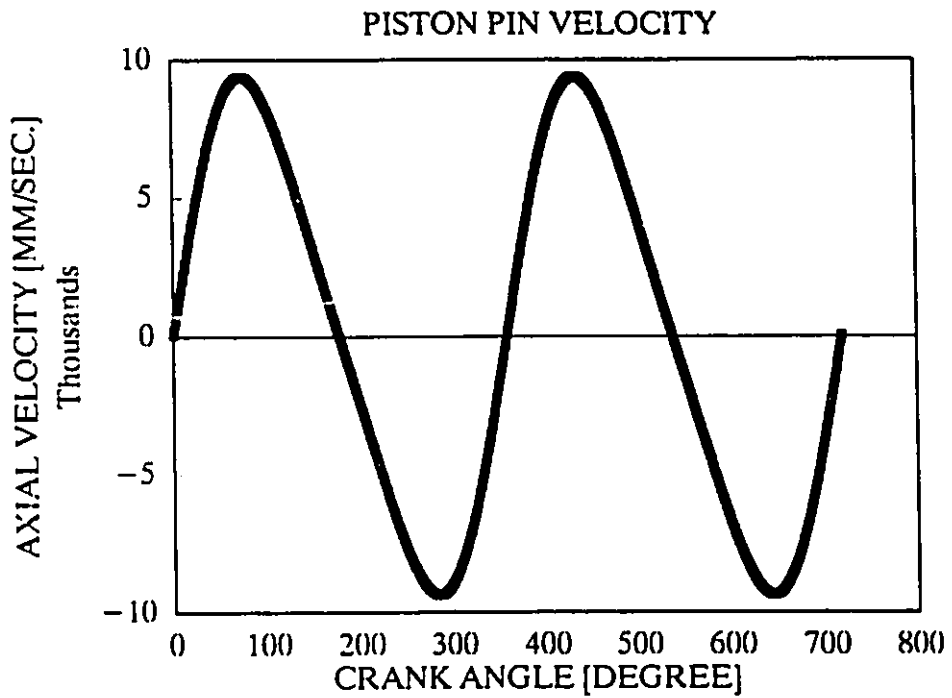
Figure 3.16 : Axial Piston Pin Velocity Versus Crank Angle.

PISTON PIN ACCELERATION
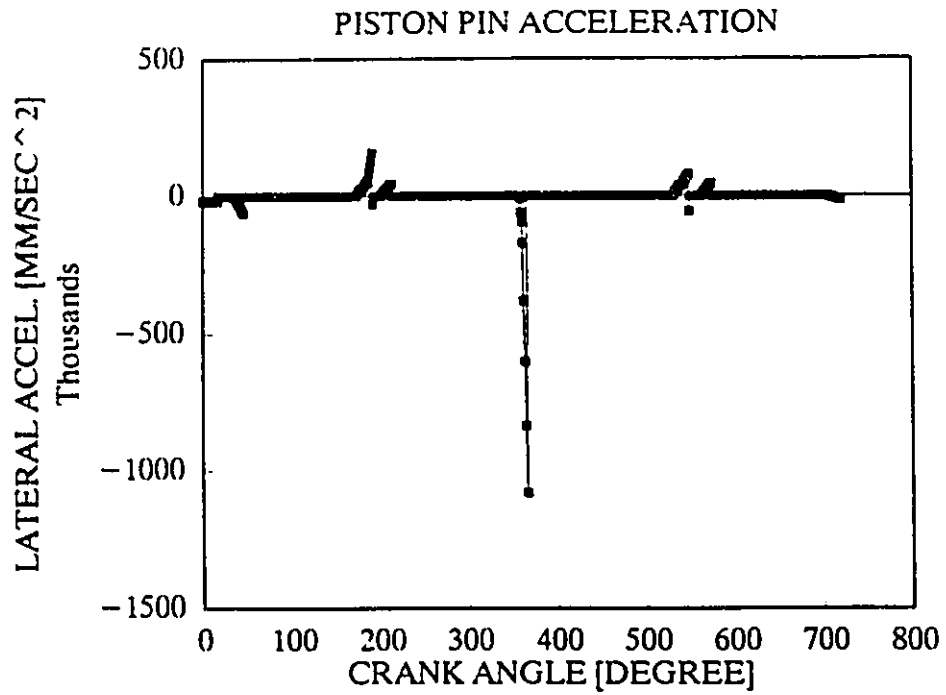
Figure 3.17 : Lateral Piston Pin Acceleration Versus Crank Angle.

PISTON PIN ACCELERATION
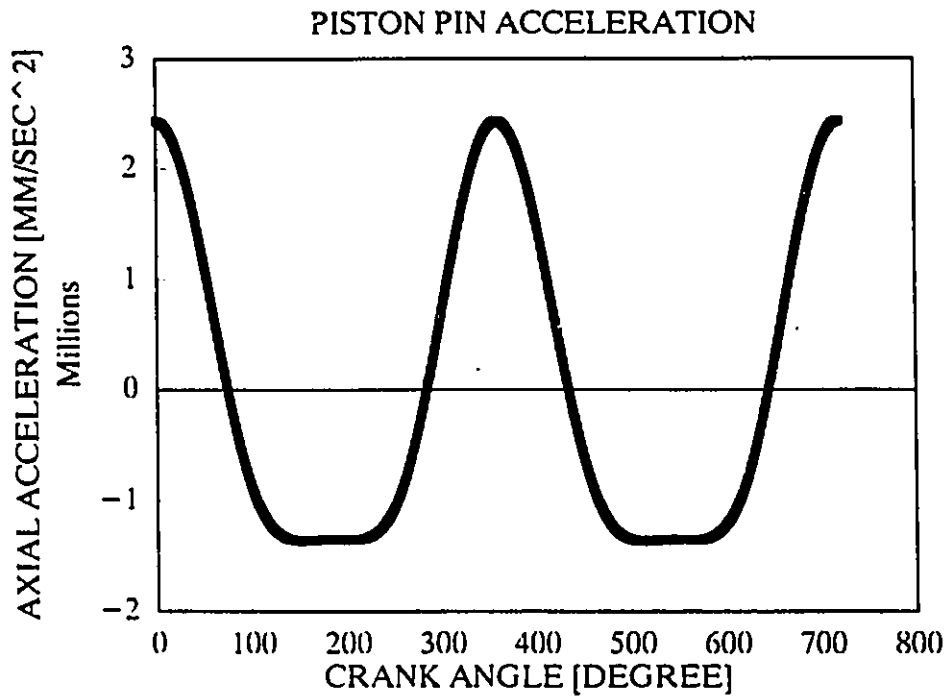
Figure 3.18 : Axial Piston Pin Acceleration Versus Crank Angle.
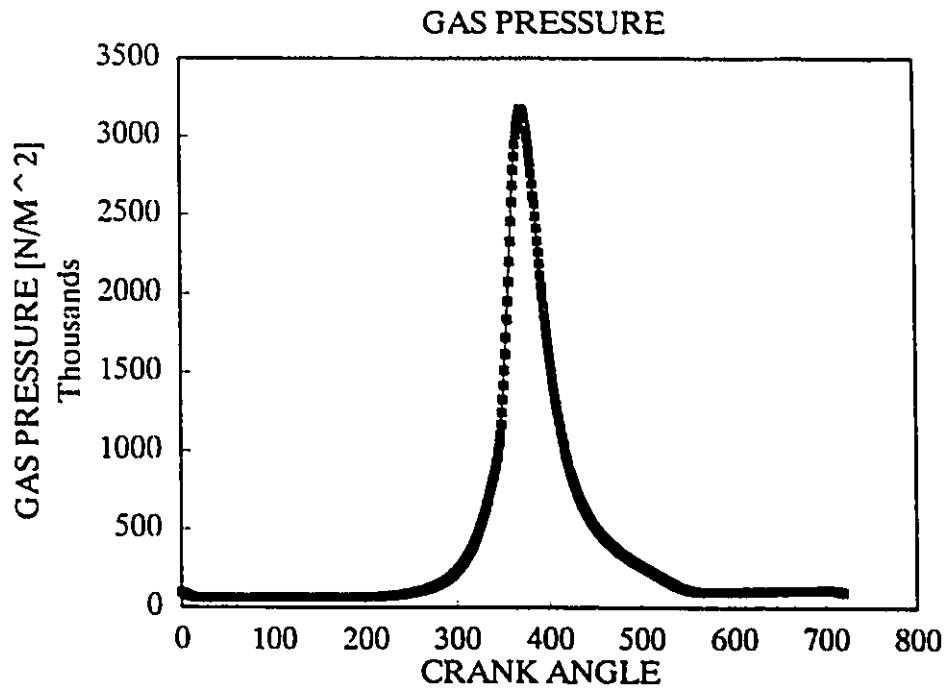
GAS PRESSURE

Figure 3.19 : Cylinder Gas Pressure Versus Crank Angle.
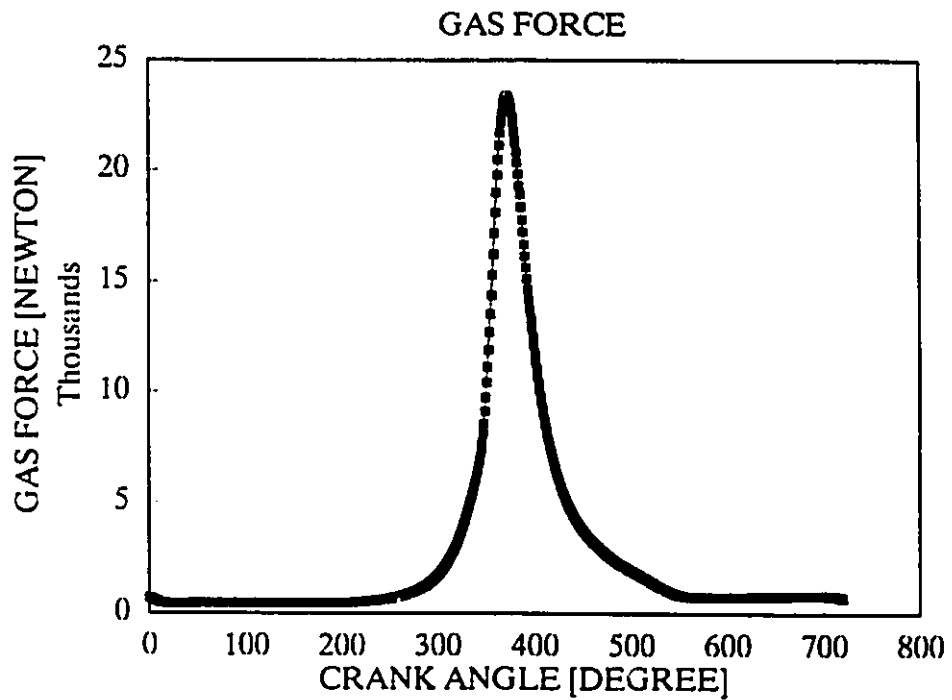
GAS FORCE

Figure 3.20 : Cylinder Gas Force Versus Crank Angle.
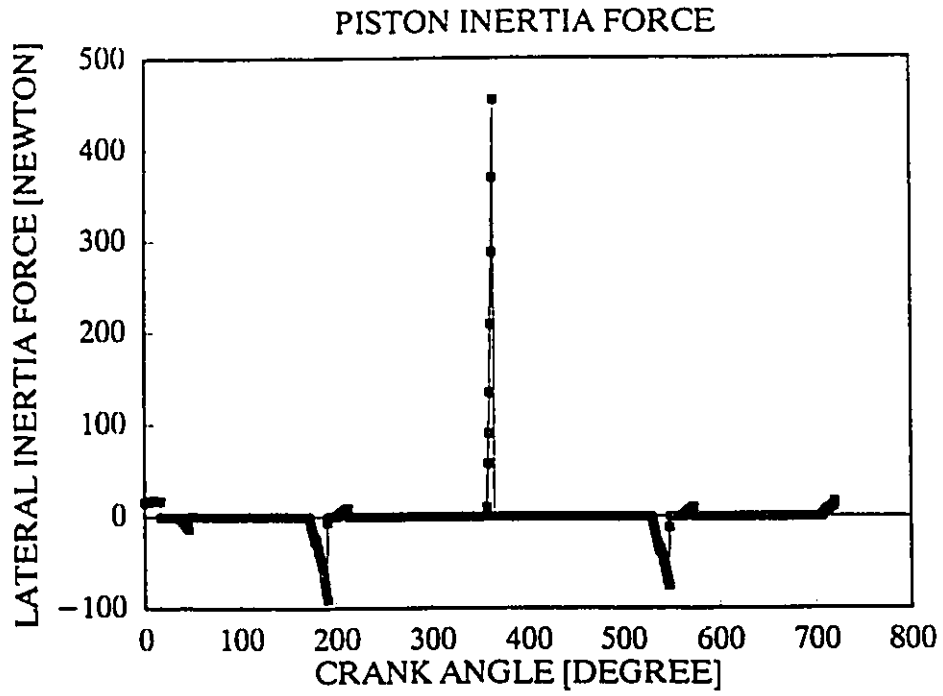
Figure 3.21 : Lateral Piston Inertia Forces Versus Crank Angle.
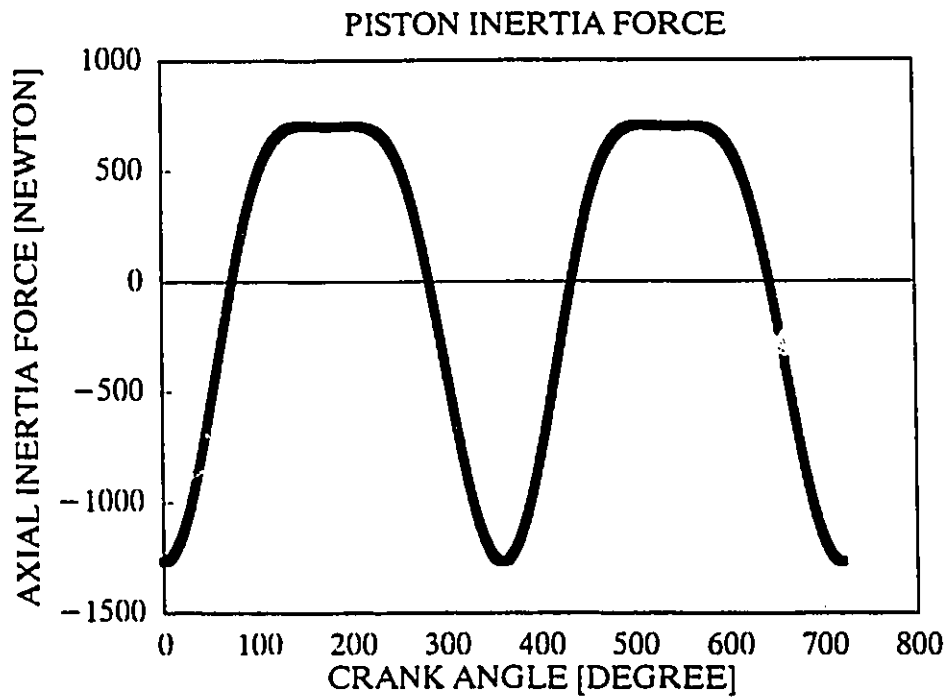
Figure 3.22 : Axial Piston Inertia Forces Versus Crank Angle.
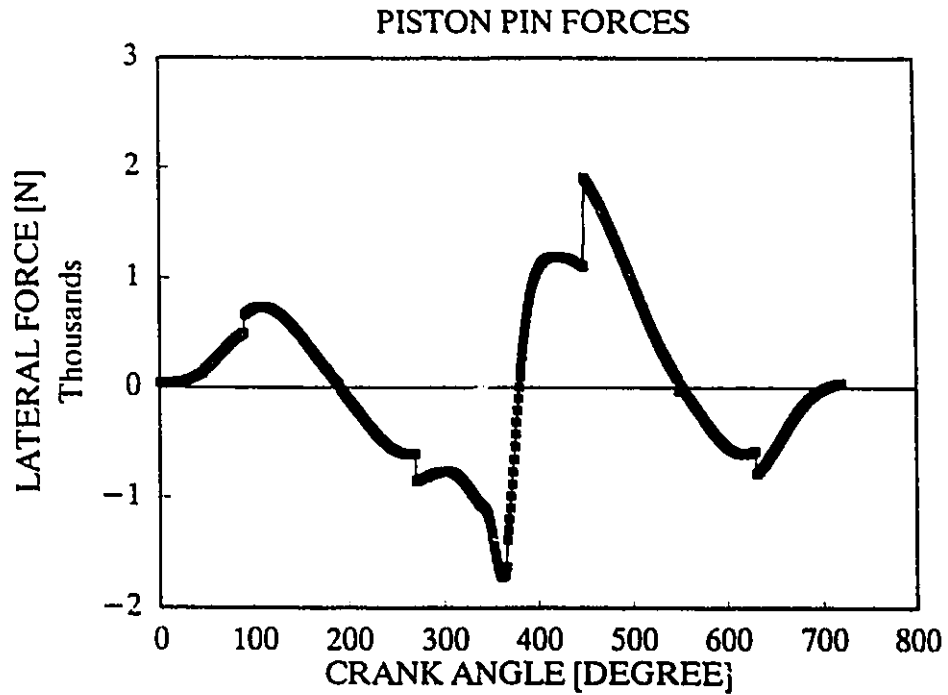
PISTON PIN FORCES

Figure 3.23 : Lateral Piston Pin Forces Versus Crank Angle.
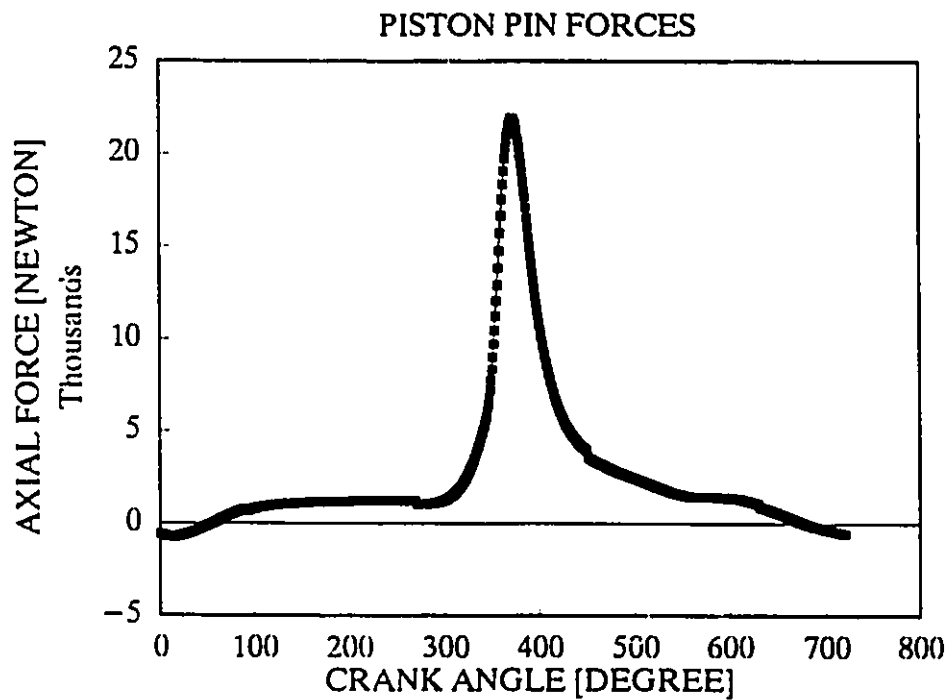
PISTON PIN FORCES

Figure 3.24 : Axial Piston Pin Forces Versus Crank Angle.

55

SKIRT CONTACT FORCE
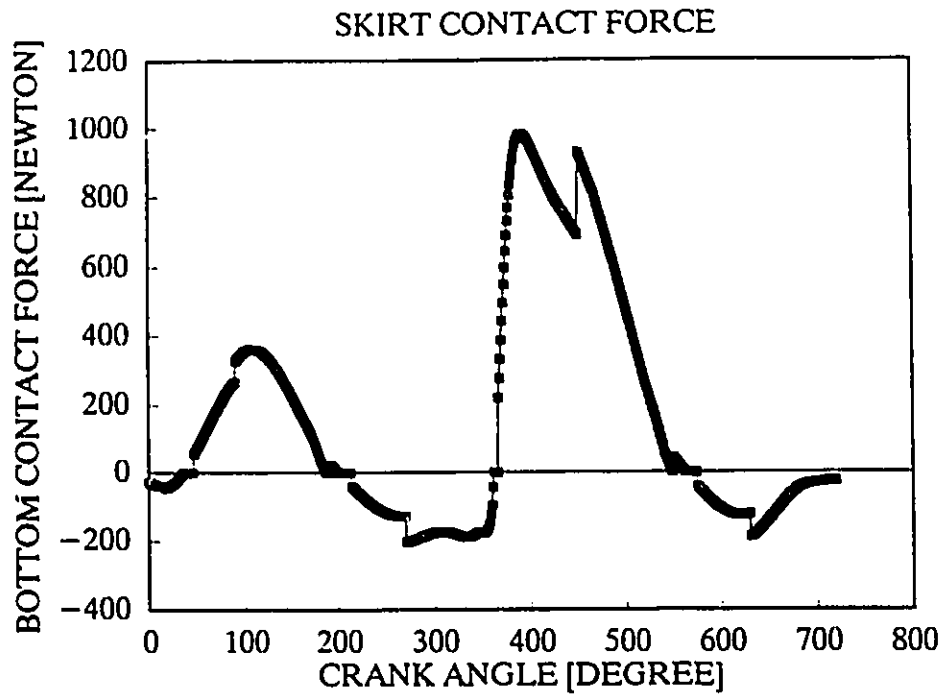
Figure 3.25 : Bottom Skirt Contact Forces Versus Crank Angle.

MOMENT ABOUT PISTON PIN
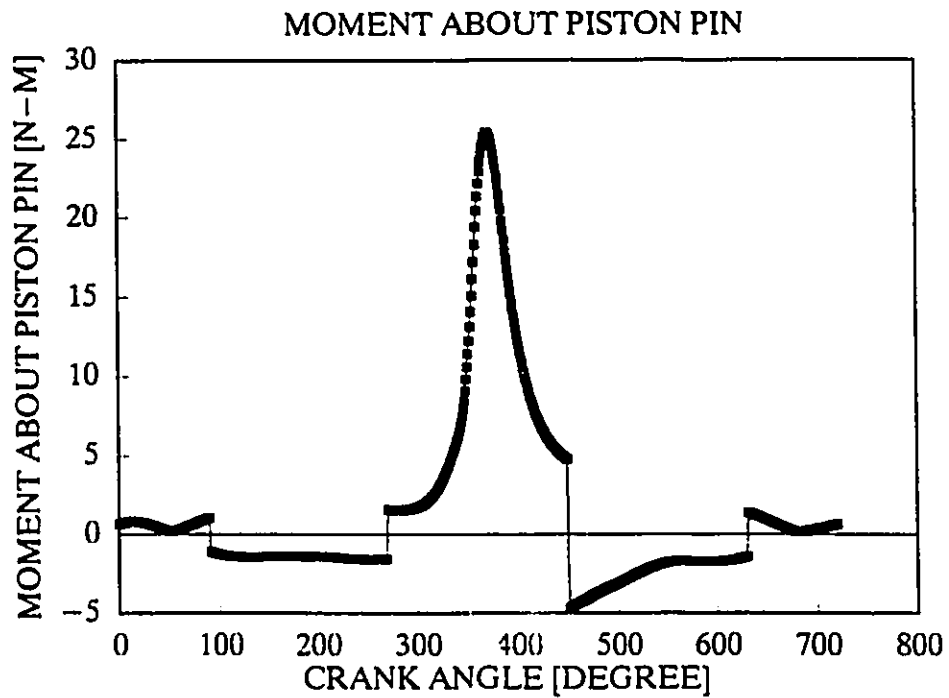
Figure 3.26 : Moment About Piston Pin Versus Crank Angle.

KINETIC ENERGY LOSS AT IMPACT	
CRANK ANGLE (Degrees)	ENERGY LOSS (Joules)
548	131E-06
576	21E-06
23	38E-06
43	25E-06
191	110E-06
194	20E-06
215	19E-06
366	181E-06
367	610E-06

TOTAL KINETIC ENERGY LOSS OVER CYCLE = 1E-03 Joules

Figure 3.27 : Kinetic energy loss during the piston impact on the cylinder.

3.2 Modal Analysis

Competition, government regulations, inflation and many other factors are putting pressure on the automotive industries to build products which weigh less, and operate more reliably with less noise and vibration than in the past. In order to effectively solve noise and vibration problems, engineers must have a good understanding of the dynamics of mechanical structures and of the influence of the proposed design modifications may have on the overall engine performance.

The primary objective of this section is to provide the detailed dynamic characteristics of the engine components.

It is important to know the modes of vibration of the structure as they provide the frequencies at which the structure can be executed into resonance and the predominant wave-like motion at the resonant frequencies. This information is useful for determining the optimized locations of sensors for automated engine data acquisition and diagnostic system.

Modal Analysis is a process of characterizing the dynamics of a structure in terms of vibration. It involves identifying the eigen-values and eigen-vectors of the equations of motion corresponding to the frequencies at which the structure is more likely to vibrate in a predominant, well identified, wave-like deformation. The amplitudes of this wave motion in the structure are specified by the corresponding eigen-vectors. (When the eigen-values are complex, they also describe the damping of the modes of vibration). Each mode of vibration, then, is defined by an eigen-value (resonant frequency and damping) and its corresponding eigen-vector (mode shape).

In this work, modal analysis is applied on engine components so as to obtain the global structural properties i.e. the modal mass, stiffness and damping. The following section gives a detailed description of the structural response of the engine assembly. This information is useful in optimizing the location of sensors in the design of automated engine data acquisition and diagnostic systems.

3.2.1 Modes of Vibration

Physically, modes of vibration are the so called "natural frequencies" at which the predominant motion of a structure occurs as a well defined waveform as shown in Figure 3.28. Mathematically, modes of vibration are defined by certain parameters of a linear dynamic model. As illustrated in Figure 3.29 each mode of vibration is defined by a resonant frequency, a damping factor and a mode shape. It should be noted that a structural dynamic model can be completely defined in terms of its modal parameters. Hence, the purpose of modal testing is to artificially excite a structure so that the frequencies, damping and mode shapes of its predominant modes of vibration can be identified.

3.2.2 Modal Testing Methods

In general, there are two fundamentally different methods of modal testing of structures: the normal mode and the transfer function methods. The normal mode method is the classical method of experimentally extracting modal parameters. This requires a large number of exciters "tuned" to excite the structure in a single desired mode of vibration. The forcing function is sinusoidal and only one mode is excited at a given time. This method however is difficult, time consuming and expensive to implement because of the following:

1) It is difficult to find the best location for the shakers on the structure without some prior knowledge of the modes of vibration

2) It is extremely difficult to excite closely coupled modes, one at a time

3) The structure must be completely instrumented with enough transducers and signal conditioning equipment so that the mode shape for all desired degrees of freedom can be measured at once.

Modes of Vibration (Mathematical):
Parameters of a Linear Dynamic Model

Modes of Vibration (Physical):
"Natural" Frequencies at which a Structure's
Predominant Motion is a Well Defined Waveform
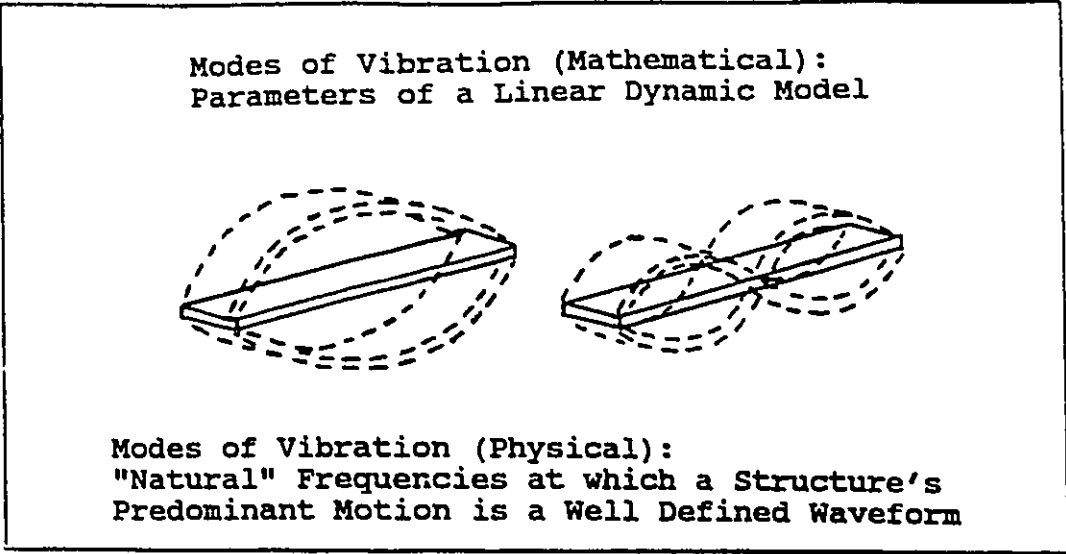
Figure 3.28 : Modes of Vibration [1]

Mode 1   Mode 2

Each Mode is defined by : a) Resonant Frequency
                           b) Damping Factor and
                           c) Mode Shape
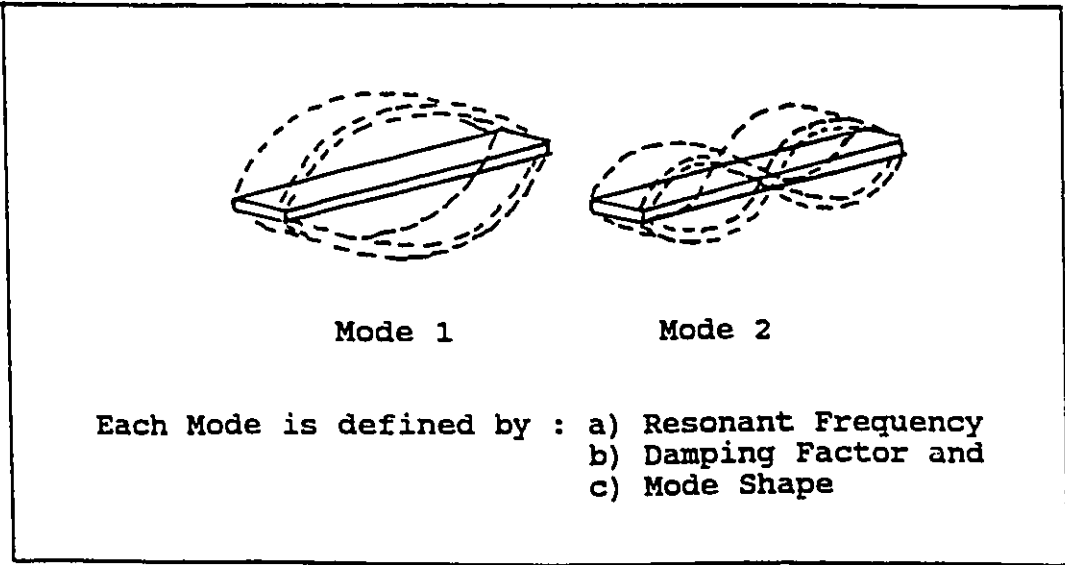
Figure 3.29 : Modes of Vibration Definition [1]

---

1 Adapted from Structural Analysis Seminar Notes by Ken Ramsey
and Mark Richardson of Structural Measurement Systems

60

However, the normal mode method is suitable for use to analyze large structures where large energy input is required. It also has good signal to noise characteristics.

The Transfer Function method is rapidly gaining wide recognition mainly due to the recent developments in computer hardware. This method is based on the use of digital signal processing techniques and the Fast Fourier Transform algorithm to measure frequency response functions between various points on the structures. Modal parameters (natural frequencies, damping and characteristic mode shapes) are identified by performing further computations (curve fitting) on the above frequency response functions.

The major differences between the Normal Mode Method and the Transfer Function Method are summarized in Figure 3.30.

The Transfer Function Method was selected for use in the investigation of modal characteristics of engine components.

MODAL TESTING METHODS

NORMAL MODE METHOD	TRANSFER FUNCTION METHOD
Multi-Shaker	Single Point Excitation
Sinusoidal	Broadband
One Mode at a Time	Many Modes at a Time
Analog Instrumentation	FFT-Based Digital Instrumentation

Figure 3.30 : Modal Testing Methods.

3.2.3 Theoretical Modal Models

In order to gain insight into the dynamics of engine structures, it is necessary to provide basic knowledge of structure modelling. Modal Analysis is based on three fundamental assumptions concerning the nature of the structure. These are:

   i) The structure is linear. This means that the response of the structure to a combination of forces, simultaneously applied, is the sum of the individual responses to each of the forces acting alone.

   ii) The structure is time invariant

   iii) The analytical equations used to describe the structure must use parameters that are measurable. It means that the input-output measurements contain enough information to generate an adequate behavioural model.

Consider the Single Degree of Freedom System (SDOF) shown in Figure 3.31 consisting of spring, mass and damper.
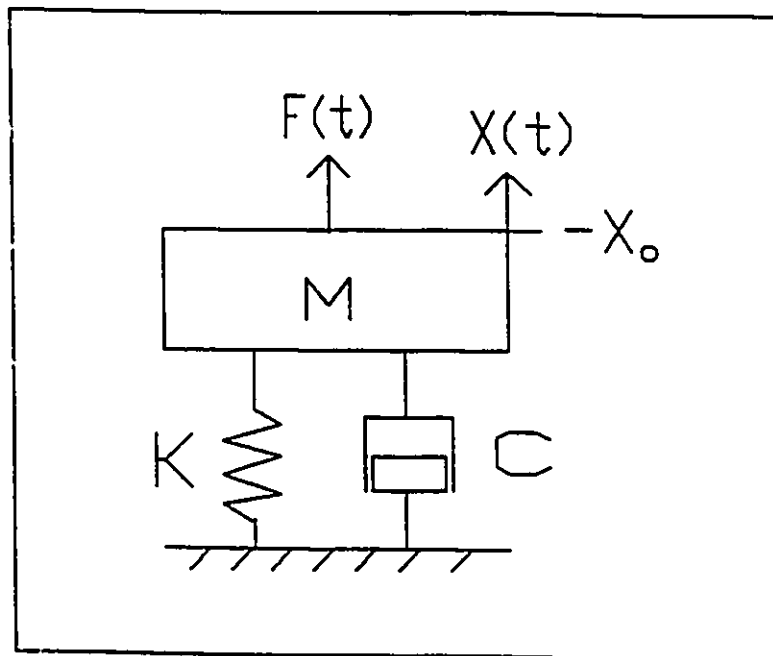
Figure 3.31 : A Single Degree of Freedom Model

The equation of motion for the system is:

$$\sum F = ma \tag{3.84}$$

$$M\ddot{x} + C\dot{x} + kx = F \tag{3.85}$$

Taking the Laplace transform of Equation (3.85)

$$(Ms^2 + Cs + k)X(s) = F(s) \tag{3.86}$$

Let

$$B(s) = Ms^2 + Cs + k \tag{3.87}$$

Then, Equation (3.86) becomes,

$$B(s)X(s) = F(s) \tag{3.88}$$

or

$$X(s) = \frac{F(s)}{B(s)} \tag{3.89}$$

A transfer function H(s) can be defined as

$$H(s) = \frac{1}{B(s)} \tag{3.90}$$

By combining (3.89) and (3.90)

$$X(s) = H(s)F(s) \tag{3.91}$$

Substituting Equation (3.87) into Equation (3.91),

$$H(s) = \frac{X(s)}{F(s)} = \frac{1}{Ms^2 + Cs + k} \qquad (3.92)$$

$$\therefore \quad H(s) = \frac{\frac{1}{M}}{s^2 + \frac{C}{M}s + \frac{k}{M}} \qquad (3.93)$$

where
$$s^2 + \frac{C}{M}s + \frac{k}{M} = 0 \qquad (3.94)$$

is the "characteristic equation".

The roots of the characteristic equation can be found by using the quadratic formula

$$s_{1,2} = \frac{-\frac{C}{M} \pm \sqrt{\left(\frac{C}{M}\right)^2 - 4\left(\frac{k}{M}\right)}}{2} \qquad (3.95)$$

$$s_{1,2} = -\frac{C}{2M} \pm \frac{1}{2}\sqrt{\left(\frac{C}{M}\right)^2 - 4\left(\frac{k}{M}\right)} \qquad (3.96)$$

or
$$s_{1,2} = -\frac{C}{2M} \pm \sqrt{\left(\frac{C}{2M}\right)^2 - \left(\frac{k}{M}\right)} \qquad (3.97)$$

When $\left(\frac{C}{2M}\right)^2 - \frac{k}{M}$ is greater than zero, the system is said to be overdamped. When it is less than zero, underdamped. When exactly equal to zero, the system is said to be critically damped.

Underdamped systems are oscillatory in nature and best represent the majority of structural systems.

Critical damping

$$\left(\frac{C}{2M} \right)^2 = \frac{k}{M} \qquad (3.98)$$

$$C_c = 2M \sqrt{\frac{k}{M}} \qquad (3.99)$$

underdamped natural frequency ω_n

$$\omega_n = \sqrt{\frac{k}{M}} \qquad (3.100)$$

$$\therefore \quad C_c = 2M\omega_n \qquad (3.101)$$

Define the Damping ratio, z, as

$$z = \frac{C}{C_c} \qquad (3.102)$$

and the Loss factor as $\qquad \eta = 2z \qquad (3.103)$

From Equations (3.97), (3.102) and (3.103)

$$s_{1,2} = -\frac{C}{2M} \pm \sqrt{\left(\frac{C}{2M} \right)^2 - \frac{k}{M}}$$

$$= -\frac{zC_c}{2M} \pm \sqrt{\left(\frac{zC_c}{2M} \right)^2 - \omega_n^2}$$

$$= -z\omega_n \pm \sqrt{z^2\omega_n^2 - \omega_n^2}$$

$$\therefore \quad s_{1,2} = \left(-z \pm \sqrt{(z^2-1)} \right)\omega_n \qquad (3.104)$$

The damping factor σ is defined as the real part of each root i.e.

$$\sigma = z\omega_n \qquad\qquad (3.105)$$

Damped natural frequency ω_d is defined as the imaginary part of each root

$$\omega_d = \omega_n\sqrt{1 - z^2} \qquad\qquad (3.106)$$

When the value of the radical in Equation (3.97) is negative, the roots of the system characteristic equation will be complex. A graphical presentation of the roots of the characteristic equation is conveniently accomplished by the use of a Laplace-plane or, simply, s-plane.

Figure 3.32 illustrates the mapping of s_1 and s_2 onto the s-plane.

Thus the simplified equation for the roots of the characteristic equation is

$$s_{1,2} = -\sigma \pm j\omega_d \qquad\qquad (3.107)$$

The roots of an underdamped system will be conjugate pairs as the imaginary part of each root is the only parameter that changes

Let

$$p = \sigma + j\omega_d \qquad\qquad (3.108)$$

$$p^* = \sigma - j\omega_d \qquad\qquad (3.109)$$

where * denotes conjugation.

The system transfer function can now be written as
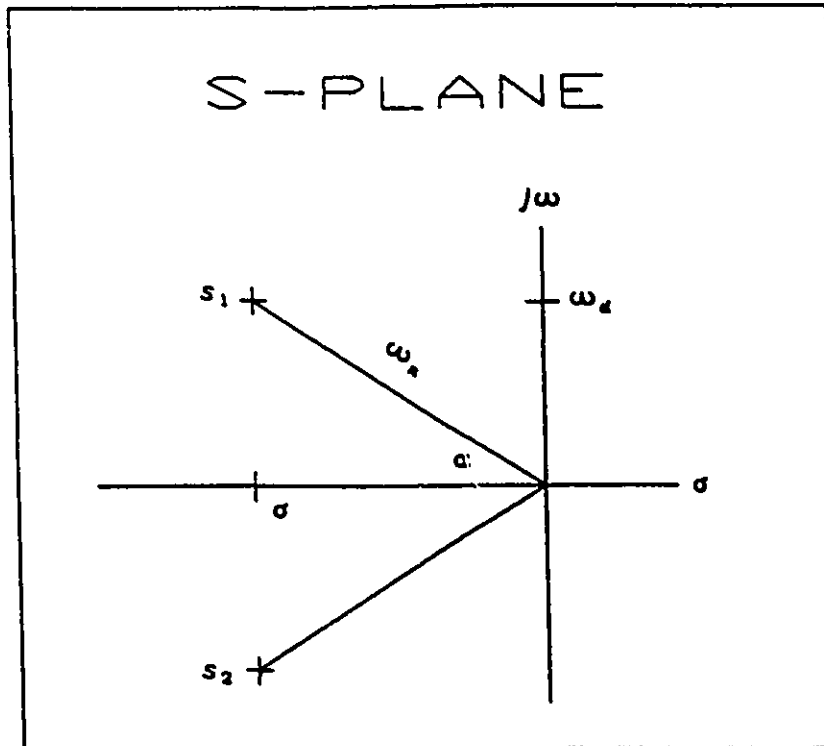
Figure 3.32 : The mapping of S_1 and S_2 onto the S-Plane
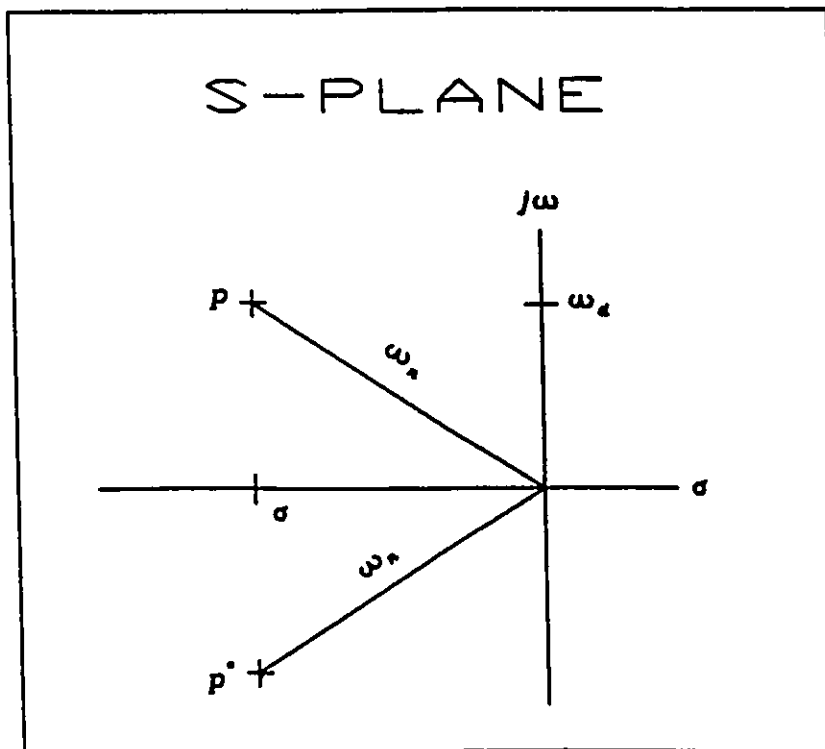
Figure 3.33 : The S-Plane Mapping

$$H(s) = \frac{\frac{1}{M}}{(s-p)(s-p^*)} \qquad (3.110)$$

The s-plane mapping of Equation (3.110) is shown in Figure 3.33.

Hence, the fundamental definitions and relationships for an SDOF system have been established. These properties must now be linked to physically measurable parameters to make them useful for measurement applications.

Performing partial fraction on (3.110)

$$H(s) = \frac{c_1}{(s-p)} + \frac{c_2}{(s-p^*)} \qquad (3.111)$$

and evaluating at s=p

$$c_1 = \frac{\frac{1}{M}}{2j\omega_d} \qquad (3.112)$$

Evaluating at $s = p^*$ gives

$$c_2 = -\frac{\frac{1}{M}}{2j\omega_d} \qquad (3.113)$$

The constant c_1 and c_2 are conjugates of one another.

Let

$$A = C_1 = \frac{\frac{1}{M}}{2j\omega_d}$$ (3.114)

$$A^* = C_2 = -\frac{\frac{1}{M}}{2j\omega_d}$$ (3.115)

Thus Equation (3.111) can be written as

$$H(s) = \frac{A}{(s-p)} + \frac{A^*}{(s-p^*)}$$ (3.116)

In order to construct a standard form of transfer function, we define a slightly different version of the complex amplitude which is called the complex residue

$$R = 2jA \quad \text{and} \quad R^* = -2jA$$ (3.117)

or

$$R = \frac{\frac{1}{M}}{\omega_d} \quad \text{and} \quad R^* = -\frac{\frac{1}{M}}{\omega_d}$$ (3.118)

Thus the standard form of the single degree of freedom transfer function now becomes

$$H(s) = \frac{R}{2j(s-p)} - \frac{R^*}{2j(s-p^*)}$$ (3.119)

So far Laplace transform does not lend itself for hardware implementation because it is a three dimensional domain: Frequency, Damping and Amplitude.

Structural analysis makes use of the fact that Fourier analysis, with its many types of hardware implementation, can be used to extract the frequency and amplitude data.

Damping can then be extracted by a variety of curve fitting techniques.

The system frequency response is defined as the system transfer function evaluated along the $j\omega$ -axis. This is the same as putting the system damping to zero. $\qquad (\sigma = 0)$

$$H(j\omega) = H(s)\,|_{s=j\omega} = \frac{R}{2j(j\omega - p)} - \frac{R^{*}}{2j(j\omega - p^{*})} \quad (3.120)$$

or

$$H(j\omega) = \frac{1}{2}\left[\frac{R}{(\omega_d - \omega) + j\sigma} - \frac{R^{*}}{(-\omega_d - \omega) + j\sigma}\right] \quad (3.121)$$

This expression can now be used directly for measurement with modern dynamic signal analyzers. In addition, the Inverse Fourier Transform of the system frequency response function (i.e. Equation 3.121) is the impulse response of the system assuming all initial conditions are set to zero.

In practice, there are very few systems that can be accurately modelled by a single degree of freedom system. For the case of an n-degree of freedom system, it can be shown that the system transfer function can be expressed as

$$H(s) = \sum_{k=1}^{n}\left[\frac{R_k}{2j(s - p_k)} - \frac{R_k^{*}}{2j(s - p_k^{*})}\right] \quad (3.122)$$

The next step is to link the equations of motion of the theoretical model to real structures. The mode shape (or eigen vector) of a system is defined as a vector which represents the motion of a given structure when excited at resonance (natural mode of vibration). The vector consists of a series of complex displacements which describe the amplitude and direction of deflections at each point on the given structure. In fact, these

70

are the system residues. By taking advantage of the symmetry inherent in the residue matrix ($h_{ij} = h_{ji}$ known as reciprocity), one can form an expression for a mode shape vector $\{U_k\}$

$$[R]_k = Q_k \{U_k\} \{U_k\}^T \qquad (3.123)$$

where

Q_k = Arbitrary scaling constant

$k = k^{th}$ mode of the system

T = transpose of the vector

Obviously the mode shape vectors have different magnitudes for a given residue matrix depending on the value of Q_k. The scale factor Q_k is generally shown as one of several standard scaling methods such as the Unit Scale Factor   (Q_k), Modal Mass = 1 and $Q_k = \frac{1}{\omega}$, etc.

Generally, it is unusual to make measurements on an SDOF system. Thus it is necessary to handle a situation where an arbitrary number of points and directions on a structure is selected for study and only a limited number of modes are of concern. Thus Equation (3.122) may be rewritten as

$$h_{rc}(s) = \sum_{k=1}^{n} \left[\frac{R_{rc}(k)}{2j(s - p_k)} - \frac{R_{rc}(k)^*}{2j(s - p_k^*)} \right] \qquad (3.124)$$

where

r = row of transfer matrix H(s)

c = column of transfer matrix H(s)

n = total of modes to be studied

k = current mode number

p_k = pole location for the kth mode = $\sigma_k + j\omega_k$

R_{rc} = residue of $h_{rc}(s)$ for the kth mode.

Note that each term in the summation expression of Equation (3.124) is an $n \times n$ matrix which represents the contribution of each mode, k, to the transfer matrix.

For each identified shape vector, a hypothetical SDOF system can be constructed using the derived modal parameters such as the modal mass, modal stiffness and modal damping. These are related to the pole locations as follows:

$$M_k = \frac{1}{Q_k \omega_k} \tag{3.125}$$

$$K_k = (\sigma_k^2 + \omega_k^2)M_k \tag{3.126}$$

and

$$C_k = 2\sigma_k M_k \tag{3.127}$$

3.2.4 Modal Parameter Extraction Techniques

So far the discussion has focussed on how modal parameters can be combined to determine the spatial deflection of structures. However, it is useful to address how these parameters are obtained from vibration measurements on the structure. An estimate of the natural frequencies of specific modes can be made simply by determining the frequency peaks in the frequency response function. This concept works very well for simple systems that have few modes, light damping, wide separation of modes, and minimal measurement noise.

The damping ratio can be obtained by finding the upper and lower frequencies

(ω_u, ω_l) on either side of the damped natural frequency which display amplitudes of 3 dB below the peak of the frequency response magnitude. Thus the expression:

$$\zeta = \frac{1}{2}\left(\frac{\omega_u - \omega_l}{\omega_d}\right)$$

(3.128)

can be used to obtain the damping ratio.

The residue can now be determined by using the following approach.

From Equation (3.121)

$$H(j\omega) = \frac{1}{2}\left[\frac{R}{(\omega_d - \omega) + j\sigma} - \frac{R^*}{(\omega_d - \omega) + j\sigma}\right]$$

At resonant $\omega = \omega_d$, $H(j\omega)$ becomes

$$H(j\omega_d) = \frac{1}{2}\left(\frac{R}{j\sigma} - \frac{R^*}{-2\omega_d + j\sigma}\right)$$

(3.129)

A convenient approximation can be made for $H(j\omega)$ in cases where the damped natural frequency is much larger than the damping factor, i.e.,

$$H(j\omega_d) \approx \frac{1}{2}\left[\frac{R}{j\sigma}\right]$$

(3.130)

This equation is valid for lightly damped structures which exhibit damped natural frequencies that are much greater than their associated damping factors.

In Equation (3.130), $H(j\omega_d)$ is purely imaginary, thus:

$$\text{IMAG}\{H(j\omega_d)\} \approx \frac{R}{2\sigma} \qquad (3.131)$$

$$\text{REAL}\{H(j\omega_d)\} \approx 0 \qquad (3.132)$$

Rearranging Equation (3.131)

$$R = 2\sigma \; \text{IMAG}\{H(j\omega_d)\} \qquad (3.133)$$

Recalling that

$$\sigma = z\omega_n$$

and, when $z \ll 1$,

$$\omega_n \approx \omega_d$$

Hence

$$\sigma \approx z\omega_d \qquad (3.134)$$

It is important to note that Equation (3.128) permits z to be determined and Equation (3.134) can be used to find σ. The residue (and ultimately the mode shape) can be obtained from Equation (3.133) because the value of the imaginary part of the frequency response function at ω_d can easily be determined from the Fourier analyzer.

The technique mentioned above is called quadrature peak picking. It is applicable to frequency response functions that are noise free, with light damping, and have enough data points to enable accurately estimate:

a) the damped natural frequency,

b) the 3 dB down points and

74

c) the magnitude of the imaginary part of the frequency response function. In addition, the modes must be widely spaced otherwise the skirt of any one mode can cause large errors in the parameter estimation.

3.2.5 Frequency Response Functions

There are six different forms transfer functions for mechanical system as shown in Figure 3.34. In general, all these transfer functions contain the same information. The decision to use one or a combination of these transfer functions depends on the capability of the equipment, the frequency range of interest, the types of transducers etc.. In this study, accelerometers, force transducers and a dynamic signal analyzer were used to obtain the "Accelerance" transfer functions.

$\dfrac{\text{DISPLACEMENT}}{\text{FORCE}}$ = DYNAMIC COMPLIANCE	$\dfrac{\text{FORCE}}{\text{DISPLACEMENT}}$ = DYNAMIC STIFFNESS
$\dfrac{\text{VELOCITY}}{\text{FORCE}}$ = MOBILITY	$\dfrac{\text{FORCE}}{\text{VELOCITY}}$ = MECHANICAL IMPEDANCE
$\dfrac{\text{ACCELERATION}}{\text{FORCE}}$ = ACCELERANCE	$\dfrac{\text{FORCE}}{\text{ACCELERATION}}$ = DYNAMIC MASS

Figure 3.34 : Summary of the Different Forms of Transfer Functions for Mechanical Systems.

3.3 Sound Intensity

The sound intensity vector, $\vec{I}$, is the net rate of flow of energy per unit area at a given position. Thus the acoustic power, W, passing through a surface, S, is defined as:

$$W = \int_s \vec{I} \, d\vec{S}$$

(3.135)

75

The usefulness of the sound intensity concept is primarily due to this fundamental relationship. In a medium without flow (i.e. without bulk movement of the medium), the time averaged intensity vector, $\vec{I}$, is equal to the product of the instantaneous pressure, p, and the instantaneous particle velocity $\vec{v}$, at the same point, i.e.,

$$\vec{I} = \overline{p\vec{v}} \qquad (3.136)$$

where the long horizontal bar denotes a time average. Hence the intensity vector in a given direction r is estimated to be,

$$\vec{I}_r = \overline{p\vec{v}_r} \qquad (3.137)$$

p is the sound pressure at the measuring position

v_r is the particle velocity at the measuring position in the direction r

3.3.1 Finite Difference Approximation

The particle velocity, $\vec{v}_r$, in a particular direction r, can be closely approximated by integrating over time the difference in sound pressure at two points, A and B, separated by a distance Δr. Mathematically:

$$\vec{v}_r = -\frac{1}{\rho_o} \int \frac{(p_B - p_A)}{\Delta r} dt \qquad (3.138)$$

where ρ_o is the density of the air, and $p_B - p_A$ is the pressure difference. In practical applications, the Bruel and Kjaer sound intensity system may be used to measure p_A and p_B.

The signals are frequency analyzed in parallel in real time and the sum and difference of the two signals for each frequency band are calculated, $p_B + p_A$ and $p_B - p_A$. The difference is integrated over time and divided by the distance between the two microphones of the probe to yield the particle velocity $\vec{v}_r$. The sum divided by two, (i.e. the sound pressure mid-way between the microphones), is then multiplied by the particle velocity to yield the sound intensity vector component, I_r, according to Equation (3.137).

It should be noted that the magnitude of the measured intensity component depends on the orientation of the probe; a maximum is measured when the probe's axis of symmetry is pointed towards the sound source and a minimum is measured when the probe is perpendicular to the line joining the probe to the source.

Intensity measurements are extremely susceptible to phase differences in the two channels of the measuring instrument. This phase mismatch comprises of:

1) the phase mismatch between the two microphones.

2) the phase mismatch between the two channels of the analyzer.

The phase mismatch is worst at low frequency for a given distance between the acoustical centers of the two microphones Δr. Hence phase mismatch limits the lowest usable frequency for a given Δr, i.e., large Δr is to be preferred at low frequency while small Δr is best at high frequency.

CHAPTER 4.

EXPERIMENTAL DETAILS

In this study, a number of V-6 engines were tested in two distinct ways i.e. externally driven (Cold Test) and Hot Test or Dynamometer Test. Vibration signals were captured and analyzed. They served as a primary parameter for monitoring the engine conditions. The engine noise and cylinder pressure were also monitored. However they served as secondary parameters. A number of experiments were performed, each of different nature and function. These were:

1. Modal analysis of the engine

2. Cold test of engines

3. Hot test of engines

4. Dimensional measurements.

The following sections will describe the experimental measurement procedures and the associated equipment used.

4.1 Modal Analysis of Engine

The vibration mode analysis of an automotive internal combustion engine block was performed in order to achieve two main objectives;

1) to study the dynamic response of the engine block and its components; and

2) to determine the proper mounting location for the vibration transducers used in the cold test diagnostic system.

Figure 4.2 shows the schematic of the modal analysis system and the equipment used in this experiment is shown in Figure 4.1.

Experiment Tasks	Equipment
Dimensional measurements of engine components	LK Micro Four Coordinate Measuring Machine
FFT Analysis	B&K 2032 Signal Analyzer
Impact Testing	PCB Model 086B05 Modally Tuned Impact Hammer
Sensor	PCB 303A02 Accelerometer
Modal Analysis	SMS Version 6.01 Structural Measurement System
Signal Analysis	Hewlett Packard HP 9000 - Model 320 with Motorola 68020 Processor

Figure 4.1 : Experimental Apparatus for Modal Analysis

In this experiment, the modal analysis of an engine block was carried out by the impulse-frequency response technique which measured the response of an impulsive force applied to the engine block as schematically illustrated in Figure 4.2.

The signals from the accelerometer and load cell on the hammer were passed through anti-aliasing filters before analog to digital conversion. The amplitude and phase angle at each point on the engine block (at natural frequency) can be evaluated by modal analysis software, SMS structural measurement systems. The major steps in the modal analysis for a given engine are:

1. The impact point and the number and location of response sites are selected.

2. The geometry of the measurement points is defined and serial numbers are marked on the engine block.

3. Dimensional measurements are carried out and recorded in a written log.

4. Frequency responses are captured through the B&K 2032 FFT analyzer and transferred to the HP 9000 computer.

5. Curve fitting of the data governing frequency, damping and residues is performed.

6. Mode shapes are evaluated and plotted. These are displayed in animated forms.

79
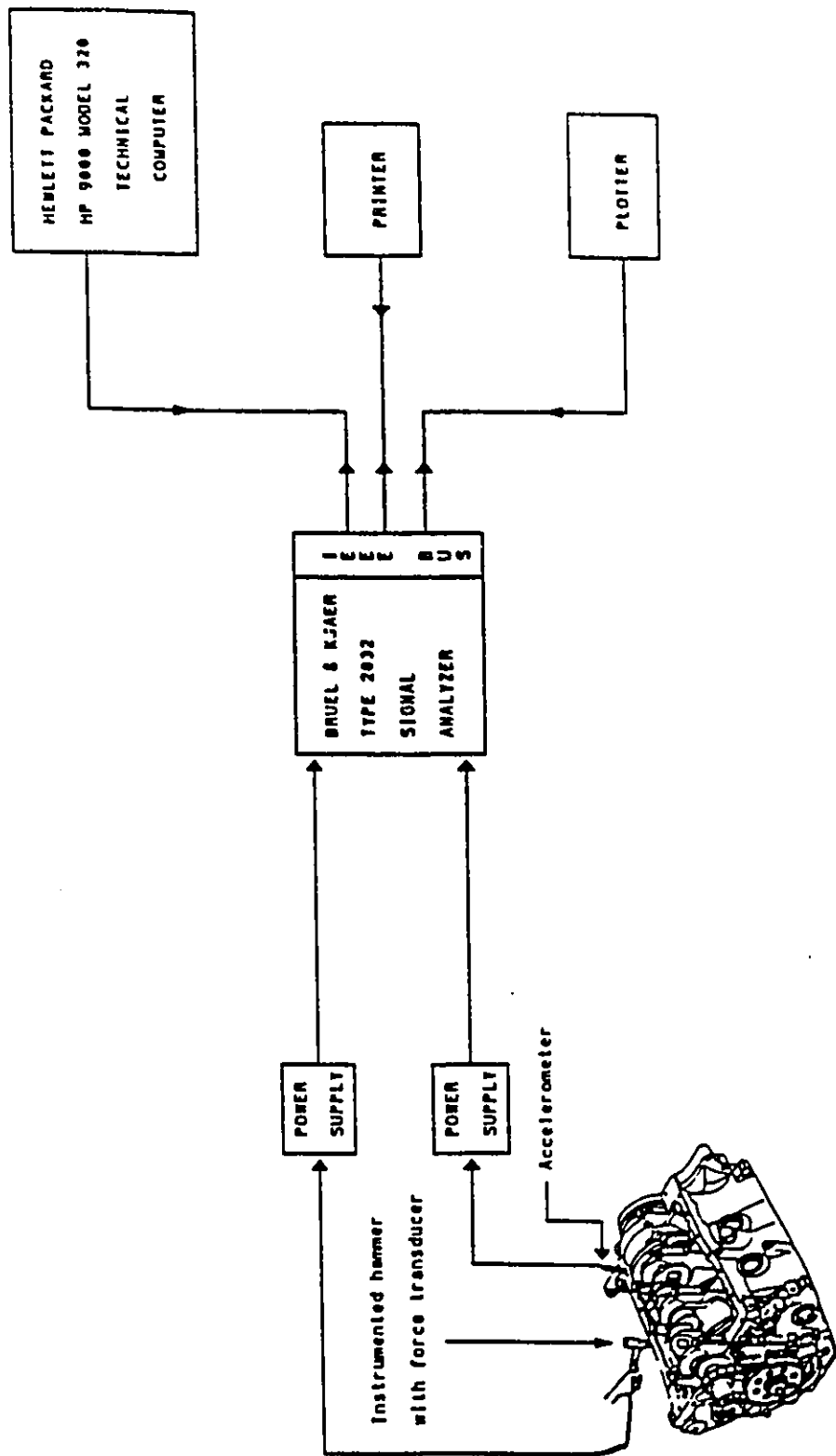
Figure 4.2 : Layout of Modal Analysis System

4.2 Cold Test of Engine

One of the conventional methods to detect a missing connecting rod bearing, in a so called "B" test (also known as cold test), is the measurement of the deck height of the piston at the location of TDC from the cylinder block deck. Decisions of pass, fail or repair will be based on the results of these tests. However, the deck-height measurement method is required to be improved due to its inconsistency in results and durability of gage. As an attempt to replace this dimensional gaging by a more reliable method, vibration and noise measurements were assessed. The following experiments were carried out as part of this effort.

4.2.1 Sound and Vibration Measurements

The vibration of the engines, both normal and defective, was monitored when the engine was driven at the speeds of 250 RPM and 420 RPM by an electric motor. To measure vibration, two PCB 308M86 transducers were mounted on the pan rail of the engine and the output was captured with the use of the Nicolet 440 Waveform Analyzer and PEC68K Data Acquisition System. The locations of the accelerometers were carefully selected from the results of a modal analysis of the engine block. The location of the microphone was determined by trial and error as shown in Figure 4.3.

More details of the data acquisition and processing equipment are discussed in the following section. The full schematic of the B-Test stand hardware is illustrated in Figure 4.4.

The Nicolet 440 Waveform Analyzer was used in conjunction with the built-in PEC68K Data Acquisition System. It has an ability to store 260K data points per sweep in its random access memory (RAM) which can then be analyzed on the oscilloscope or saved on a Bernoulli hard disk. Every sweep of the Waveform Analyzer was triggered at the same crank angle by utilizing a position sensor. The feature of the autocycle function of

Microphone

Spring

Accelerometer No. 1
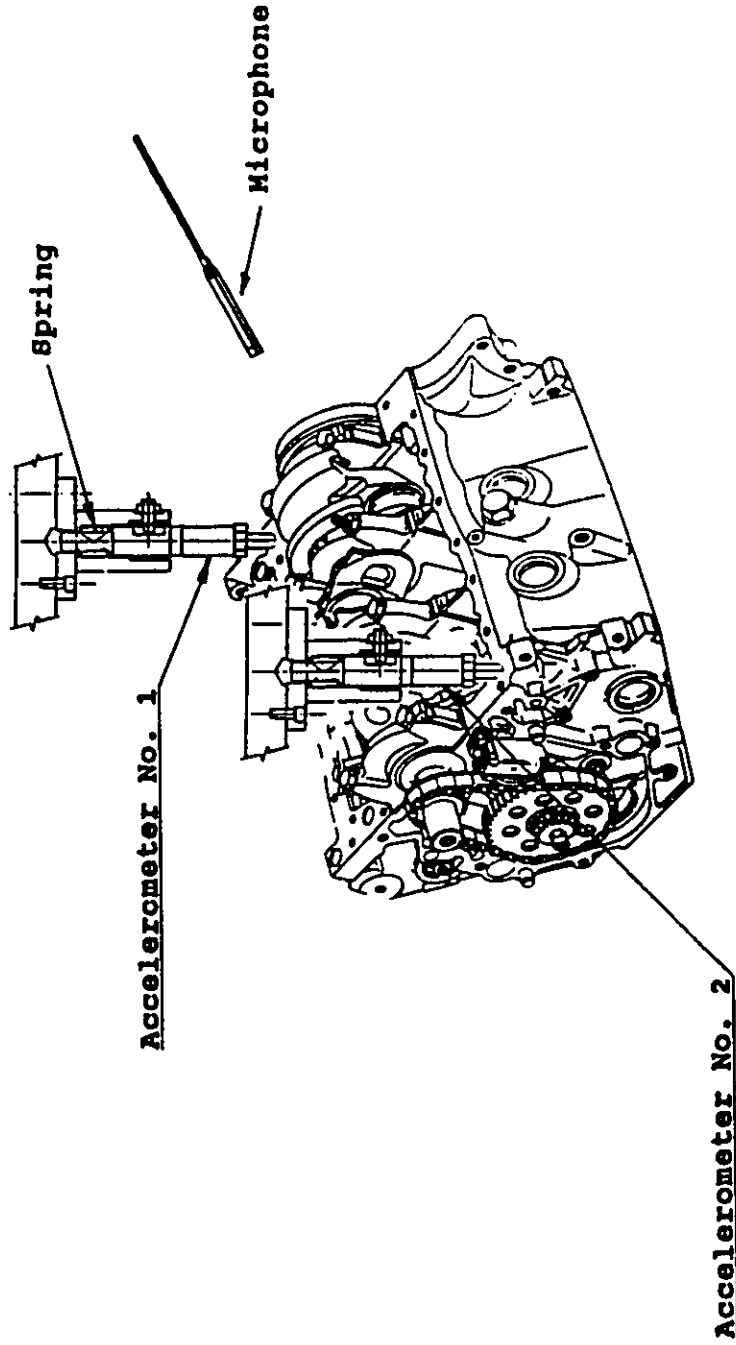
Accelerometer No. 2

Figure 4.3 : B-test stand showing locations of accelerometers and Microphone.

82
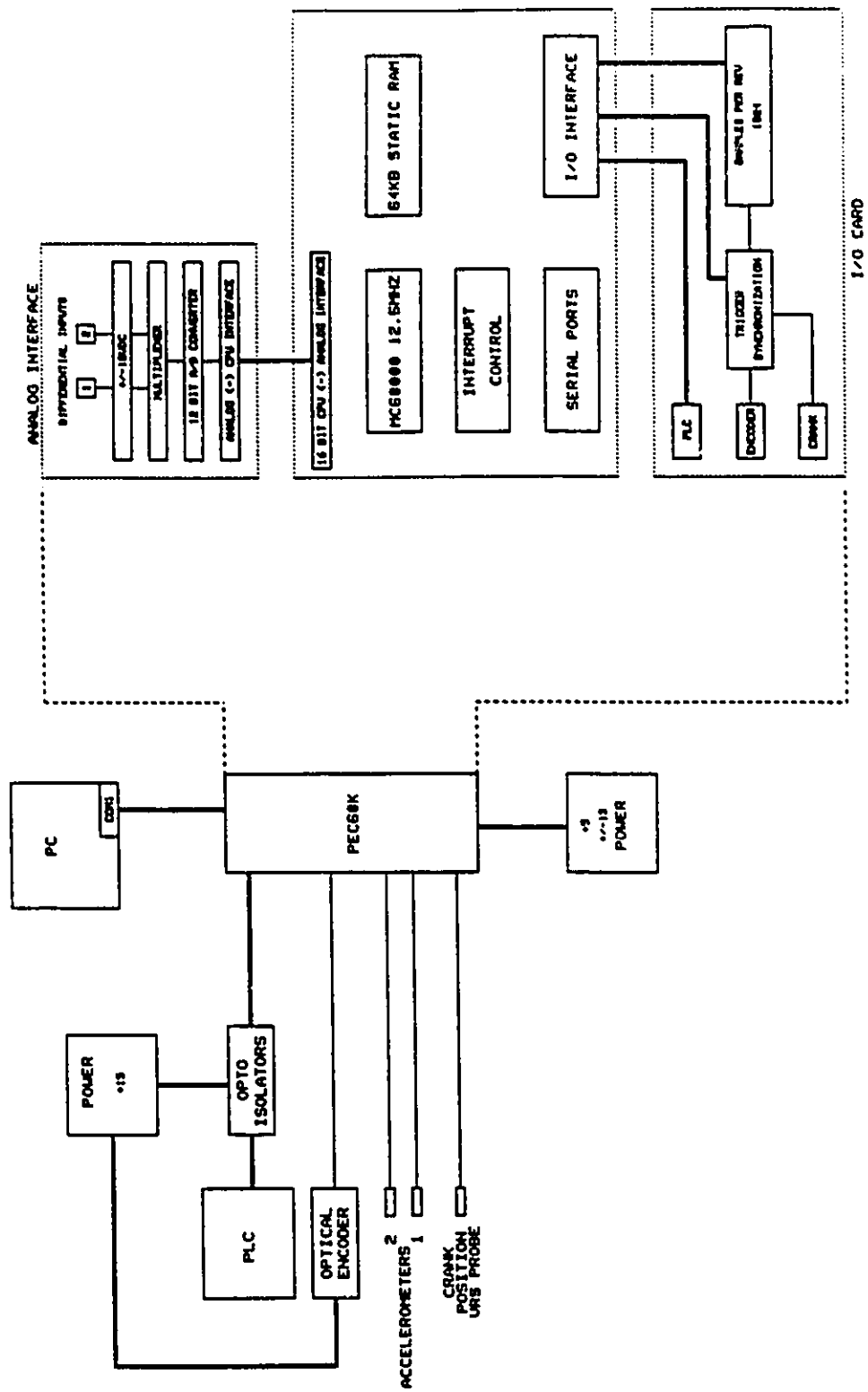
Figure 4.4 : The Full Schematic of Cold Test Stand Hardware

the system enabled the data acquisition and storage to be obtained with a minimum loss of time domain history due to data processing.

The overall test cycle involving the test stand is represented by the flowchart in Fig. 4.5. The solid line elements of the chart signify the additions proposed for the vibration test. The vibration test was executed as a substitution of the conventional deck height test. The detail flowcharts of the vibration test of the current production system and the development system are found in Appendix B.

Each test was executed as a module. The overall test cycle was initiated by a PLC (Programmable Logic Controller) bit indicating that the engine was fully clamped and that all the sensors were in position. As depicted in the flowchart, the modules were executed in the following order:

1) Breakaway Torque (60 Nm low limit and 110 Nm high limit),

2) Running Torque (13 Nm low limit and 24 Nm high limit) and

3) Vibration Test (Variance 0.25 g^2 at 250 rpm, 0.71 g^2 at 420 rpm).

At the completion of each test, the result of the test was checked and the remainder of the test sequence was aborted if there was a reject.

4.2.2 Data Acquisition

Once the encoder interrupts were enabled, data acquisition began. The vibration data was acquired in the ISR's (Interrupt Service Routine) for each accelerometer. When the ADC indicated that a conversion was completed, the Motorola 68000 microprocessor executed an ISR based on the multiplexer channel selected. The ISRs for both accelerometers stored the result of the conversion, and accumulated the sum of all the vibration measurements taken. The sums were later used to calculate the mean of the signal.

The ISRs for the accelerometers were not the same. However, when an encoder interrupt occurred, on either rising or falling edge, both accelerometer outputs have to be
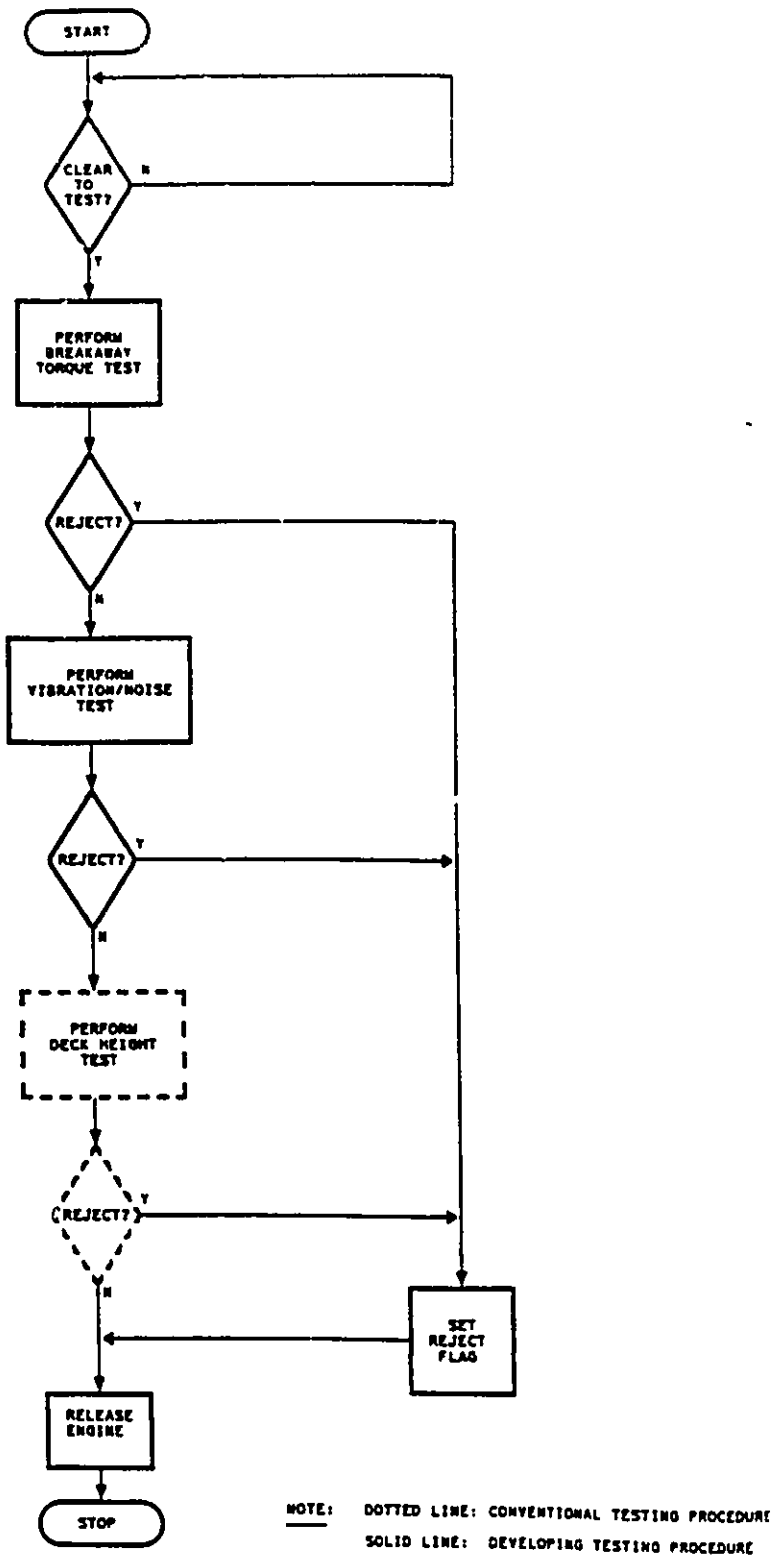
Figure 4.5 : Flowchart of Overall Test Cycle.

sampled. To accomplish this, a "glitch" in the ADC (Analog to Digital Converter) was exploited. Whenever the ADC was read, another conversion was initiated and, when it was completed, another interrupt was triggered. In other tests, this was avoided by turning the ADC interrupt off prior to reading the result of the conversion of accelerometer #1, then the multiplexer channel was changed to accelerometer #2. Reading the output of the ADC at this point resulted in another conversion being initiated. Like ISRs for the other tests, the ISR for accelerometer #2 disabled the ADC interrupt prior to reading its value. The ADC was then read, and the multiplexer was set back to the channel for accelerometer #1. The next encoder interrupt then reenabled the ADC interrupt and the process was repeated.

Because the ADC was not a simultaneous sample and hold device, the accelerometers were not read at exactly the same time. There was a time differential between readings of 25 microseconds (the conversion time for the ADC). However, the conversion time did not affect the performance of the test because this period is short compared to the time span for the highest frequency response of the signal.

Vibration was sampled in the above manner for eight revolutions. The storage location of the sampled data was reset when sample #2047 was obtained. This indicated the last sample for each revolution.

In the initial acquisition of data, reference signals were captured from a normal engine. Thereafter, the engine was checked dimensionally in the standard room and proved within engineering specifications. Subsequently, the engine was operated with missing or defective parts in piston No. 1. These were repeated for every piston with missing or defective parts, by the firing order. The characteristics of the defective engine components were as follows:

1. Missing connecting rod bearings

2. Unbalanced crank

3. Nick on balance shaft gear

4. Loose connecting rod nuts

5. Reversed bearing cap

6. Mismatched bearing cap

7. Cylinder bores defective machining

8. Tight piston pin

9. Missing main bearings

10. Loose main bearing bolts.

The results of these tests will be discussed in Chapter 6.

4.3 Hot Test or Dynamometer Test of Engine

In the automotive industry, a hot test is performed to measure engine performance capability to pre-established minimum acceptance criteria in the dynamometer laboratory. Vibration, noise, and cylinder pressure measurements were carried out during the hot test and the results were compared to that of the cold test. The general procedure used for this test and equipment is described in this section.

4.3.1 Engine Test Stand, Dynamometer and Control System.

The schematic of an engine test stand is illustrated in Figure 4.6. It consists of

a) a T-slotted base plate on isolated foundation

b) engine mounts

c) a drive shaft

d) the engine

e) a dynamometer and control system

f) the test stand control and data acquisition system.

The test engine was mounted on a separate base plate to that of the

87
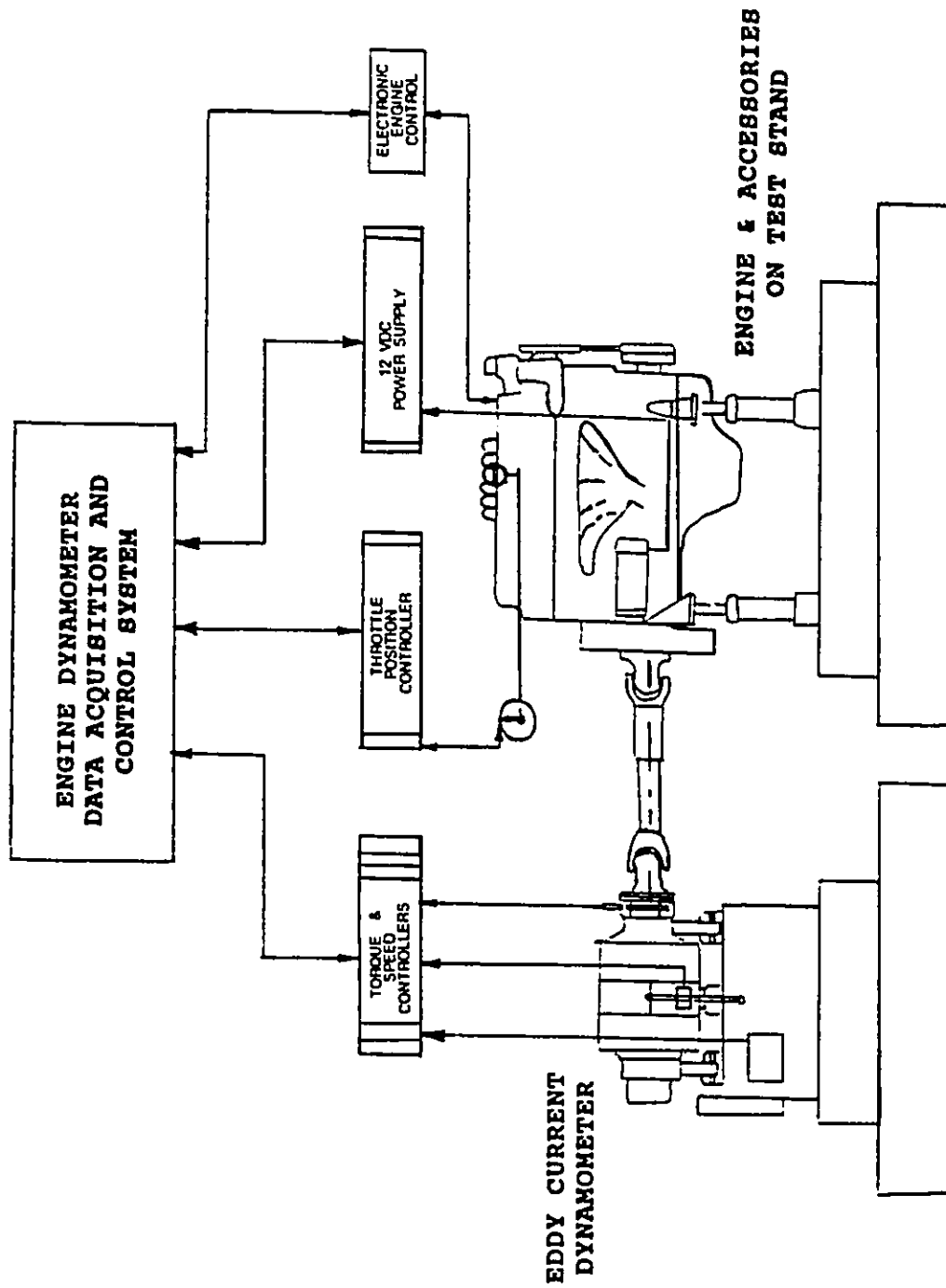
Figure 4.6 : A Schematic Diagram of an Engine Test Stand

dynamometer. This set-up was desirable so that any motion of the engine frame would not cause any detrimental effect to the engine itself and would not transmit any vibration to the adjacent area. The connection of the test engine and the dynamometer was through a special elastic drive shaft which allowed an axial mis-alignment and reduced variations in the torque and running speed.

In this study, the eddy current dynamometer shown in Figure 4.7 was used for measuring the engine torque and speed. The system is an assembly of four different components:

a) Rotating eddy current machine

b) Cradle

c) Torque measuring equipment

d) Speed measuring equipment.

The eddy current dynamometer is easily controlled by a d.c. input. Its main advantages include high power absorption, high speed capabilities and relatively low cost.

The d.c. flowing through the exciting coil, which is fixed to the dynamometer casing, produces a magnetic field which counteracts the rotary motion because the dynamometer casing is connected to the torque measuring equipment (load cell) through a lever arm. The moment of reaction is indicated as a force for a definite length of lever arm. To determine the power output it is essential to measure the speed: a proximity sensor senses the slots in a toothed disc at the shaft end of the dynamometer and produces voltage impulses. These impulses are converted into a speed-dependent voltage which is used for speed indication and control.

The standalone independent data acquisition and control system is coupled with the dynamometer to provide a complete engine test system. The system is based on a Digital Equipment Corporation PDP 11/73 computer and peripherals and the software using DEC's RSX-11M Plus operating system. The system was designed to ensure
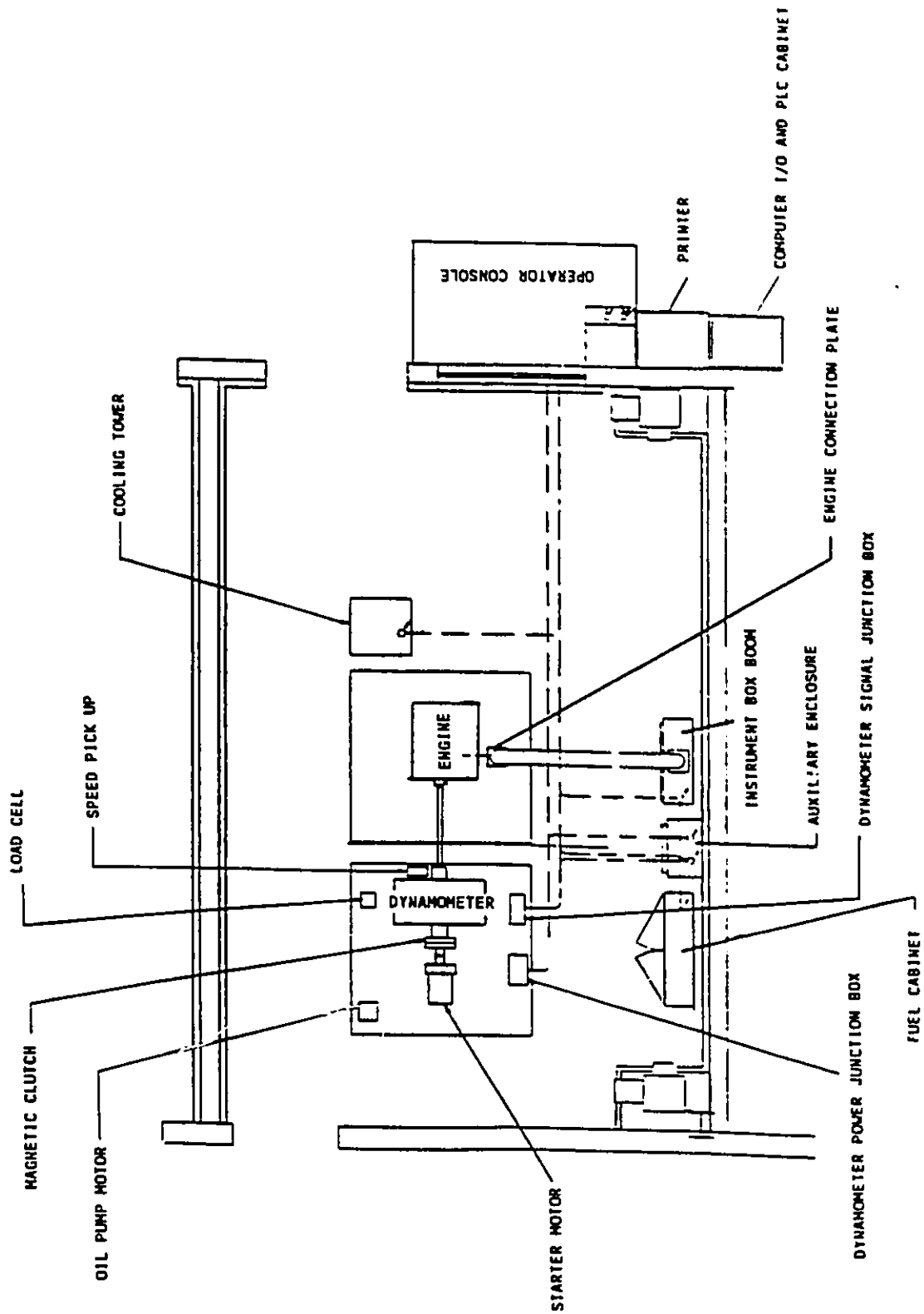
Figure 4.7 : A Block Diagram of a Complete Test Cell

COOLING TOWER

SPEED PICK UP

LOAD CELL

MAGNETIC CLUTCH

OIL PUMP MOTOR

STARTER MOTOR

ENGINE

DYNAMOMETER

OPERATOR CONSOLE

PRINTER

COMPUTER I/O AND PLC CABINET

ENGINE CONNECTION PLATE

INSTRUMENT BOX BOOM

AUXILIARY ENCLOSURE

DYNAMOMETER SIGNAL JUNCTION BOX

DYNAMOMETER POWER JUNCTION BOX

FUEL CABINET

ease of use by laboratory test personnel and to provide the power and flexibility necessary to run various test procedures. The block diagram of a complete test cell is illustrated in Figure 4.7.

The software for the test system is structured to provide two distinct levels of interaction: operation level and configuration level. The operation level provides the function needed to start and stop a test procedure, display data print data and operate the safety shutdown system. The configuration level provides various menu-driven interactive programs that allow a user to adjust the system to specific requirements.

A sample of the parameters measured and displayed in typical engine operating conditions is shown in Figure 4.8.

4.3.2 Data Acquisition System for Hot/ Dynamometer Test

The data acquisition for the Hot/Dynamometer test was divided into three different systems. Each system had its advantages and disadvantages and these will be summarized in the analysis of the engine test data.

4.3.2.1 System No. 1: Data Acquisition System Using Dynamic Analyzer

The block diagram in Figure 4.9 illustrates the interaction of the equipment in the complete measurement system. The basic components are the trigger box, transducers, dynamic signal analyzer, computer and its control system.

The trigger system consists of the signal inductive pick-up and a conditioning box. The conditioning box converts the spark plug signal to a TTL (Transistor-Transistor Logic) compatible voltage signal that is suitable for the external trigger of the dynamic signal analyzer.

The data acquisition system contains a computer with software, analyzer, a

TEST #		CODE		ENG. SER. #			ENG B.D.				
PROCEDURE # TITLE POWER TEST S/C							OPERATOR				

STEP #		1	2	3	4	5	6	7	8	9	10		
AM/PM													
ENGSP RPM	800	1000	1500	2000	2500	2750	3000	3250	3500	4000	4500		
OTORQ NM	0	249	271	366	396	404	406	413	410	395	360		
OBHP KW	0	25.4	42.4	75.5	103.3	115.3	127.0	139.3	150.2	164.3	167.7		
FUELF KG/HR	1.6	10.7	15.2	22.2	28.8	32.6	35.4	39.4	44.4	54.1	59.6		
OBSFC KG/KWH	0.02	0.011	0.006	0.008	0.007	0.008	0.008	0.008	0.008	0.009	0.010		
TIMING BTDC	10	10.4	10.1	13.5	16.9	17.9	18.8	19.0	19.6	21.4	21.5		
CINT c	71.0	71.5	74.9	75.2	77.1	78.2	79.8	81.6	83.4	86.2	87.9		-
COUT c	85.5	86.0	83.0	85.1	86.6	87.8	89.3	91.2	92.8	95.0	96.5		
OILT c	90.1	106.9	105.7	103.9	105.6	108.8	111.2	116.2	119.1	126.5	129.7		
AIRCT c	31.2	39.8	39.5	38.8	42.4	43.8	42.5	45.7	43.2	46.3	46.8		
EXHRT c	354	697	722	795	837	862	878	887	883	865	879		
EXHLT c	348	696	721	796	847	870	888	900	901	892	903		
OILP BAR	2.69	2.06	3.38	3.84	3.91	3.89	3.86	3.86	3.83	3.69	3.50		
FUELP BAR	2.42	3.11	3.26	3.29	3.42	3.36	3.36	3.41	3.51	3.43	3.47		
MANFP MM-HG	475	185	283	378	430	450	480	495	503	513	545		
COOLP KPA	97.2	98.9	99.1	98.7	99.2	99.1	99.9	98.8	98.9	99.0	99.2		
DUR HRS													
TOT HRS													

STEP #									COMPRESSION TEST RESULTS			
AM/PM									CYL. #	KPA		⊙ 360 RPM
ENGSP RPM									1	1275		
OTORQ NM									2	1250		
OBHP KW									3	1250		
FUELF KG/H									4	1250		
OBSFC KG/KWH									5	1250		
TIMING BTDC									6	1275		
CINT c									STARTING PARAMETERS			
COUT c									BAROMETER READING		734	MMHG
OILT c									AMBIENT AIR TEMP		25	C
AIRCT c									WET BULB TEMP		23	C
EXHRT c									DRY BULB TEMP		34	C
EXHLT c												
OILP BAR									FINISH PARAMETERS			
FUELP BAR									BAROMETER READING		734	MMHG
MANFP MM-HG									AMBIENT AIR TEMP		25	C
COOLP KPA									WET BULB TEMP		24	C
DUR HRS									DRY BULB TEMP		35	C
TOT HRS												

Figure 4.8 : A Sample of Engine Operating Conditions
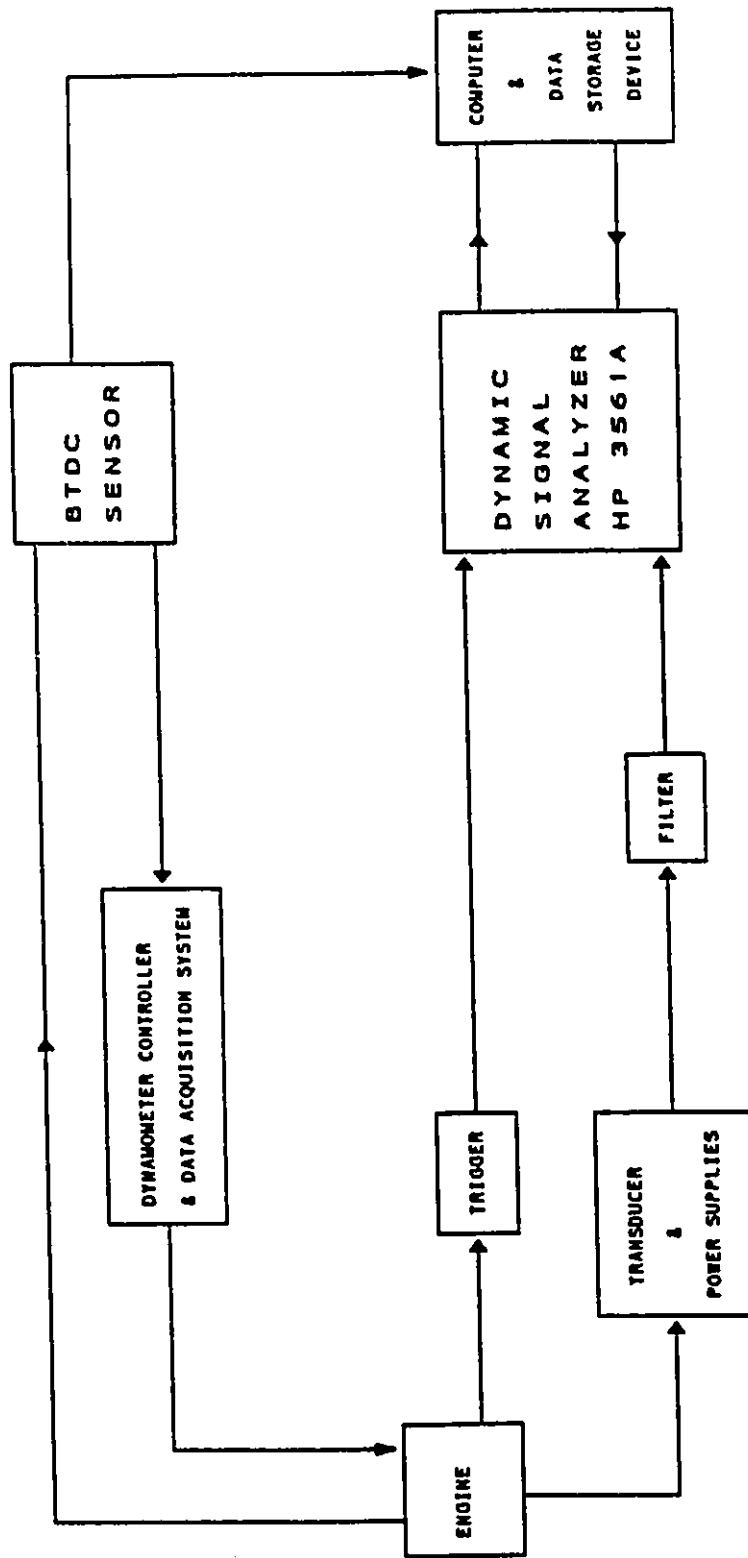
Figure 4.9 : System No. 1, Data Acquisition using a Dynamic Signal Analyzer.

1. MASS STORAGE IS :,700,1

2. DO YOU WANT TO AVERAGE TIME DATA : N

3. HOW MANY TIME AVERAGES : 50

4. DO YOU WANT FREE RUN DATA : N

5. NO. OF RECORDS OF FREE RUN : 1

6. FILTER PRESENT : Y

7. CUTOFF FREQUENCY (LP) : 4000

8. FREQUENCY SPAN : 5000

9. FREQUENCY START : 0

10. ENGINE RPM : 1500

11. SETTLED ANALYZER RANGE : 15

12. TRIGGER VOLTAGE : -9.8

13. PERCENTAGE OF RANGE TO TRIGGER : -140

14. BEFORE TOP DEAD CENTER (DEG) : 30

15. CALIBRATION VOLT/UNIT : 0.100

16. THE FILTER DELAY (SEC) : 0.000233

SELECT APPROPRIATE SOFTKEY

MENU1   MENU2   TESTMENU   CHANGE
                                    PARAMETER

Figure 4.10 : Typical Data Acquisition Menu

programmable filter and transducers. The signal passes through the filter where aliasing frequencies are removed. After triggering, the data is collected by digital sampling in the HP 3561A analyzer. The computer is programmed to control the analyzer, filter, mass storage and printer functions. The typical menu is shown in Figure 4.10. The programs are written in HP BASIC for both the data acquisition and analysis. The listings of these programs are found in Appendix C.

4.3.2.2 System No. 2: Data Acquisition System Using Nicolet 440

The schematic in Figure 4.11 shows the system which uses the Nicolet 440 Benchtop Waveform Acquisition System which is a four channel, 12 bit, 10 mega samples per second system. This system digitizes and stores the signals in memory and shows them on the display screen. The displayed waveforms can then be used to measure time and voltage values, manipulate the waveform either internally (which has a 260 k data points sweep capability) or send it to an external computer.

Six transducer bases were glued down on the engine block (centre line of the pistons) and B&K 4384 transducers were mounted. The signal was amplified through a B&K 2635 Charge Amplifier and then captured by a Benchtop Waveform Data Acquisition System. Modal analysis was performed earlier in the experiment to determine the location of the transducers to avoid the vibration nodes of the engine block.

The vibration signal was captured at the time of number 1 engine spark plug firing. This was made possible by using the external trigger signal generated by the induction of the #1 engine spark plug cable. The crank angle at the firing of the spark plug was recorded. Twenty five engine cycles of traces of vibration data, which represented 50 revolutions of the crank shaft, were swept in the oscilloscope and then saved to a built-in data storage system as one set of data. Forty sets of data were acquired for different engine operation conditions. Figure 4.12 is a sample of the data acquisition system set-up.
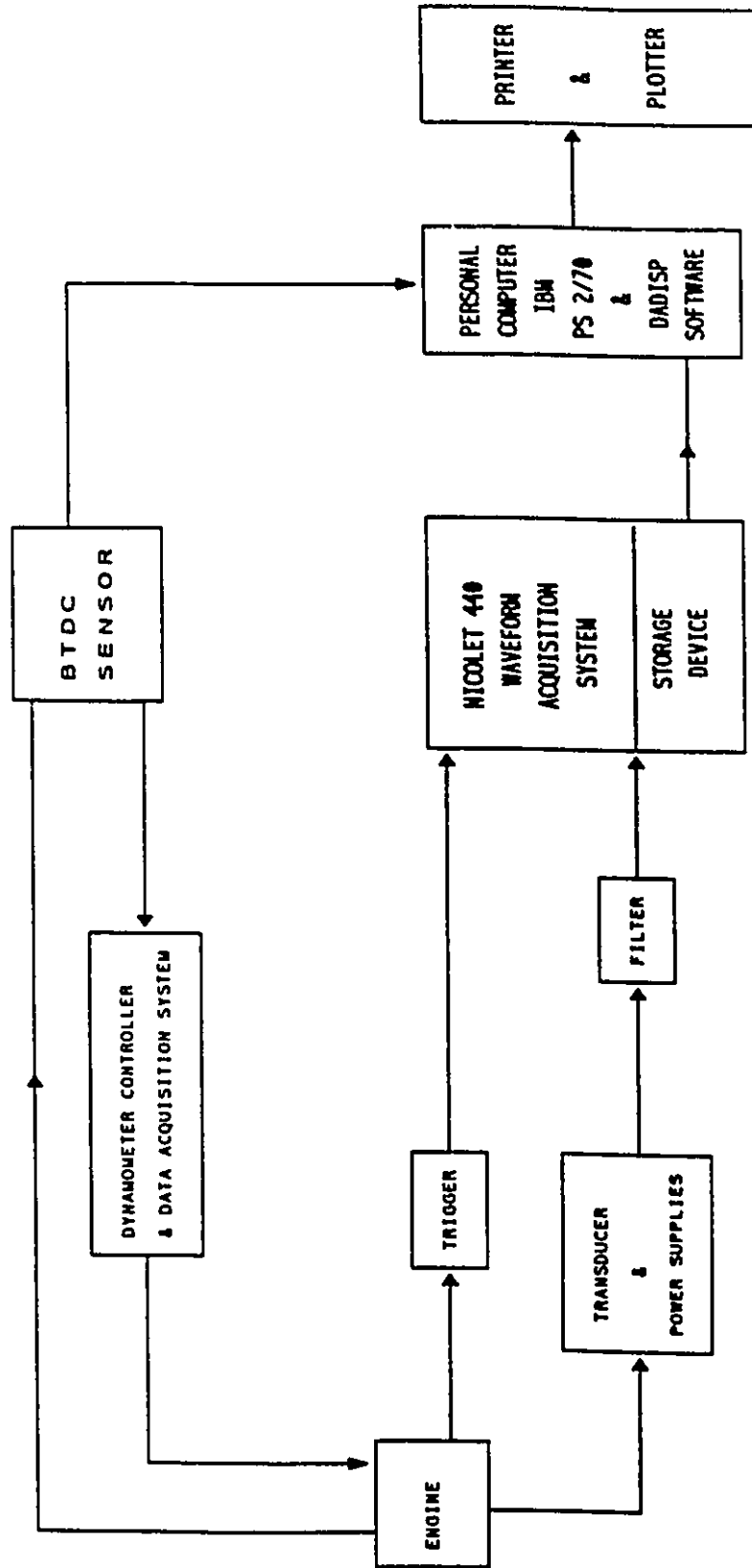
Figure 4.11 : System No. 2, Data Acquisition using Nicolet 440.

DATE : May 5, 1992	EXPERIMENT No. 203
DATA : WAVE 0110-0134. wft.	
External Trigger Level	5.18 ± 0.15 Volts
Sampling Time	100 microseconds
Sweep Points	18000 (1.8 seconds)
Amplitude Range Channel No. 1 Channel No. 2	5 Volts . 5 Volts
Engine R.P.M.	1667
Engine Timing	28° BTDC

Figure 4.12 : A Sample of Data Acquisition System No. 2 Set-up.

4.3.2.3 SYSTEM NO.3 : 8 Channel Data Acquisition System

The block diagram of the 8-channel data acquisition system is illustrated in Figure 4.13. The heart of the system consists of Motorolla 68020 CPU (Central Processing Unit), 1 Megabyte of RAM (Random Access Memory), interrupt control, serial port, I/O (input/output) interface. The data acquisition box is connected to six transducers, a magnetic pick-up, Engine PIP (Profile Ignition Pickup) and CID (Cylinder Identification) signals from the Electronic Engine Controls and finally a personal computer with programs to handle the data acquisition and analysis. The flowchart of the data acquisition programs for both the Box and the personal computer can be found in Appendix D.
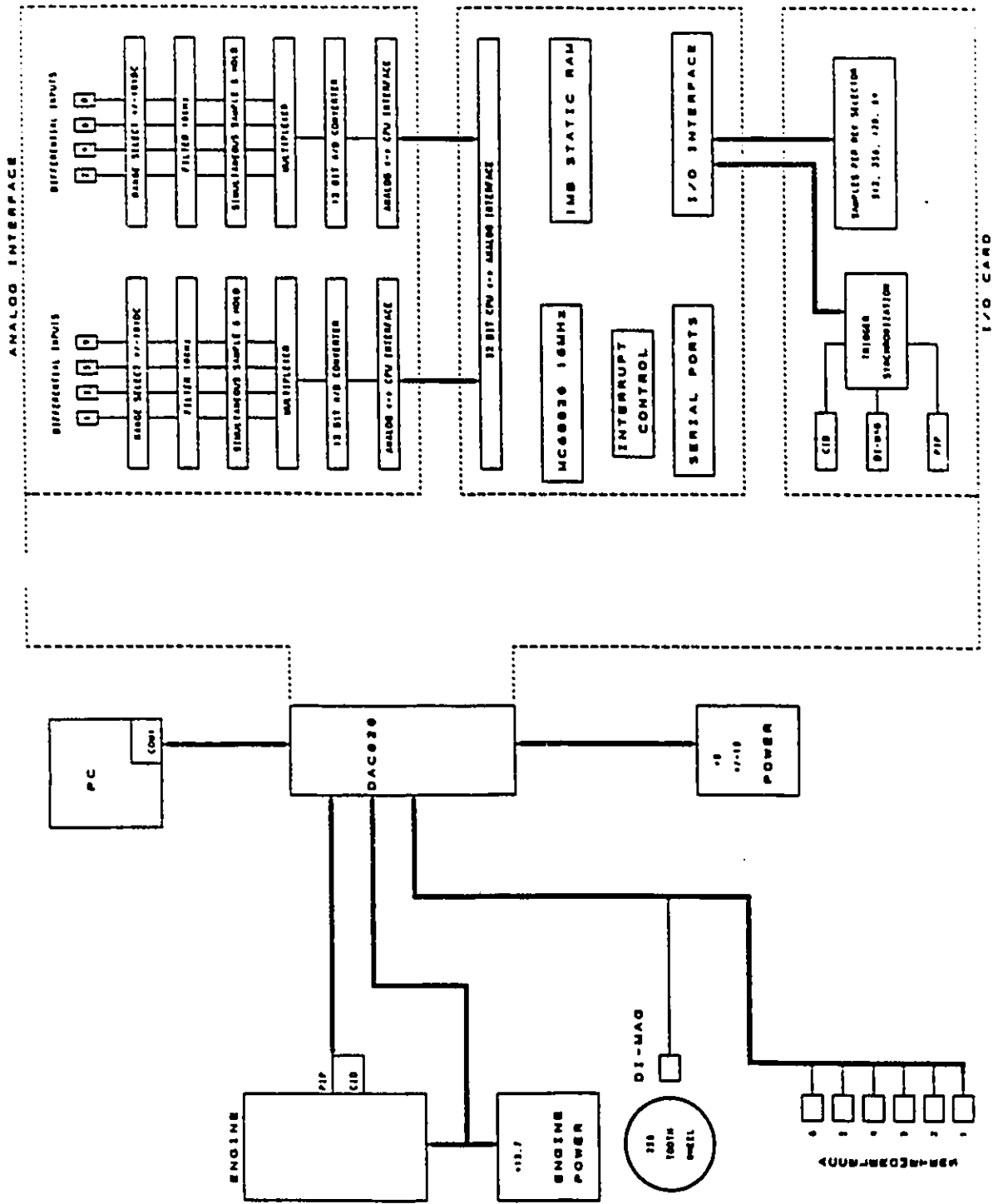
Figure 4.13 : System No. 3, 8-channel Data Acquisition System.

98

4.4 Sound Pressure and Sound Intensity Measurements

The Bruel and Kjaer Type 3360 Sound Intensity Analysis System consists of the Sound Intensity Analyzer Type 2134, the Display Unit Type 4715, the Sound Intensity Probe Type 3519 and Remote Indicating Unit ZH 0250. The 3360 can measure the vector quantity sound intensity level in real time 36 third-octave bands with center frequencies from 3.2 Hz to 10 kHz and in the 12 octave bands with center frequencies from 4 Hz to 8 kHz. The results are displayed on the separate, calibrated Display Unit Type 4715 where not only the sound intensity level can be measured but also the direction of the incident sound intensity can be inferred.

The 2134 and 4715 combination can also be used as a digital frequency analyzer in real time for measurements of sound pressure levels and in a wide variety of analyses of acoustical, vibrational and other signals. For sound pressure measurements, a real-time analysis is performed in the 42 third-octave bands with center frequencies from 1.6 Hz to 20 kHz and the 14 octave bands with center frequencies from 2 Hz to 16 kHz.

For both modes of operation, i.e., sound pressure level mode and the sound intensity level mode, the input signal may be A-weighted in the input amplifier before displaying the resulting spectrum.

4.4.1 Sound Intensity Analyzer Type 2134

The Type 2134 is a digital frequency analyzer with two input channels primarily designed for sound intensity measurements. Either channel can be used for sound pressure measurements and both channels are employed simultaneously when the Type 2134 is used to measure sound intensity. The sound pressure and sound intensity modes of operation are push-button selectable on the front panel.

4.4.2 Calibration

The probe can be calibrated, one microphone at a time, by means of a known sound pressure level such as that provided by the Pistonphone Type 4220 (which provides 124 dB re 20 μPa sound pressure level at 250 Hz with an accuracy of ± 0.15 dB). A calibrated barometer is provided with the pistonphone to determine the necessary correction due to the atmospheric pressure.

It can be shown that when calibrating the system for use in the sound intensity mode only half the atmospheric pressure correction (which is indicated on the barometer in dB) must be applied to each microphone.

The reference for the sound pressure is 20 μPa and the reference intensity for sound intensity level is $1\ pW/m^2$. These reference values have been chosen so that, for a freely propagating plane wave, the intensity level, IL, is practically equivalent to the sound pressure level, SPL. The actual relationship is:

$$IL = SPL - 0.16\ dB.$$

Therefore with pressure calibration, the intensity levels are 0.16 dB too high, which can be allowed for, if desired, by adjusting the sensitivity control. This calibration with a known sound level automatically calibrates the system for sound intensity level and the sound intensity levels on the display unit are given in dB re $1\ pW/m^2$.

4.4.3 Sound Intensity Vector Component Calculations

The Bruel and Kjaer 2134 contains four, front panel selectable programmes to calculate the sound intensity vector component, I_r for the four permissible combinations of spacer, δr, and microphone (i.e. for $\delta r = 6$ mm or 12 mm with the 1/4" microphones or for $\delta r = 12$ mm or 50 mm for the 1/2" microphones). Before performing a measurement, the optimum probe configuration range should be chosen for a particular application by considering the probe size, probe sensitivity and frequency range.

4.4.4 Display Unit Type 4715

Measurement results are displayed on the Display Unit Type 4715 in the form of a bar-graph in third octave or octave bands. For sound pressure measurements the bars on the display all have the same brightness. For sound intensity measurements however, there are two different levels of brightness for the bars on the display unit; "grey", "normal" brightness columns for the sound intensity which is incident on the front probe (referred to as "positive" intensity); "white" columns for the sound intensity which is incident on the rear of the probe.

4.4.5 Remote Indicating Unit ZH 0250

In very confined spaces or where the quantity of information presented by the Display Unit is more confusing than helpful, it can be preferable to use the probe in conjunction with the Remote Indicating Display Unit ZH 0250. The small, hand-held ZH 0250 enables a single channel, either octave or third octave, of either sound pressure level or sound intensity level to be read out from the 2134 in the form of a bar graph. The unit can also initiate integrations and can operate up to 50 m from the 2134.

4.5 Transducers and Accessories

There are several transducers and their supporting equipment used in this study. The specifications and functions are discussed in the following sections.

4.5.1 Bruel and Kjaer Type 4384 Accelerometer

The active elements of this accelerometer consist of a piezoelectric disc loaded by seismic masses and held in position by a clamping ring. When the accelerometer is subjected to vibration, the combined seismic mass exerts a variable force on the

piezoelectric element. This force then produces a corresponding electric charge due to the piezoelectric effect. The key specifications are listed in Figure F.1 (Appendix F). This accelerometer is also supplied with calibration chart and measured frequency response curve.

4.5.2 Bruel and Kjaer Type 2635 Charge Amplifier

This is a portable low noise charge amplifier for use with piezoelectric accelerometers. Accurate three digit conditioning networks allow dial-in of exact sensitivity to give amplifier output rating between 0.1 to 1000 mV/unit. The major specifications of this unit are outlined in Figure F.2.

4.5.3 PCB Model 302A21 Accelerometer

This is low impedance quartz accelerometer designed for operation in high $(400°F)$ temperature environment. The accelerometer operates from low cost power unit and connects directly to some FFT analyzers equipped with ICP (Integral Circuit Piezoelectric) current source. The major characteristics are tabulated in Figure F.3.

The accelerometer is also supplied with an individual NBS (National Bureau of Standards) traceable calibration certificate.

4.5.4 PCB Model 308M86 Accelerometer

The accelerometer is built with a proven, quartz element and advanced microelectronic circuit capable of withstanding dirty factory environment. The specifications are outlined in Figure F.4.

4.5.5 PCB Model 408D06 Power Supply

This power supply is used with ICP (Integrated Circuit Piezoelectric) transducers. Its functions include powering the transducer electronics, amplifying the signal, debiasing the output signal and indicating normal or faulty system operation. The main specifications are listed in Figure F.5.

4.5.6 Bruel and Kjaer Type 4249 Calibration Exciter

This accelerometer calibrator is completely self-contained, pocket-sized, vibration reference source for laboratory and field applications. It is designed to produce a reference acceleration level of 10 ms^{-2} rms at a frequency of 159.2 Hz ($\omega = 1000 rads^{-2}$) and is intended for rapid calibration of vibration measurement, monitoring and recording systems utilizing piezoelectric accelerometers. The main specifications are outlined in Figure F.6.

4.5.7 Bruel and Kjaer Laser Velocity Transducer Set Type 3544

The Laser Velocity transducer set consists of the Laser Velocity Transducer and Power Supply. By attaching a small piece of retroreflective tape to the surface of the vibrating object (or painting the surface with reflective liquid), vibration velocity at that point can be measured by aiming the Laser on the object.

It is designed for use in all those applications where an accelerometer cannot be used. Such applications includes measurement on:

    a. hot surfaces of structures (e.g. engine exhaust)

    b. light structures (such as disk drive head) and

    c. rotating surfaces (sides or ends of shafts)

    The specifications of this equipment are summarized in tabular form on Figure F.7.

4.5.8 PCB Model 086B05 Impulse Force Hammer

The hammer consists of an integral, ICP, quartz force sensor mounted on the striking end of the hammer head. It is structured with rigid quartz crystals and a built-in microelectronic unity gain, isolation amplifier. The hammer sensitivity is outlined in Figure F.8.

4.5.9 PCB MODEL 303A02 Accelerometer

This miniature ICP (Integrated Circuit Piezoelectric) accelerometer is designed specifically for high frequency response. The size makes it ideal for structural measurement where the effect of the accelerometer on the structure is critical. The specifications and calibration specifications are tabulated in Figure F.9.

4.5.10 PCB Model 112A Pressure Transducer

A standard spark plug is modified to mount a miniature quartz pressure transducer in a spark ignition engine for measuring combustion pressures. The specifications for this transducer are tabulated in Figure F.10.

4.5.11 Bruel and Kjaer Type 4155 Microphone

This is a free field, half inch condenser microphone used for general and low sound level measurements. The free frequency response from 4 Hz to 16 kHz is $\pm 2dB$. The sensitivity is 50 mV/Pa. The influence of $1\,ms^{-2}$ axial vibration is typically 60 dB equivalent sound pressure level. The influence of relative humidity is 0.004 dB/% RH while the influence of static pressure is -0.001 dB/mbar.

4.5.12 Bruel and Kjaer Type 2231 Sound Level Meter

The Bruel and Kjaer Type 2231 is a precision hand held sound level meter. With Microphone type 4155, it has a measuring range of 24 dB to 153 dB. The availability of interchangeable application modules allow measurement of acoustical parameter of wide range of acoustical parameter. The other main specifications are summarized in Figure F.11.

4.5.13 Rockland Model 2783 Signal Processing Filter

Rockland Model 2783 is a high pass/ low pass filter/ signal conditioner with near-ideal passband and stopband characteristics. It has the following main features;

1) 3 digit resolution from 0.1 Hz to 110 kHz

2) 8 pole/8 zero Elliptic response

3) differential inputs with low noise amplifier to handle signals from 1 mV to 31.6 V full scale.

4) selectable bipolar or unipolar output swing to suit all A to D converters.

5) overload indicators to avoid signal distortion.

6) opto-isolated GPIB and RS 232 interfaces.

The detailed specifications are outlined in Figure F.12.

4.6 Time and Frequency Domain Analysis Equipment

4.6.1 Bruel and Kjaer 2032 Dual Channel Signal Analyzer

The Bruel and Kjaer 2032 analyzer is a two channel Fast Fourier Transform (FFT) analysis system having 801 lines of resolution. It is fast because of its high real time frequency of 5 kHz. It has a fully instrumented front-end and user defined calibration. The full specifications are listed in Figure F.13.

4.6.2 Hewlett Packard HP3561A Dynamic Signal Analyzer

The Hewlett Parkard HP3561A is a single channel narrow band dynamic signal analyzer with a frequency range of 100 kHz. It weighs only 16 Kilograms. The analyzer is equipped with a buble memory capable of storing more than 100 time traces and frequency spectra. The analyzer measures input signals from 22.39V rms to 2.82 mV rms. The 80 dB dynamic range of this equipment allows measurement of signal of interest exists in the presence of large unwanted signals. The signal processing capabilities include rms averaging, rms exponential weighting averaging, and time averaging. It also has software for mathematical operations which can be applied to measurement data for additional processing. The A-weighting filter is available for acoustic measurements. The Integrated Circuit Piezoelectric (ICP) current source is available for powering ICP accelerometers.

Most important of all in automated measurement, this analyzer is equipped with the Hewlett Packard Interface Bus so that it can be controlled remotely by a computer. Since measurement data can be remotely input or output, it is possible to extend, with a computer, the basic measurement capability of this instrument. The detailed specifications are summarized in Figure F.14.

4.6.3 Nicolet 440 Benchtop Waveform Acquisition System

Vibration data during an engine test was captured in the Nicolet 440 Benchtop Waveform Acquisition System which is a four channel, 12 bit, 10 megasamples per second system. This system digitizes analog input signals, stores the digitized signals in memory and shows them on the display screen. The displayed waveforms can then be used to measure time and voltage values, manipulate the waveforms either internally in the system or send it to an external computer, Which has a 260K data points sweep capability. The detailed system specifications are outlined in Figure F.15.

106

4.7 Data Presentation

The acquired data and results obtained were presented, with the use of various computer programs developed and DADiSP. The computers and peripherals used include the following:

1. IBM PS/2 Model 90 computer,

2. Hewlett Packard 9000 Model 360 computer,

3. Hewlett Packard HP 7550 plotter,

4. Hewlett Packard Laserjet III printer and

5. Hewlett Packard Thinkjet printer.

4.8 Engine Teardown Analysis

The test engine is mounted on the engine teardown stand for complete dimensional and torque measurements. Typical torque and dimensional measurements of the engine are shown in Figures 4.14 and 4.15, respectively.

ENGINE TEARDOWN ANALYSIS REPORT

PART NAME	QTY	ACCEPTABLE TORQUE(NM)		RUNNING TORQUE TAKEN IN LOOSENING DIRECTION ONLY (CIRCLE FIGURES OUT OF LIMITS)							
				1	2	3	4	5	6	7	8
OIL PUMP (M-8)	4	20-40		38	40	40	38				
FRONT	6	11-39	R	22	20	20	22	18			
COVER			L	12	15	15	15	10			
WATER PUMP	9	14-35		30	28	20	24	28			
OIL PAN	16	9-35	R	19	15	16	14	17	13	14	15
(ALUMINUM)			L	14	14	17	19	19	18	15	12
OIL LEVEL SENSOR	1	17-55									
OIL PUMP PICK-UP	2	12-35		15	16						
OIL PUMP PICK-UP NUT	1	40-60		48							
DAMPER BOLT	1	140 MIN		180							
ENGINE TORQUE		BEFORE TEST									
TO TURN		AFTER TEST		30							
CAMSHAFT SPROCKET	1	40-70		65							
TIMING CH. TENSIONER	3	8-19		14	14	14					
CONNECTING ROD	12	41-80	R	60	58	66	68	70	68		
			L	64	60	60	64	70	68		
MAIN BEARING	8	110-180	R	155	155	140	160				
			L	150	150	145	155				
OIL PUMP (M-6)	2	8-20		14	14						
CYLINDER HEAD	8	60 MIN	R	120	120	120	120				
(SHORT)			L	120	110	120	120				
CYLINDER HEAD	8	60 MIN	R	120	130	115	120				
(LONG)			L	120	120	120	115				
ROCKER	12	25-50	R	34	34	36	36	34	35		
ARM			L	34	36	32	36	34	34		
LOWER INTAKE	14	11-20	R	8	6	10	12	10	10	12	
MANIFOLD			L	16	8	8	10	4	6	4	
FUEL INJECTION	4	8-20	R	12	12						
RAIL			L	13	12						
UPPER	6	26-45	R	40	42	42	38				
INTAKE			L		NA	38					
THROTTLE BODY	4	18-32		26	22	26	28				

Figure 4.14 : Torque Measurement Data

DATE: 10/14/92	RWD			AUDITED BY:	B.P.	
TORQUE TO TURN 14-23NM	18	CRANKSHAFT END PLAY .10-.20				0.10
CAM END PLAY .025-.100	0.04	BALANCE SHAFT END PLAY .075-.16				N/A

MAIN BEARING TO JOURNAL CLEARANCE

MASTER GAGE	BEARING	64.021 - 64.059			CLEARANCE .013 - .058		
	JOURNAL	63.983 - 64.003			BORE DIA 68.885 - 68.905		

NUMBER	1	2	3	4	5	6	AVERAGE
BORE	68.896	68.892	68.898	68.899			68.896
BEARING	64.025	64.024	64.012	64.009			
JOURNAL	63.993	63.988	63.991	63.992			63.991
CLEARANCE	0.032	0.036	0.021	0.017			0.027

CAMSHAFT BEARING TO JOURNAL CLEARANCE

MASTER GAGE	BEARING	52.133 - 52.158			CLEARANCE .025 - .076		
	JOURNAL	52.082 - 52.108					

BEARING	52.152	52.145	52.139	52.154			AVERAGE
JOURNAL	52.095	52.093	52.095	52.092			
CLEARANCE	0.057	0.052	0.044	0.062			0.054

BALANCE SHAFT BEARING TO JOURNAL CLEARANCE

MASTER GAGE	BEARING	52.133 - 52.158			CLEARANCE .025 - .076		
	JOURNAL	52.082 - 52.108					

BEARING							AVERAGE
JOURNAL							
CLEARANCE							

CON ROD BEARING TO JOURNAL CLEARANCE

MASTER GAGE	BEARING	58.724 - 58.762			CLEARANCE .022 - .069		
	JOURNAL	58.682 - 58.702					

BEARING	58.742	58.752	58.750	58.742	58.762	58.750	AVERAGE
JOURNAL	58.692	58.696	58.692	58.696	58.696	58.696	
CLEARANCE	0.050	0.056	0.058	0.046	0.066	0.054	0.055

PISTON TO CYLINDER BORE CLEARANCE

MASTER GAGE	BORE	96.800 - 96.890	S/C PRODUCTION		.101 - .114
	PISTON	96.754 - 96.874	BASE PRODUCTION		.030 - .056
			S/C BARREL		.038 - .063

BORE	96.828	96.830	96.834	96.828	96.831	96.830	AVERAGE
PISTON	96.801	96.793	96.804	96.787	96.799	96.793	
CLEARANCE	0.027	0.037	0.030	0.041	0.032	0.037	0.034
LINEGRADE/ACTUAL	G /P	P /P	G /P	P /P	G /P	P /P	BORE
LINEGRADE/ACTUAL	G /G	P /G	G /P	P /P	G /G	P /G	PISTON

PISTON TO BLOCK DECK HEIGHT

SPECIFICATION	+.25mm TO -.27mm						
FRONT	-0.01	-0.06	-0.02	-0.13	0.06	-0.03	AVERAGE
REAR	-0.11	-0.10	-0.12	-0.16	-0.16	-0.08	
AVERAGE	-0.06	-0.08	-0.07	-0.15	-0.05	-0.06	-0.08

All dimensions are in mm

Figure 4.15 : Dimensional Measurement Data

109

4.8.1 Piston to Bore Clearance

The air gages with electronic column readout are calibrated with the masters. Before measurements, the piston and the cylinder bore were thoroughly cleaned and were free of oil residue. The piston to bore clearance was then measured using the air gage system shown in Figure 4.16.

4.8.2 Offset Piston Skirt with respect to Ringland

In the production environment, any dimensional measurement has to be performed in an effective and reliable manner. The measurement of the runout of the piston skirt with respect to ringland number 1 is accomplished using the gage shown in Figure 4.17.

Using Figure 4.18 as a guide, the measurement procedure for the runout of the piston skirt with respect to the ringland is as follows:

  i) Orient the piston as shown.

  ii) Push the piston against a stop at indicator base.

  iii) Zero the indicator.

  iv) Rotate the piston 180 $^\circ$.

  v) Record the measurement AC (including sign).

  vi) Similarly BD can be measured by zeroing the indicator at B and measuring at D.

  vii) The offset is thus calculated using the formula.

$$\text{Offset} = \sqrt{(AC)^2 + (BD)^2}.$$

4.8.3 Concentricity of Ringland with respect to Skirt

This measurement is performed in the laboratory where the environment (temperature, humidity, and cleanliness) is controlled. This is done using a special Coordinate Measuring Machine. After positioning the piston skirt, the measuring head
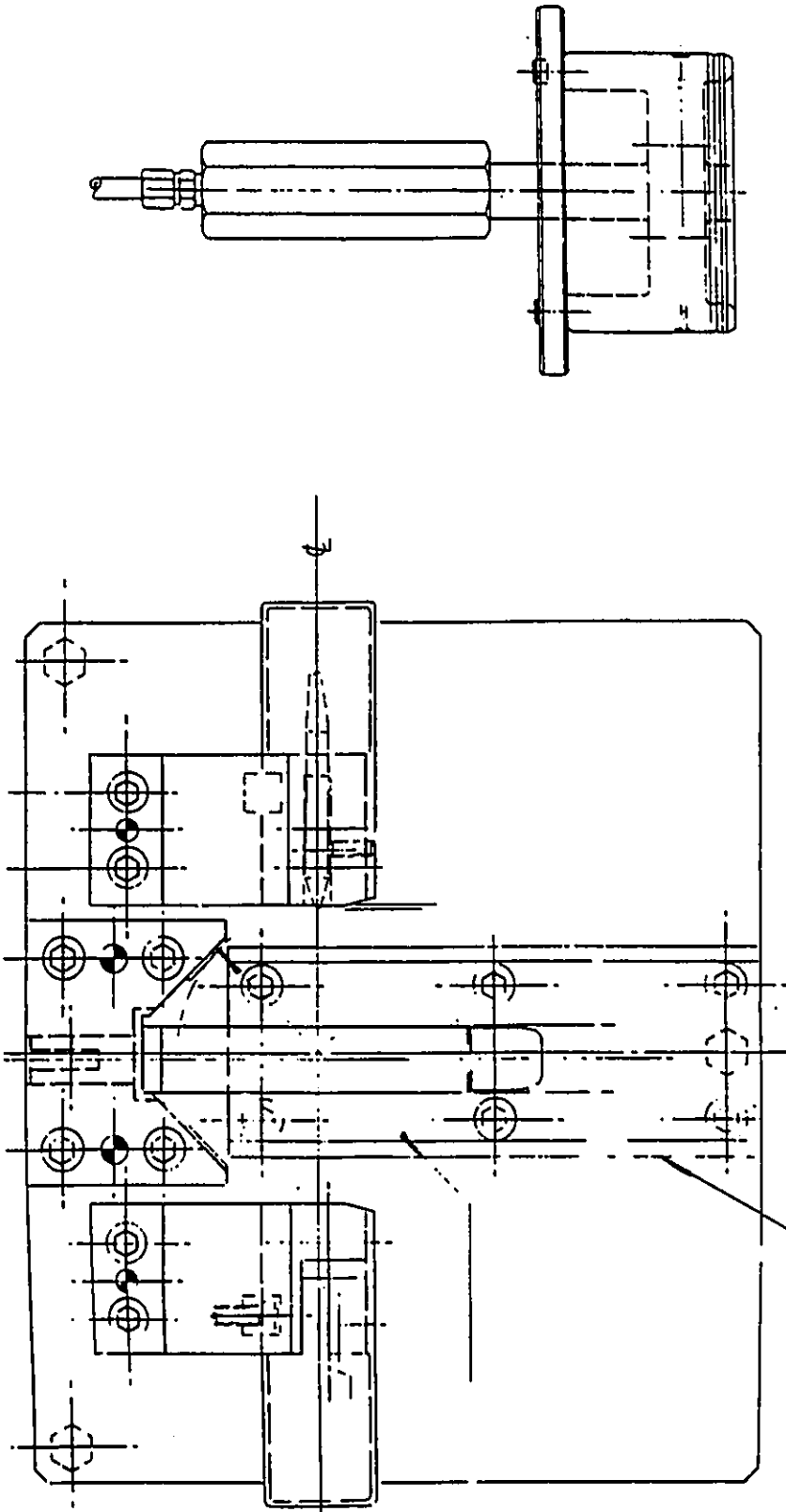
Figure 4.16 : Gages Used for Measuring Piston to Bore Clearance

111

DIAL INDICATOR GUARD
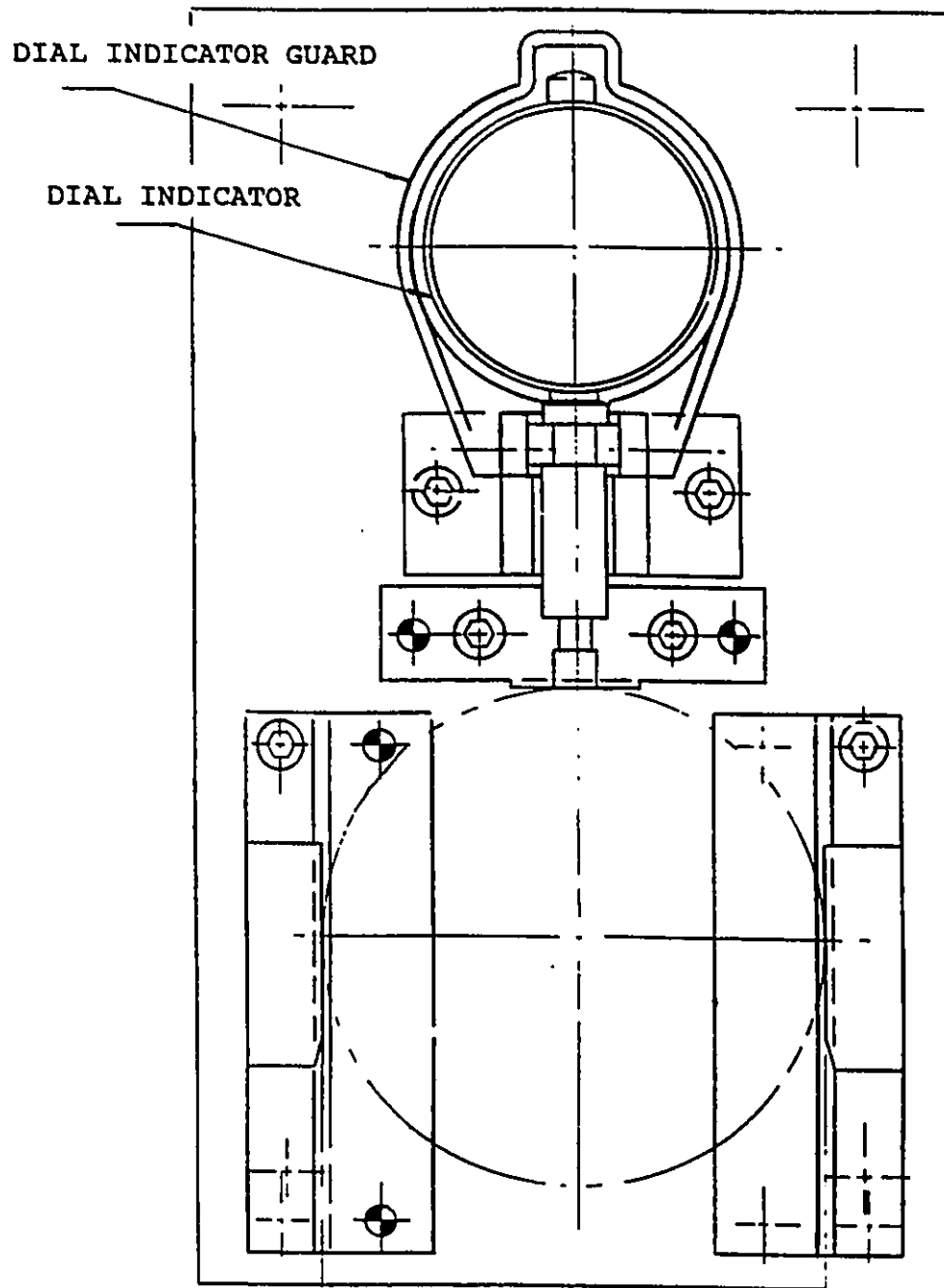
DIAL INDICATOR

Figure 4.17 : Dial Indicator Gage for Checking Concentricity
of Piston Ringland to Skirt

Zero Gauge At Point "A"
Rotate Piston To Point "C"
Take Reading At Point "C"
This Value Becomes Reading "A - C"
Rotate Piston So Gauge Aligns With Point "B"
Zero Gauge At Point "B"
Rotate Piston To Point "D"
Take Reading At Point "D"
This Value Becomes Reading "B - D"
Find Values For Readings "A - C" and "B - D"
On Concentricity Chart, The Value At The Intersection Of The Readings
Gives The Piston's Concentricity FIM
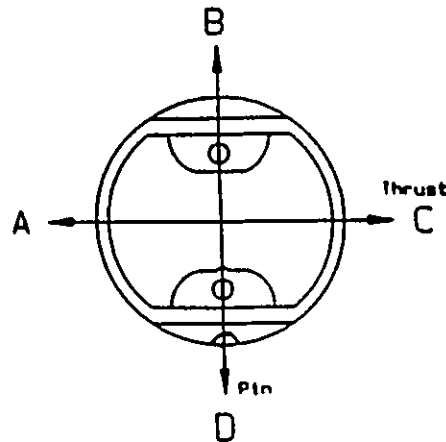
FIM	A-D	0.000	0.010	0.020	0.030	0.040	0.050	0.060	0.070	0.080	0.090	0.100
B-D												
0.000		0.000	0.010	0.020	0.030	0.040	0.050	0.060	0.070	0.080	0.090	0.100
0.010		0.010	0.014	0.022	0.032	0.041	0.051	0.061	0.071	0.081	0.091	0.100
0.020		0.020	0.022	0.028	0.036	0.045	0.054	0.063	0.073	0.082	0.092	0.102
0.030		0.030	0.032	0.036	0.042	0.050	0.058	0.067	0.076	0.085	0.095	0.104
0.040		0.040	0.041	0.045	0.050	0.057	0.064	0.072	0.081	0.089	0.098	0.108
0.050		0.050	0.051	0.054	0.058	0.064	0.071	0.078	0.086	0.094	0.103	0.112
0.060		0.060	0.061	0.063	0.067	0.072	0.078	0.085	0.092	0.100	0.108	0.117
0.070		0.070	0.071	0.073	0.076	0.081	0.086	0.092	0.099	0.106	0.114	0.122
0.080		0.080	0.081	0.082	0.085	0.089	0.094	0.100	0.106	0.113	0.120	0.128
0.090		0.090	0.091	0.092	0.095	0.098	0.103	0.108	0.114	0.120	0.127	0.135
0.100		0.100	0.100	0.102	0.104	0.108	0.112	0.117	0.122	0.128	0.135	0.141
0.110		0.110	0.110	0.112	0.114	0.117	0.121	0.125	0.130	0.136	0.142	0.149
0.120		0.120	0.120	0.122	0.124	0.126	0.130	0.134	0.139	0.144	0.150	0.156
0.130		0.130	0.130	0.132	0.133	0.136	0.139	0.143	0.148	0.153	0.158	0.164
0.140		0.140	0.140	0.141	0.143	0.146	0.149	0.152	0.157	0.161	0.166	0.172
0.150		0.150	0.150	0.151	0.153	0.155	0.158	0.162	0.166	0.170	0.175	0.180

All dimensions are in mm.

Figure 4.18 : Measurement Guide for Concentricity of Piston Ringland to Skirt

113

was programmed to sweep through the ringland and measure the coordinates of 1500 points on the ringland. Typical results of the measurement are shown in Figure 4.19.

This measurement is far more accurate than the production gage. The correlation between these measurement methods is shown in Figure 4.20. The correlation R is equal to 0.957 which indicates a "strong' linear relationship between the production gage measurement and the CMM measurement.

4.8.4 Piston Skirt Ovality and Taper Measurement

The Adcole Model 910 auto inspection gage (computer controlled) shown in Figure 4.21 is used to measure the piston skirt ovality and taper measurement. In this measurement, the piston is chucked in the headstock machine while a carbide follower records the movement as the piston rotates. The piston skirt profile is shown in Figure 4.22. The skirt ovality is summarized in Figure 4.23.
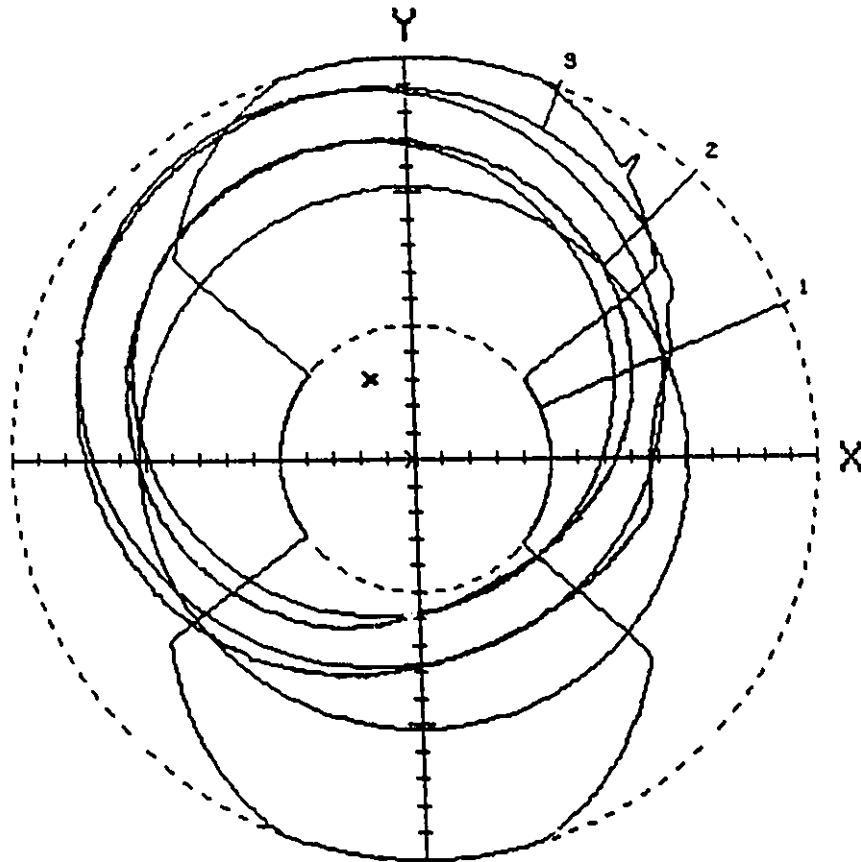
	1. measurem.	2. measurem.	3. measurem.
Meas.point:			
Calculation	LSC	LSC	LSC
Filter (U/R):	0-500	0-500	0-500
Graduation (mym):	50.00	50.00	50.00
Position (mm) :	44.0	5.6	12.4
X0 (mym):	-4	-75	-77
Y0 (mym):	1	150	150
P+V (mym):	506	20	64

All dimensions are in microns.

Figure 4.19 : Concentricity of Piston Ringland to Skirt

CMM VS. PRODUCTION MEASUREMENT
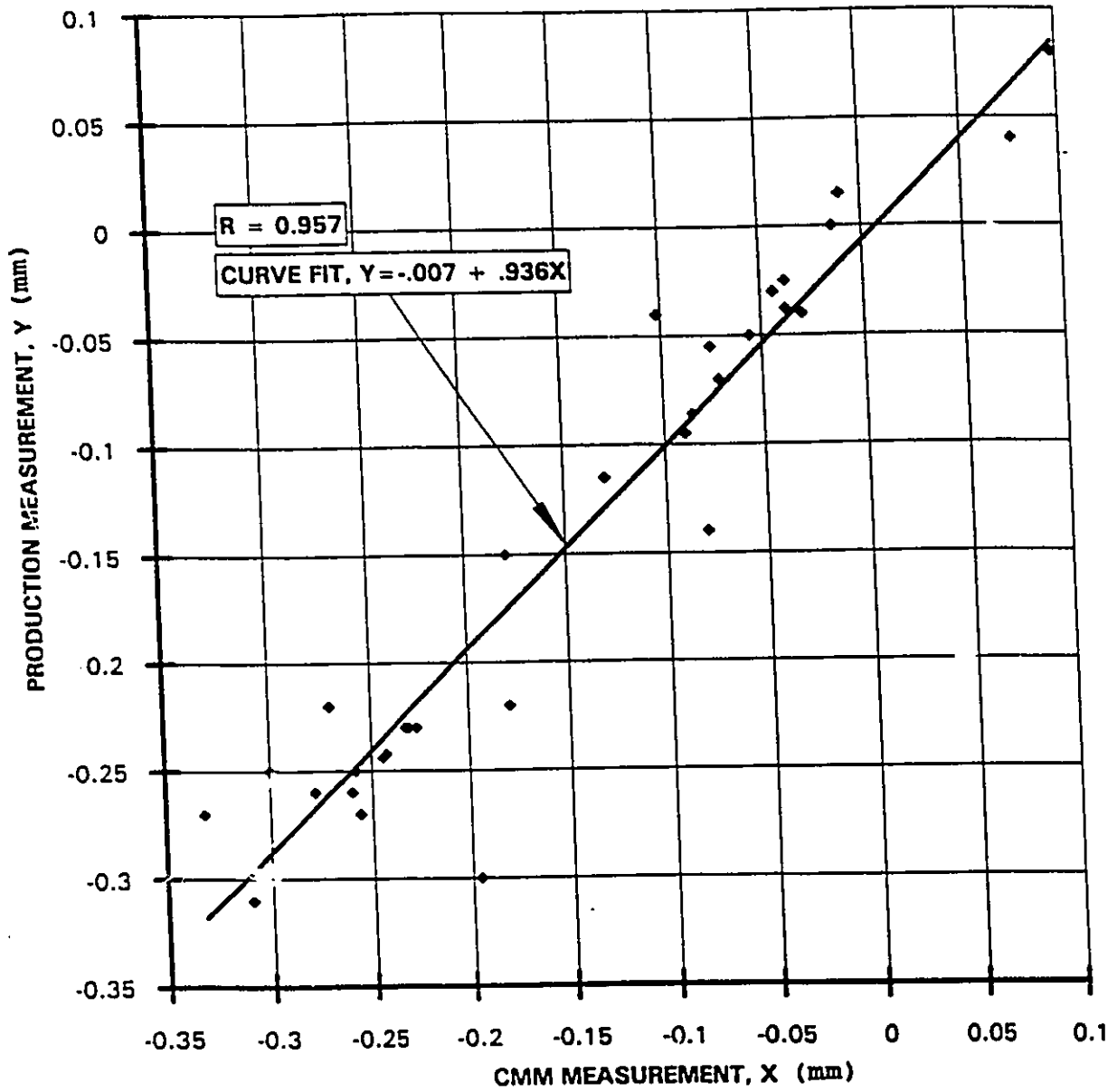
Figure 4.20 : Correlation between Production Gage and CMM
Measurements
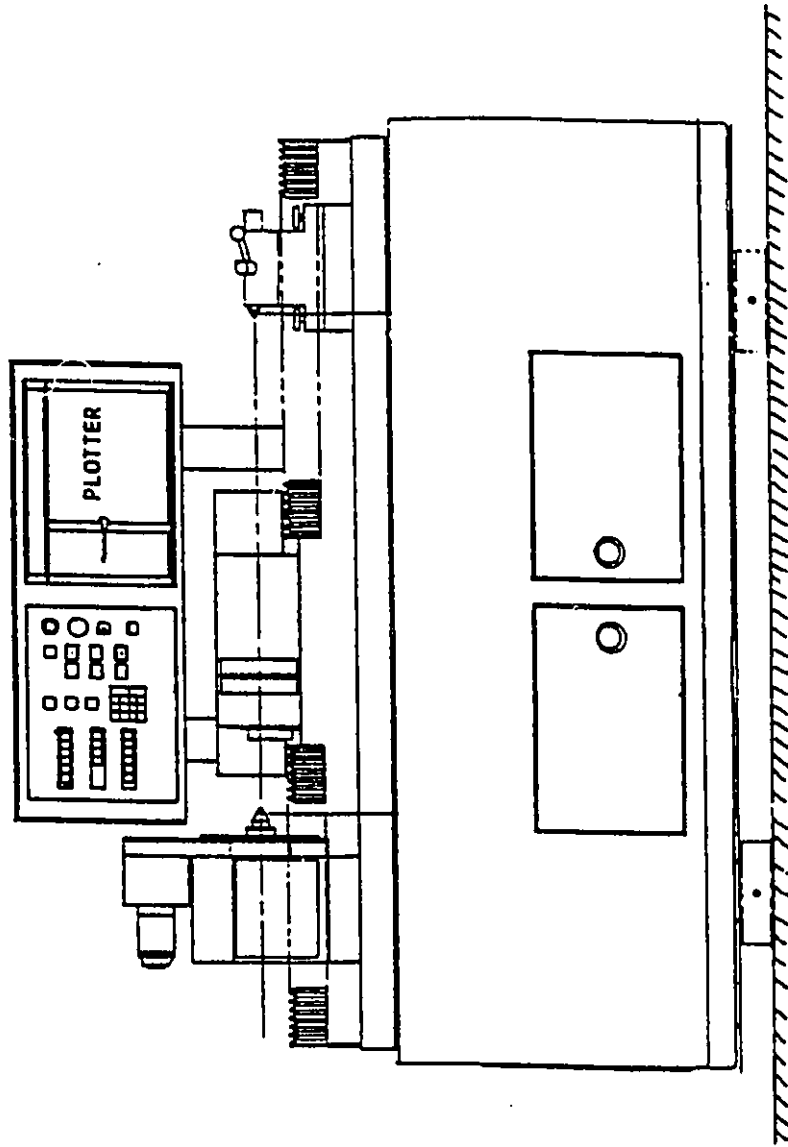
Figure 4.21 : Piston Skirt Profile and Ovality Inspection Gage
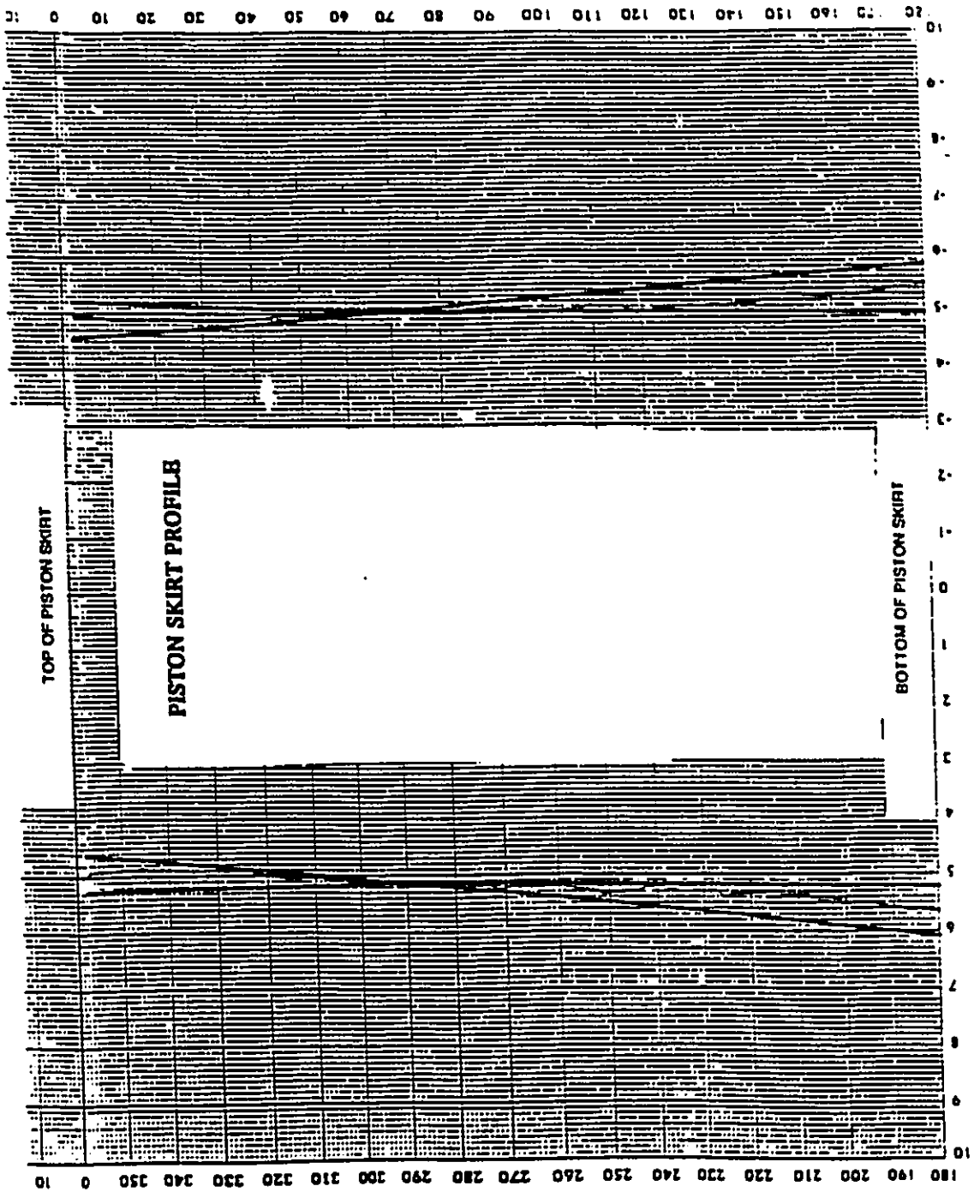
Figure 4.22 : Piston Skirt Profile

118
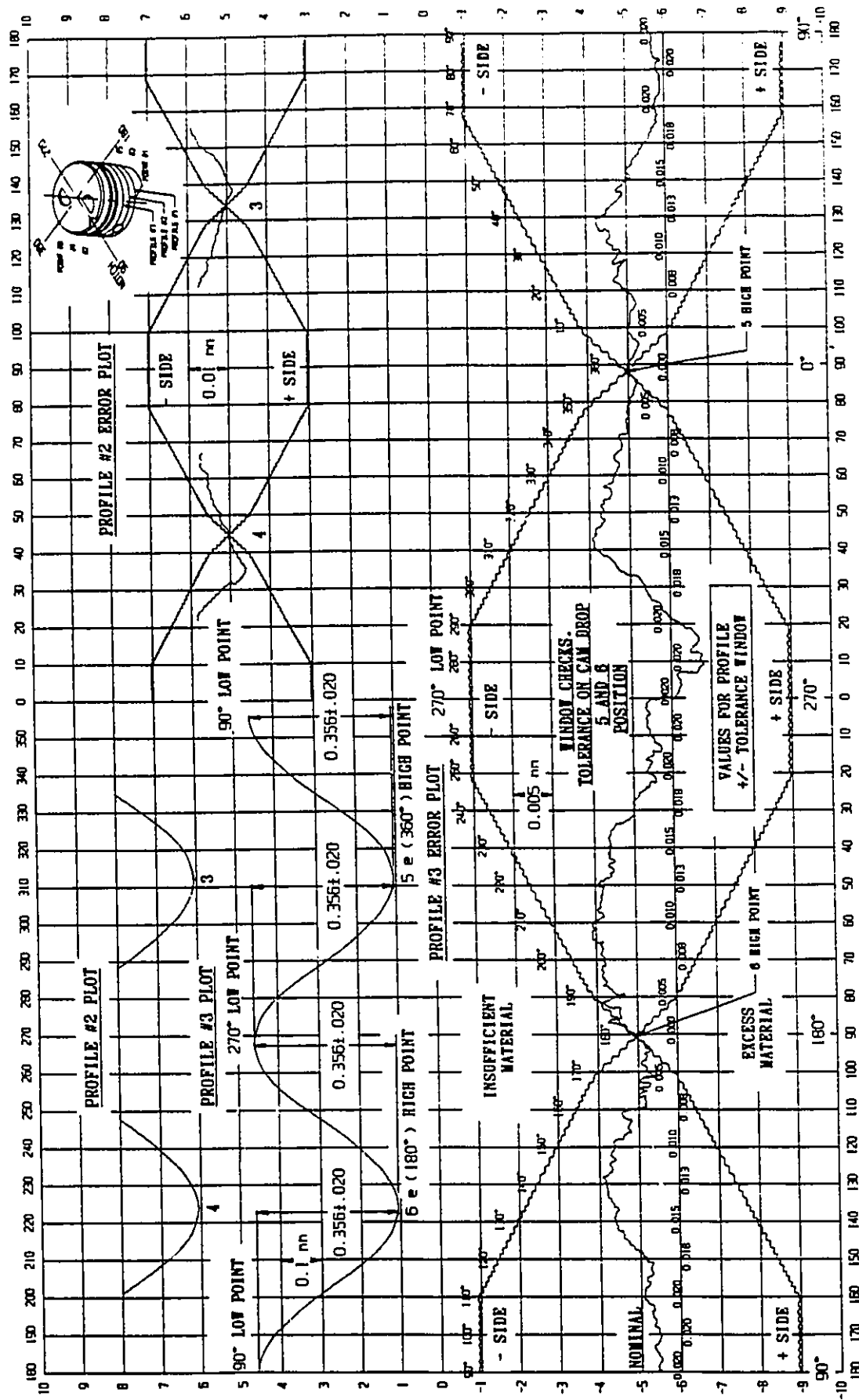
Figure 4.23 : Piston Skirt Ovality Measurements

119

CHAPTER 5.

DATA ANALYSES

The important variables which are related to the combustion and mechanical impacts to be monitored are as follows:

1) Vibration signals, either acceleration or velocity,

2) Noise signals,

3) Cylinder pressure of engine and others.

As a set-up guide, a preliminary measurement of vibration, noise and cylinder pressure signals was made to observe the engine characteristics. It was found that the vibration, noise and pressure signals are deterministic in nature. In addition, there was a distinct increase in the amplitudes of the vibration signals when the engine was running with defective engine components. Therefore, the descriptor which is able to represent these distinct characteristic changes when the defective engine runs will be meaningful and effective in this engine diagnosis study. Vibration signals were selected as the primary signals while noise and cylinder pressure signals were used to verify the results.

In this study, data analyses were carried out as follows:

1. The vibration signals obtained from the engine operations were analyzed in the time and frequency domains. Appropriate methods of analysis in the two domains were derived, separately, through visual inspection of the time-amplitude vibration signals and the frequency spectra obtained.

2. Time domain averaging and variance analysis were then performed with respect to the time datum or location datum of the data.

3. Four statistical descriptors were selected and calculated for the time domain analysis, namely: mean, standard deviation, skew, kurtosis.

4. In the frequency domain analysis, peak value of the frequency spectrum was used.

5.1 Time Domain Averaging

A typical vibration signal from normal engines is shown in Figure 5.1. In this research, a time domain averaging (TDA) technique was used to analyze the vibration signal. It is accomplished by simply averaging desired time traces. Even though simple to implement, it is a powerful technique for extracting periodic components from a raw signal. It is also useful for detection of any fault that is consistently regular, but not if transient or irregular [2]. Therefore, the time domain signal averaging technique is employed in this research. It is accomplished by simply averaging desired time traces.

A typical vibration signal from one engine cycle as shown in Figure 5.2 can separated into periodic and semi-periodic components as illustrated in Figures 5.3 and 5.4, respectively. In the separation procedure, the periodic components are determined by time domain averaging of 15 engine cycles of vibration signals, and the semi-periodic components are derived by subtracting the periodic components from the composite (original) signal.

As an attempt to relate these time traces to the history of the piston movement, in terms of crank angle, each time record is initiated at a common trigger point in both the hot and cold tests. After a sufficient length of time sweep, a new trace of time series is triggered at the same crank angle. A mathematical description of the TDA (including its properties as a filter in eliminating non-cycle linked signals), is provided in reference [22].
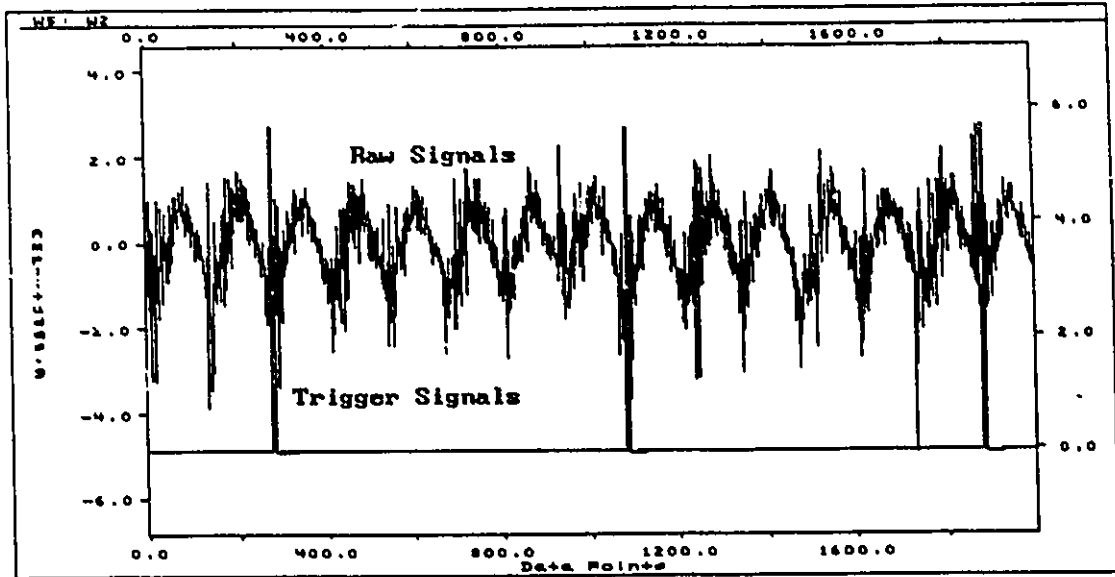
Figure 5.1 : A Typical Vibration Signal from Normal Engine
and its Trigger Signals
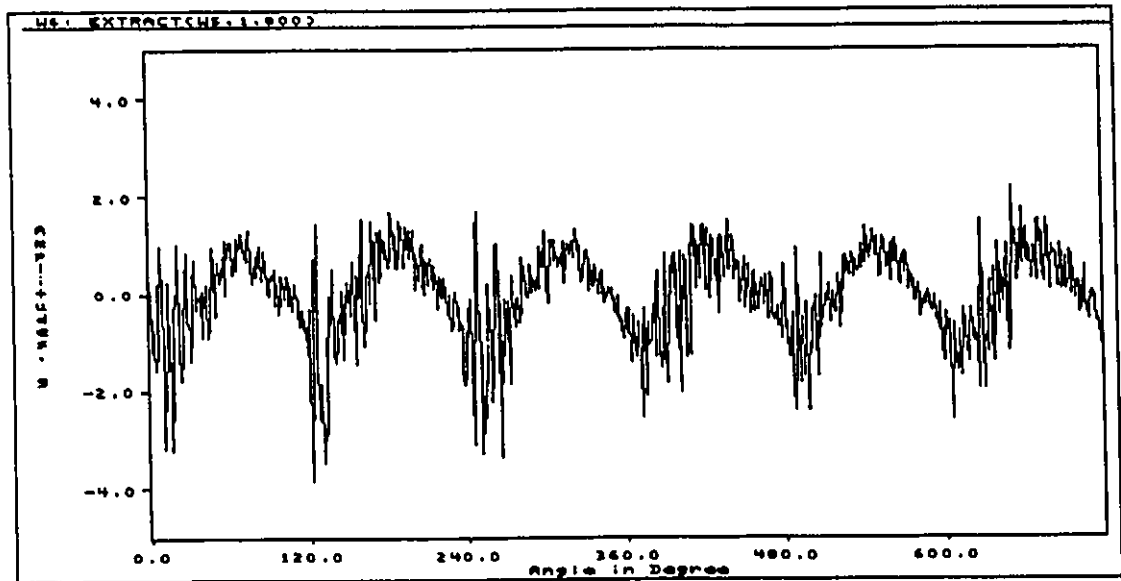
Figure 5.2 : A Typical Vibration Signal from One Engine
Cycle

122
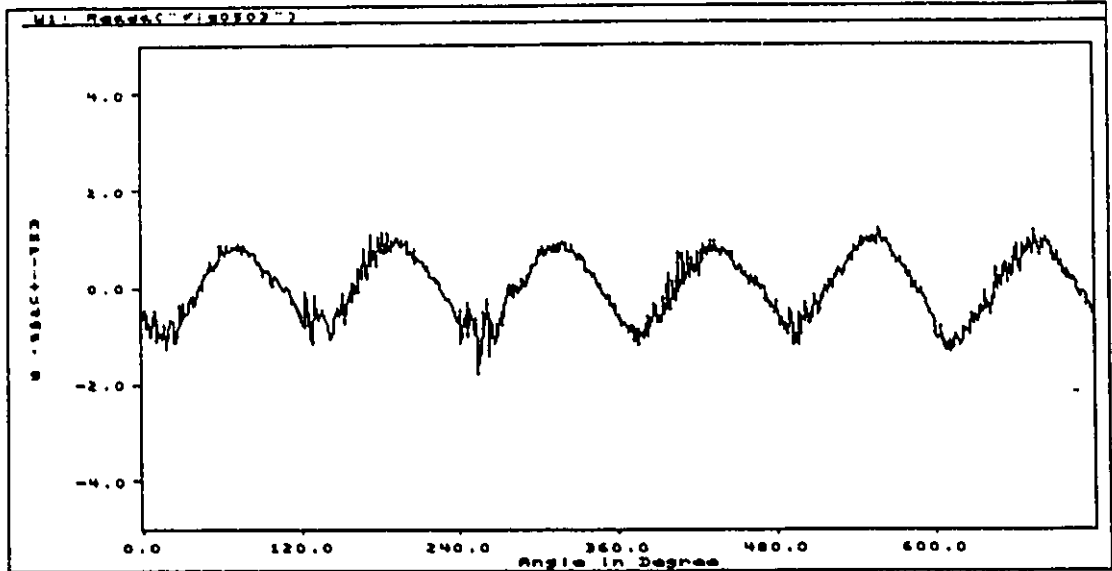
Figure 5.3 : Time Domain Average Vibration Signals from 15
Engine Cycles
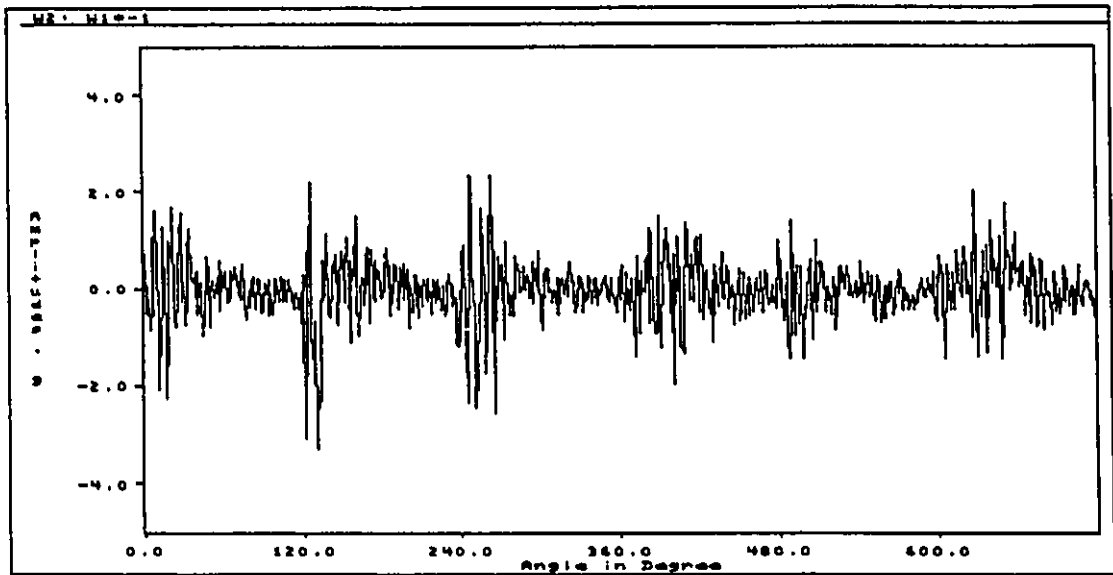
Figure 5.4 : Semi-Periodic Components of Vibration Signals

123

5.2 Statistical Parameters

In this study, three statistical descriptors were selected to describe the overall amplitude characteristics of the signals, such as its spread/dispersion, symmetry, and peakedness. They are:

1. Variance (a measure of spread)

2. Skew (a measure of symmetry)

3. Kurtosis (a measure of peakedness)

To calculate these statistical descriptors, vibration signals were first grouped according to amplitude classes. The most obvious advantage of performing computations on the grouped data is the significant reduction in the computation speed. In the grouping process, the amplitude scale was divided into classes of equal interval and the number of times data values fall in each class was tallied. As such resultant grouped data (or frequency distribution) is known as the amplitude distribution of the signal.

5.2.1 Variance Analysis

Dispersion can be defined as the degree of spread of observations about the mean. This characteristic of the distribution can be measured by either the variance (second order central moment, M2) or the standard deviation σ, (the square root of variance).

In the last section time domain averaging was described. Time domain averaging allows the extraction of periodic components which are always present in the signal. Other components, which are not always present but occur at specific positions in a cycle, are termed semi-periodic. These types of signal can be valuable in detecting faults such as bearing defects, piston slap, etc.. The mathematical development of the variance method can be found in references [22, 23] and examples of its use are presented in references [139, 143]. The basic equations needed to perform this analysis are briefly described as follows:

124

$$AV(X(i)) = Y(i) = \frac{1}{m} \sum_{r=0}^{m-1} X(i) \tag{5.1}$$

$$Z(i) = VAR(X(i)) = (X(i) - Y(i))^2 \tag{5.2}$$

where

m = the number of traces collected

i = an index for vector data points

r = the index of a particular race

$X(i)$ = the ith component of a vector X

$Y(i)$ = the average vector for all traces

$Z(i)$ = the ith component of the variance vector

In these computations, the removal of the periodic function is accomplished and, by squaring the result, the semi-periodic function information is exaggerated. This exaggeration protects the semi-periodic information from being filtering out, while at the same time noise components converge to a specific constant value over the whole variance vector. Figure 5.5 shows a typical variance of the vibration signals from a normal engine during a hot test and the waterfall plots of the variance of each engine cycle, are shown in Figure 5.6.

5.2.2 Measurement of Central Tendency and Asymmetry

Observations of the tendency to center or group themselves around a central value and the peakedness of the distribution of the vibration signals were also observed. However, no noticeable trend in data analyses was observed.
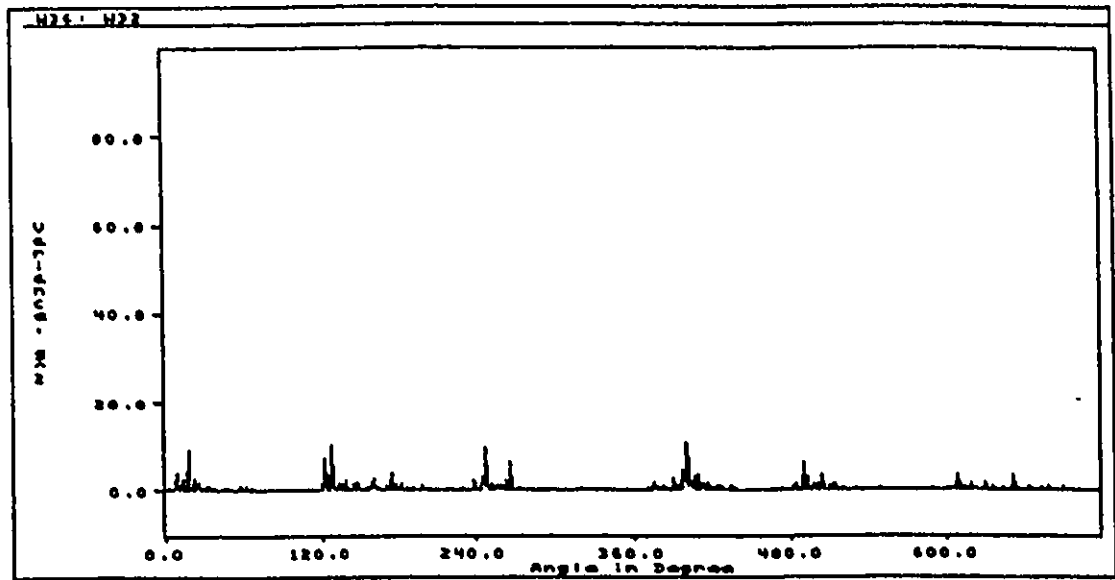
Figure 5.5 : Variance of Vibration Signals from Normal
Engine during Hot Test
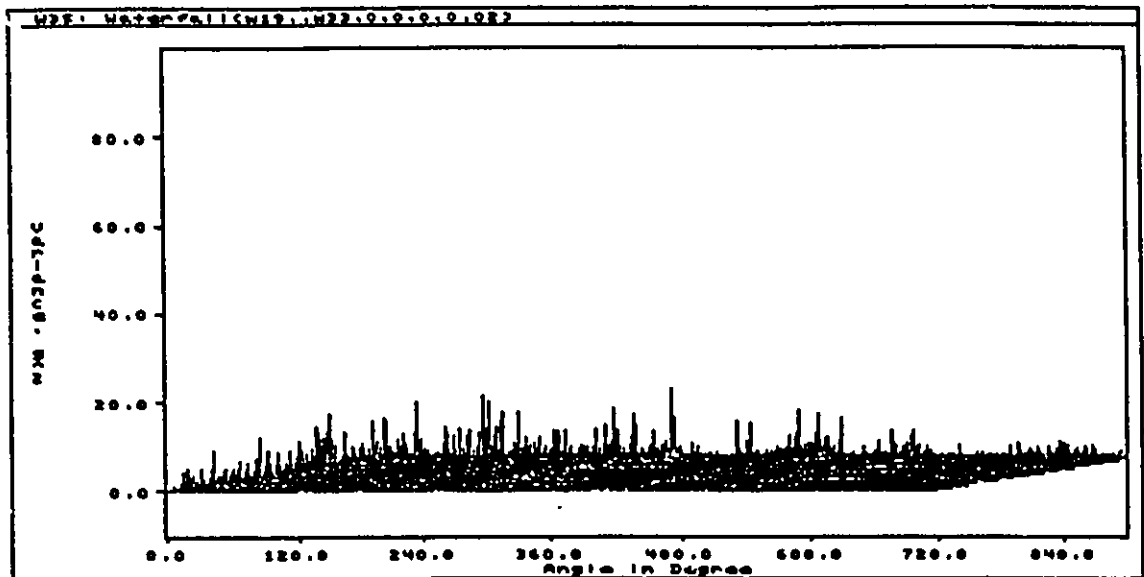
Figure 5.6 : Running Variance of Vibration Signals from
Normal Engine during Hot Test

5.3 Frequency Domain Analysis

The HP3561A FFT analyzer includes an anti-aliasing device that samples at 2.56 times the highest frequency of interest and the resulting transformed data (frequency spectrum) is represented by a set of 400 sampled values. Figure 5.7 shows a typical frequency spectrum of a vibration signal when the engine is running at 2000 rpm. Even though the engine is excited at all frequencies from 0 to 20 kHz and the measuring system response is linear within the same range, in this research only components in the range from 0 to 5 kHz were considered in the analysis. This is due to the fact that most mechanical components in engines do not respond readily to frequencies greater than 5 kHz.

Figure 5.8 illustrates a typical frequency spectrum of the engine vibration signal with a component defect, such as a reversed piston skirt taper. It was observed that, for different engine defects, the amplitude of the frequency spectrum was different. Therefore, the global peak value of the spectrum was chosen as one of the descriptors.
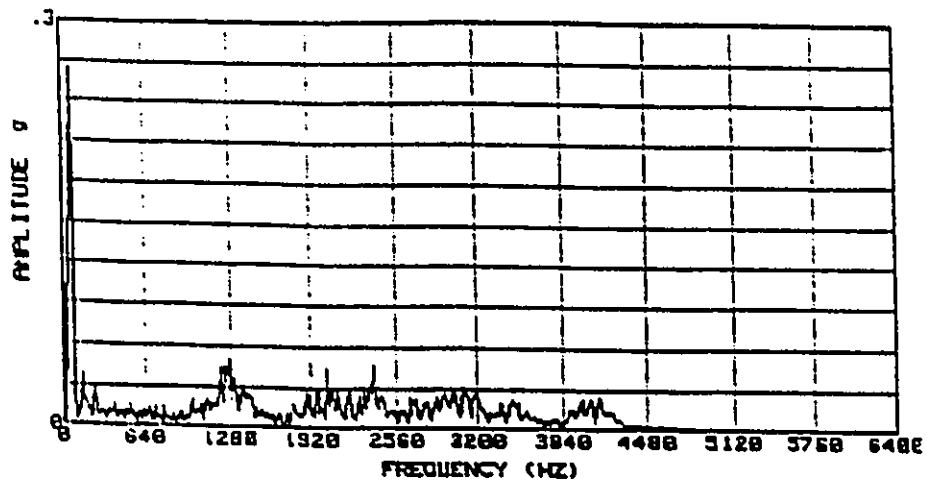
Figure 5.7 : Frequency of a Normal Engine.
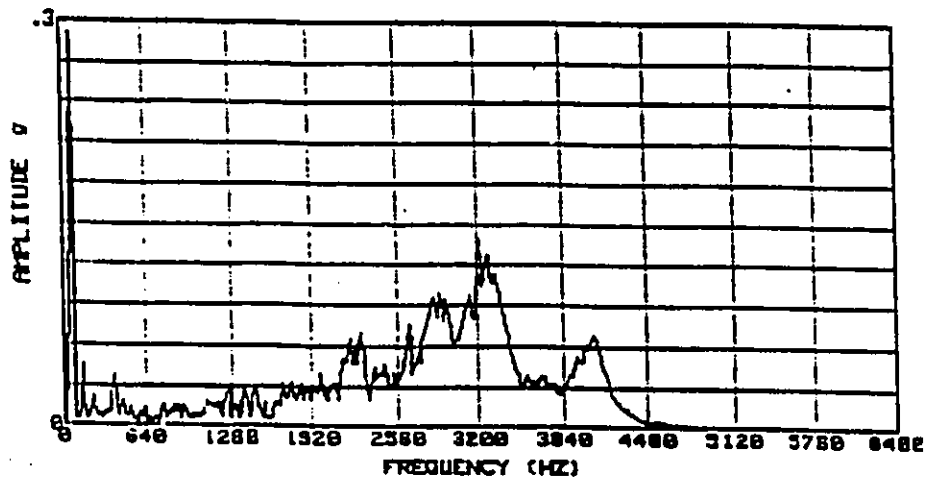
Figure 5.8 : Frequency Spectrum of an engine with Reversed Taper Piston #2.

128

CHAPTER 6.

RESULTS AND DISCUSSIONS

In this chapter, the experimental results of monitoring defective engine conditions with the use of vibration, noise and cylinder pressure signals are presented. The modal analysis of the engine block is dealt with at the beginning. This is followed by the results of the cold and hot test of the engine with different parameters and different methods. Next, the effects of the location of transducers to the corresponding amplitudes are discussed. Finally, the determination of optimum parameters to monitor the defective engine condition is also discussed.

6.1 Modal Analysis of an Engine

The vibration mode analysis of an automotive internal combustion engine block was performed in order to achieve two objectives;

1) to study the dynamic response of the engine block and its components, and

2) to determine the proper mounting locations for the vibration transducers.

Initially, 19 points on the oil pan rail surface of the engine assembly (Figure 6.1), including proposed mounting locations of two accelerometers, were selected for the frequency response function measurements. The dynamic behaviour of the oil pan rail (Figure 6.2) at different resonance frequencies is depicted in Figures 6.3 to 6.8. The corresponding frequency response functions for points #1 and #2 are shown in Figures 6.9 and 6.10.

By examining the dynamic behaviour of the oil pan rail in detail, it was observed that the first mode of the engine block appeared at the frequency of 460 Hertz with the nodal points of the structure at locations #5 and #15 respectively (Figure 6.3). A second mode of the structure appeared at a frequency of 730 Hertz with the nodal
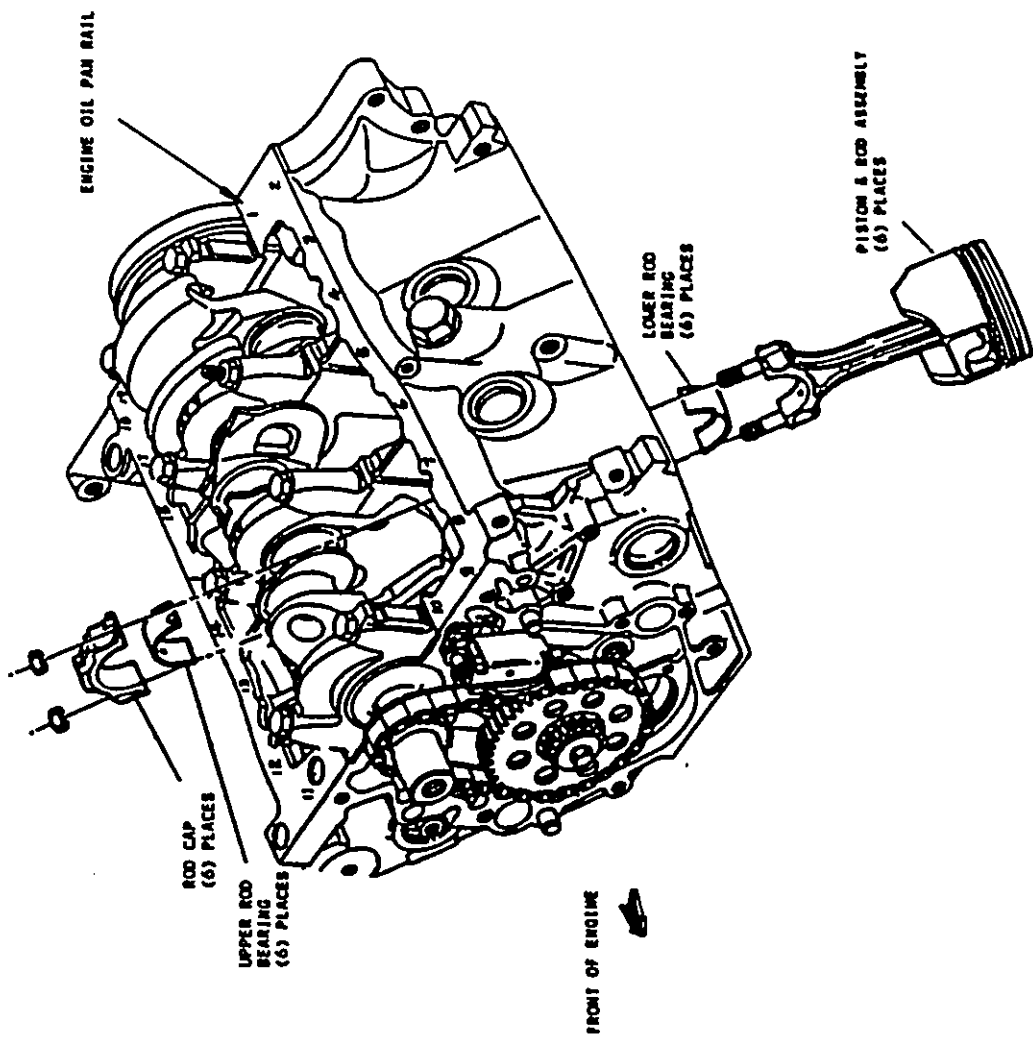
Figure 6.1 : Partially completed engine assembly

ENGINE OIL PAN RAIL

PISTON & ROD ASSEMBLY
(6) PLACES

LOWER ROD
BEARING
(6) PLACES

ROD CAP
(6) PLACES

UPPER ROD
BEARING
(6) PLACES

FRONT OF ENGINE

130

Undeformed Structure
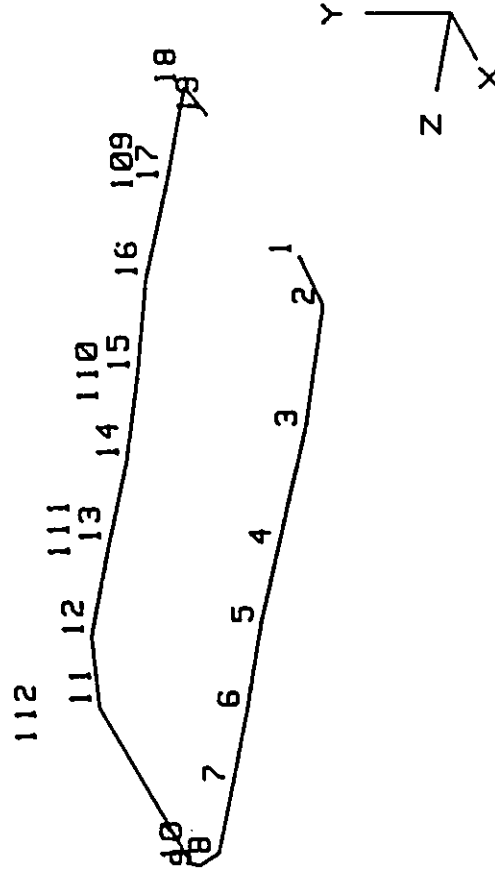
Figure 6.2 : Undeformed Shape of Oil Pan Rail & Main Bearing Caps.

Mode: 1
Freq: 460.32 Hz Damp: 1.48 %
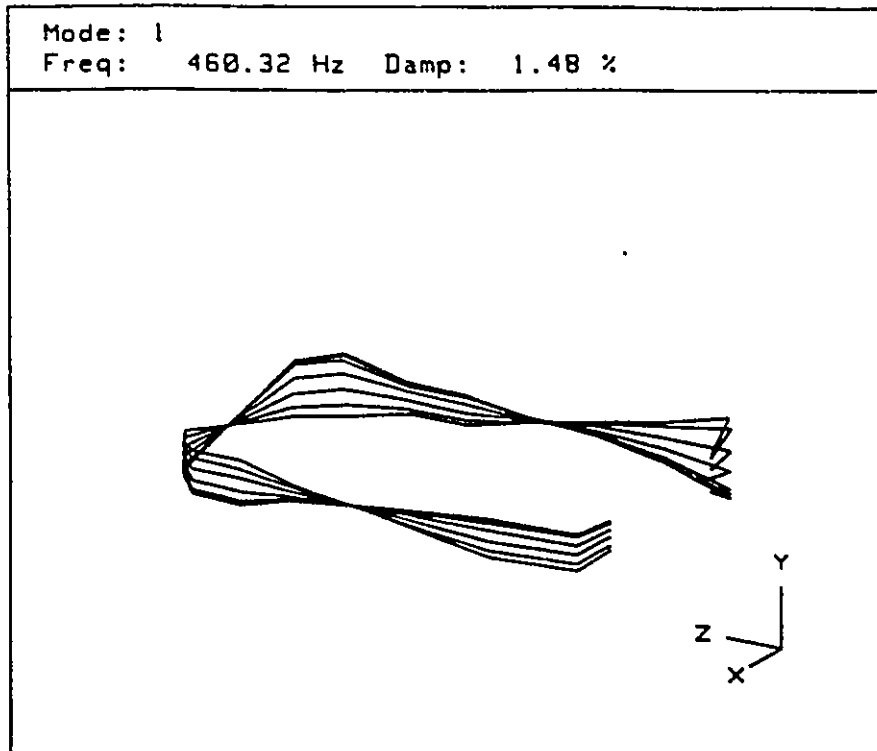
Figure 6.3 : First Mode Shape of Oil Pan Rail.

Mode: 2
Freq: 729.72 Hz Damp: .56 %
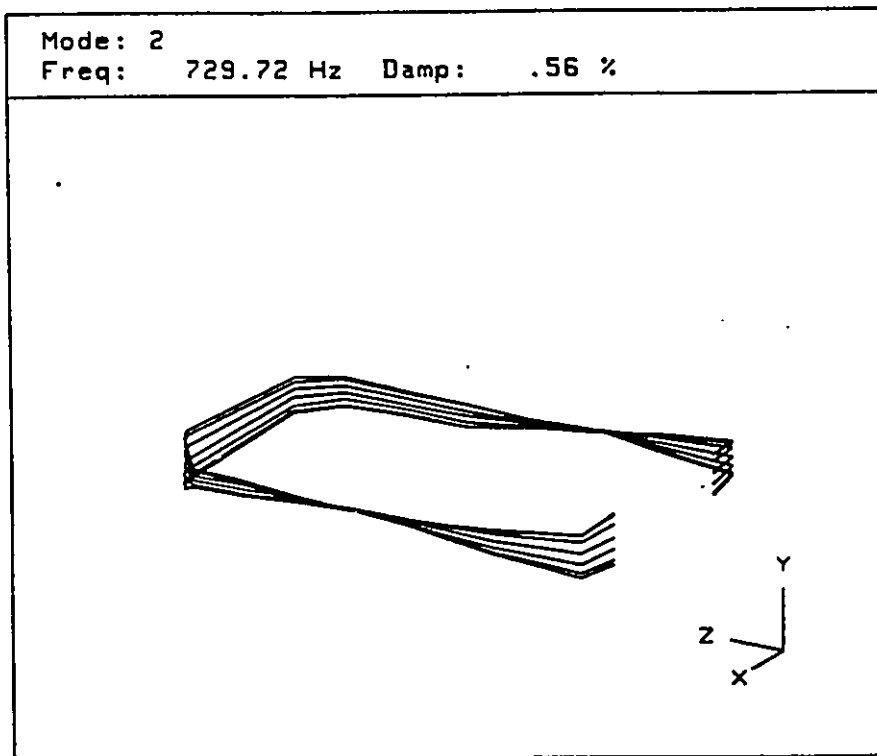
Figure 6.4 : Second Mode Shape of Oil Pan Rail.

132
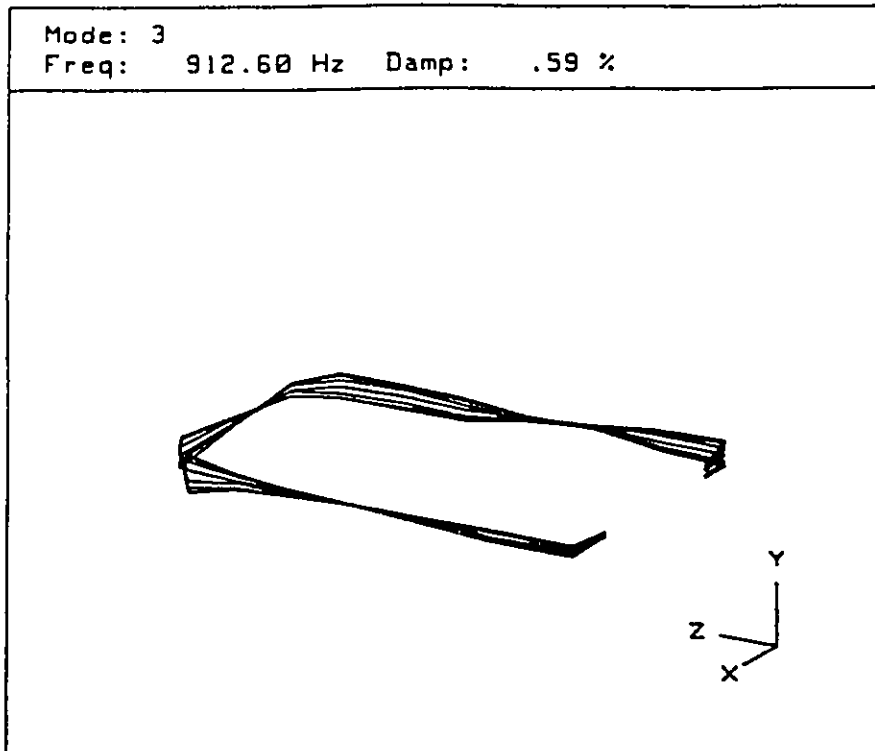
Figure 6.5 : Third Mode Shape of Oil Pan Rail.
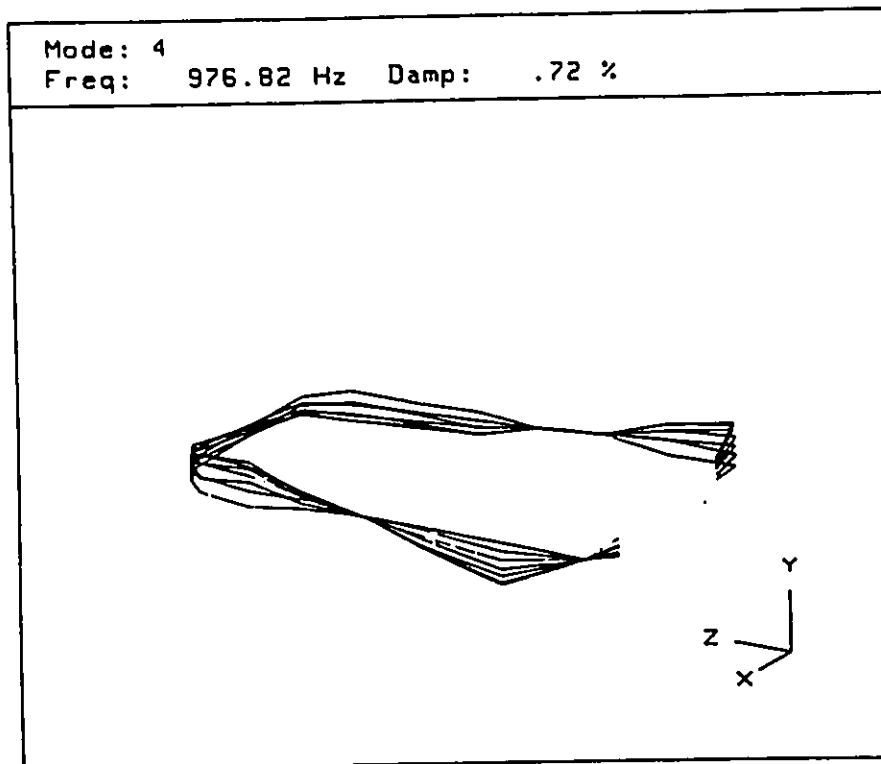
Figure 6.6 : Fourth Mode Shape of Oil Pan Rail.

133
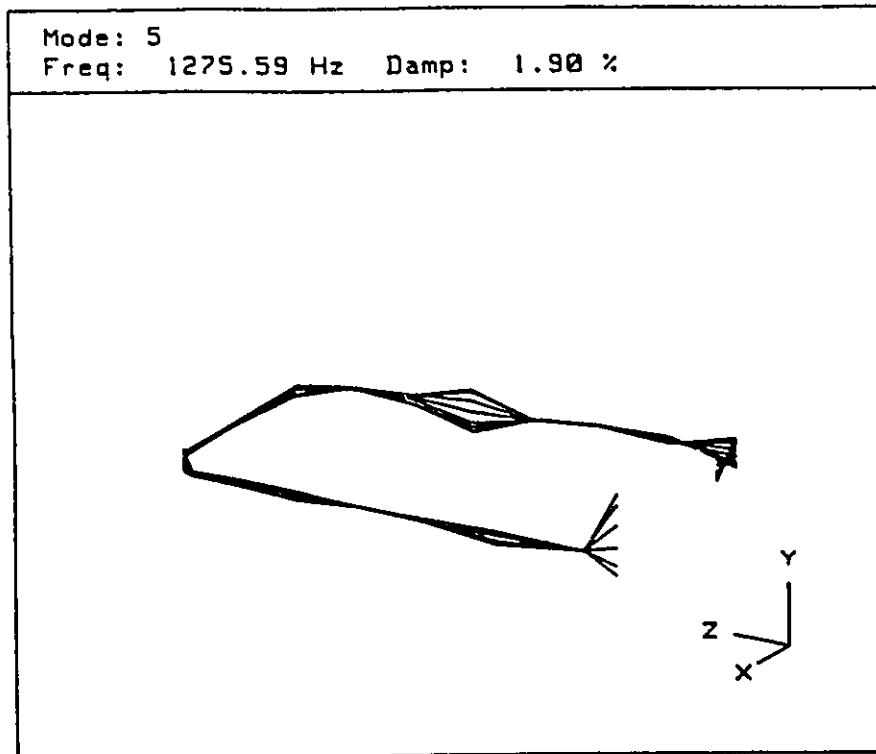
Figure 6.7 : Fifth Mode Shape of Oil Pan Rail.
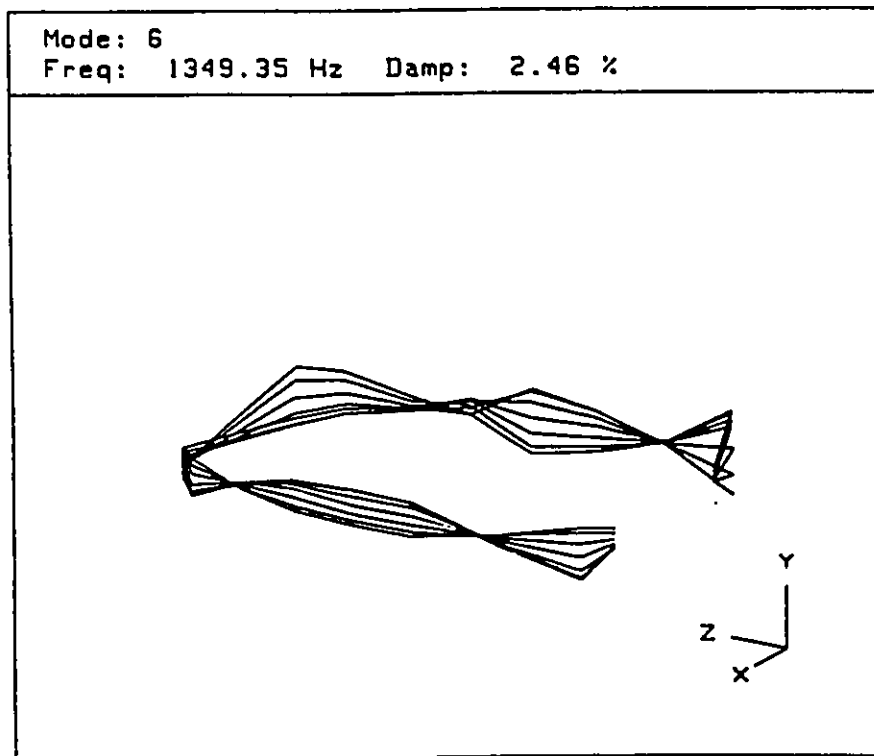
Figure 6.8 : Sixth Mode Shape of Oil Pan Rail.

134
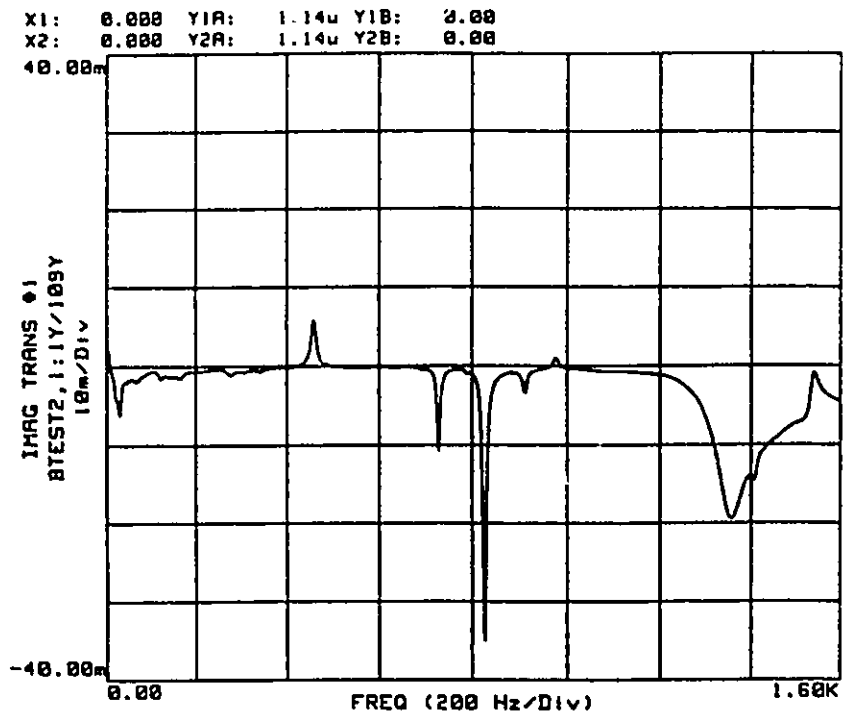
Figure 6.9 : Frequency Response Function of Point 1.
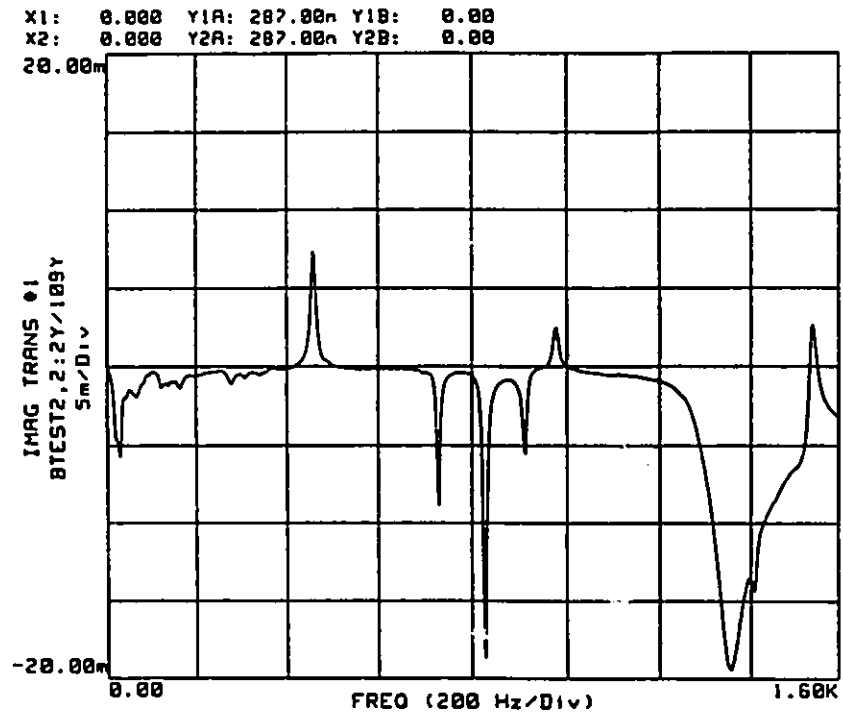
Figure 6.10 : Frequency Response Function of Point 2.

135

points also at locations #5 and #15 (Figure 6.4). Finally, the sixth mode of vibration was observed at the frequency of 1349 Hertz (Figures 6.8, 6.9 and 6.10).

In light of these results, points #9 and #18 were selected as the locations of the two accelerometers in the cold test. This selection was made essential for sensing the highest vibration response and avoiding the nodal points.

6.2 Effects of Data Processing

The effects of different signal processing methods for the defective engine monitoring are discussed in this section. Initially, different data triggering methods are discussed followed by an assessment of the different processing systems used. The results from different methods are compared and finally, optimum procedures for this study are discussed.

6.2.1 Effect of Triggering Methods

Time domain signals from an engine reflect the instantaneous motion of the various components. As the dynamic motion of the engine is cyclic (due to combustion characteristics), the time domain signals need to be examined cycle by cycle. To achieve this objective, the engine signals need to be acquired from a reference relative to the angular position of the crankshaft. However, different triggering algorithms in the data acquisition process may lead to different results in the analysis. To test this hypothesis, two different triggering methods were used in the experiments and the results will be compared in the following section.

Initially, data was captured when the acquisition system was triggered by TTL (Transistor-Transistor Logic) signals which were generated by an induction voltage at the #1 spark plug firing. The number of data points (for one engine cycle) was determined by the time period per cycle and the data sampling rate, as follows:

136

[Data points] = [sampling rate] * [period of one engine cycle].

Figure 6.11 shows the trace of a typical data set which was acquired by the use of time locked triggering method. In this figure, the upper trace represents the time domain engine signal while the lower trace represents a combination of the header signal and time locked triggering signal. The data points for one cycle were set at 1024 points which was determined by the sampling rate at a specified engine speed. However, when the engine speed is varying, the 1024 data points do not exactly cover one engine cycle. Thus any fluctuation in the speed of the engine causes difficulty in capturing exactly one cycle of engine data. Figure 6.12 shows the variation of the engine vibration signals which were captured by means of the Nicolet 440 Digital Data Acquisition System (System No. 2) when the engine speed was controlled at 1500 rpm (± 5 rpm). Although there are fluctuations in the amplitude with the cycles, the location of the peaks is consistent at approximately 390 degree of crank angle. However, when the engine speed was oscillated between 1500 rpm to 1800 rpm, the locations of distinct peaks were scattered, as shown in Figure 6.13.

Similar experiments were repeated with a different data acquisition system. Figure 6.14 shows a variance of the time domain vibration which was captured by the HP3561A Dynamic Signal Analyzer (System No. 1) at 1500 ± 5 rpm while Figure 6.15 was acquired at 1500 to 1800 rpm. These results showed similar behaviour to that obtained by means of the Nicolet 440 system..

To overcome the disadvantage of time locked triggering, position locked triggering was employed to acquire the data. In this method, the signals for triggering the trace are from the pulses generated from a custom designed encoder attached to the crankshaft.

For this set of tests, the results indicated that the location of the peak amplitudes is consistent for both constant and varying engine speeds (Figure 6.16 and Figure 6.17). After testing, the engine was disassembled for mechanical and visual inspections to

137
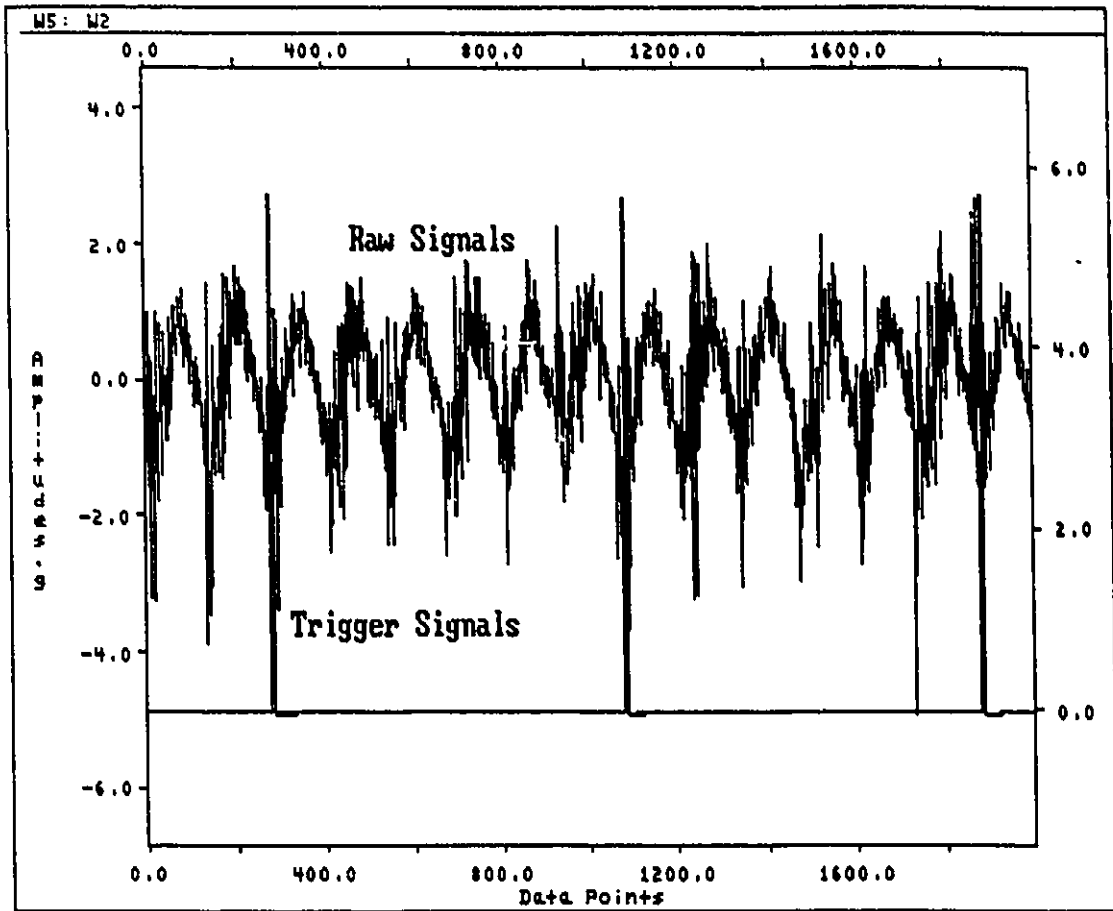
Figure 6.11 : A Typical Vibration Signal from a Normal
Engine and its Trigger Signal
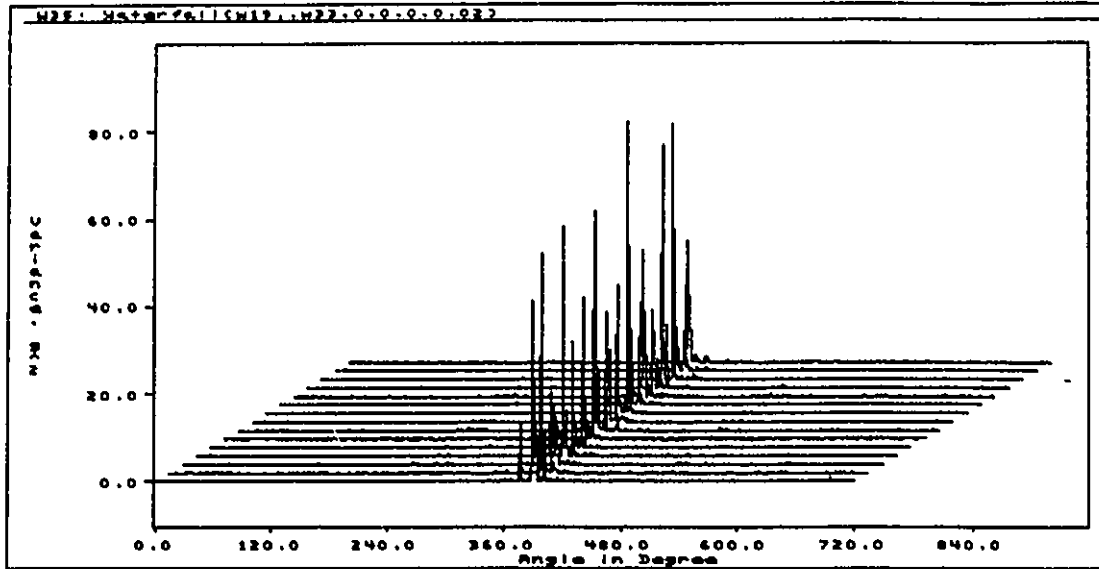
Figure 6.12 : Vibration Variance of an Engine with
Defective #5 Piston using System No. 2, i.e.
Time Locked Triggering Method
(Constant 1500 rpm)
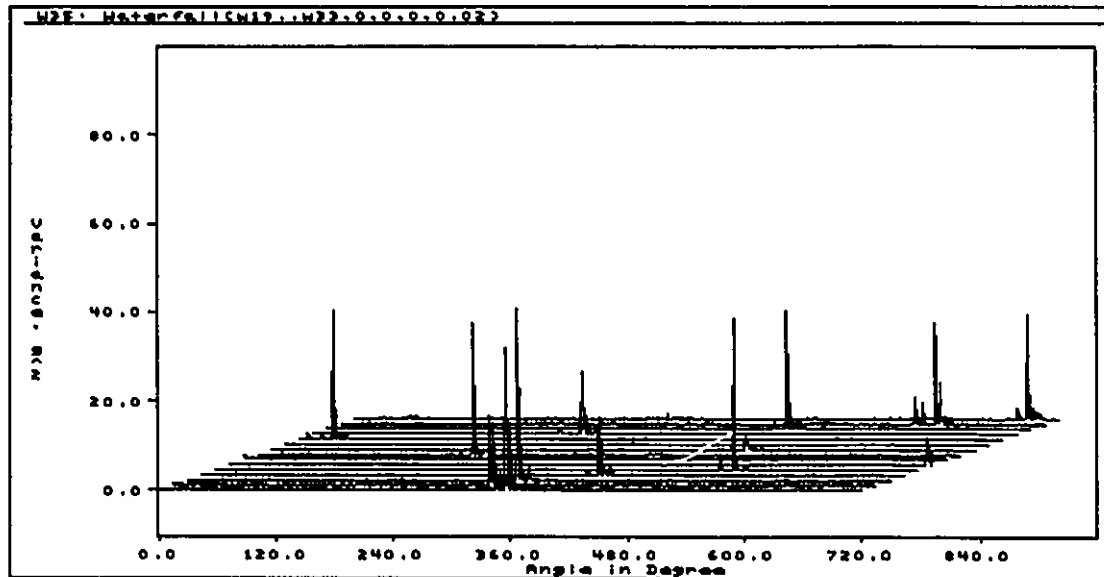
Figure 6.13 : Vibration Variance of an Engine with
Defective #5 Piston using System No. 2, i.e.
Time Locked Triggering Method
(1500 to 1800 rpm)

139
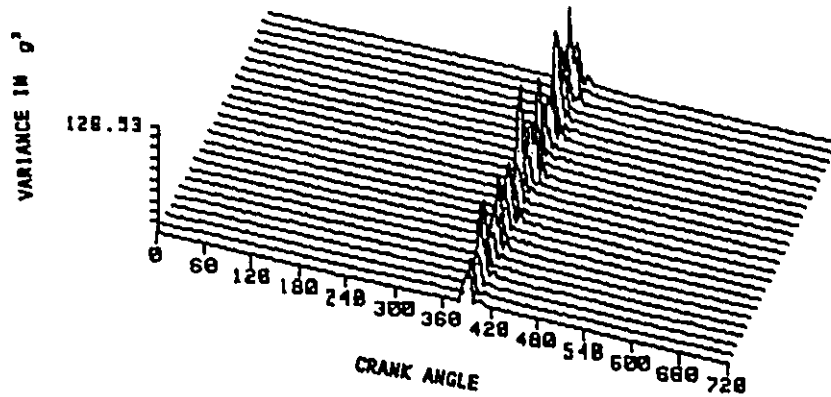
Figure 6.14 : Vibration Variance of An Engine with
Defective #5 Piston Using System No. 1, i.e.
Time Locked Triggering Method (Constant 1500
rpm)
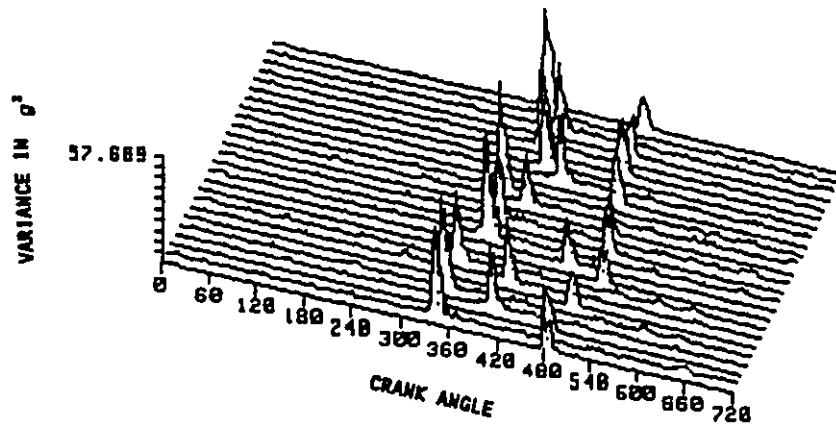
Figure 6.15 : Vibration Variance of an Engine with
Defective #5 Piston Using System No. 1, i.e.
Time Locked Triggering Method (1500 to 1800
rpm)
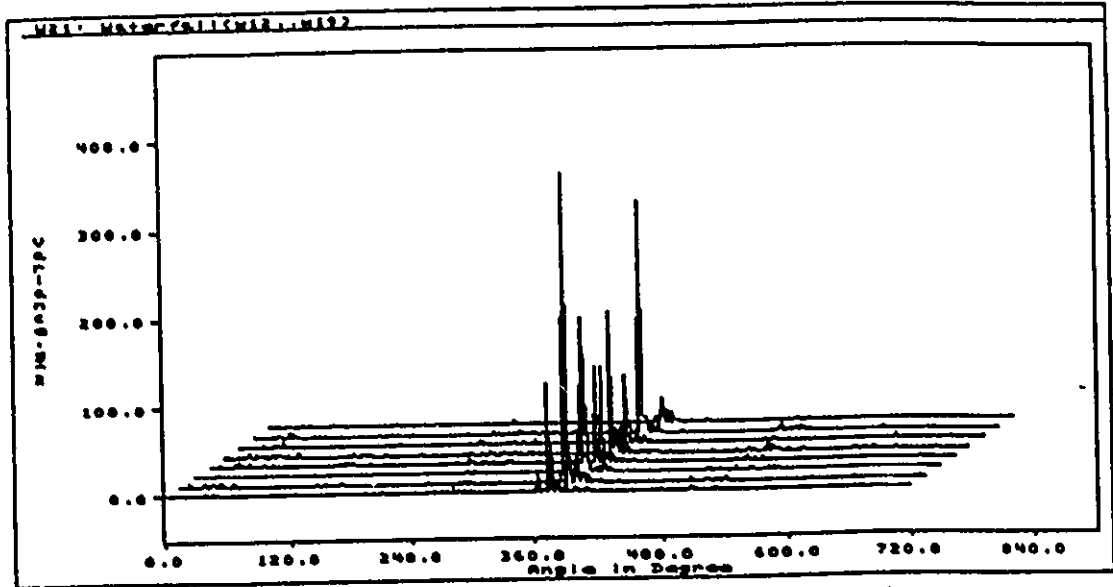
Figure 6.16 : Vibration Variance of an Engine with
Defective #5 Piston Using System No. 3,
i.e. Position Locked Triggering Method
(Constant 1500 rpm)
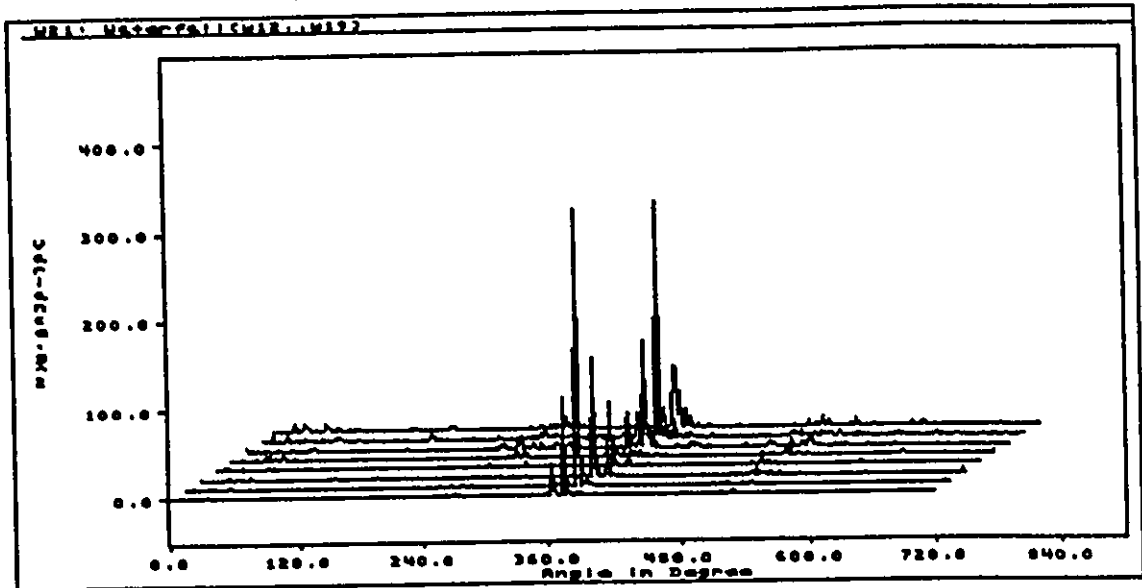
Figure 6.17 : Vibration Analysis of an Engine with
Defective #5 Piston using System No. 3,
i.e. Position Locked Triggering Method
(1500 to 1800 rpm)

141

identify the defective components.

After performing more than 100 engine tests using the position locked triggering method, it was found that the results were repeatable and reliable. Thus, this method is selected for the triggering mechanism for subsequent data collection.

6.2.2 Effect of Signal Processing

In this section, the effect of signal processing on the detection of faults is analyzed. In the experiments, three different vibration data acquisition systems - HP3561 Dynamic Signal Analyzer, Nicolet 440 Digital Signal Analyzer and the custom made 8 Channel Data Acquisition System were employed. The data were evaluated to select the most effective system to monitor the defective parts in engines.

Initially, the Hewlett Packard Dynamic Signal Analyzer was employed to capture the vibration and noise signals. This system captures 1024 data points for each sweep and the time and/or frequency records are compressed to 399 data points for display. As an illustration of the typical results of this method, the variance of the vibration signals versus crank angle is plotted in Figures 6.18 and 6.19. It should be noted that the firing order of the six cylinder engines used in this study was 1, 4, 2, 5, 3, 6. In these results, it was observed that the distinct vibration amplitudes were originated from number 2 cylinder in the engine. This distinct noise was identified as well by the experienced stethoscope operator at number 2 cylinder.

There is a drawback with this system. As the data collection and processing were carried out serially, there will be a gap in the recorded trace. This gap creates difficulty in analyzing the data as illustrated below.

Figure 6.20 shows a sample result of variance of random vibration signals from a customer returned engine. According to the average variance of the signal, as shown in Figure 6.21, it is evident that there are certain occurrences of excessive vibration at every 120 degrees span. However, non-periodic random amplitudes are also observed in the
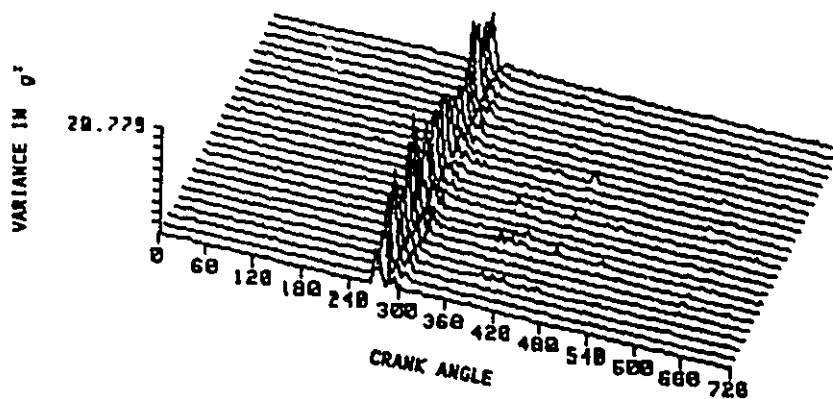
Figure 6.18 : Vibration Variance of an Engine with
Defective #2 Piston with Accelerometer on
Location 2.
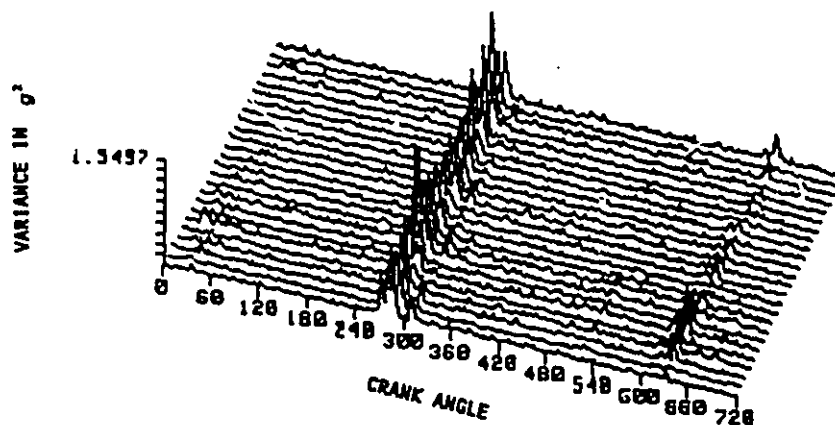
Figure 5.19 : Vibration Variance of an Engine with
Defective #2 Piston with Accelerometer on
Location 6
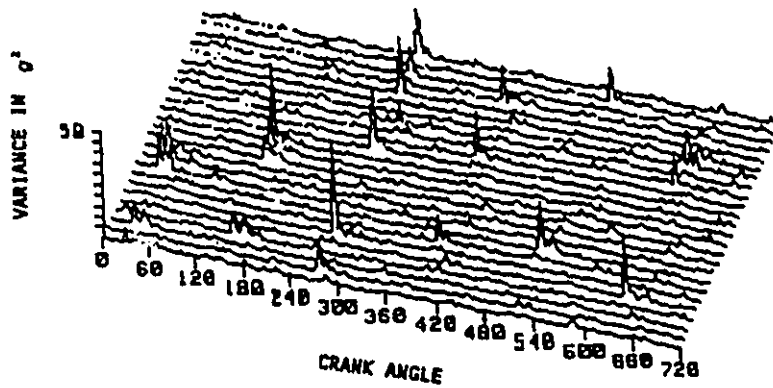
Figure 6.20 : Vibration Running Variance of an Engine with
Defective #6 Piston
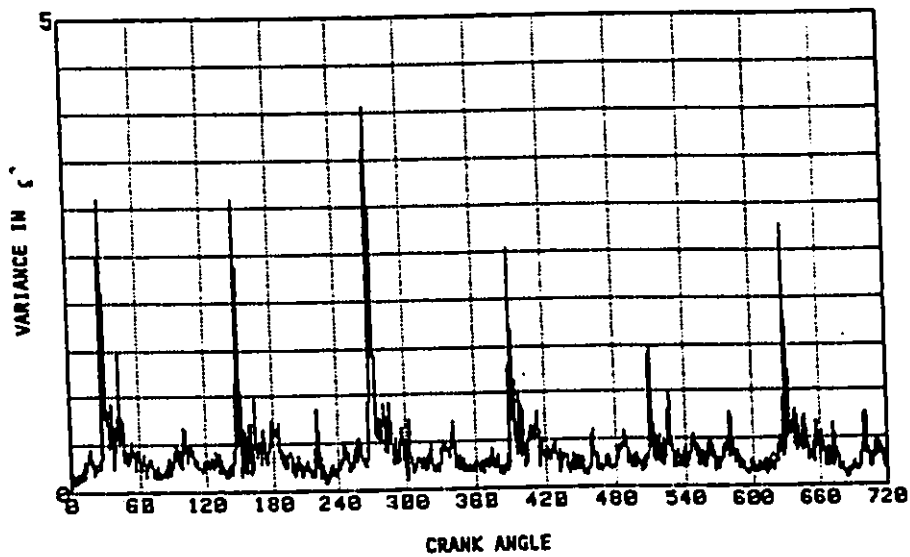
Figure 6.21 : Vibration Average Variance of an Engine with
Defective #6 Piston

144

waterfall plot due to the discontinuity in the measured vibration signals. A check with a stethoscope indicated that the noise source was from piston number 6, and the audible ticking noise was perceived at every piston pin reversal point. A subsequent engine teardown analysis showed that the defect was an oversized ringland diameter of piston number 6. Thus there is a possibility of misdiagnosis of the engine defect with this method especially if the defect is associated with a random vibration. To overcome this problem, it is necessary to use a system which is capable of capturing and storing time data continuously.

Therefore, a custom designed eight channel data acquisition system was employed to monitor the engine conditions. In this study, however, only six of the channels are used.

Vibration data was captured with the eight channel data acquisition system when the engine was running at 2000 rpm. All the transducers were calibrated before being installed on the engine and the vibration signals for 64 revolutions of the engine were monitored. The variations of the vibration signals were then analyzed and plotted as shown in Figures 6.22 to 6.24. Distinct amplitudes of variation can be observed at the crank angle of 385 degree, which is equivalent to the top dead center of piston number 5. In order to assess the efficiency/ effectiveness of the defect detection method, the following are to be considered:

a) the effect of location of transducers on the amplitude of variance and

b) consistency of the amplitudes of variance between engine cycles.

Considerable differences in amplitudes of variance exist, depending on the location of transducers. As shown in Figures 6.22 to 6.24, the results from three channels exhibit distinct amplitudes at the same location in each cycle. However, their magnitudes are different depending on the location of transducers. Especially the amplitudes from channel number 5, (with the transducer located on the defective cylinder), are considerably higher than others. From these experiments, it is concluded

145
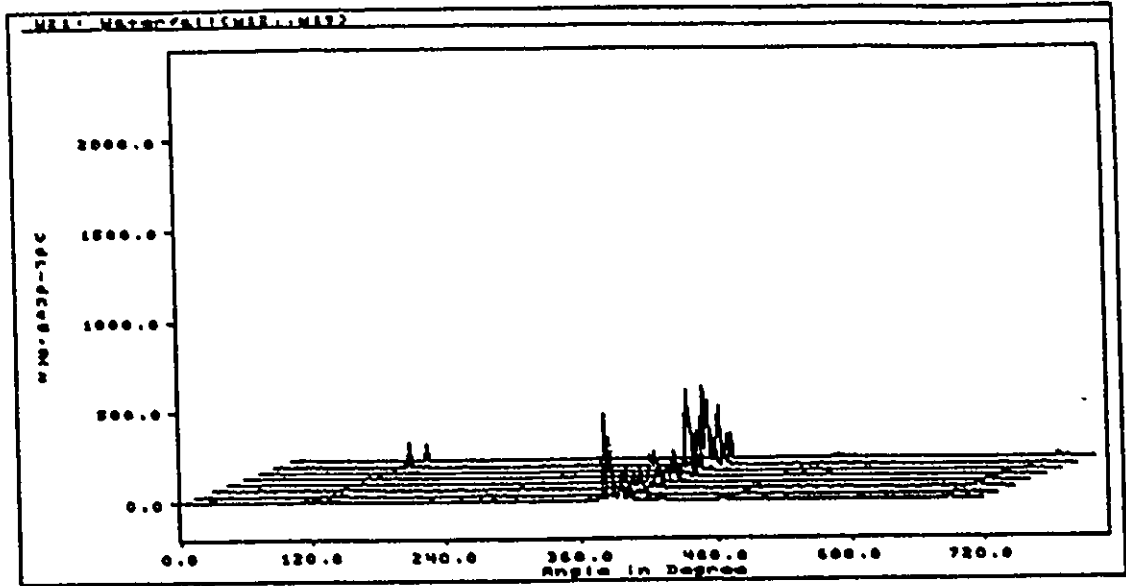
Figure 6.22 : Vibration Variance of an Engine with
Defective #5 Piston at Location of the
Accelerometer on Cylinder Wall #4
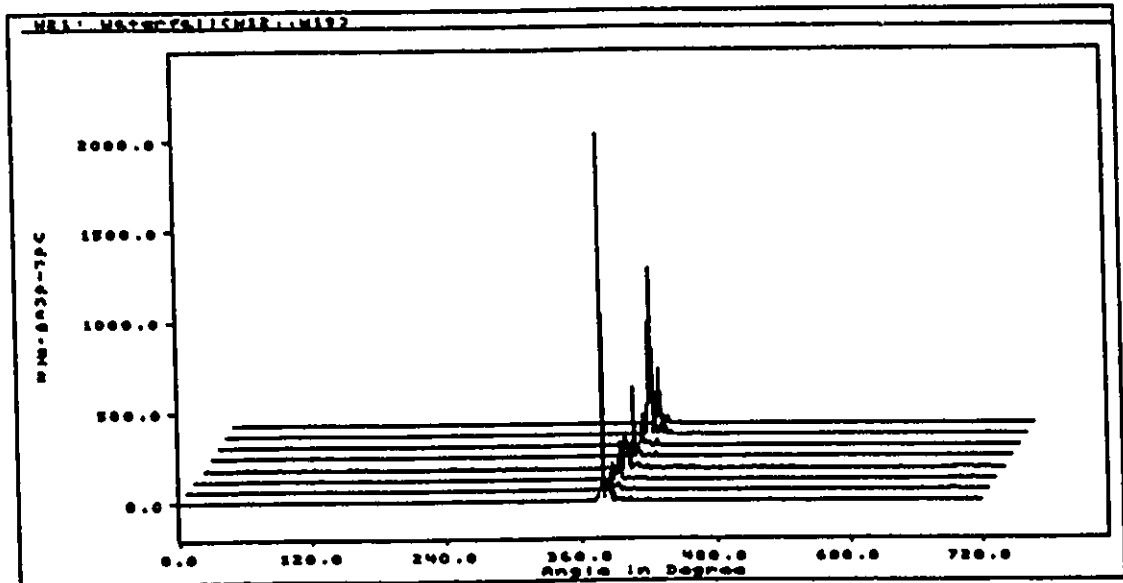
Figure 6.23 : Vibration Variance of an Engine with
Defective #5 Piston at Location of the
Accelerometer on Cylinder Wall #5

146
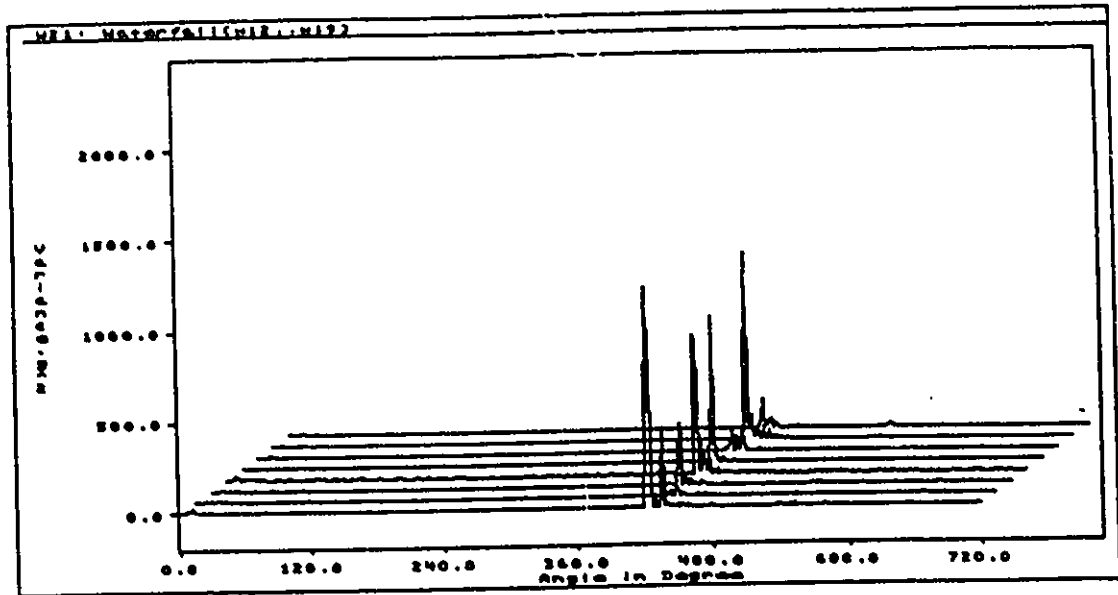
Figure 6.24 : Vibration Variance of an Engine with
Defective #5 Piston at Location of the
Accelerometer on Cylinder Wall #6

that:

1) Multi channel data acquisition systems are required to compensate for the inconsistency of amplitudes due to the location of the transducers.

2) An optimum engine speed for data acquisition has to be determined in order to achieve the minimum data processing time and to compensate for the inconsistency of amplitudes between cycles.

6.3 Cold Test of Engine

The vibration and noise of engines were monitored when driven at the specified speeds of 250 and 420 rpm by an electric motor for both normal and defective engines. Higher speeds were avoided to prevent possible damage of engine due to insufficient lubrication.

To measure vibration, two accelerometers were mounted on the pan rail of the engine block. The outputs were captured using a six channel data acquisition system through an Allen-Bradly Portable Programming Terminal.

To measure noise, a Bruel and Kjaer Type 4150 microphone was used with the sound level meter Type 2231.

In the data acquisition, reference vibration and noise signals were initially captured from a normal engine whose components were within engineering specifications. The vibration and noise signals from defective engines were then recorded from two accelerometers or a microphone. The details of the measurement will be considered in the next section

6.3.1 Vibration Measurements

Vibration signals from the engine which was driven by an electrical motor, were acquired through two accelerometers. Data was obtained for a time period of 0.24

seconds which is equivalent in duration to 8 revolutions of the crankshaft when the engine is running at 250 rpm. The number of data points was reduced to 1024 points per revolution to minimize the data processing time. Experiments were repeated for 35 engines with different defective characteristics. A position locked encoder signal, which was modulated to generate 5 volts TTL signal at a particular location (10 degrees before TDC of the piston) of the crankshaft, was used to trigger the data acquisition system to capture the vibration signals.

Figures 6.25 and 6.26 show composite vibration signals from a normal engine during a cold test. It can be seen that the vibration response from a normal engine is low and consistent. These measurements were compared to the vibration signals from engines with missing or defective engine parts in piston #1. This was repeated for every piston in the firing order sequence and for 35 engines. Figures 6.27 and 6.28 show the vibration signals (of two different channels) from a defective engine during the cold test. A normal engine has low and consistent amplitude distribution whereas the defects produce large and distinct peaks.

In the experiment it was observed that the amplitudes of vibration are dependent upon the location of the accelerometer as illustrated in Figures 6.27 and 6.28. Higher engine speed also causes the vibration signal to increase as shown in Figures 6.29 and 6.30.

Once captured, the signals were analyzed by means of time domain averaging, variance, and frequency analysis which will be discussed in the next section.

6.3.1.1 Time Domain Averaging and Variance Analysis of Vibration Signals

The averaging of vibration waveforms was performed for 15 engine cycles for a normal engine. No significant differences were observed in signal amplitudes as shown in Figure 6.31. However, for defective engines, distinct spikes appeared in the trace (Figure 6.32). These spikes correspond to the location of side force reversals in the

149
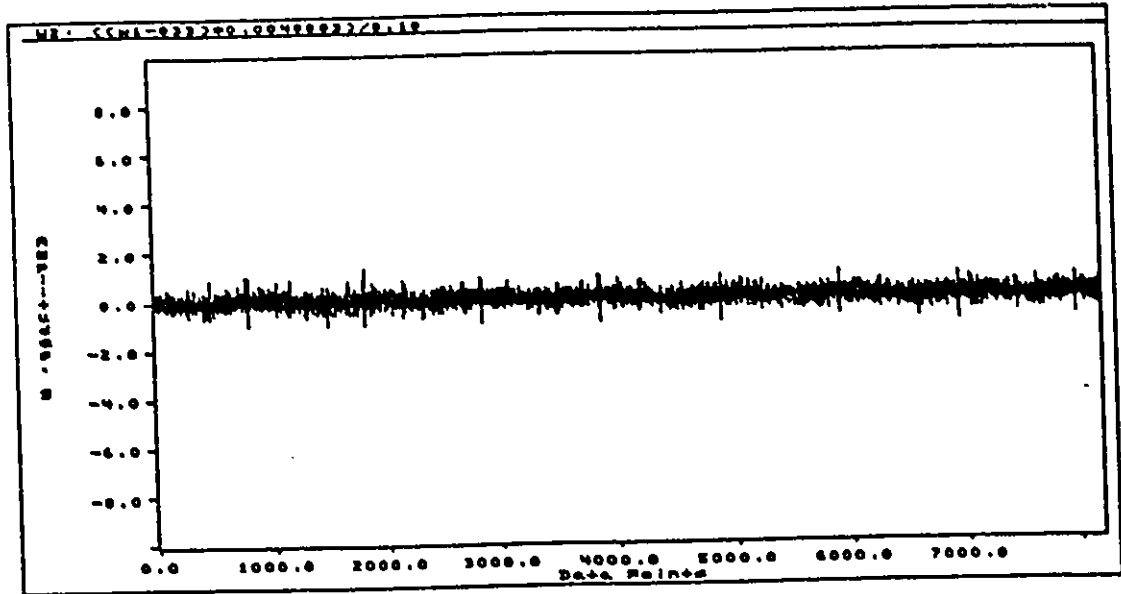
Figure 6.25 : Channel 1 Raw Vibration Data for Normal
Engine
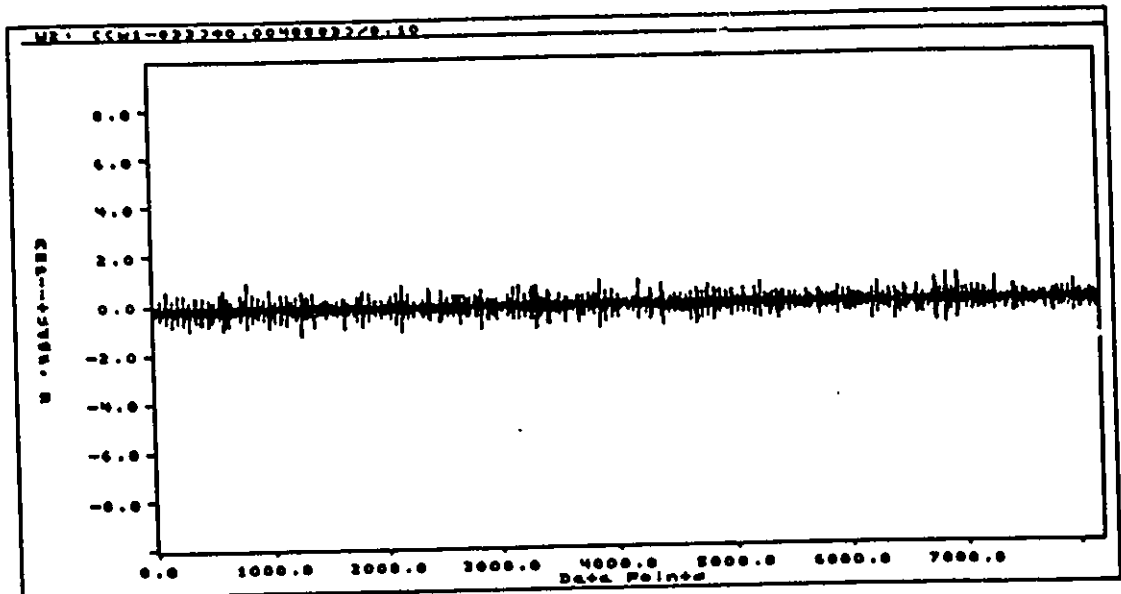
Figure 6.26 : Channel 2 Raw Vibration Data for Normal
Engine
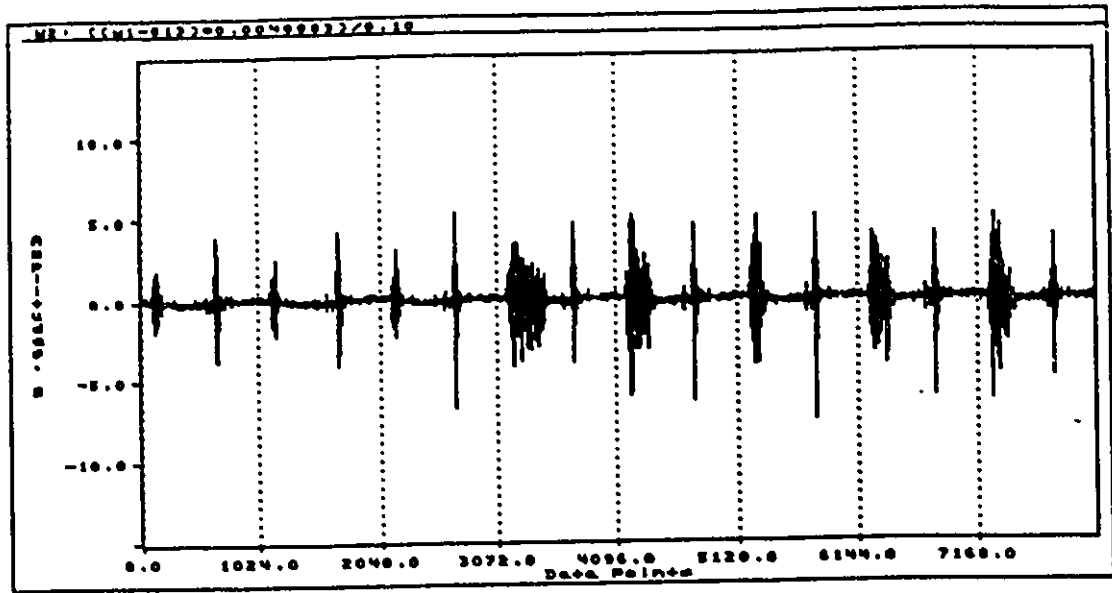
Figure 6.27 : Channel 1 Raw Vibration Data for Defective Engine
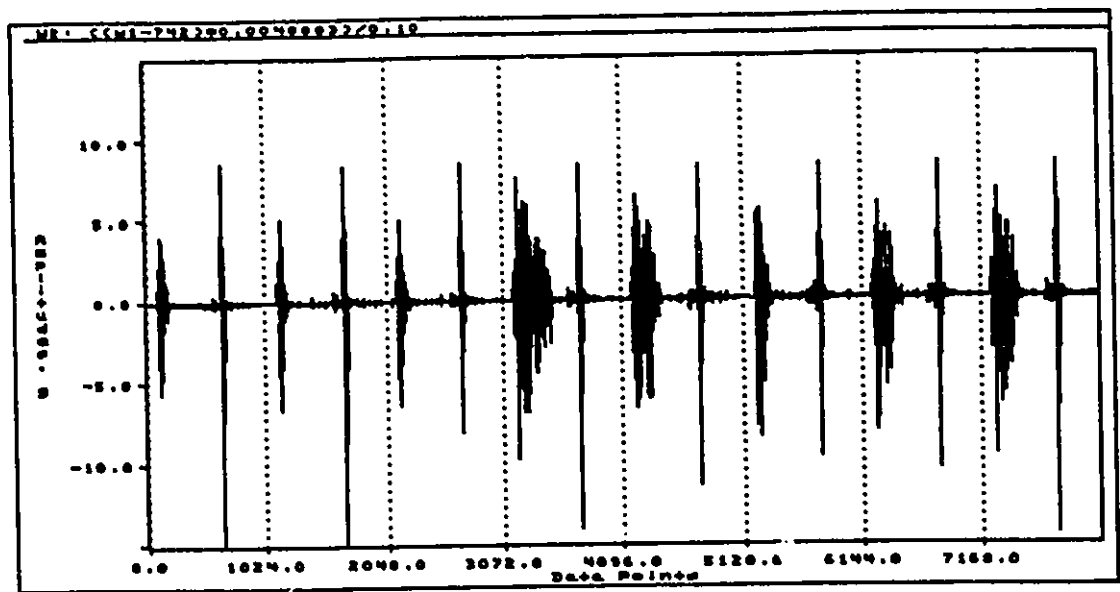
Figure 6.28 : Channel 2 Raw Vibration Data for Defective Engine

151
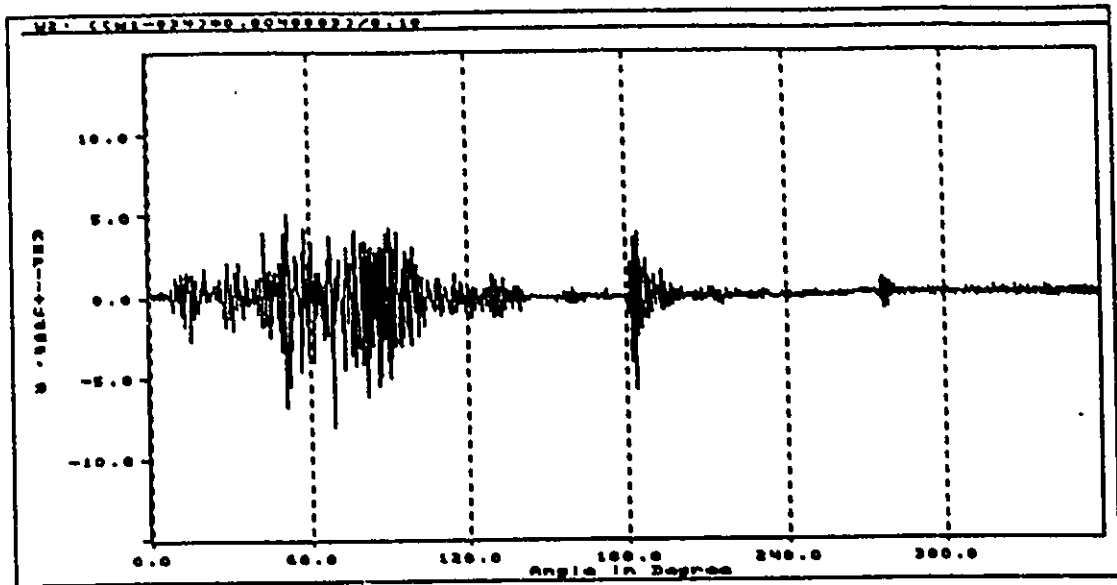
Figure 6.29 : Raw Vibration Data for Defective Engine at
Low Speed (250 rpm)
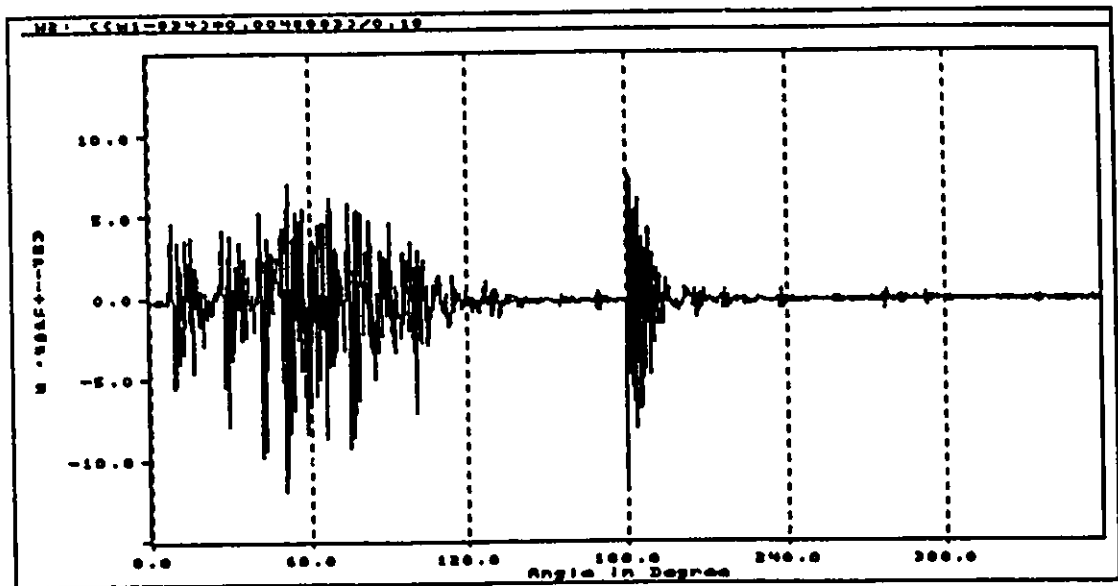
Figure 6.30 : Raw Vibration Data for Defective Engine at
High Speed (400 rpm)

152
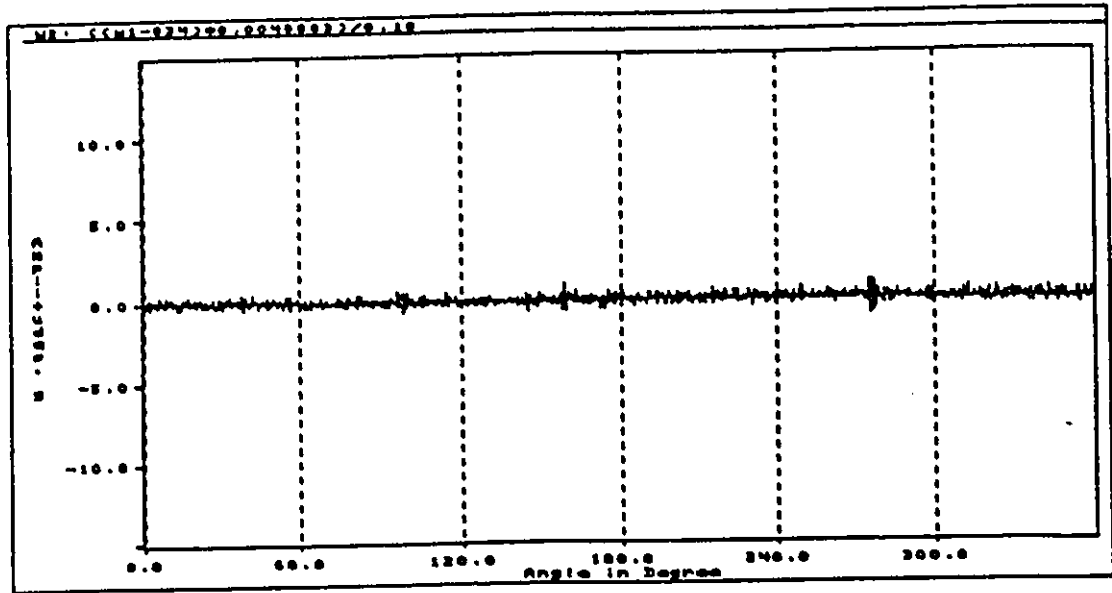
Figure 6.31 : Average Waveform of a Normal Engine
During Cold Test
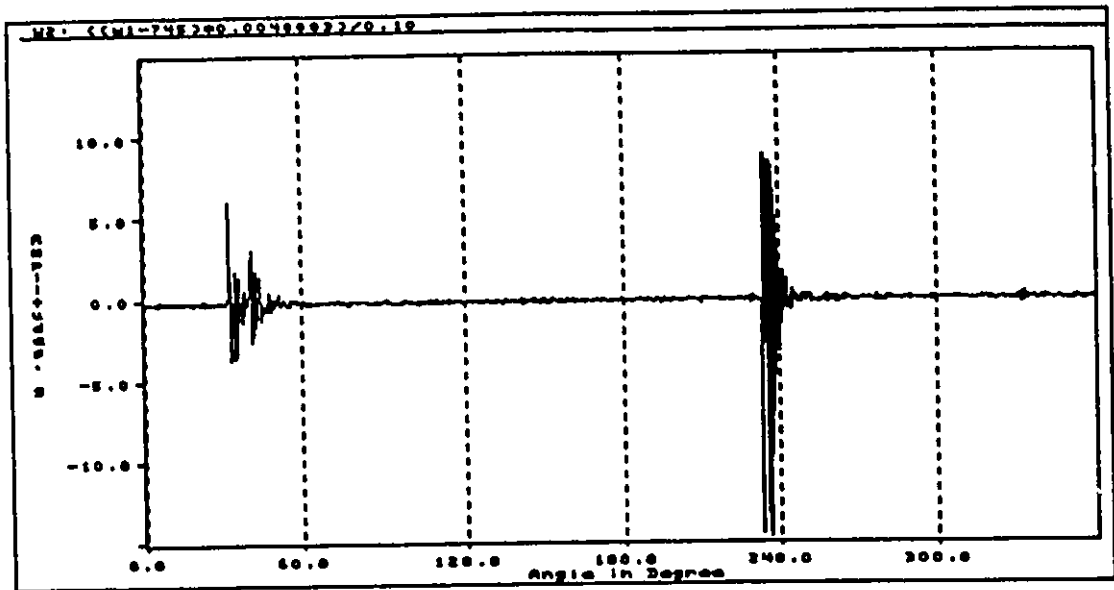
Figure 6.32 : Average Waveform of a Defective Engine
(#1 Cap Bearing Omitted) during Cold Test

153

piston.

Better results were obtained when the variance analysis was performed on the raw signals. This is illustrated by the waterfall plot of variance of vibration signals for seven engine cycles during a cold test of a defective engine (with the cap bearing of #1 piston connecting rod missing). Distinct amplitudes are present at TDC and BDC of #1 piston. Because of the success, this test was repeated for different defective parts on different pistons of the engine.

6.3.1.1.1 Detection of Missing Connecting Rod Bearings

With the test configuration discussed previously, the engine was operated with a missing connecting rod bearing in piston #1. Measurements were then taken and the process was repeated in turn for every piston of the engine with a missing bearing. Figure 6.32 shows a sample of a TDA signal from an engine with a missing rod bearing cap on #1 piston. The distinct peaks appeared at crank angles of 20 and 220 degrees which are slightly off the TDC and BDC of the piston. Similar results were observed for engines with different defects as shown in Figures 6.33 to 6.40. After reviewing these results, the following conclusions are drawn:

1. the vibration levels measured for the normal engine are very low and consistent,

2. there are two vibration pulses per revolution for each missing bearing and

3. the pulses occur over a finite period which is relatively short in duration.

A summary matrix of performance factors was devised to indicate the feasibility of this vibration measurement procedure for detection of any defective engine components. Table 6.1 shows a sample matrix of obtained results when the engine was running with one missing connecting rod bearing cap on each piston in turn and on four engines. It can be seen that all of the faults were detected satisfactorily with this

154
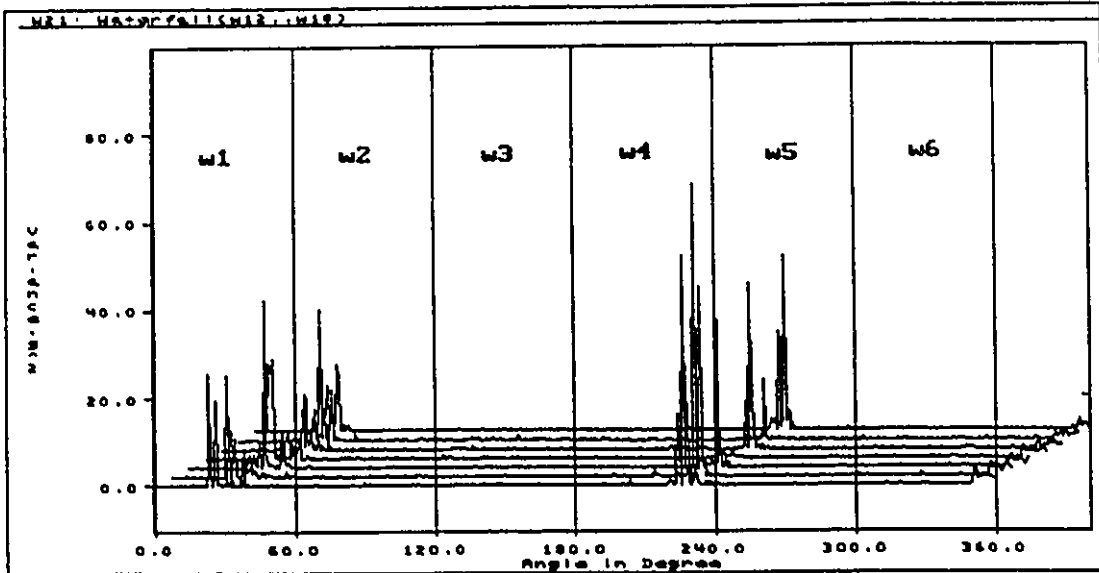
Figure 6.33 : Vibration Variance Data from a Defective
Engine (#1 Cap Bearing Omitted) During Cold
Test
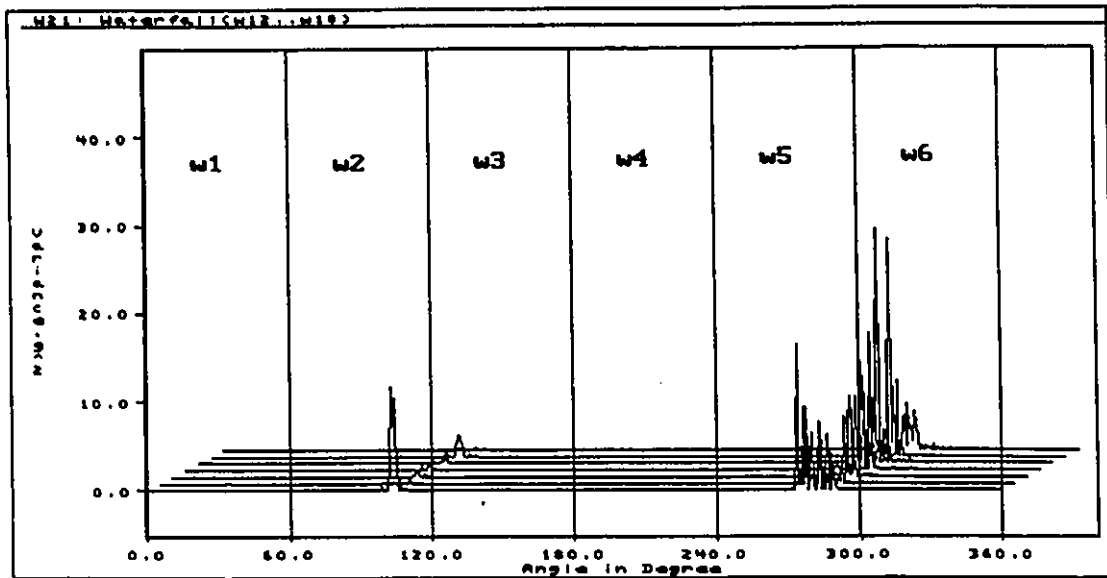
Figure 6.34 : Vibration Variance Data from a Defective
Engine (#2 Cap Bearing Omitted) During Cold
Test

155
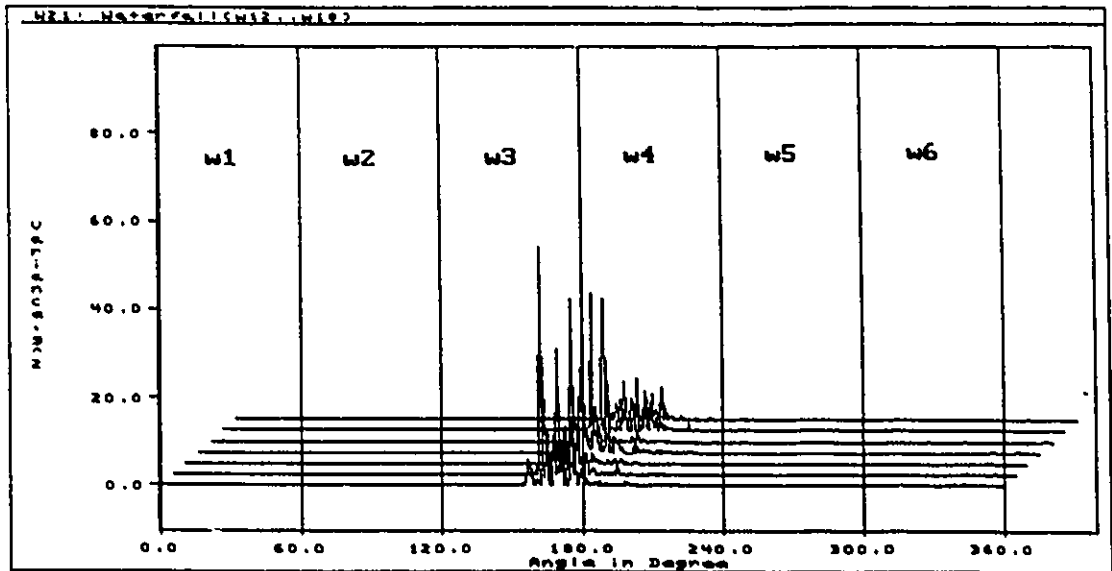
Figure 6.35 : Vibration Variance Data from a Defective
Engine (#3 Cap Bearing Omitted) During Cold
Test
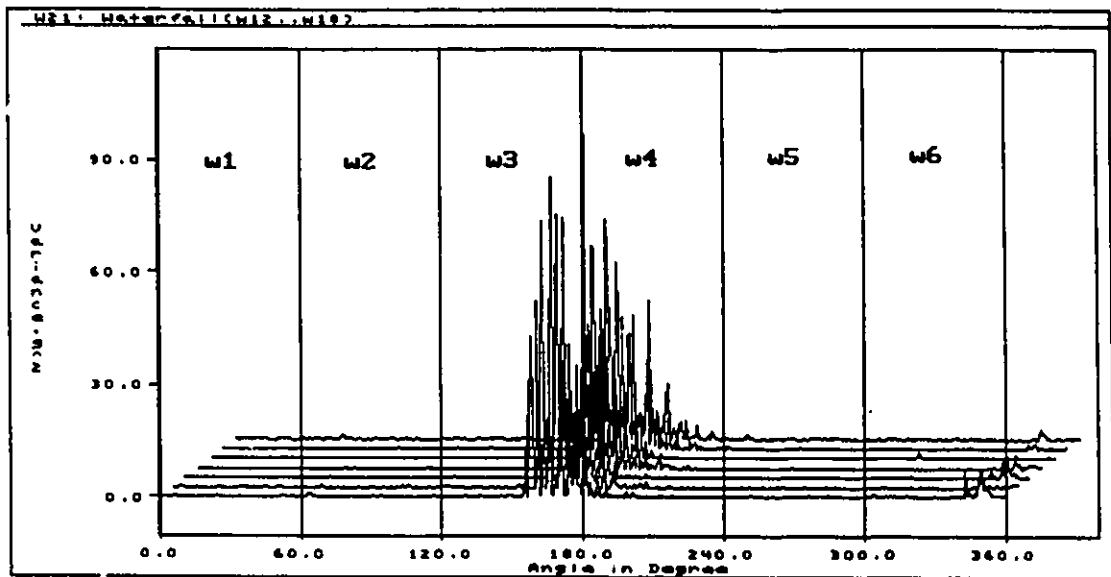
Figure 6.36 : Vibration Variance Data from a Defective
Engine (#4 Cap Bearing Omitted) During Cold
Test
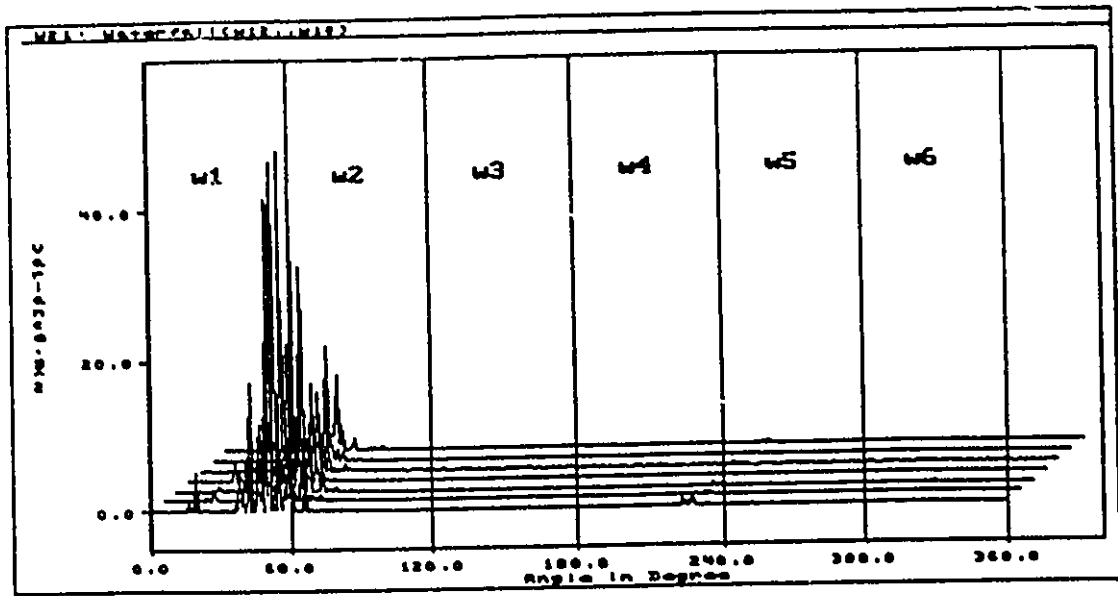
Figure 6.37 : Vibration Variance Data from a Defective
Engine (#5 Cap Bearing Omitted) During Cold
Test
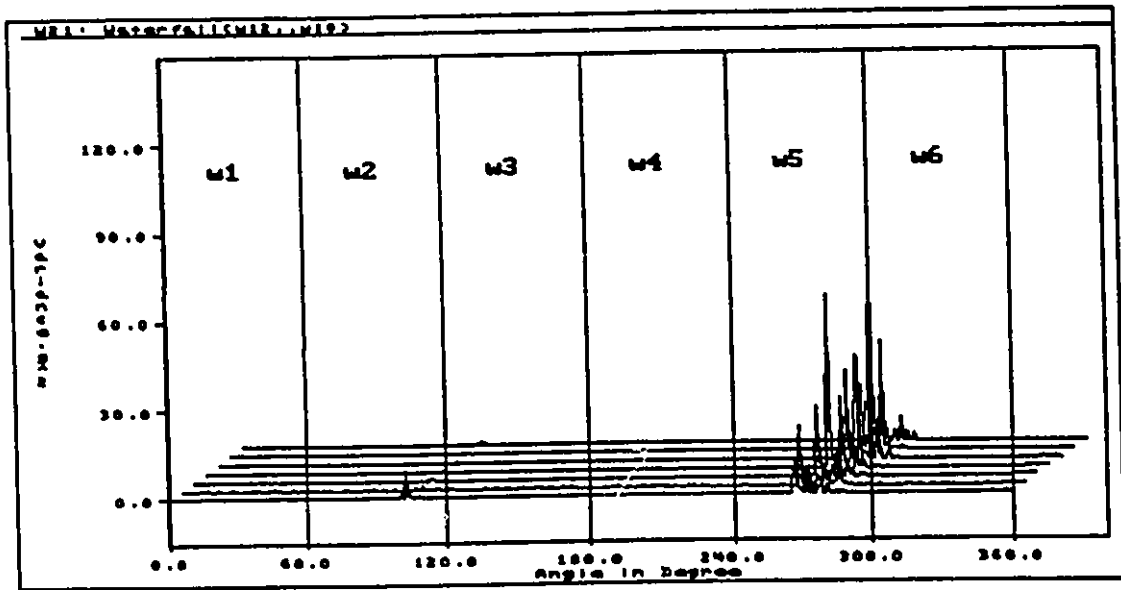
Figure 6.38 : Vibration Variance Data from a Defective
Engine (#6 Cap Bearing Omitted) During Cold
Test

157
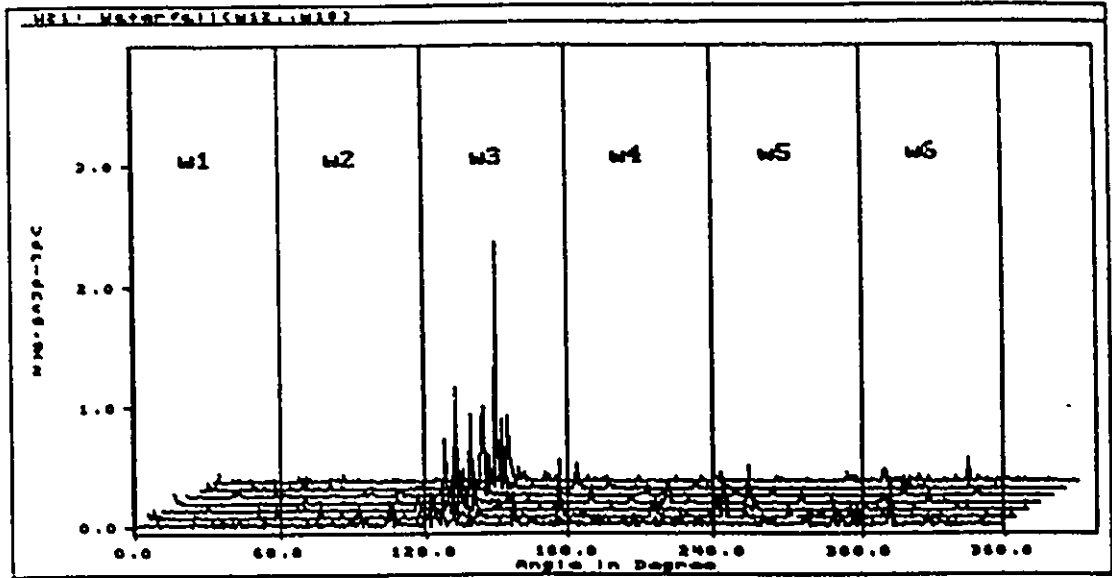
Figure 6.39 : Vibration Variance Data from a Defective
Engine (#4 Rod Nut Omitted) During Cold Test
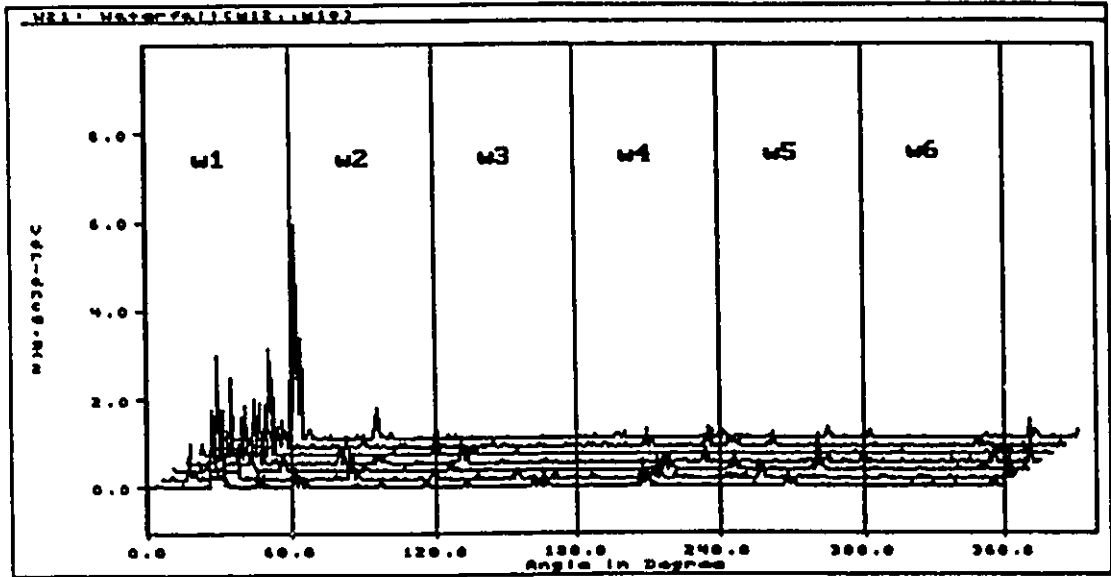
Figure 6.40 : Vibration Variance Data from a Defective
Engine (#1 Rod Cap Reversed) During Cold Test

158

procedure. Table 6.2 shows the same level of success when the engine speed is increased to 420 rpm. Although higher speed produces better result, low speed is preferred so as to avoid damaging crankshaft when a rod bearing is missing. For the case where the connecting rod bearing is missing, Table 6.3, similar results were obtained.

Engine Number	Accelerometer #1 Piston #						Accelerometer #2 Piston #					
	1	2	3	4	5	6	1	2	3	4	5	6
1	ST	SB	ST	ST	ST	S	S	SB	ST	ST	ST	S
2	S	S	ST	ST	S	S	SB	S	S	S	S	S
3	ST	S	ST	ST	ST	SB	ST	SB	ST	ST	ST	ST
4	S	S	ST	ST	ST	SB	SB	SB	ST	ST	ST	SB

Note:

1. S = satisfied fault detection at both TDC and BDC.

2. ST = satisfied fault detection only at TDC.

3. SB = satisfied fault detection only at BDC.

4. US = unsatisfied fault detection.

5. F = failure of fault detection.

Table 6.1 : Performance Matrix of Engine Fault Detecting Experiments -Engine Speed 250 rpm with Rod Bearing Cap Missing

Engine Number	Accelerometer #1 Piston #						Accelerometer #2 Piston #					
	1	2	3	4	5	6	1	2	3	4	5	6
1	S	SB	S	S	SB	S	S	SB	ST	ST	ST	S
2	SB	S	SB	S	S	S	S	S	S	S	S	ST
3	S	SB	S	ST	ST	SB	S	SB	ST	S	ST	S
4	S	ST	S	ST	ST	SB	ST	SB	S	S	SB	ST

Note:

1. S = satisfied fault detection at both TDC and BDC.

2. ST = satisfied fault detection only at TDC.

3. SB = satisfied fault detection only at BDC.

4. US = unsatisfied fault detection.

5. F = failure of fault detection.

Table 6.2 : Performance Matrix of Engine Fault Detecting Experiments -Engine Speed 420 rpm with Rod Bearing Cap Missing

160

Engine Number	Accelerometer #1 Piston #						Accelerometer #2 Piston #					
	1	2	3	4	5	6	1	2	3	4	5	6
1	ST	SB	ST	ST	ST	SB	ST	SB	ST	S	S	SB
2	S	S	S	S	S	SB	S	SB	S	S	S	S
3	ST	S	S	S	S	S	S	S	S	S	S˙	S
4	S	ST	ST	ST	ST	S	S	S	ST	SB	ST	S

Note:

1. S = satisfied fault detection at both TDC and BDC.

2. ST = satisfied fault detection only at TDC.

3. SB = satisfied fault detection only at BDC.

4. US = unsatisfied fault detection.

5. F = failure of fault detection.

Table 6.3 : Performance Matrix of Engine Fault Detecting Experiments -Engine Speed 420 rpm with Rod Bearing Missing

6.3.1.1.2 Detection of Miscellaneous Defective Components

The same procedure outlined in section 6.3.1.1 was repeated for an engine with different defective components. The results summarized in Table 6.4 indicate the feasibility of using this method to detect a missing rod bearing cap, a missing rod bearing, and loose connecting rod nuts. However, the remaining of the defective conditions, i.e., mismatched bearing cap, missing main bearing and unbalanced crankshaft, were not detected consistently.

| Defective Engine Components | Location of Defective Part | | | | | |
| | Piston # | | | | | |
	1	2	3	4	5	6
Rod bearing cap missing	S	S	S	S	S	S
Rod bearing missing	S	S	S	S	S	S
Loosen connecting rod nuts	S	S	S	S	S	S
Reversed rod bearing cap	US	US	US	US	US	US
Mismatched bearing cap	US	US	US	US	US	US
Missing main bearing	US	US	US	US	US	US
Unbalanced crankshaft	F	F	F	F	F	F

Note:

1. S = satisfied fault detection.

2. US = detection with inconsistency

3. F = failure to detection.

Table 6.4 : Performance Matrix of Defective Engine Test Utilizing Vibration Measurements.

6.3.1.2 Frequency Analysis of the Noise Signals

To determine the frequency characteristics of noise signals from defective engines, noise signals were first obtained from a normal engine, whose components were thoroughly inspected. The signal characteristics were then examined. This was followed by an equivalent evaluation of the noise signals from a defective engine with a missing cap rod bearing. Figure 6.41 shows a typical time domain noise signal

RANGE: -51 dBV   STATUS: PAUSED

A: STORED

97.4
dBEU

10
dB
/DIV

17.4
START: 0 Hz   BW: 47.742 Hz   STOP: 5 000 Hz

B: STORED

208.3
kEU

52.09
kEU
/DIV

-208.3
START: 0 Sec   STOP: 80 mSec

X: 0 Hz   Y: 49.14 dBEU
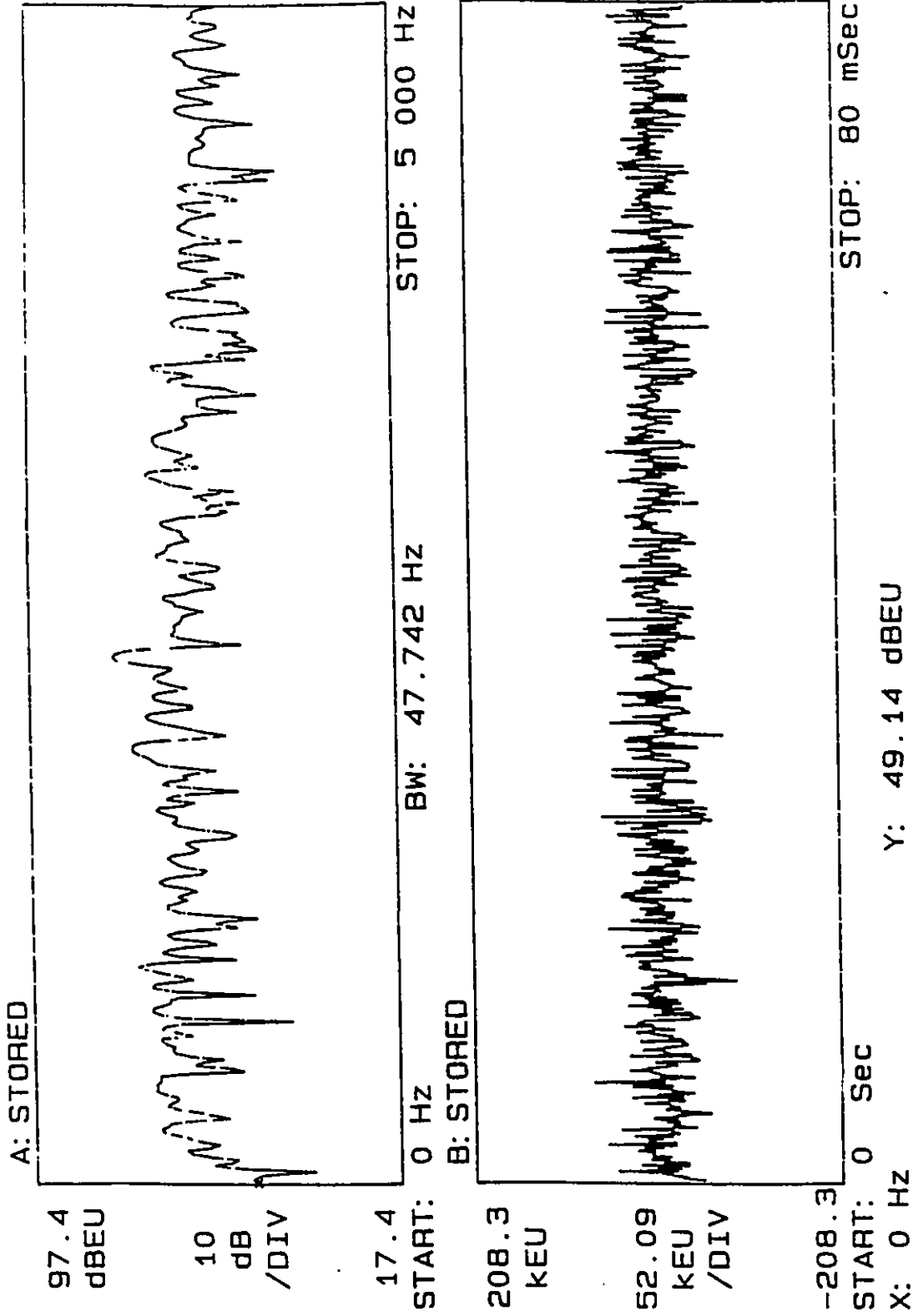
Figure 6.41 : Frequency Spectrum and Time Domain Trace for a Normal Engine

163

and the frequency spectrum from a normal engine while the corresponding results of the defective engine are shown in Figure 6.42. By comparing these, it was observed that there was no distinct differences in amplitudes of the spectra that would allow us to discern the defective engine from a normal engine.

6.3.2 Noise Measurements

Noise measurements were also carried out during engine running in the cold test stand utilizing a sound level meter. The same set of engine defective conditions were also used in the noise measurements.

Two different sizes of microphones, 1/2 inch and 1/4 inch diameters, were used to monitor the noise signals from the engine. It was found that the noise measurements using 1/2 inch microphone gave a larger amplitude and less noise than the 1/4 inch microphone. Therefore, the 1/2 inch diameter microphone was employed for subsequent noise measurements.

To ensure the feasibility of noise measurement as one of the monitoring methods of defective engines, noise and vibration signals were captured simultaneously. Figures 6.43 and 6.44 show the variance of the vibration signal, while Figures 6.45 and 6.46 depict that of the noise signal. As shown in these figures, for defective engines, both noise and vibration analyses portray similar characteristics in terms of amplitude distributions of the variances.

Experiments were repeated for the different defective engine components and also for defects at different locations. The results from the testing of 25 engines indicated that the noise measurements showed the same characteristics as the vibration measurements. As shown in Table 6.5, missing rod bearing, missing rod bearing cap and loose connecting rod nuts were entirely detected with the measurements of engine noise during cold engine motoring while reversed rod bearing caps, mismatched bearing caps and missing main bearings are partially detected.
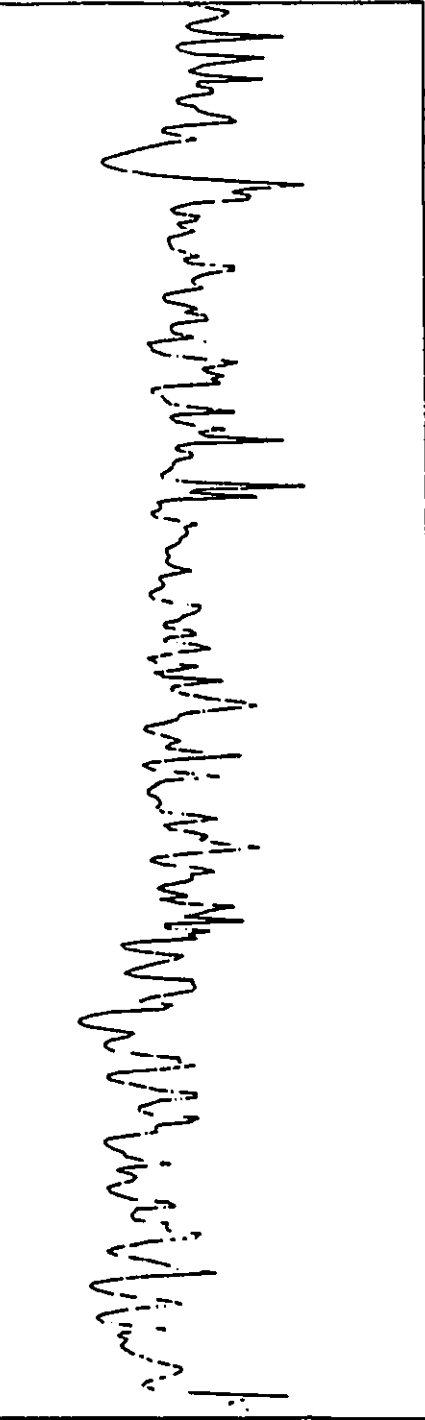
164
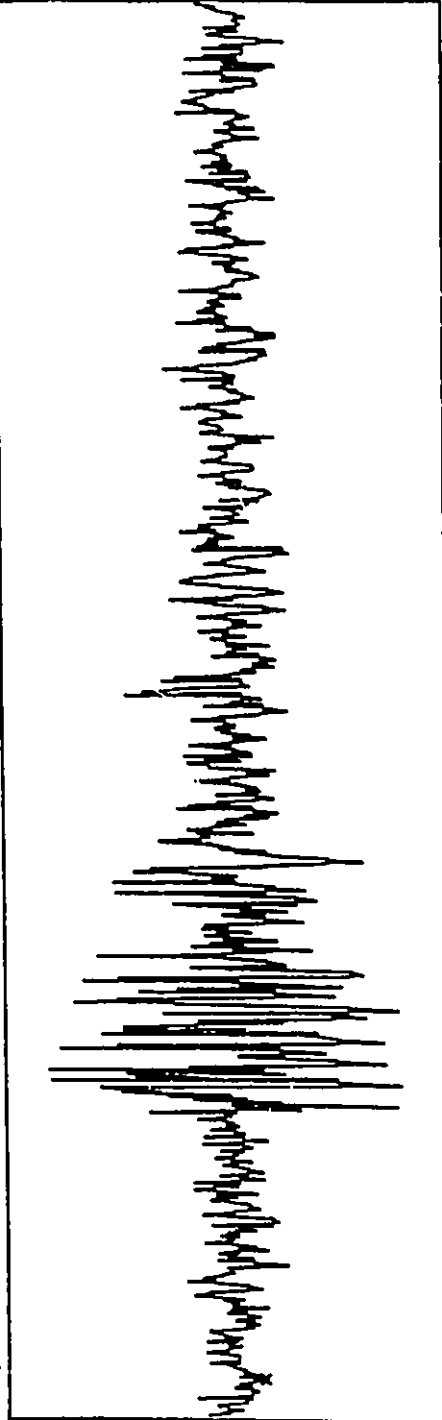
Figure 6.42 : Frequency Spectrum and Time Domain Trace for a Defective Engine

165
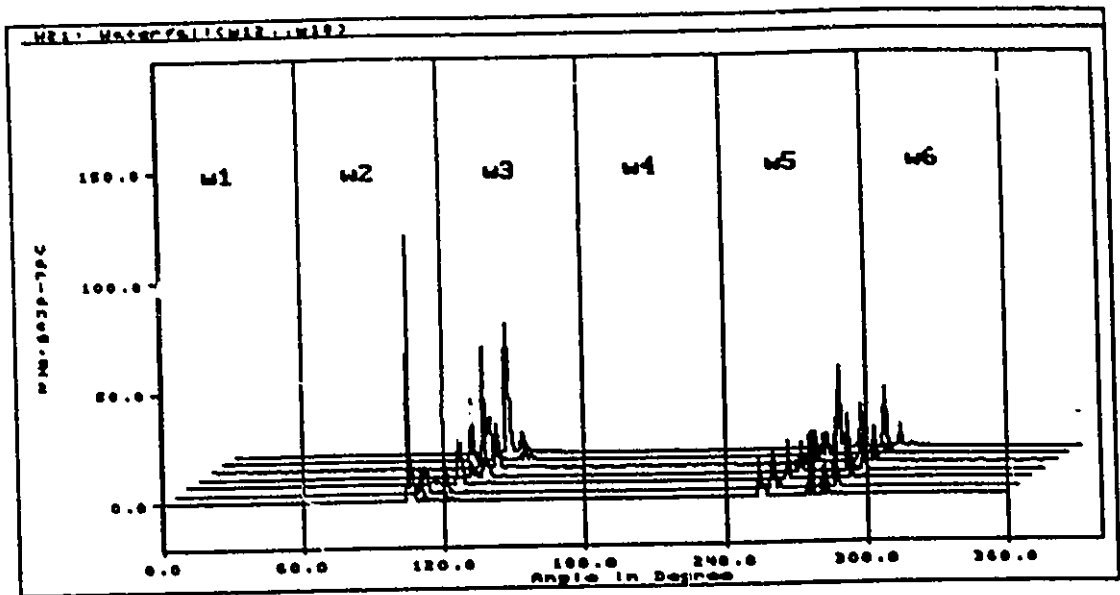
Figure 6.43 : Channel 1 Vibration Variance Data for
Defective Engine
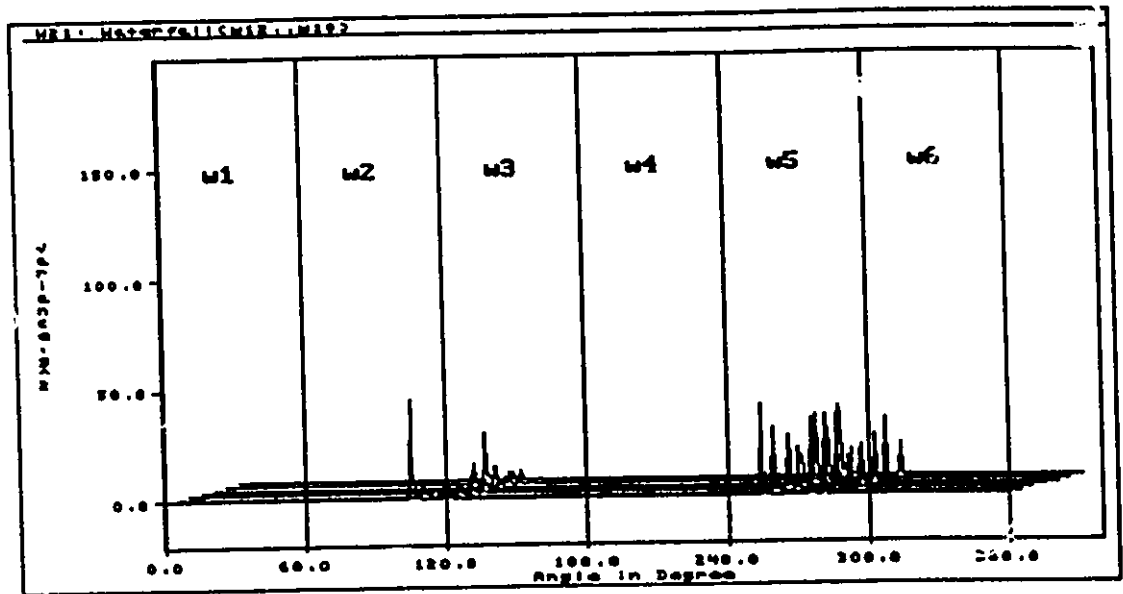
Figure 6.44 : Channel 2 Vibration Variance Data for
Defective Engine

166
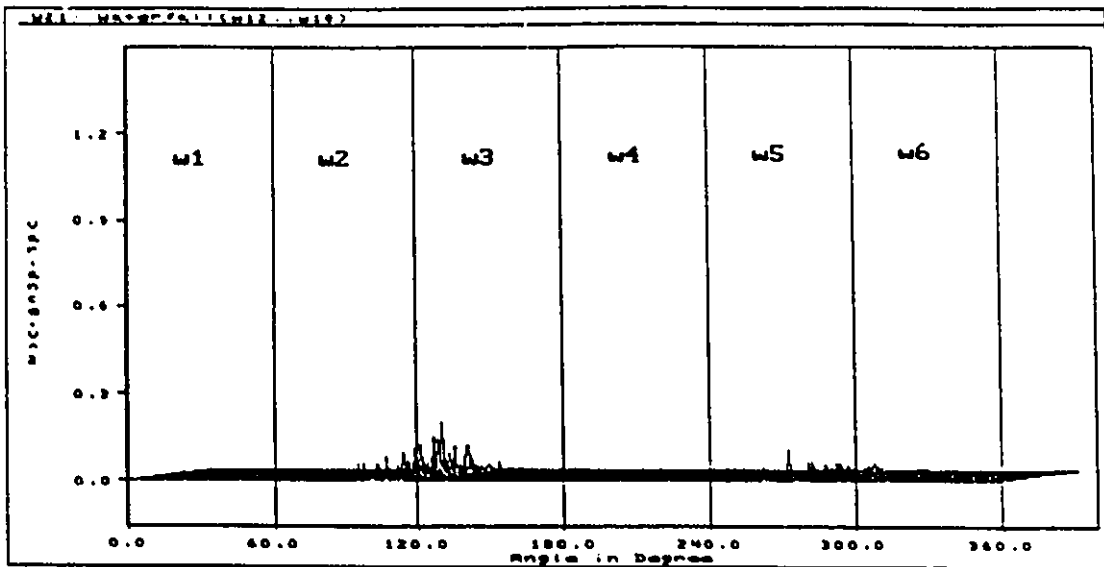
Figure 6.45 : Channel 1 Noise Variance Data for Defective Engine
(1/4" Microphone, Sensitivity = 4 mV/Pa)
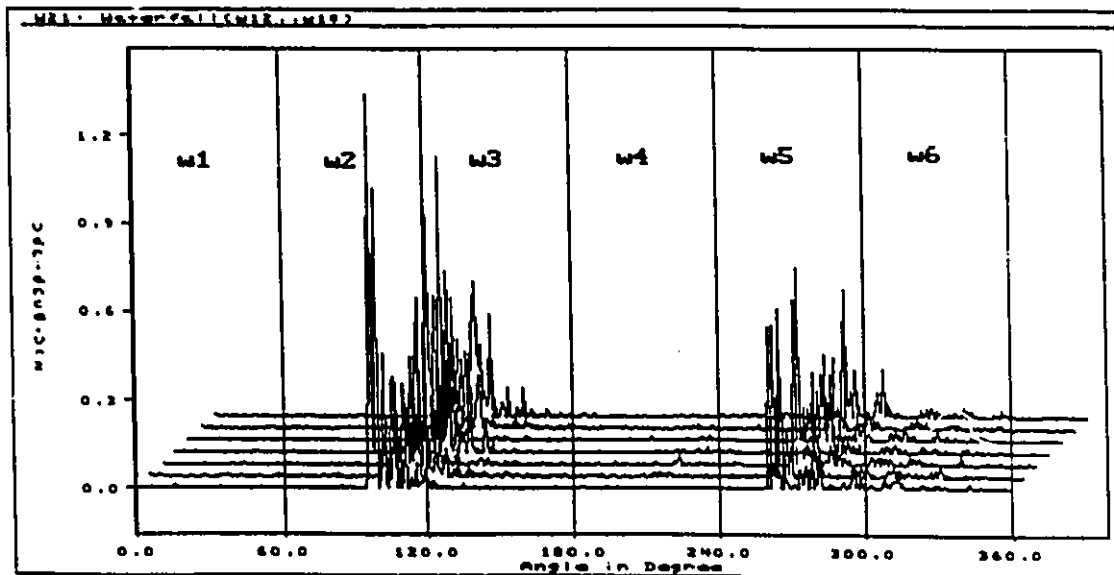
Figure 6.46 : Channel 2 Noise Variance Data for Defective Engine
(1/2" Microphone, Sensitivity = 50 mV/Pa)

Defective Engine Components	Location of Defective Part Piston #					
	1	2	3	4	5	6
Rod bearing cap missing	S	S	S	S	S	S
Rod bearing missing	S	S	S	S	S	S
Loosen connecting rod nuts	S	S	S	S	S	S
Reversed rod bearing cap	US	US	US	US	US	US
Mismatched bearing cap	US	US	US	US	US	US
Missing main bearing	US	US	US	US	US	US
Unbalanced crankshaft	F	F	F	F	F	F

Note:

1. S = satisfied fault detection.

2. US = detection with inconsistency

3. F = failure to detection.

Table 6.5 : Performance Matrix of Defective Engine Test Utilizing Noise Measurements.

6.4 Hot Test of Engine

A variety of engines, normal or with different defective conditions were tested at the dynamometer laboratory. Vibration, sound, and cylinder pressure of the engines were measured. The induced TTL signal from #1 spark plug wire or PIP (Profile Ignition Pickup) signal from the electronic engine control system was used as an external triggering signal to start the signal sweep at the same crank angle, i.e. 10 degrees before top dead center of

the piston. Teardown analysis of the engines was subsequently performed by dimensional and visual inspection of the engine components. Correlations were made between the processed signal characteristics of each pistons and their dimensional characteristics. These will be discussed in the following sections.

6.4.1 Vibration Measurements

Vibration signals from more than 250 engines were monitored utilizing different data acquisition systems at engine speeds of 1500 to 2000 rpm. Operating conditions of the engine, i.e., engine speed, inlet and outlet engine coolant temperatures and applied load to the engine, were monitored and controlled. The acquired vibration signals were analyzed in terms of variance, time domain averaging and running variance.

6.4.1.1 Variance and Time Domain Averaging Analysis

The vibration signal (in the time domain) from a defective engine (Figures 6.48) can nr w be compared to that from a normal engine (Figure 6.47). There are differences, but it is difficult to distinguish the difference which is attributed to the defective conditions. To improve this , a new method of signal analysis was used. In this method, the time domain averaging was first performed for 15 engine cycles of vibration signal and no significant differences were observed in six group of amplitudes as illustrated in Figure 6.48. The time domain average signal was then subtracted from the composite (raw) signal. Distinct pseudo-random signals were found which were observed to correspond to the location of the side force reversals in the piston, as shown in Figure 6.49. Similar results were found in the variance of the signal plot of the same engine (Figure 6.50). However, the peaks in this case are more pronounced than in the previous case.

169
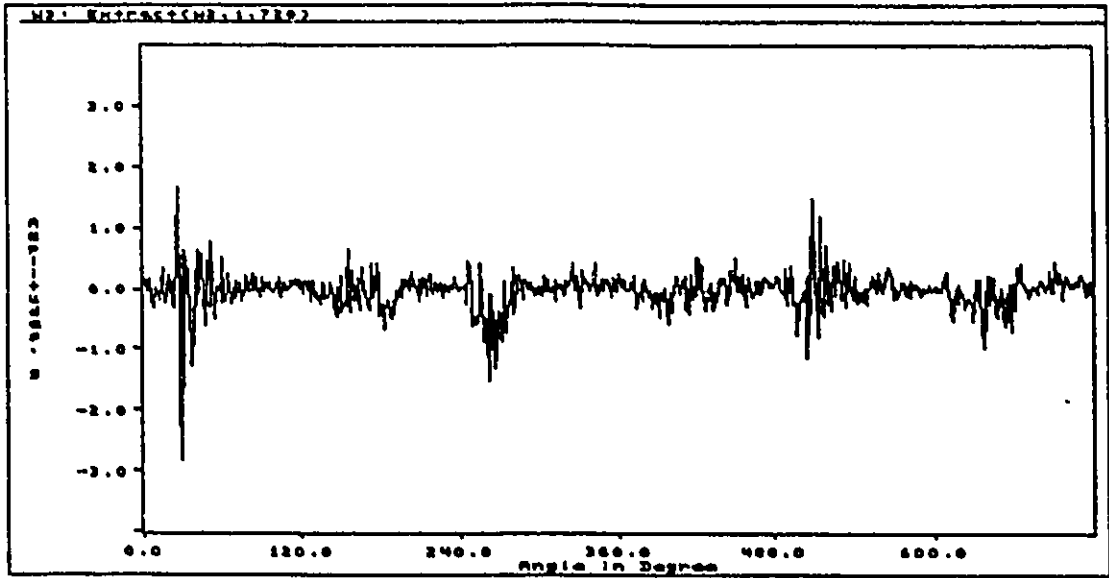
Figure 6.47 : Vibration Signals from Defective Engine
During Hot Test - One Engine Cycle
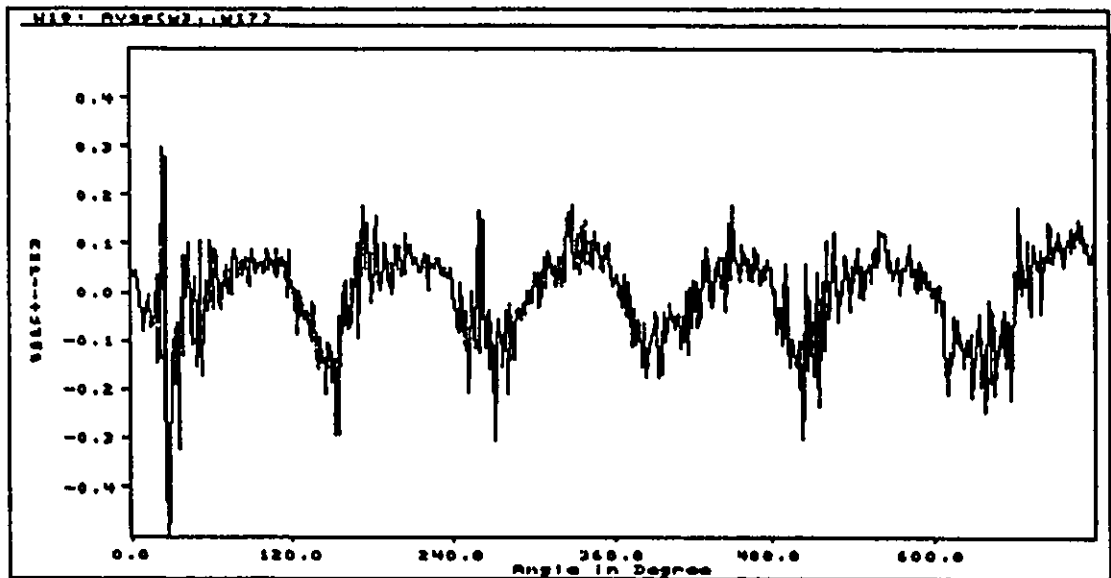
Figure 6.48 : Time Domain Average Signals from Defective
Engine During Hot Test

170
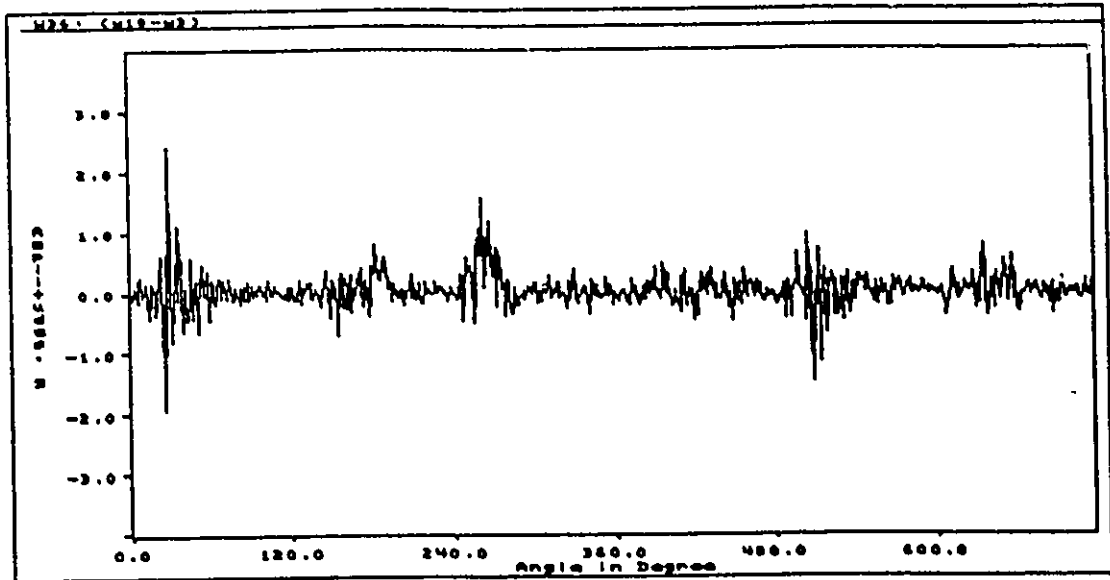
Figure 6.49 : Random Repetitive Component of Vibration
Signals
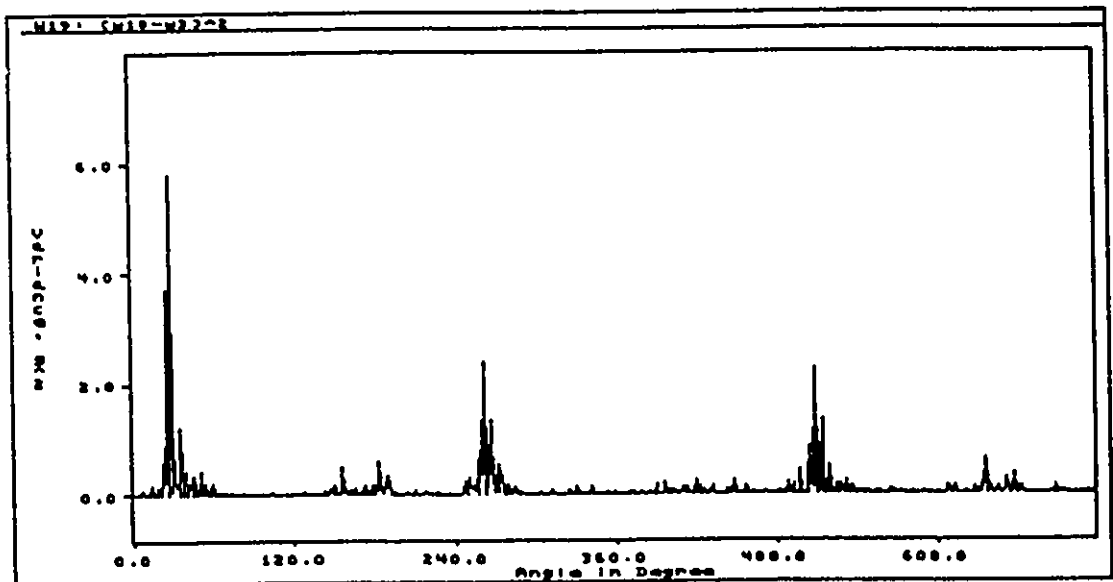
Figure 6.50 : Variance of Signatures from Defective Engine
During Hot Test

171

Figures 6.51 shows a waterfall plot of the variance of signals, from a defective engine (customer complaint). Distinct amplitudes of variance are also observed at piston #1. A remark can be made here that the signature introduced by the defect in the piston, while being repetitive, is not truly periodic. This is clearly illustrated by observing Figures 6.47 and 6.48 which are relatively similar. From the results, it can be concluded that the variance function (Figure 6.51) clearly shows the effects of defective conditions and can certainly be used for diagnostic purposes.

Similar experiments were repeated for more than 250 engines. The amplitudes of variance were observed and then they were related to the defective components in the cylinder. To confirm the cause of the high magnitude vibration level, engine teardown analysis was later performed.

6.4.1.2 Frequency Analysis of Vibration Signals

The objective here is to determine the feasibility of using frequency analysis for detecting engine faults. In the frequency analysis, vibrations were first monitored from a defective engine which had a reversed skirt taper piston in cylinder #5. The defective piston was then replaced by a good (within specifications) piston and vibration signals were recorded from the same engine. Figure 6.52 shows a typical time domain vibration signal from the defective engine while that from a normal engine is shown in Figure 6.53. Frequency characteristics of both signals were analyzed. In the frequency spectrum of the defective engine, as shown in Figure 6.54, distinct amplitudes are observed in the frequency range of 2700 to 3500 Hz. However, these distinct amplitudes are not visible in the frequency spectrum of a normal engine as illustrated Figure 6.55. Repeatable results were observed in additional experiments, as shown in Figure 6.56 and 6.57.

The results from this method are promising, however, the reliability of this method in on-line defective engine monitoring is questionable because of some exceptions.

172

W35: Waterfall(w19..w33.0.0.0.0.02)
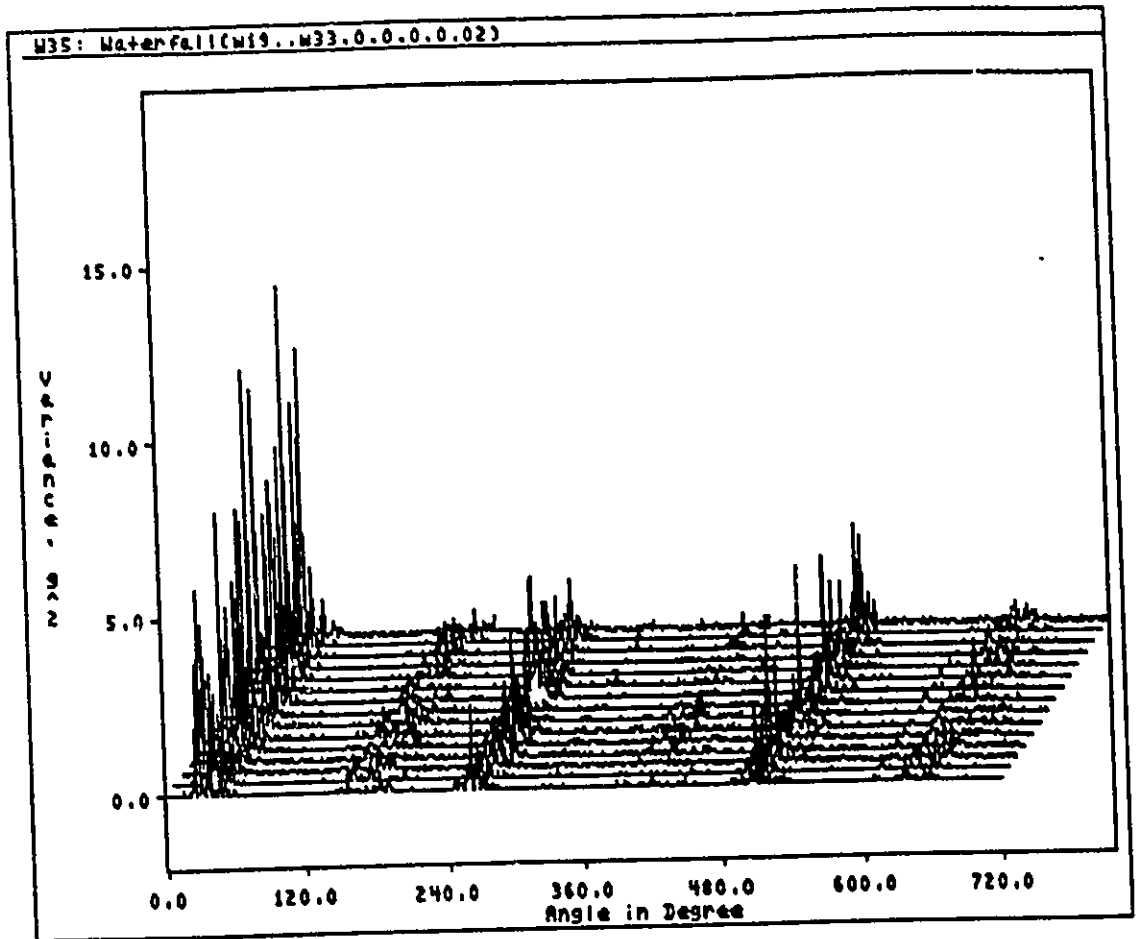
Figure 6.51 : Variance of Signatures from Defective Engine
During Hot Test - Waterfall Plot
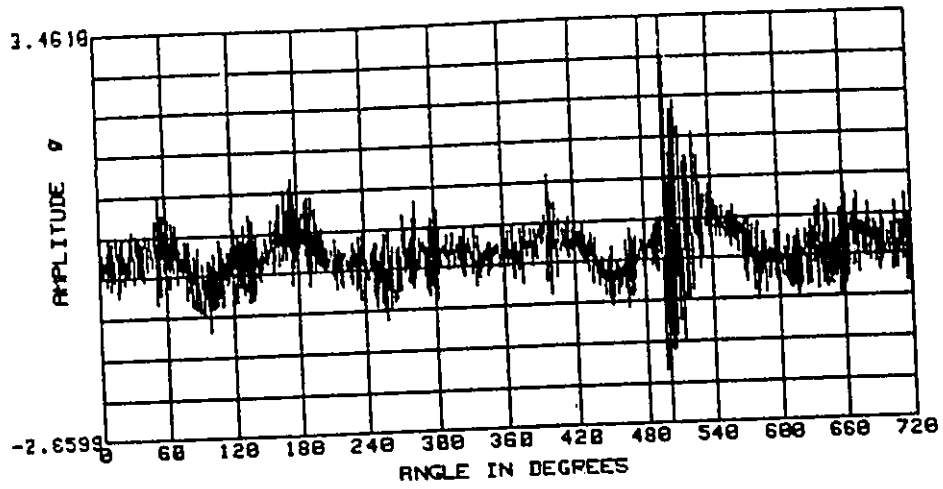
Figure 6.52 : A Typical Time Domain Signal of a Defective Engine
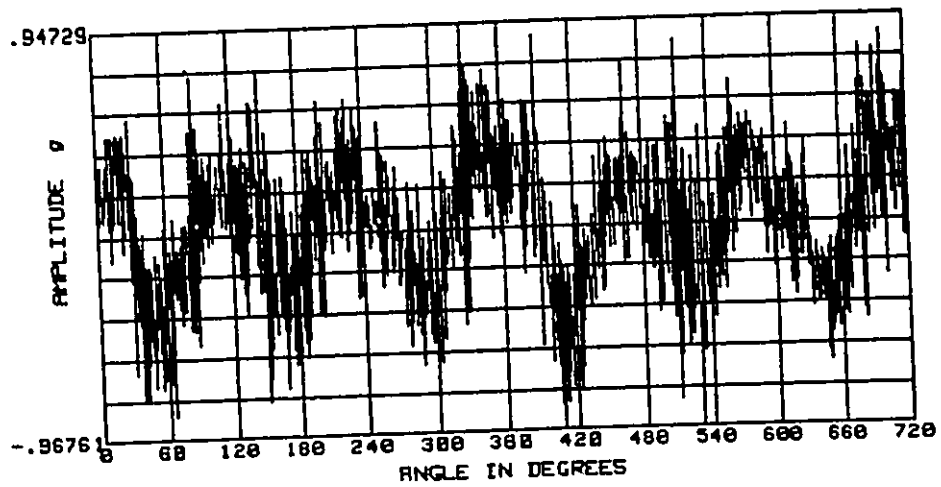
Figure 6.53 : A Time Domain Signal of a Normal Engine

174
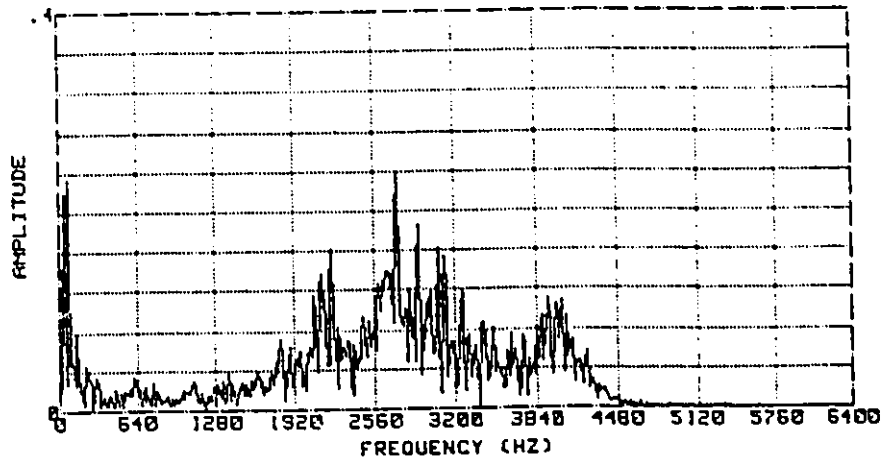
Figure 6.54 : Frequency Spectrum of Defective Engine
(Reversed Taper Piston)
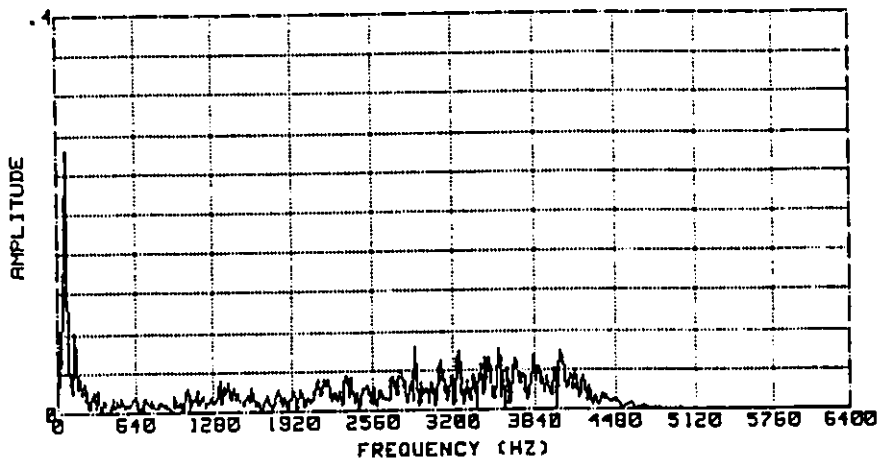
Figure 6.55 : Frequency Spectrum of the Same Engine (Normal
Piston)

175
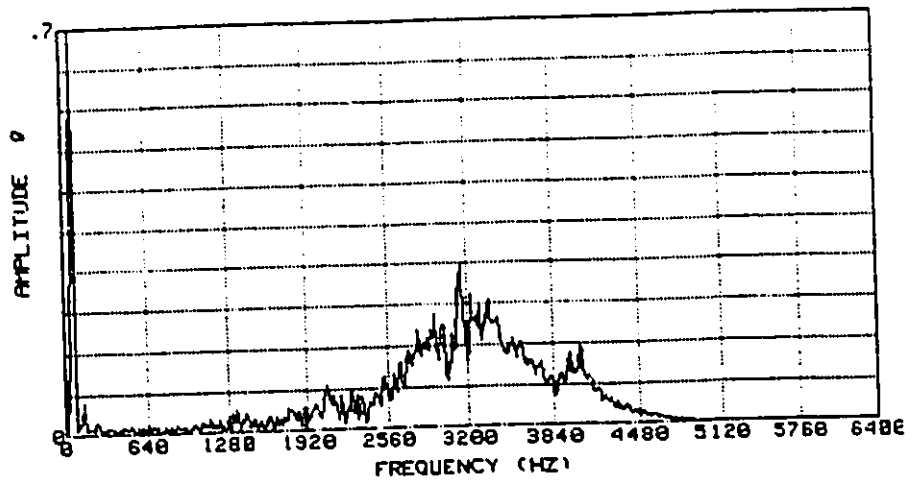
Figure 6.56 : Frequency Spectrum of Defective Engine
(Concentricity of Piston Ringland to Skirt
Out of Specification)
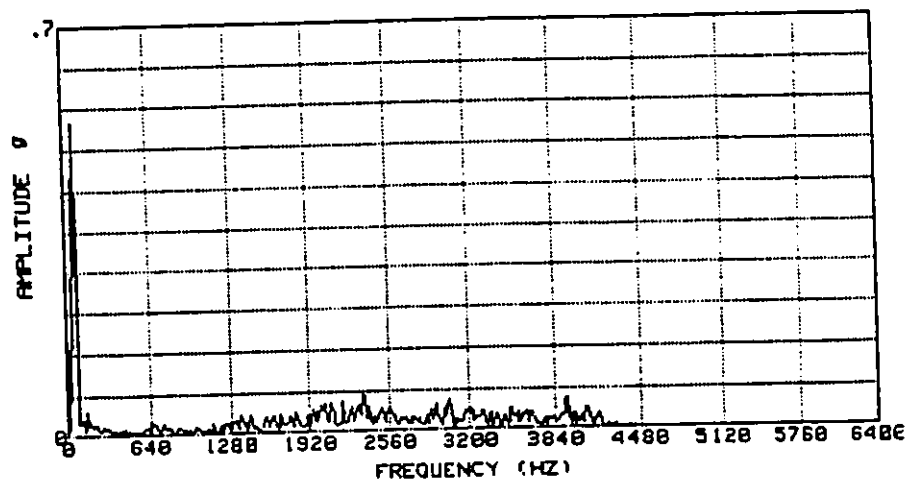
Figure 6.57 : Frequency Spectrum of the Same Engine
(Barrel Shape Skirt Profile Piston)

Figure 6.58 shows a running variance of the vibration signal from a defective engine which has oversized ringland in piston #6. The corresponding frequency spectrum is shown in Figure 6.60. These are compared to the time and frequency domain signal from a normal engine as illustrated in Figures 6.59 and 6.61 respectively. No significant differences in the frequency spectra were observed which indicates that the detection of a fault is not effective.

6.4.2 Engine Teardown Analysis

After vibration, sound and pressure measurements were accomplished, the dimensional characteristics of the engine components – piston taper, piston skirt to ringland concentricity, piston to cylinder bore clearance and piston ringland diameters – were measured, as shown in Table 6.6. Further measurements such as piston skirt ovality, skirt profile were also performed. These were then compared to the analyzed vibration signals and correlations were made.

6.4.2.1 Effect of Piston Skirt Off-set with Respect to Ringland

As described earlier in the experimental details of a teardown analysis, the piston ringland offset with respect to the piston skirt was measured in two directions. For the sign convention of the readout in A-C axis, the negative sign represents the (piston ringland) offset to the major thrust side while the positive sign represents that of the minor thrust side. The amplitudes of vibration signals from 35 engines, in terms of variance, were plotted against the measured piston skirt offset in the A-C axis (See Figure 4.19 for illustration).

As shown in Figure 6.62, the variance in the signal is high when the offset is less than -0.2 mm . As the offset in the thrust direction approaches -0.100 mm, the variance is consistently low. Thus it can be concluded that the piston ringland offset to the
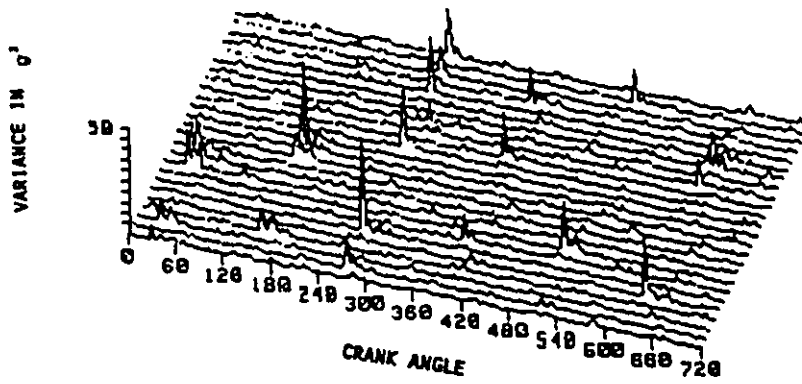
Figure 6.58 : Running Variance of Defective Engine
(Ringland Diameter out of Specification)
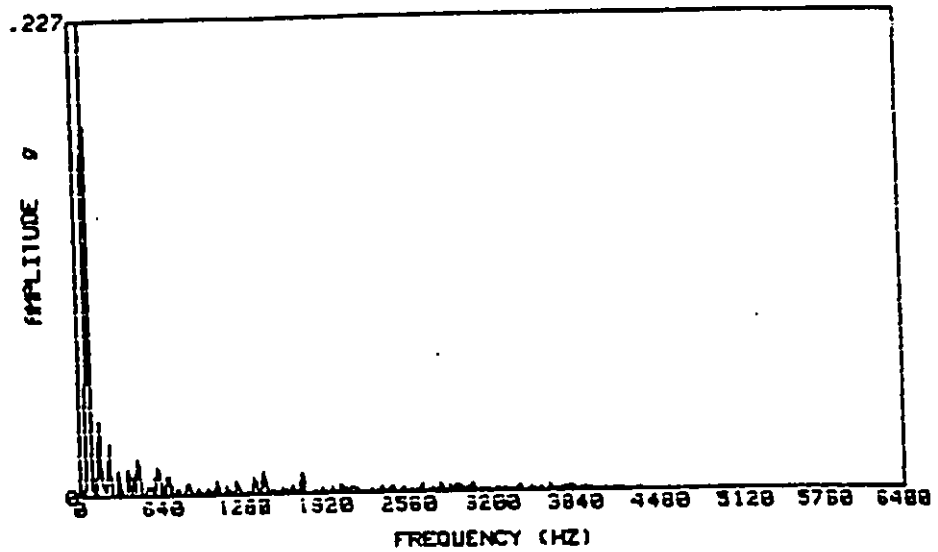
Figure 6.59 : Frequency Spectrum of Defective Engine
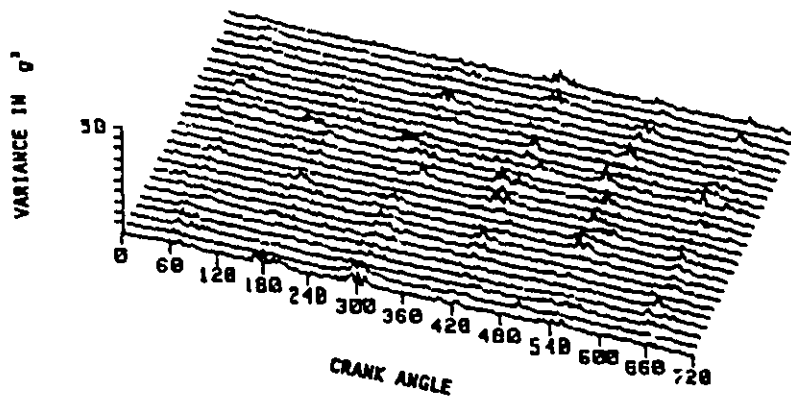
Figure 6.60 : Running Variance of a Normal Engine
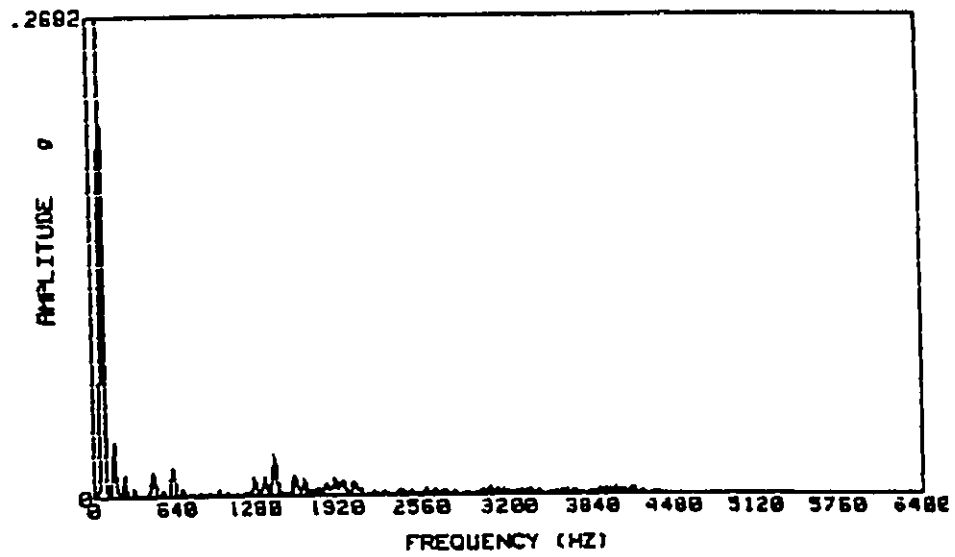
Figure 6.61 : Frequency Spectrum of a Normal Engine

ENG	C	A	W	B	#1 ringland diameter		#2 ringland diameter		SKIRT TAPER		CONCENTRICITY		PISTON TO BORE
					1 PIN	1 THRUST	2 PIN	2 THRUST	B–W	W–A	AC–THRUST	BD–PIN	CLEARANCE
1	5	96.762	96.767	96.791	96.048	96.081	96.099	96.285	0.024	0.005	-0.15	-0.19	0.033
2	5	96.772	96.776	96.787	96.106	96.101	96.306	96.301	0.011	0.004	-0.25	0.08	0.027
3	5	96.784	96.792	96.819	96.035	96.025	96.257	96.25	0.027	0.008	-0.24	0.08	0.055
	4	96.785	96.787	96.805	96.048	96.029	96.268	96.254	0.018	0.002	-0.04	0.17	0.037
4	6	96.767	96.773	96.805	96.081	96.078	96.298	96.298	0.032	0.006	-0.22	0.06	0.063
	2	96.768	96.779	96.801	96.122	96.103	96.285	96.259	0.022	0.011	0.08	0.14	0.059
5	2	96.78	96.787	96.811	96.127	96.112	96.329	96.3	0.024	0.007	-0.086	0.26	0.05
	5	96.778	96.783	96.813	96.105	96.081	96.31	96.296	0.03	0.005	-0.31	0.08	0.053
6	6	96.789	96.795	96.819	96.113	96.096	96.321	96.294	0.024	0.006	-0.25	0.07	0.09
	5	96.786	96.796	96.833	96.065	96.075	96.271	96.278	0.037	0.01	-0.055	0.15	0.041
7	5	96.784	96.792	96.797	96.056	96.055	96.28	96.278	0.005	0.008	0	0.07	0.051
	6	96.786	96.792	96.804	96.062	96.056	96.281	96.274	0.012	0.006	-0.23	0.13	0.009
8	5	96.771	96.774	96.772	96.073	96.067	96.277	96.267	-0.002	0.003	0.015	0.13	0.064
	6	96.783	96.785	96.814	96.068	96.055	96.27	96.256	0.029	0.002	-0.23	0.11	0.047
9	2	96.763	96.768	96.771	96.132	96.13	96.316	96.312	0.003	0.005	-0.23	0.08	0.055
	5	96.774	96.783	96.806	96.124	96.107	96.331	96.305	0.023	0.009	-0.25	0.1	0.05
10	1	96.778	96.782	96.813	96.14	96.118	96.32	96.3	0.031	0.004	0.06	0.22	0.044
	2	96.763	96.772	96.798	96.029	96.027	96.243	96.241	0.026	0.009	-0.22	0.13	0.054
11	6	96.781	96.786	96.808	96.076	96.082	96.275	96.276	0.022	0.005	-0.26	0.05	0.054
	5	96.785	96.789	96.8	96.049	96.049	96.273	96.277	0.011	0.004	-0.03	0.04	0.042
12	2	96.778	96.78	96.788	96.06	96.054	96.282	96.28	0.008	0.002	-0.22	0.13	0.054
	3	96.774	96.78	96.807	96.053	96.062	96.252	96.254	0.027	0.006	-0.025	0.16	0.051
13	4	96.763	96.774	96.801	96.135	96.124	96.313	96.308	0.027	0.011	-0.095	0.2	0.059
	6	96.772	96.782	96.81	96.142	96.126	96.319	96.307	0.028	0.01	-0.115	0.2	0.053
14	6	96.774	96.793	96.822	96.099	96.103	96.314	96.315	0.029	0.019	-0.04	0.17	0.049
	2	96.772	96.788	96.808	96.072	96.073	96.281	96.279	0.02	0.016	0.078	0.214	0.051
15	6	96.776	96.788	96.797	96.03	96.031	96.239	96.231	0.009	0.012	-0.23	0.06	0.042
	5	96.781	96.789	96.804	96.105	96.088	96.304	96.301	0.015	0.008	-0.3	0.08	0.045
16	1	96.789	96.791	96.812	96.057	96.033	96.26	96.248	0.021	0.002	-0.04	-0.06	0.028
	6	96.777	96.781	96.804	96.091	96.371	96.29	96.282	0.023	0.004	-0.25	0.04	0.056
17	1	96.77	96.784	96.803	96.054	96.037	96.258	96.244	0.019	0.014	-0.07	0.07	0.044
	2	96.769	96.786	96.786	96.038	96.03	96.245	96.228	0	0.017	-0.27	-0.22	0.048

TABLE 6.6 : Critical Dimensional Characteristics of Engine
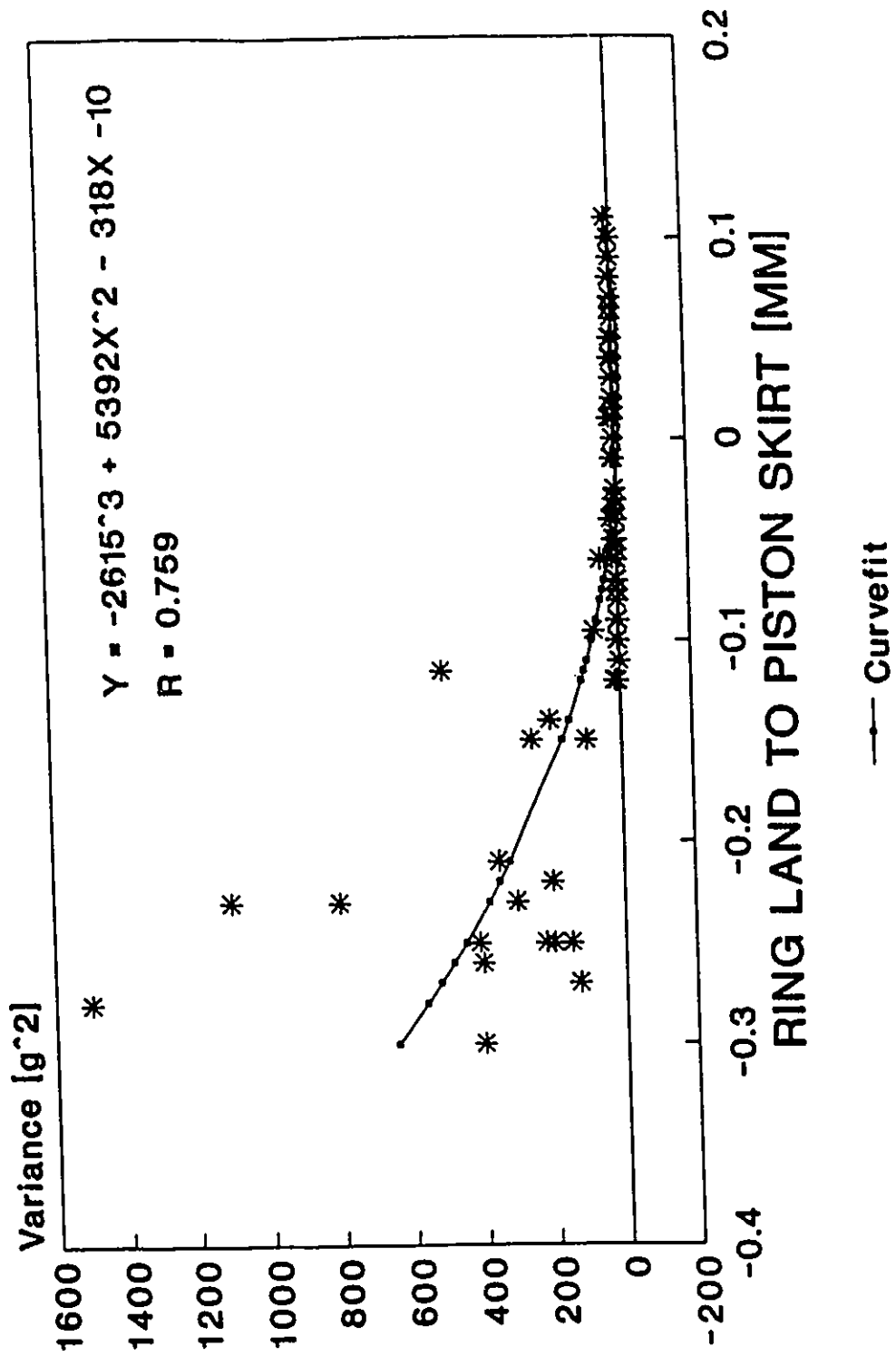
Figure 6.62 : Peak Vibration Variance Versus Offset of Piston
Ringland to Skirt in the Thrust Direction.
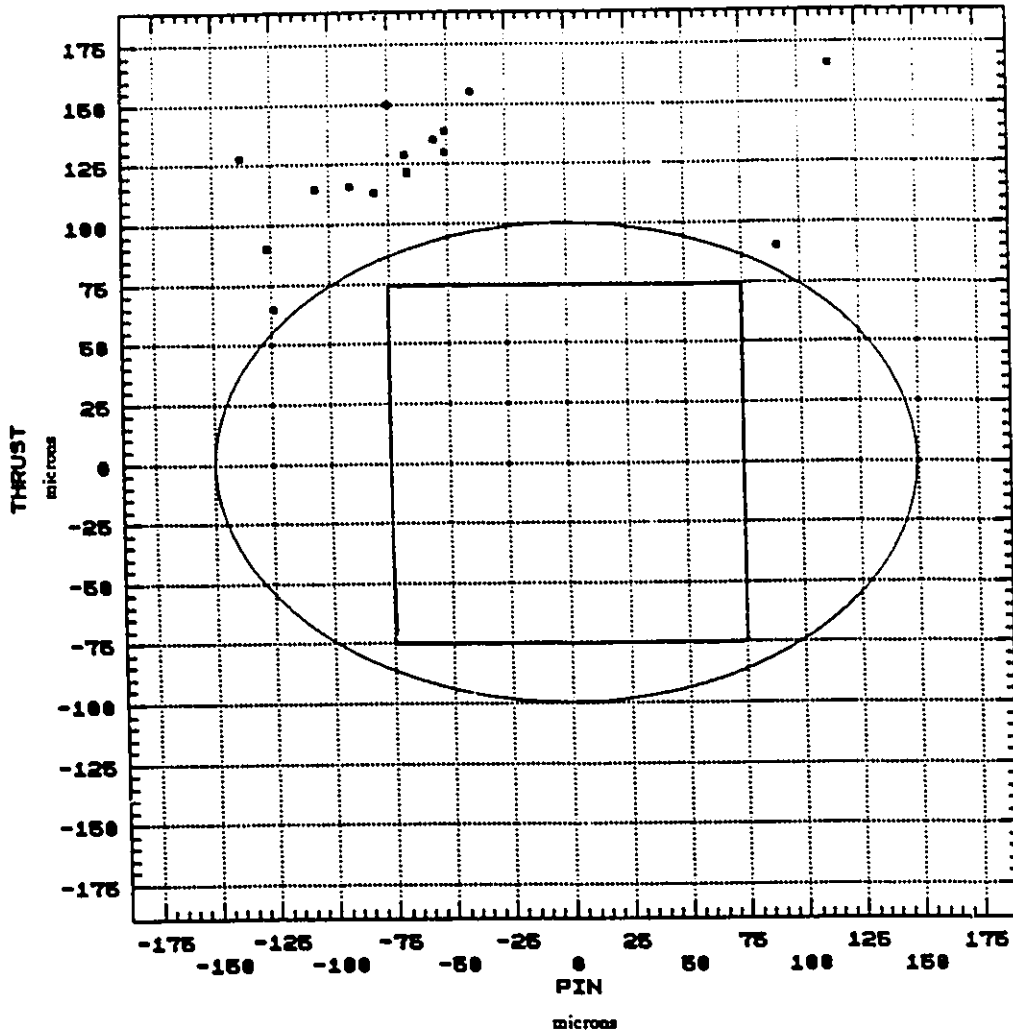
Figure 6.63 : Plot Concentricity of Piston Ringland to Skirt of All Noisy Pistons

minor thrust side is not the major cause of high level vibration signals. The offset to the major thrust side, however, is the main contributor to piston noise and vibration. The offset in question (0.100 mm) is within the current blue-print specifications of the production piston. Steps were immediately taken to retarget the machining operation so as to reduce the off-set as much as possible. The target zone for the machining operation is shown in Figure 6.63. As illustrated in this figure, all of the engine noise complaints resulting from high levels of vibration are concentrated outside the target zone which clearly indicates that this zone is effective in eliminating piston noise caused by concentricity of the piston skirt to ringland.

Further attempts were made to correlate vibration signals to the component dimensions obtained in the engine teardown analysis (such as piston skirt taper, piston ringland diameters and piston to cylinder bore clearance). The results obtained from a study of more than 50 customer return engines indicate that as long as all these characteristics are within specifications (whether at the minimum or maximum), the piston does not generate vibration and noise levels that are objectionable to the customers.

6.5 Feasibility of Vibration Analysis Method in On-Line Monitoring

According to the statistics of one engine manufacturer, missing or misassembled components during assembly, and customer engine noise complaints are the major roadblocks in achieving higher productivity and customer satisfaction. Thus, it is important to find effective ways to detect these defects. In this section, the feasibility of vibration analysis in defective engine monitoring is discussed. It is mainly focused on the results of the cold test of engines as being one solution to the problem of releasing defective engines to the final assembly process and finally to the customer.

.

6.5.1 The Use of Preliminary Threshold Level of Vibration Variance

The determination of the threshold level to detect a defective engine in the cold test will be discussed in this section. An Analysis of the vibration signals obtained from engines indicates the following characteristics:

1. There are two vibration pulses per revolution during the cold test when the defective condition is a missing bearing, as shown in Figures 6.64 and 6.65.

2. The generated vibration pulses are a combination of signals from two cylinders which have the same piston movement (with respect to the top dead center of the pistons). The matching cylinder pairs are as follows: cylinders 1 & 5, 2 & 6, 3 & 4. It is assumed that the output amplitudes from matching cylinders during the cold test are similar.

3. The acquired vibration amplitudes from normal engines are very low compared to those that from defective ones. This facilitates the signal processing of the vibration from defective engines.

4. There is a discontinuity or fluctuation in the vibration amplitudes between the cycles, as shown in Figures 6.66 and 6.67.

5. There are differences in amplitudes of vibration signals from two accelerometers.

6. The duration of the signal peak (which can be attributed to the defective part) is relatively short compared to the engine cycle (see Figure 6.66).

From the above considerations, it is possible to divide the one revolution of the engine into a number of intervals (or windows) of equal spacings. Such a window would contain only a set of variance peaks which is attributed to a specific engine defect. In this study, on an engine revolution is divided into 6 identical windows as shown in Figure 6.65 and Table 6.7. Now, the next task is to determine the threshold level.

The initial threshold level for rejecting defective engines was set up using the average variance value of 15 defective engines (e.g. with missing rod bearings). The
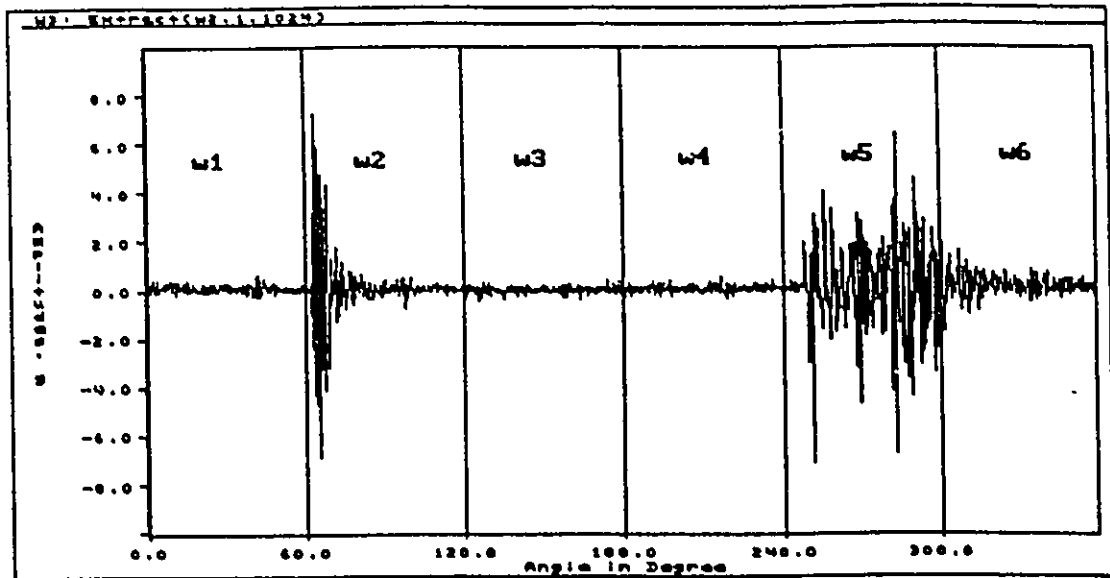
Figure 6.64 : Accelerometer #1 Raw Vibration Data for
Defective Engine (#2 Rod Bearing Omitted)
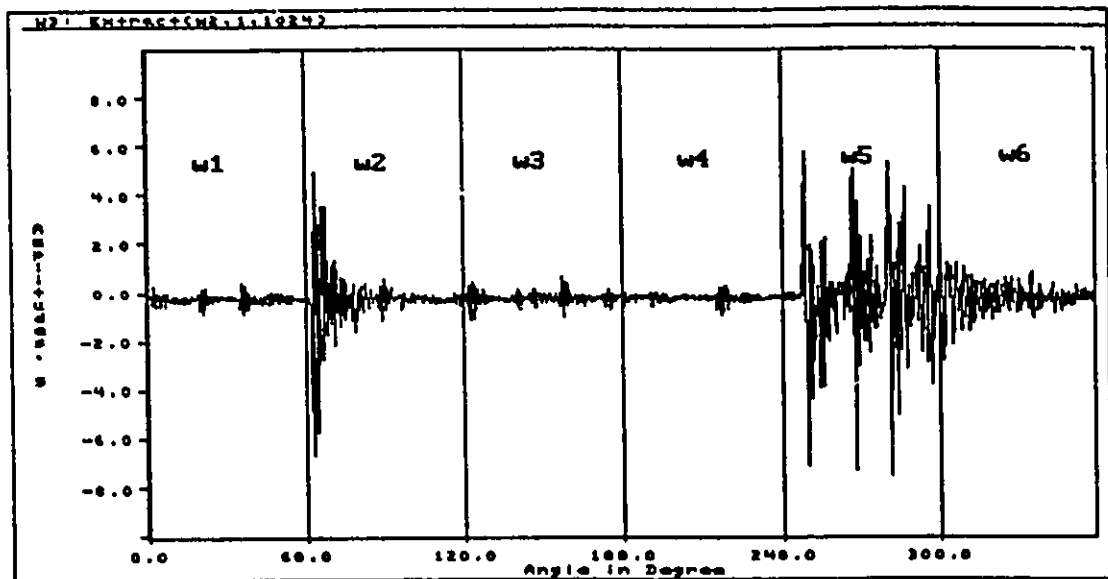
Figure 6.65 : Accelerometer #2 Raw Vibration Data for
Defective Engine (#2 Rod Bearing Omitted)
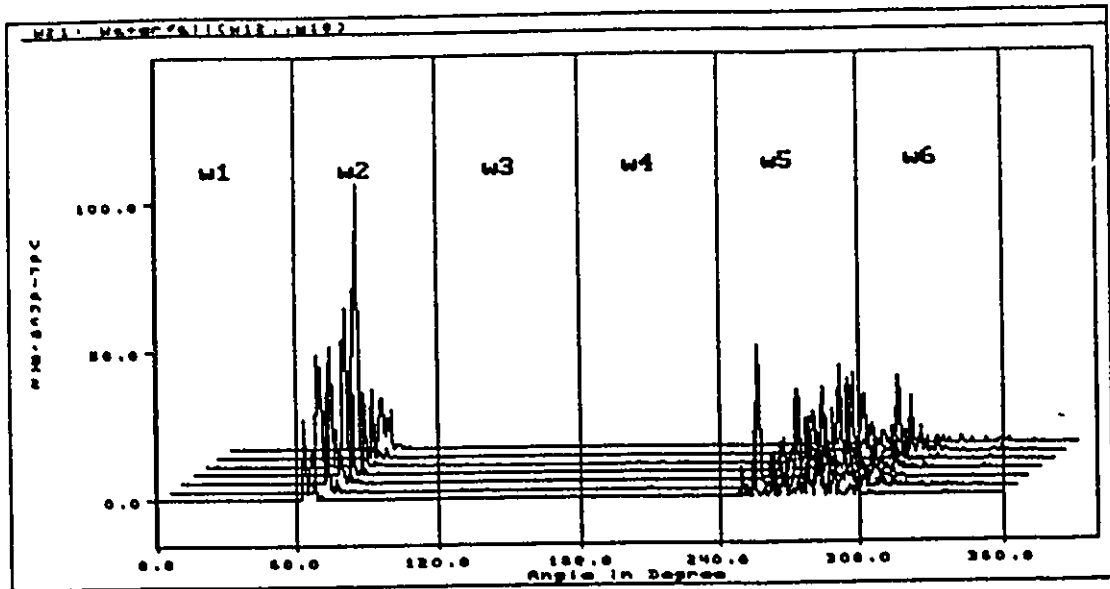
Figure 6.66 : Accelerometer #1 Vibration Running Variance
for Defective Engine (#2 Rod Bearing Omitted)
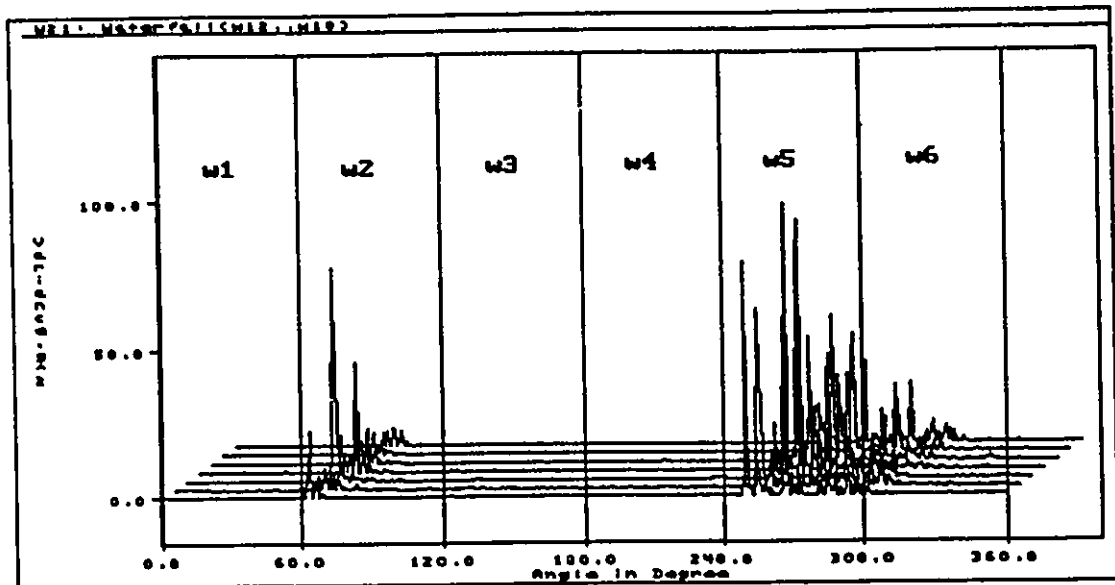
Figure 6.67 : Accelerometer #2 Vibration Running Variance
for Defective Engine (#2 Rod Bearing Omitted)

186

operating threshold value was defined as the minimum value of the vibration measured at different locations on the engine with a missing rod bearing. These values were then adjusted by trial and error until no defective engine was passed. A typical result of this monitoring method is shown in Table 6.8.

LOCATION	POSITION WINDOW
0°- 60°	1
61°- 120°	2
121°- 180°	3
181°- 240°	4
241°- 300°	5
301°- 360°	6

Table 6.7 : Position Windows Associated with Crank Angle.

Possible Location of faults (piston #)	Window No. Where Signal is Greater Than Threshold Level
1 & 5	1 and 4
2 & 6	2 and 5
3 & 4	3 and 6
4 & 3	3 and 6
5 & 1	1 and 4
6 & 2	2 and 5

Table 6.8 : Possible Results of Missing Connecting Rod Bearing

In this table, row 1 for example, if the measured vibration signal is greater than threshold level in window no. 1 and 4, then it is possible that the defect is either at piston #1 or #5.

Reliable and consistent results are being obtained using the above algorithm for identifying missing rod bearing on the cold test.

6.5.2 Implementation of Production Cold Test Stand

The vibration measurements were taken when the partially assembled engine is first driven at 250 rpm (low speed) and then 420 rpm (high speed). Threshold variance amplitudes of the rejected defective engines were determined by a trial and error method. This was achieved by sending selected defective engines to the system, exercising the reject procedure and applying different threshold variance amplitudes. Experiments were repeated until the system achieved 100 percent success in rejecting defective engines.

When the vibration (variance) exceeds a target limit of 0.25 g^2 (equivalent to 100 units)

at low speed, the engine is rejected without going through the 420 rpm (high speed) test cycle thus eliminating the possibility of damaging the engine. The limit for the high speed test is 0.71 g^2 (equivalent to 300 units).

Typical frequency distributions of the variance data for both accelerometers 1 and 2 at low and high speeds are illustrated in Figure 6.68 to Figure 6.71. The percentage of rejects due to high vibration at the high speed test ranges from 0.04 to 0.34%. For a daily production of 2000 engines, that translates to, from 1 to 7 engines per day.

The percentage of rejects due to high vibration at the low speed test ranges from 0.21 to 0.29 which translates to, from 4 to 6 engines per day.

For practical reasons, the limits for the threshold were set based on approximately 120,000 engines tested without having an incident of abnormal engine passing the vibration test. The rejected engines are moved to the reject bay area where they are repaired and then sent to be retested.

6.6 Dynamometer Test

From the results of the vibration signal analysis and the related teardown investigation, it is evident that the piston ringland offset with respect to skirt has a major role in generating high amplitude vibration signals. In other words, vibration analysis, in terms of variance analysis, is one of the very effective methods for identifying and isolating defective engine components during the combustion process. To verify the feasibility of this method, vibration was measured after swapping or replacing the noisy piston of a customer-complaint engine.

Figure 6.72 shows typical vibration signals from a noisy engine in terms of variance. Distinct vibration amplitudes are observed from piston #5 as indicated by the location of the maximum amplitude in the vicinity of the firing of cylinder #5.

After the vibration signals were monitored, a teardown analysis was performed and

```
                    *** DATA FREQUENCY DISTRIBUTION ***

         NAME:HIGH SPEED VARIANCE-ACCELEROMETER #1 REQUEST-START: 11-04-92 12:00 AM
DATA CODE :   9      UNITS: *0.002384 g^2               -END  : 11-06-92 04:59 PM

MIN      4.000        MEAN      21.911     SAMPLE SIZE 4759    HIGH LIMIT = 300
MED     16.000        SIGMA     19.901
MAX    484.000     +3 SIGMA     81.613     %REJECT =  0.042    # REJECT =    2
                   -3 SIGMA    -37.792     %ACCEPT = 99.958    # ACCEPT = 4757

       CELL LOW PT        38   228   418   608   798   988  1178 1368  1558 1748 1938 2128
                           |    |     |     |     |     |    |    |     |    |    |    |
            OVER     2
             370     0
             360     0
             350     0
             340     0
             330     0
             320     0
             310     0
             300     0
             290     0
             280     0
             270     0
             260     0
             250     3
             240     0
             230     0
             220     2
             210     0
             200     0
             190     2
             180     0
             170     0
             160     1
             150     0
             140     9
             130     0
             120    17
             110     0
             100    22    *
              90     0
              80    51    *
              70     0
              60    90    **
              50     0
              40   155    ****
              30   295    ********
              20  *1037   ****************************
              10   2077   *******************************************(*******************
               0   996    **************************
```

Figure 6.68 : High Speed Variance Frequency Distribution for Accelerometer # 1

```
                    *** DATA FREQUENCY DISTRIBUTION ***

        NAME: HIGH SPEED VARIANCE-ACCELOMETER #2 REQUEST-START: 11-04-92 12:00 AM
DATA CODE :   11       UNITS: *0.002384 g^2                -END  : 11-06-92 04:59 PM


MIN     4.000         MEAN      27.531     SAMPLE SIZE 4759    HIGH LIMIT - 300
MED    16.000         SIGMA     45.149
MAX  1089.000    +3 SIGMA     162.978    %REJECT  =   0.337    # REJECT =     16
                 -3 SIGMA    -107.916    %ACCEPT  =  99.663    # ACCEPT =   4743


CELL LOW PT            37  222  407  592  777  962 1147 1332 1517 1702 1887 2072
                        |    |    |    |    |    |    |    |    |    |    |    |
          OVER    10
          370      0
          360      2
          350      0
          340      0
          330      0
          320      4
          310      0
          300      0
          290      0
          280      7
          270      0
          260      0
          250     10
          240      0
          230      0
          220     12
          210      0
          200      0
          190     17
          180      0
          170      0
          160     26  *
          150      0
          140     34  *
          130      0
          120     40  *
          110      0
          100     64  **
           90      0
           80     80  **
           70      0
           60    105  ***
           50      0
           40    158  ****
           30    247  *******
           20  * 760  ********************
           10   2027  ******************************************************************
            0   1156  *****************************
```

Figure 6.69 : High Speed Variance Frequency Distribution for Accelerometer #2

191

```
                    *** DATA FREQUENCY DISTRIBUTION ***

DATA NAME: LOW SPEED VARIANCE-ACCLEROMETER #1  REQUEST-START: 11-04-92 12:00 AM
DATA CODE :    5      UNITS: *0.002384 g^2              -END  : 11-06-92 04:59 PM

MIN     1.000      MEAN        9.337    SAMPLE SIZE 4780   HIGH LIMIT = 100
MED     4.000      SIGMA      36.845
MAX  2401.000   +3 SIGMA     119.871    %REJECT =  0.29    # REJECT =    14
                -3 SIGMA    -101.197    %ACCEPT = 99.71    # ACCEPT = 4766

     CELL LOW PT       74   444   814 1184 1554 1924 2294 2664 3034 3404 3774 4144
                        |    |     |   |    |    |    |    |    |    |    |    |
          OVER    1
           370    0
           360    0
           350    0
           340    0
           330    0
           320    1
           310    0
           300    0
           290    0
           280    1
           270    0
           260    0
           250    1
           240    0
           230    0
           220    1
           210    0
           200    0
           190    1
           180    0
           170    0
           160    1
           150    0
           140    5
           130    0
           120    2
           110    0
           100    3
            90    0
            80    3
            70    0
            60   13
            50    0
            40   24
            30   73   *
            20  169   **
            10  430   *****
             0 *4051  ****************************************************************
```

Figure 6.70 : Low Speed Variance Frequency Distribution for Accelerometer #1

192

```
                    *** DATA FREQUENCY DISTRIBUTION ***

DATA NAME: LOW SPEED VARIANCE-ACCELEROMETER #2 REQUEST-START: 11-04-92 12:00 AM
DATA CODE :    7      UNITS: *0.002384 g^2              -END  : 11-06-92 04:59 PM

MIN     1.000       MEAN        8.261   SAMPLE SIZE 4780   HIGH LIMIT = 100
MED     4.000       SIGMA      49.820
MAX  3364.000   +3  SIGMA     157.720   %REJECT =  0.21    # REJECT   =   10
                -3  SIGMA    -141.198   %ACCEPT = 99.79    # ACCEPT   = 4770

    CELL LOW PT          76   456   836 1216 1596 1976 2356 2736 3116 3496 3876 4256
                          |    |     |    |    |    |    |    |    |    |    |    |
          OVER     1
           370     0
           360     0
           350     0
           340     0
           330     0
           320     0
           310     0
           300     0
           290     0
           280     0
           270     0
           260     0
           250     0
           240     0
           230     0
           220     0
           210     0
           200     0
           190     1
           180     0
           170     0
           160     1
           150     0
           140     2
           130     0
           120     3
           110     0
           100     2
            90     0
            80    14
            70     0
            60    25
            50     0
            40    36
            30   107  *
            20   160  **
            10   300  ****
             0 *4128  ***********************************************************
```

Figure 6.71 : Low Speed Variance Frequency Distribution for Accelerometer #2

193
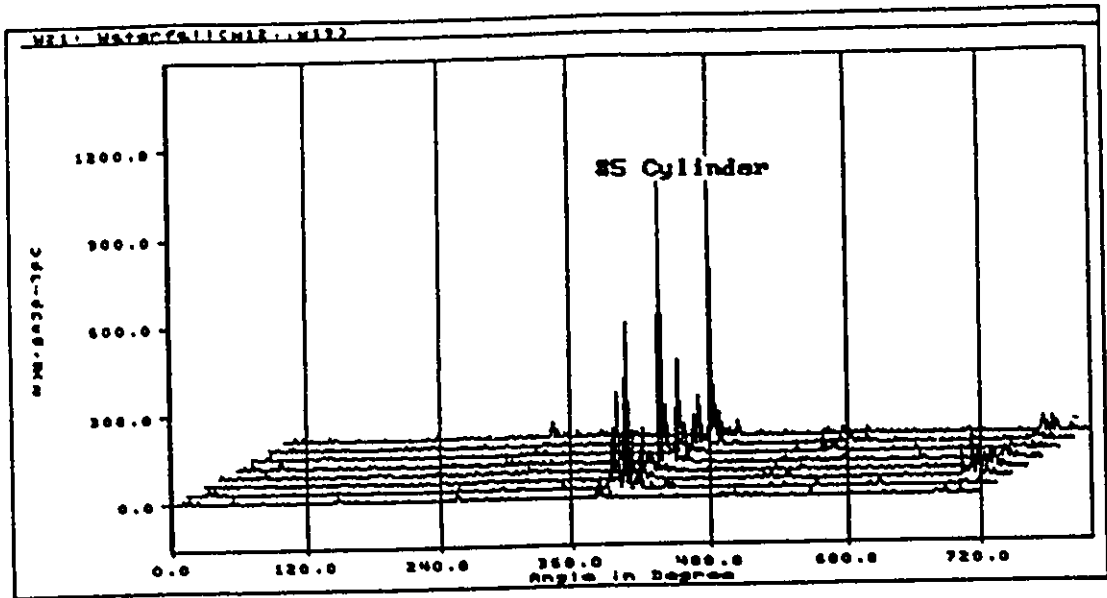
Figure 6.72 : Vibration Variance Data of Original Warranty
Return Engine
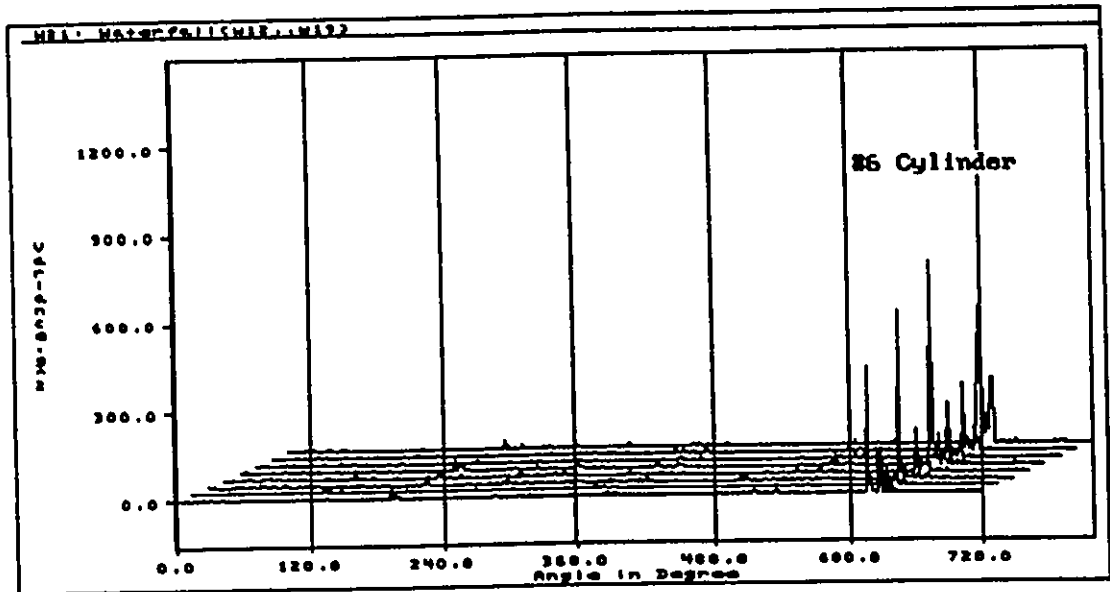
Figure 6.73 : Vibration Variance Data of Warranty Return
Engine with #5 and #6 Piston Swapped

194

dimensional characteristics of piston and cylinder #5 were investigated. As shown in Table 6.9, the maximum piston skirt offset in the negative direction was observed at piston #5.

Piston #5 was then swapped with piston #6 and the vibration was measured at the original engine operating conditions. As it can be seen from Figure 6.73, the distinct vibration from piston #5 disappeared and new peaks exist at the location of piston #6 firing.

Additional verifying experiments were carried out by replacing the noisy piston with a new piston. When the vibration was then measured at the same engine operating conditions, it was practically eliminated, as shown in Figure 6.74. These experiments were repeated for three more engines after swapping and replacing the faulty pistons. Conclusive results were consistently obtained.

6.7 Sound Pressure and Sound Intensity Analysis of Engine

The feasibility of using sound pressure and sound intensity measurements to detect defective engines is discussed in this section.

6.7.1 Sound Pressure and Sound Intensity Mapping

A sound intensity mapping was performed on an engine with a faulty piston #6 and the results are shown in Figure 6.75 for the left hand side and in Figure 6.76 for the right hand side of the engine. These figures illustrate (a) the sound intensity data mapping, (b) the mapping of equal intensity contours and (c) the 3-Dimensional plot of the intensity. Figure 6.77 shows the main frequency components of the same engine.

The results (Figures 6.75 and 6.76) indicate that the highest intensity level occurs between cylinder number 5 and cylinder number 6. Thus it is concluded that the approximate physical location of the engine noise source can be determined. However,

195

SUBJECT : PISTON MEASUREMENTS

CLAIM #.	B&A RETURN
ENGINE CODE	5K 535 084
ENGINE #	111 223 456
BUILD DATE	01-10-92
CYL. LOC. OF NOISE	#5
DATA FILE :ACCEL	

PISTON NUMBER	#1	#2	#3	#4	#5	#6
TAPER	OK	OK	OK	OK	OK	OK
RUN-OUT [mm]	0.05	0.11	0.061	0.256	0.242	0.12
PISTON CENTER [A-C, B-D]	-0.05 / 0	-0.01 / 0.11	-0.06 / -0.01	0.09 / 0.24	-0.15 / -0.19	0.01 / 0.12
PISTON TO BORE CLEARANCE						
RING DIAMETER [mm]						
TOP 96.12/96.02	96.06	96.08	96.09	96.07	96.05	96.12
MIDDLE 96.32/96.22	96.25	96.28	96.28	96.26	96.25	96.29
BOTTOM 96.07/95.87	95.96	96.02	95.96	95.89	96.05	96
REPLACED PISTON					0.11 / 0.18	

Table 6.9 : Engine Teardown Dimensions
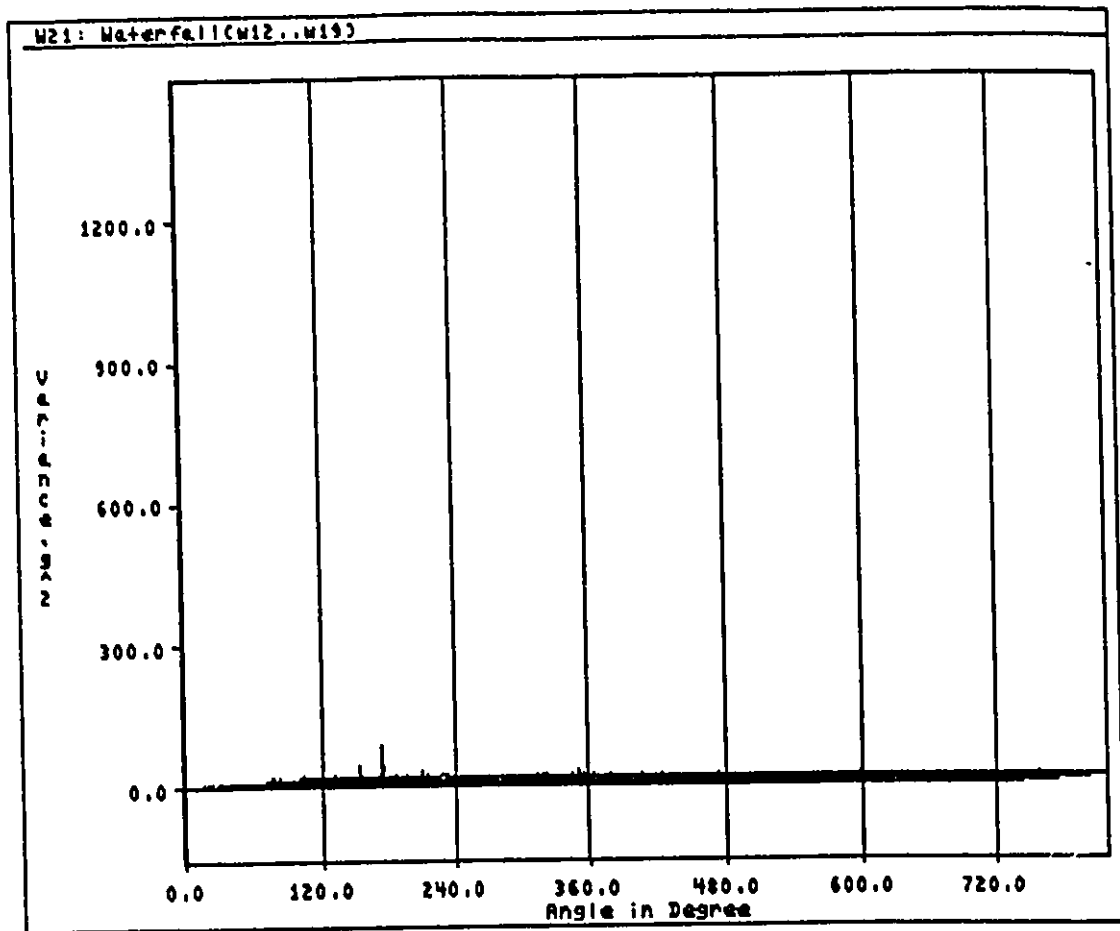
Figure 6.74 : Vibration Variance Data of Warranty Return
Engine with #5 Piston Replaced

RHINTEN PLUG3POS1
PLUG3POS1INTEN

SOUND INTENSITY

12 mm MIC. SPACER
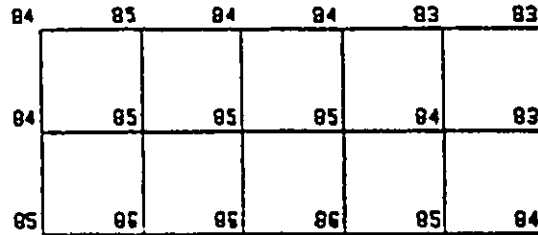
LINEAR RANGE:
125 Hz - 5000 Hz

REF. LEVEL: 50 dB

84	85	84	84	83	83
84	85	85	85	84	83
85	86	85	86	85	84

RHINTEN PLUG3POS1
PLUG3POS1INTEN

POSITIVE INTENSITY

12 mm MIC. SPACER

LINEAR RANGE:
125 Hz - 5000 Hz

REF. LEVEL: 50 dB

BASE LINE: 50 dB

DELTA LEVEL: 0.5 dB

LOG. INTERPOL.: 20
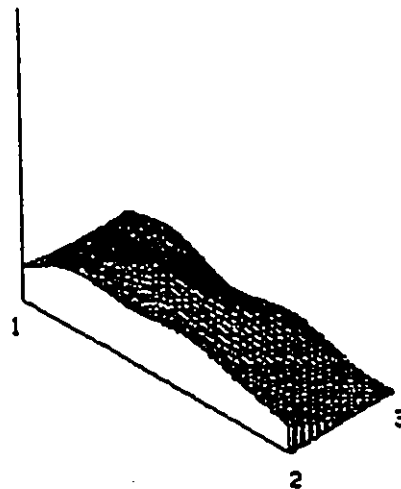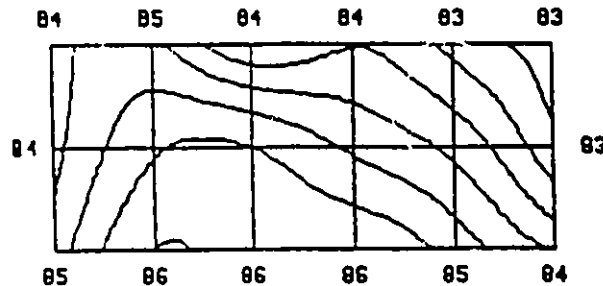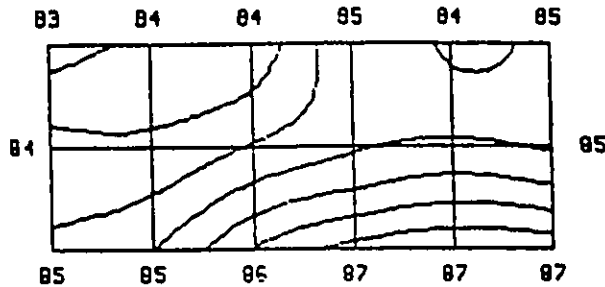
84 85 84 84 83 83
84   83
85 86 86 86 85 84

RHINTEN PLUG3POS1
PLUG3POS1INTEN

POSITIVE INTENSITY

12 mm MIC. SPACER

LINEAR RANGE:
125 Hz - 5000 Hz

REF. LEVEL: 50 dB

BASE LINE: 83 dB

GAIN FACTOR: 10

LOG. INTERPOL.: 20

Figure 6.75 : Sound Intensity Mapping of Left Hand Side of
a Defective Engine

```
83    84    84    85    84    85

84   84   85   85    85   85


85   85   86   87    87   87
```

```
83    84    84    85    84    85




84                              85




85    85    86    87    87    87
```
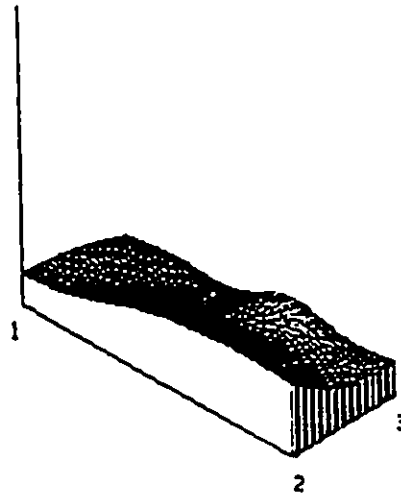
Figure 6.76 : Sound Intensity Mapping of Right Hand Side of
a Defective Engine
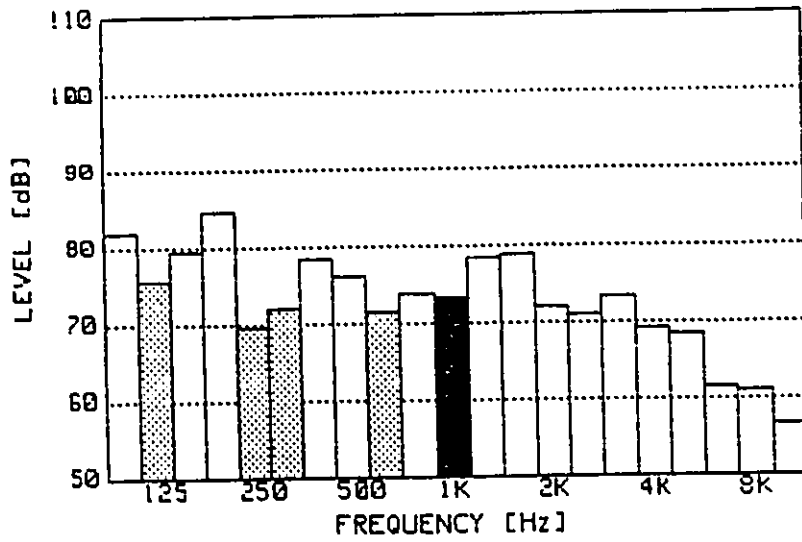
IO. : CYLINDER NO 6
WINDOW NO. : 8
FREQUENCY : 1 kHz   LEVEL : 73.3 dB

Figure 6.77 : Frequency Spectrum of the Defective Engine

it is not possible to determine the exact defective component or the exact time / location (within the cycle) when it occurs. Therefore this method was not considered for use in the monitoring procedure.

6.7.2 Gated Sound Intensity Analysis

The gated sound intensity technique is used for analyzing repetitive non-stationary signals in different applications. The sound intensity from a source is measured using a two-microphone sound intensity probe. The detailed explanation of the technique is found in Appendix G. In this study, gated sound intensity measurements were performed in an attempt to locate and define the noise source of a defective engine that was analyzed in the previous section by sound intensity mapping.

Figures 6.78 to 6.83 are the noise intensity plots from one point in space about two inches from the wall of the cylinders, from cylinder number one to six respectively. The three axes in the 3 dimensional plot are the frequency axis, the sound intensity level axis and the crank angle of engine rotation from 0 degrees to 720 degrees. The engine was running at 1500 rpm and at 100 Nm of torque.

It is shown in these previous figures that this method of analysis can approximately identify the frequency of occurrence of the noise as well as the approximate crank angle. However these results cannot distinctly differentiate the normal versus the abnormal cylinders.

6.8 Cylinder Pressure Measurement

One of the main difficulties in measuring vibration and noise is to differentiate the noise and vibration signals which are generated by the normal engine from those produced by combustion knocks. To investigate the mechanical defects in engines by measurement of vibration and noise, it is essential to eliminate the combustion knocking
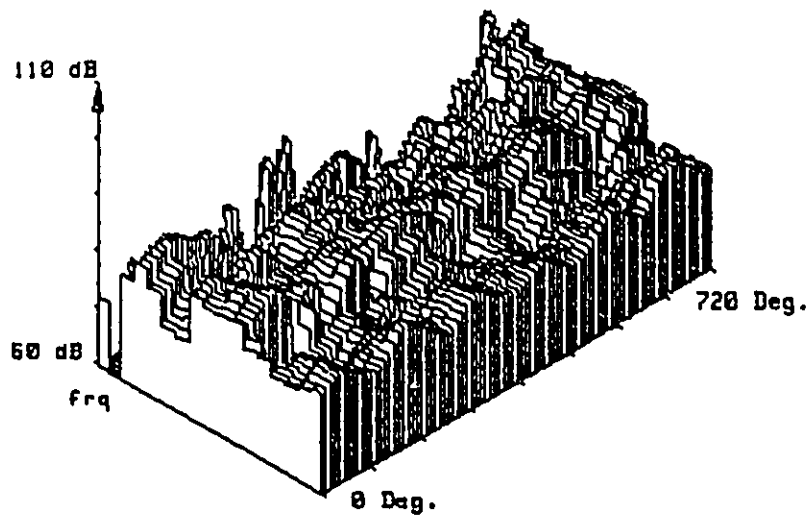
ID. : CYLINDER NO 1

FREQUENCY : 125 Hz

Figure 6.78 : 3D Plot of Sound Intensity of Defective Engine
(Location of Microphone at Cylinder #1)
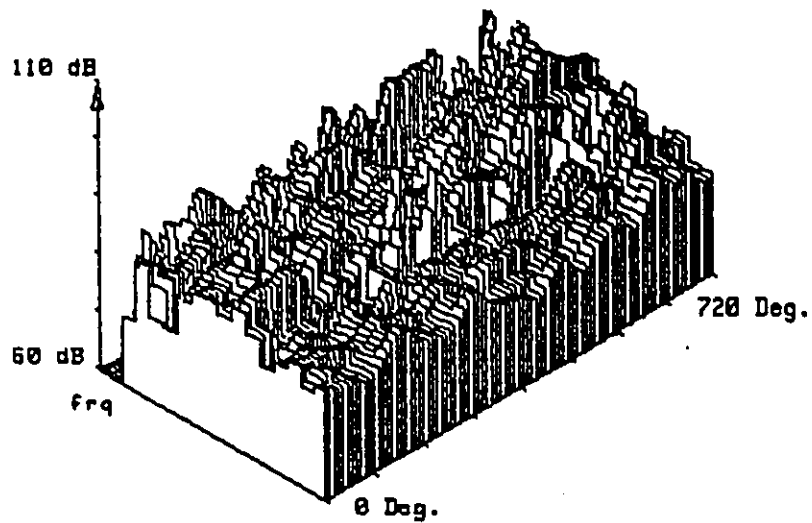
ID. : CYLINDER NO 2

FREQUENCY : 125 Hz

Figure 6.79 : 3D PLot of Sound Intensity of Defective Engine
(Location of Microphone at Cylinder #2)
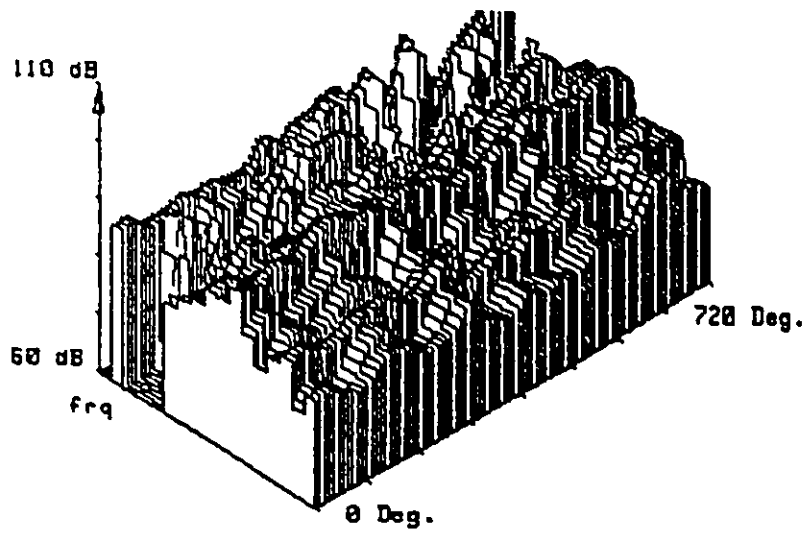
ID. : CYLINDER NO 3

FREQUENCY : 125 Hz

Figure 6.80 : 3D Plot of Sound Intensity of Defective Engine
(Location of Microphone at Cylinder #3)
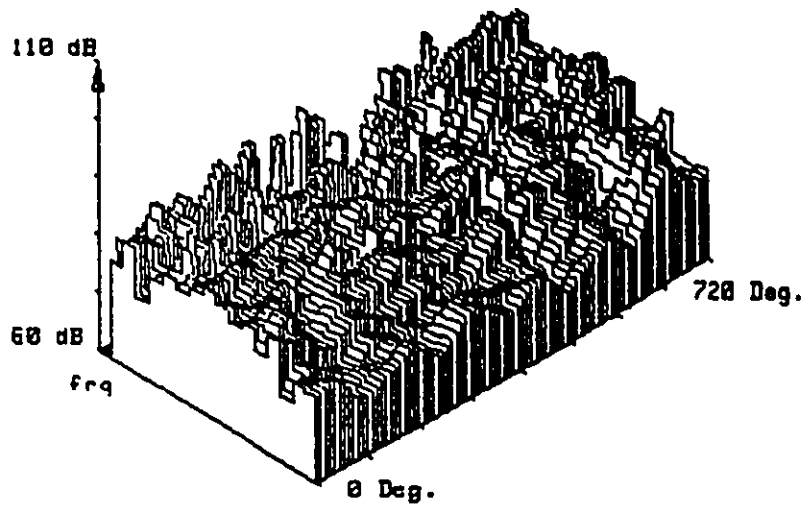
ID. : CYLINDER NO 4

FREQUENCY : 125 Hz

Figure 6.81 : 3D Plot of Sound Intensity of Defective Engine
(Location of Microphone at Cylinder #4)

203
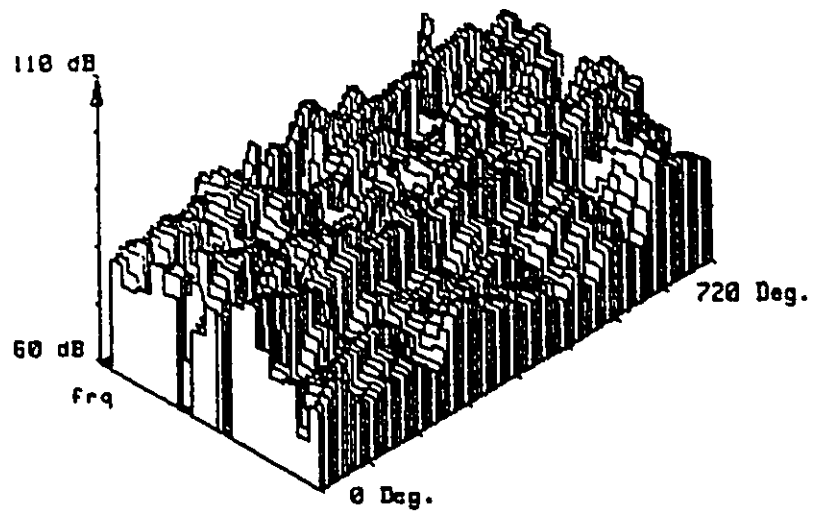
ID. : CYLINDER NO 5

FREQUENCY : 125 Hz

Figure 6.82 : 3D PLot of Sound Intensity of Defective Engine
(Location of Microphone at Cylinder #5)
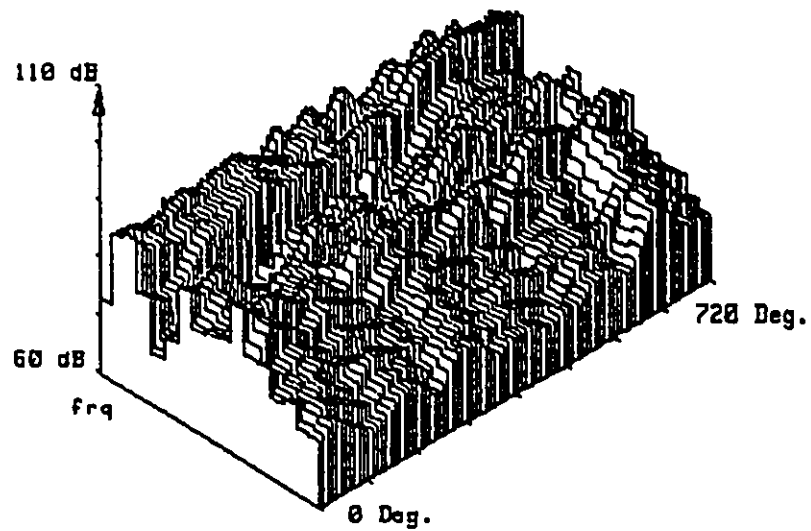
ID. : CYLINDER NO 6

FREQUENCY : 125 Hz

Figure 6.83 : 3D Plot of Sound Intensity of Defective Engine
(Location of Microphone at Cylinder #6)

phenomenon.

According to Groschel [165], the astonishingly high sensitivity of the human ear for detecting knock cannot be achieved by electronic means, because of the complicated signal processing capability of the ear. Therefore, most of the engine knocking occurrences were detected by experienced operators. These results were confirmed by measurement of the cylinder pressure which enabled these engines to be excluded from the process of identification of engine defects by means of vibration signature analysis.

Figure 6.84 shows a typical cylinder pressure signal which was measured by the PCB type 112A pressure transducer from a normal engine. However, distinct patterns of pressure signals are observed when the pressure was measured for the knocking engine, as shown in Figure 6.85 and its waterfall running variance plots are shown in Figure 6.86. Similar results were obtained by Groschel and Douaud (165) as illustrated in Figures 6.87 and 6.88.

The observed knocking signal patterns in this study were similar to the previous researches so that, measurement of the cylinder pressure was used for identifying combustion knocking engines. This process was used to ensure that the engine vibration obtained from all operating engines, is mainly due to imperfections in the manufacturing and assembly processes.
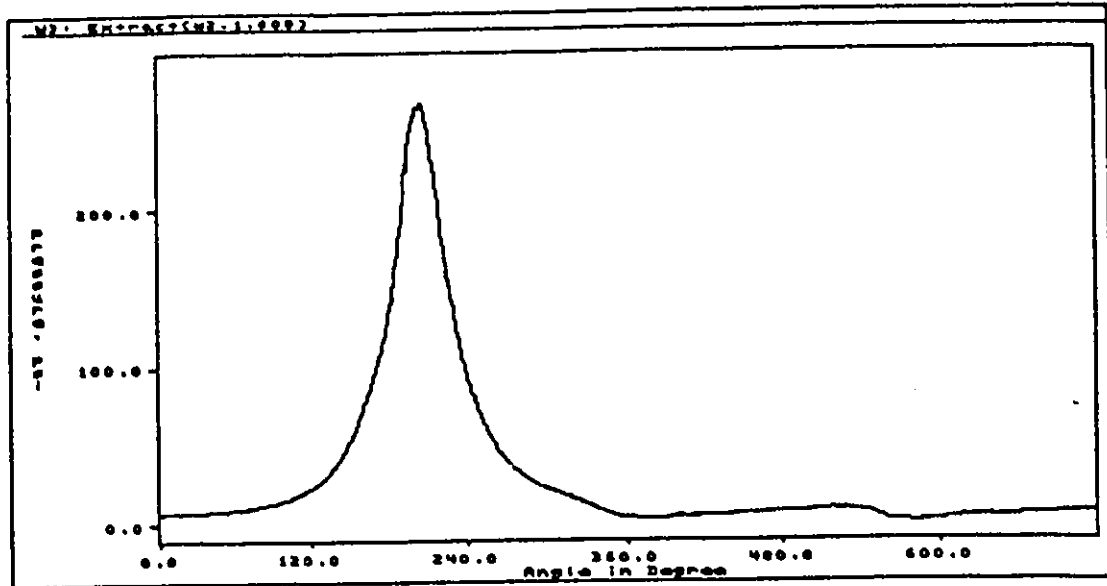
Figure 6.84 : Cylinder Pressure Signal of a Normal Engine
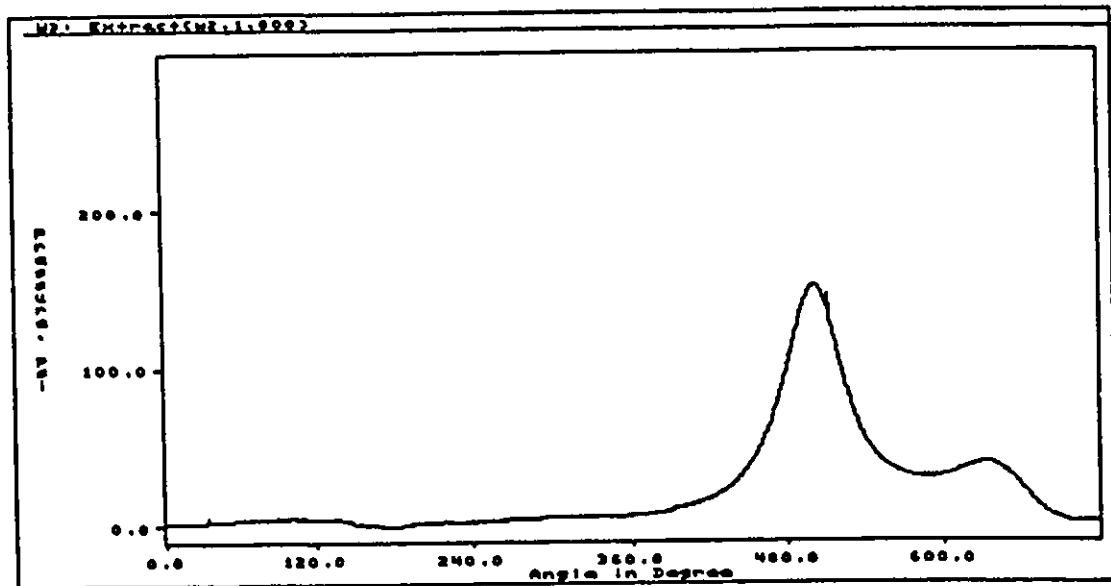
Figure 6.85 : Cylinder Pressure Signal of an Engine with
Combustion Knock

206
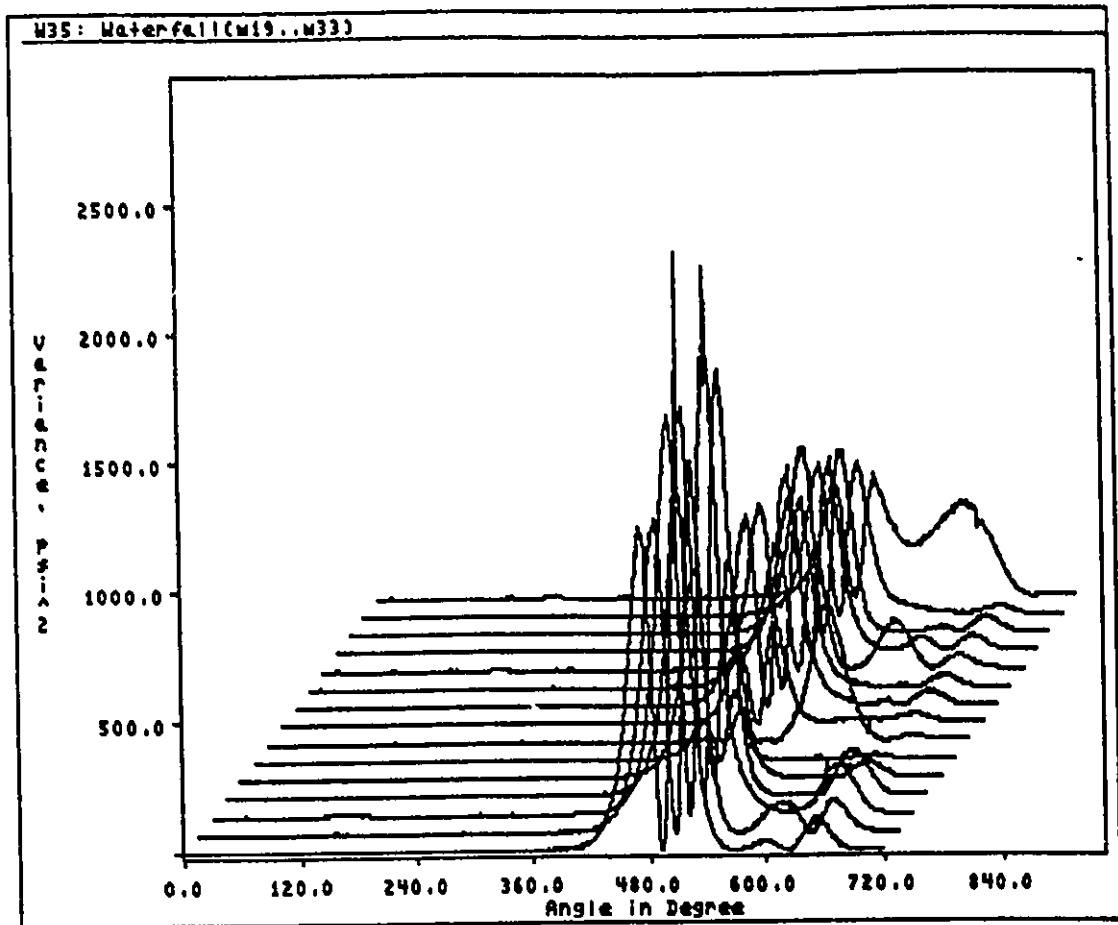
Figure 6.86 : Cylinder Pressure Running Variance Data of an
Engine with Combustion Knock
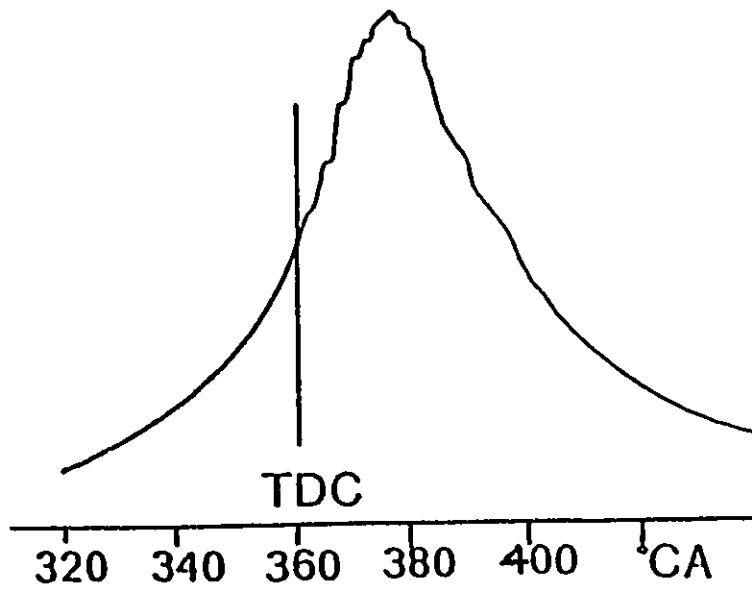
Figure 6.87 : Cylinder Pressure Signal of a Normal Engine as
Reported by Groschel and Douaud (165)
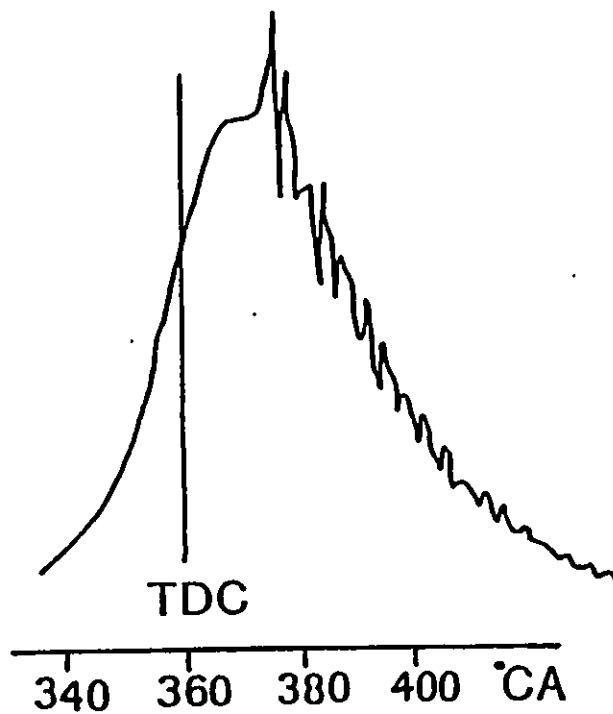
Figure 6.88 : Cylinder Pressure Signal of a Knocking
Combustion Engine as Reported by Groschel and
Douaud (165)   208

CHAPTER 7.

CONCLUSIONS

The following conclusions have been reached after examining the results of this study.

1. The vibration signature analysis techniques, in terms of time domain averaging and variance analysis, provide sufficient data for the development of a program for identifying and isolating manufacturing and assembly defects in engines.

2. A noise analysis during the motoring of an engine also indicates reliable results in monitoring missing components. However, the problem of maintenance of microphones in hostile manufacturing environments makes this method impractical. Hence, accelerometers are used in this application.

3. The selection of a proper triggering method in monitoring vibration, noise and pressure signals is critical. The position locked TTL triggering signal provided satisfactory data acquisition. This avoids signal drift due to varying engine speeds in all experiments.

4. The variance analysis of vibration signals can be used to identify the location of defective components in the engine. Using this method, almost 75 percent of teardown analysis time is saved in finding defective components in customer returned engines due to noise. The offset of piston ringland with respect to skirt is found to be a major contributor of engine noise generation. However, there is no evidence that the piston skirt taper, piston to bore clearance are the cause of major noise generation.

5. Engines with defects caused by manufacturing and assembly processes can be identified in terms of their frequency components. However, a large number of engines with special defects cannot be detected by using this method. Hence the reliability and consistency of this method does not warrant application to on-line engine signal monitoring and diagnostics.

6. Successful results in identifying and isolating defective engines have been obtained for

thousands of engine assemblies in an on-line engine monitoring system.

7. Based on this study, two systems were launched simultaneously in the engine manufacturing facility. One system was successfully implemented in June, 1992 for on-line monitoring and diagnosing of partially completed engines with a capability of testing 3000 engines daily. The second system was launched in May of 1992 for diagnosing warranty field-returned engines and evaluating the noise and vibration characteristics of engines before and after design changes. The projected annual cost saving is estimated to exceed 500,000 dollars. This is derived from the reduction in the number of defective engines going to the final phase of assembly or to the customer, a reduction in time required for diagnosing faults, and finally providing design and testing tools for development work.

7.1 Contributions

The major contributions of this research can be summarized as follows:

1. A unique automated engine test and diagnostics system was developed for rapid detection and diagnosis of various manufacturing and assembly defects, resulting in increased productivity and quality, and reduced manufacturing cost.

2. A new eight channel data acquisition system for the evaluation of noise and vibration characteristics and component development testing was designed and implemented in the dynamometer laboratory of an engine manufacturing plant.

3. A new approach in engine noise and vibration data reduction and interpretation was also proposed. This approach has been successfully applied in determination of the root cause of engine noise and in engine component development work.

CHAPTER 8.

RECOMMENDATIONS

The following recommendations represent enhancements of the present work as well as of future research, with emphasis on the successful implementation of complicated online engine monitoring and diagnostic systems.

1. Further investigations have to be carried out using a laser velocimeter as a non-contact transducer.

2. The currently available diagnosing programs using the acoustic intensity method need to be improved for use in locating noise sources in the engine.

3. The development of a more advanced engine dynamic signal monitoring and diagnostic system capable of identifying, isolating and rejecting multiple defects in completely assembled engines, has to be immediately established. This work is currently under way in one of the engine manufacturing facilities and its expected date of completion is May of 1993.

4. Application of the already developed systems is to be extended to the diagnosing of engine noise in the vehicle. This enhances the capability of the automotive mechanics involved in the diagnosis of a vehicle.

REFERENCES

1. Abe, T., Anderton, D., "Digital Acoustic Intensity Techniques in Gasoline Engine Noise Studies", SAE Paper 820363, 18 pages.

2. Akiba, K., Kakiuchi, T., "A Dynamic Study of Engine Valving Mechanisms: Determination of the Impulse Force Acting on the Valve", SAE Paper 880389, 1988, 5 pages.

3. Alfredson R., "The Partial Coherence Technique for Source Identification on a Diesel Engine", J. of Sound and Vibration, 55(4),1977, pages 487-494.

4. Alpini, A., Busso, M., Ruspa, G., Turino, G., "Analysis Techniques of Combustion Noise and Vibrations in Diesel Engines", SAE Paper 800406, 1980, 12 pages.

5. Anderton, D., Halliwell, N., "Noise from Vibration", SAE Paper 800407, 1980, 12 pages.

6. Anderton, D., "Relation between Combustion System and Engine Noise", SAE Paper 790270, 1979, 16 pages.

7. Anderton, D., Dixon, J., Chan, C., Andrews, S., "The Effect of Structure Design on High Speed Automotive Diesel Engine Noise", SAE Paper 790444, 1979, 18 pages.

8. Andrew, S., Anderton, D., "The Analysis and Mechanism of Engine 'Crank Rumble' ", I. Mech. E. Conference Publication 1979-10, pages 99-110.

9. Aoyama, F., Tanaka, S., Miura, Y., "Vibration Mode Analysis for Controlling Noise Emisssion from Automotive Diesel Engine", SAE Paper 790361, 1979, 10 pages.

10. Arrigoni, V., Calvi, G., Gaetani, B., Giavazzi, F., Zanoni, G., "Recent Advances in the Detection of Knock in S.I. Engines", SAE Paper 780153, 10 pages.

11. Arrigoni, V., Cornetti, G., Spallanzani, G., Calvi, F., Tontodonati, A., "High Speed Knock in S.I. Engines", SAE Paper 741056, 25 pages.

12. Aspinall, D., Hillarby, S., Townsend, G., "Application of Advanced Techniques to Noise and Vibration - Phase 1", MIRA Released Research Report 1984 / 2,

13. Austen, A., Priede, T., "Noise of Automotive Diesel Engines: Its Causes and Reduction", SAE Paper 650165, 37 pages.

14. Barton, R., Lestz, S., Duke, L., "Knock Intensity as a Function of Engine Rate of Pressure Change", SAE Paper 700061, 5 pages.

15. Baxa, D.E., "Noise Control in Internal Combustion Engines", John Wiley & Sons, 1982

16. Bendat, J.S., " The Hilbert Transform and Applications to Correlation Measurements", Bruel and Kjaer Technical Review, 1988, 42 pages.

17. Bianchi, F.J., "Advances in Engine Pressure Waveform Analysis", The Second International Conference On Condition Monitoring, Lodon, May, 1988, pages 147-165.

18. Bosch, R., "Automotive Handbook", Robert Bosch Publication 1979.

19. Bosch, R., "Automotive Electric / Electronic Systems", Robert Bosch Publication 1988, 347 pages.

20. Bouchillon, S., Shoureshi, R., Knurek, T., Schilke, P., "Optimal Tuning of Adaptive Hydraulic Engine Mount", SAE Paper 891160, 1989, 8 pages.

21. Brandeis, J., "The Use of Finite Element Techniques to Predict Engine Vibration", SAE Paper 820436, 1982, 12 pages.

22. Braun, S.G., Seth B.B., "Signature Analysis Methods and Applications For Rotating Machines", ASME 77-WA/Aut-5, 1977, 8 pages.

23. Braun, S.G., Seth,B.B., " Analysis of Repetitive Mechanism Signatures" Journal of Sound and Vibration, 1980, 70(4), 513-526 pages.

24. Bruel and Kjaer Company, Technical and Lecture Notes

25. Burton, D., O'Keeffe, J., Williams, R., "A Combined Analytical and Experimental Approach Fro Evaluating Engine Design For Low Noise Levels", I. Mech. E. Conference Publication 1979-10, pages 161-168.

26. Carr, I.E., Lalor, N., "The Prediction and Reduction of Noise from Engine Covers Using Energy Methods", Proc. I. Mech. E. C20/88, 1988, pages 159-165.

27. Cawthorne, A., Tyler, J., "The Transport and Road Research Laboratory Quiet Heavy Vehicle Project", SAE Paper 790452, 1979, 28 pages.

28. Challen, B., Croker D., "A Review in Diesel Engine Noise Reduction", Proceedings of Engine Noise Symposium P-106, 1982, pages 1-32.

29. Chan, C., Anderton, D., "Correlation between Engine Block Surface Vibration and Radiated Noise of In-Line Diesel Engines", Noise Control Engineering, Winter, 1974, pages 16-24.

30. Charzinski, H., Hiereth, H., "Some Aspects Concerning Noise Reduction on Diesel Passenger Cars", SAE Paper 790445, 1979, 10 pages.

31. Chung, J., Pope, J., Feldmaier, D., "Application of Acoustic Intensity Measurement to Engine Noise Evaluation", SAE Paper 790502, 1979, 12 pages.

32. Chung, J.Y., "The Use of Digital Forier Transform Methods in Engine Noise Research", SAE Paper 770010, 1977, 10 pages.

33. Clerck, J., Van Karsen, C., Shapton, W., "The Influence of Frequency Response Function Estimators on the Approximation of Modal Parameters", SAE Paper 891165, 1989, 8 pages.

34.   Cornetti, G., Arrigoni, V., Sezzi, F., Zanoni, G., "Measurement of the Extent of Abnormal Combustion by Means of an external Devices", SAE Paper 730085, 1973, 14 pages.

35.   Cortina, E., Engel, H., Scott, W., "Pattern Recognition Techniques Applied to Diagnostics", SAE Paper 700497, 12 pages.

36.   Corcione, F., Mattia, M., Paciucci, R., "Acoustic Intensity Measurements of Noise Emission From A Light Duty T.C.D.I. Diesel Engine", SAE Paper 891130, 1989, 13 pages.

37.   Crocker, M., Robb, A., "The Design and Development of an Automated System for Sound Intensity Measurement", SAE Paper 891168, 1989, 8 pages.

38.   Crocker, M., Tyrrell, R., "Engine Noise - Practicalities and Prediction Part 4 - Hardware Optimisation", SAE Paper 891128, 1989, 7 pages.

39.   Crocker, M., "The Analysis and Control of Engine Noi ɔ Quality", Proc. I. Mech. E., C16/88, 1988, 10 pages.

40.   Crocker, D., "Digital Processing Revitalises Old Techniques", SAE Paper 820366 18 pages.

41.   Crocker, D., Lalor, N., Petyt, M., "The Use of Finite Element Techniques For The Prediction of Engine Noise", I. Mech. E. Conference Publication 1979-10, pages 131-140.

42.   Crocker, M., Hamilton, J., "Modeling of Diesel Engine Noise Using Coherence", SAE Paper 790362, 1979, 12 pages.

43.   Crocker, M.J., "The Use of Existing and Advanced Intensity Techniques to Identify Noise Sources on Diesel Engine", SAE Paper 810694, 1981, 12 pages.

44.   Crocker, M.D., "Engine Structure Analysis For Low Noise - The Options", SAE Paper 850970, 1985, 11 pages.

45.   Dejong, R.G., Parsons, N.E., "Piston Slap Noise Reduction in a Vee-Block Diesel Engine", SAE Paper 820240, 1982, 9 pages.

46.   Dejong, R., Manning, J., "Modeling of Vibration Transmission in Engines to Achieve Noise Reduction", SAE Paper 790360, 1979, 12 pages.

47.   Dixon, J., Grover, E., Priede, T., "Simulation of Combustion Induced Noise in a Non-Running Engine Structure by Impulsive Hydraulic Excitation", SAE Paper 820364, 1982, 10 pages.

48.   Dourson, S., Joyce, J., "Building an Expert System to Diagnose Noise in Automotive Engine Cooling Systems", SAE Paper 850964, 1985, 19 pages.

49.   Enochson L., "Digital Techniques in Data Analysis", Noise Control Engineering, Nov, 1977, pages 138-154.

50.   Fachbach, H., Thien, G., "An Approach to a Quiet Car Diesel Engine", SAE Paper 790441, 1979, 12 pages.

51. Feitzelmayer, K., Shroder, W., "Research Project For Reducing the Noise of Truck Diesel Engines", SAE Paper 790450, 1979, 9 pages.

52. Ferraro, C.V., "A Knock Intensity Meter Based on Kinetic Criterion", SAE Paper 780154, 1978, 11 pages.

53. Fielding, B.J., Skorecki, J., "Identification of Mechanical Sources of Noise in a Diesel Engine: Sound Emitted form the Valve Mechanism", Proc. Instn. Mech. Engrs., 181(1), 1966, pages 437-446.

54. Flower, W., "Understanding Hydraulic Mounts for Improved Vehicle Noise, Vibration and Ride Qualities", SAE Paper 850975, 1985, 10 pages.

55. Ford, D., "An Analysis and Application of a Decoupled Engine Mount System for Idle Isolation", SAE Paper 850976, 1985, 10 pages.

56. Ford, D., Hayes, P., Smith, S., "Engine Noise Reduction By Structural Design Using Advanced Experimental and Finite Element Methods", SAE Paper 790366, 1979, 8 pages.

57. Fujimoto, T., Chikatani, Y., Kojima, J., "Reduction of Idling Rattle in Manual Transmission", SAE Paper 870395, 1987, 11 pages.

58. Fujimoto, Y., Suzuki, T., Ochiai, Y., "Some New Results Concerning Parameters Influencing Piston Slap In Reciprocating Machinery", I. Mech. E. Conference Publication 1979-10, pages 33- 38.

59. Galotto, C., Giorcelli, C., Levizzari, G., Ruspa, G., "The Use of Logic Electronic Device for Detection and Evaluation of Mechanical Defects of Vehicle Gearboxes in the Inspection Room", SAE Paper 740951, 1974, 8 Pages.

60. General Motors Corporation, "Balance Engineering Manual", Third Edition, 110 pages.

61. Genuit, K., Gierlich, H., "Investigation of the Correlation between Objective Noise Measurement and Subjective Classification", SAE Paper 891154, 1989, 10 pages.

62. Griffiths, W., Skorecki, J., "Some Aspect of Vibration of a Single Cylinder Diesel Engine", J. of Sound and vibration, 1(4), 1964, pages 345-364.

63. Grover, E., Perry, R., "An Experimental Passenger Car Diesel Engine", SAE Paper 790443, 1979, 8 pages.

64. Haddad, S., Pullen, H., "Piston Slap as a Source of Noise and Vibration in Diesel Engines", J. of Sound and Vibration, 34(2), 1974, pages 249-260.

65. Hanaoka, M., Fukumura, S., "A Study of Valve Train Noises and a Method of Cam Design to Reduce the Noises", SAE Paper 730247, 1973, 12 pages.

66. Hayes, P.,Quantz, C., "Determining Vibration, Radiation Efficiency, and Noise Characteristics of Structural Designs Using Analytical Techniques", SAE Paper 820440, 1982, 8 pages.

67. Hayes, P., Seybert, A., Hamilton, J., "A Coherence Model for Piston Generated Impact Noise", SAE Paper 790274, 1979, 8 pages.

68. Hera, R., "Transmission Noise Reduction Using Holographic Source Identification and Constrained Layer Damping", SAE Paper 790363, 1979, 8 pages.

69. Hickling, R., Kamal, M., "Engine Noise : Excitation, Vibration, and Radiation", Plenum Press, 1982.

70. Hirako, O., Murakami, N., Akishino, K., "Influence of Valve Noise On Knock Detection in Spark Ignition Engines", SAE Paper 880084, 1988, 13 pages.

71. Hodgetts, D., McDonald, A., "The Transmission of Piston Forces to the Mounts of An Engine", I. Mech. E. Conference Publication 1979-10, pages 1-8.

72. Hogh, G., Powell, B., Lawson, G., "Real Time Engine Dynamic Analysis and Control", SAE Paper 885104, 1988, 10 pages.

73. Honda, Y., Saito, T., Wakabayashi, K., Kodama, T., Iwamoto, S., "A Simulation Method for Crankshaft Torsional Vibration by Considering Dynamic Characteristics of Rubber Dampers", SAE Paper 891172, 1989, 16 pages.

74. Jiang, J., Whittlesey, M., "An Analytical Method of Noise Source Identification Using Boundary Element Technique", SAE Paper 891152, 1989, 16 pages.

75. Kadomatsu, K., "Hydraulic Engine Mount for Shock Isolation at Acceleration on the FWD Cars", SAE Paper 891139, 1989, 8 pages.

76. Kaiser, H., Schmillen, K., Spessert, B., "Acoustical Optimization of the Piston Slap by Combination of Computing and Experiments", SAE Paper 880100, 1988, 12 pages.

77. Kamiya, T., Atsumi, T., Tasaka, K., "Toyota's New Type of Crankshaft Pulley to Improve the Compartment Tone Quality", SAE Paper 880078, 1988, 7 pages.

78. Kemmer, U., Rollwage, M., Rose, K., "New Generation of BOSCH Electrical Fuel Pump - Improvement in Hot Fuel Handling and Noise", SAE Paper 870120, 13 pages.

79. Kindt, J., Marty, J., "Experimental Study of a High Speed Diesel Engine by Acoustical Power Method", SAE Paper 790446, 1979, 16 pages.

80. Kinoshita, M., Sakamoto, T., Okamura, H., "An Experimental Study of a Torsional / Bending Damper Pulley for an Engine Crankshaft", SAE Paper 891127, 1989, 12 pages.

81. Kirkup, S., Henwood, D., Tyrrell, R., "Engine Noise - Practicalities and Prediction Part 3: Noise Prediction using Boundary Element Method", Proc. I. Mech. E., C33/88, 1988, 8 pages.

82. Kochanowski, H., Kaiser, W., Esche, D., "Noise Emission of Air-Cooled Automotive Diesel Engines and Trucks", SAE Paper 790451, 1979, 10 pages.

83. Kojima, N., Okamura, S., Zhou, H., "The Use of Vibration Intensity Measurement in Identifying the Source of Impact in an Engine Structure", SAE Paper 891167, 1989, 8 pages.

84. Kojima, N., Murata, M., Fukuda, M., "Impulse Response and Radiated Noise in an Air-cooled Small Engine", Bull. of the JSME, 25(200), Feb. 1982, pages 234-240.

85. Krenz R., "Vehicle Response to Throttle Tip-In / Tip-Out", SAE Paper 850967, 1985, 9 pages.

86. Krisper, G., Kratochwill, H., "Concept for a Chasis Mounted Capsule of Engine and Gearbox for Heavy Trucks", SAE Paper 790449, 1979, 10 pages.

87. Kuroda, O., Fujii, Y., "An Approach to Improve Engine Sound Quality", SAE Paper 880083, 1988, 10 pages.

88. Lalor, N., Grover, E., Priede, T., "Engine Noise Due to Mechanical Impacts at Pistons and Bearings", SAE Paper 800402, 7pages.

89. Lalor, N., "Computer Optimised Design of Engine Structures for Low Noise", SAE Paper 790364, 1979, 10 pages.

90. Lyon, R., "Machinery Noise and Diagnostics", Massachusetts Institute of Technology, 418 pages.

91. McCandless J., "High Tech in Small Engine Design and Development", ISER, Sept. 1985, 27 pages.

92. McGary M., Crocker, M., "Surface Intensity Measurements on Diesel Engine", Noise Control Engineering, Jan-Feb, 1981, pages 27-36.

93. McKinlay, W.P., Woods, M., Pickles, M., "Vehicle Noise Source Identification Techniques", Proc. I. Mech. E., C34/88, 1988, 12 pages.

94. Meier, R.C., Goetz, T.G., "Cost Effective Engine Diagnostics For Production Engine Hot Test", SAE Paper 851564, 1986, 8 pages.

95. Meier, R.C., "Diagnostic Computer Interface and Sensor hardware Description and Recommendations", Ford Motor Company Internal Report, 1981.

96. Meier, R.C., "Frequency Domain Engine Defect Signal Analysis", U.S. Patent No. 4,424,709, Jan 10, 1984.

97. Meier, R.C., Gable, S.V., Patil, P.B., "Application of a Short Transient Engine Cycles to Production Hot Test Facilities", Ford Motor Company Internal Report, 1979.

98. Meier, R.C., and Gable, S.V., "Frequency Domain Engine Diagnostic System, A new Approach to Production Engine Hot Test Defect Detection", Ford Motor Company Internal Technical Report, 1981.

99. Meier, R.C., "Piston slap / bearing Knock Noise Evaluation Study", Ford Motor Company Internal Report, 1983.

100. Milenkovic, V., Shmuter, S., Field, N., "ON-Line Diagnostics of Rear Axle Transmission Errors", J. of Engineering for Industry, Nov., 1984, V106, pages 331-338.

101. Monaghan, M.L., "Engine Design and Development - A View to the Future" ISER, sept. 1985, 16 pages.

102.   Morrison, D., Challen, B., "A Survey of Passenger Car Diesel Engine", SAE Paper 790442, 1979, 10 pages.

103.   Munro R., Parker A., "Transverse Movement Analysis and Its Influence on Diesel Piston Design", SAE Paper 750800, 1975, 11 pages.

104.   Murphy, C.,"Effects of Engine oil Supply on Rocker Arm and Ball Wear", SAE Paper 740540, 1974, 6 pages.

105.   Nivi, H., "Axle In-Process Diagnostic Test: Gear Nick Detection", Ford Motor Company Internal Technical Report, 1982.

106.   Nivi, H., Field, N., Seth, B., "Optimum Phasor Tolerances for 90° V-6 Engine Balance", Ford Motor Company Internal Technical Report, 1982.

107.   Ochiai, K., Nakano, M., "Relation between Crankshaft Torsional Vibration and Engine Noise", SAE Paper 790365, 1979, 8 pages.

108.   Oetting, H., Papez, S., "Reducing Diesel Knock BY Means of Exhaust Gas Recirculation", SAE Paper 790268, 1979, 12 pages.

109.   Oguri, A., Totii, H., Hosokawa, T., Nakada, M., "Development of Analysis Model For Piston Movement", SAE Paper 885031, 1988, 8 pages.

110.   Okamura, H., Shinno, A., Sogabe, K., "Dynamic Stiffness Matrix Method for the Three-Dimensional Analysis of Crankshaft Vibration", Proc. I. Mech. E., C23/88, 1988, 14 pages.

111.   Okuma, M., Ohara, T., Nagao, K., Nagamatsu, A., "Application of a New Experimental Identification Method to Engine Rigid Body Mount System", SAE Paper 891139, 1989, 8 pages.

112.   Ordubadi, A., "Fault Detection in Internal Combustion Engines Using an Acoustic Signal", SAE Paper 820365, 6 pages.

113.   Otte, D., Fyfe, K., Sas, P., Leuridan, J., "Use of the Pricipal Component Analysis for Dominant Noise Source Identification", Proc. I. Mech. E., C21/88, 1988, 10 pages.

114.   Padoan, R., Monrozier, M., "Statistical Approach For Diesel Engine Noise Analysis", SAE Paper 790454, 1979, 10 pages.

115.   Petitdidier, A., "Practical Investigation of Noise Reduction of a Diesel Passenger Car", SAE Paper 790447, 1979, 10 pages.

116.   Pettitt, R., Towch, B., "Noise Reduction of a Four Litre Direct Injection Diesel Engine", Proc. I. Mech. E., C22/88, 1988, 8 pages.

117.   Pischinger, F., Schmillen, K., Leipold, W., "A New Measuring Methods for the Direct Determination of Diesel Engine Combustion Noise", SAE Paper 790267, 1979, 10 pages.

118.   Pope, J., Hickling, R., Feldmaier, D., Blaser, D., "The Use of Acoustic-Intensity Scans for Sound Power Measurement and For Noise Source Identification in Surface Transportation Vehicles", SAE Paper 810401, 9 pages.

119.   Potter, R., Gribler, M., "Computed Order Tracking Obseletes Older Methods", SAE Paper 891131, 1989, 6 pages.

120.   Priede, T., Dutkiewicz, R., "The Effect of Normal Combustion and Knock on Gasoline Engine Noise", SAE Paper 891126, 1989, 14 pages.

121.   Priede, T., Baker, J, Grover, E., Ghazy, R., "Characteristics of Exciting Forces and Sructural Response of TurboCharged Diesel Engines", SAE Paper 850972, 1985, 9 pages.

122.   Priede, T., "Problems and Developments in Automotive Engine Research", SAE Paper 790205, 1979, 16 pages.

123.   Rasmussen, G., "Sound Intensity Measurement : Vancouver Skytrain", Bruel & Kjaer Report, 1987.

124.   Rhodes, D., Phillips, A., Abbott, B., "Prediction of Engine Vibration From Combustion Pressure Measurements and Examination of the Effect of Combustion Variations in the Frequency Domain", Proc. I. Mech. E., C28/88, 1988, 12 pages.

125.   Richmond J., Parker, D., "The Quantification and reduction of Piston Slap Noise", Proc. of Instn Mech Engrs, Vol 201, No. D4, 1987, pages 235-244.

126.   Rivin, E., "A Low Noise Gear Transmission", Proc. I. Mech. E., C27/88, 1988, 18 pages.

127.   Ross, D., Ungar, E., "On Piston Slap as a Source of Engine Noise", ASME Paper 65-OGP-10, 1965, 8 pages.

128.   Russell, M., Worley, S., Young, C., "An Analyzer to Estimate Subjective Reaction to Diesel Engine Noise", Proc. I. Mech. E., C30/88, 1988, 10 pages.

129.   Russell, M., Haworth, R., "Combustion Noise form High Speed Direct Injection Diesel Engines", SAE Paper 850973, 1985, 22 pages.

130.   Russell, M.F., "Diesel Engine Noise: Control at Source", SAE Paper 820238, 1982, 19 pages.

131.   Russell, M., Cavanagh, E., "Establishing a Target for Control of Diesel Combustion Noise", SAE Paper 790271, 1979, 14 pages.

132.   Russell, M., Pullen, R., "The Influence of Mountings on Injector Pump Noise", SAE Paper 790273, 1979, 10 pages.

133.   Russell, M., "Automotive Diesel Engine Noise and Its Control", SAE Paper 730243, 1973, 18 pages.

134.   Russell, M., "Reduction of Noise from Diesel Engine Surfaces" SAE Paper 720135, 1972, 11 pages.

135.   Sacks, M., Brackett, S., "Subjective Evaluation of Simulated Engine Induction Noise", SAE Paper 891156, 1989, 10 pages.

136.   Sander, W., Steidle, W., Wacker, E., "Piston Movement and Its Influence on Noise of Automotive Engines", SAE Paper 790272, 1979, 12 pages.

137. Schenck Trebel, "Fundamentals of Balancing", March 1983.

138. Schneider, M., Schmillen, K., Pischinger, F., "Regularities of Cylinder Pressure Oscillations and Their Effects on the Combustion Process and Noise", SAE Paper 872248, 1987, 9 pages.

139. Seth, B.B., and Field, N.L., "Oil Pressure Signature For Engine Lubrication System Monitoring", SAE Paper 840063, 1984, 8 pages.

140. Seth, B.B., "Application of Statistical Process Control Methodology to IN-Process Cold Test At EEP", Ford Motor Company Internal Technical Report.

141. Seth, B.B., "Balancing Algorithms For 3.8L, V-6 Engine Production Test Stands", Ford Motor Company Internal Technical Report, 1983.

142. Seth, B., Stuart, B., Field, N., "3.8 L V-6 Engine Cold Test Process Control", Ford Motor Company Internal Technical Report, 1983.

143. Seth, B., "Multiple Defects Diagnostics of 3.8L, V-6, Engines Using Signature Analysis", Ford Motor Company Internal Technical Report, 1983.

144. Sherrington, I., Smith, E., "The Measurement of Piston-Ring Friction by the 'floating -Liner' Method", I. Mech. E. Conf. On Experimental Methods in Engine Research and Development, March 1988, 11 pages.

145. Shinkle, G.A., " Automotive Component Vibration: A practical Approach to Accelerated Vibration Durability Testing", SAE Paper 840501, 1984, 15 pages.

146. Shmuter, S.L., "Pericision Measurement of Torsional Oscillations Induced by Gear Errors", The Shock and Vibration Bulletin, Part 3, June 1984, pages 77-87.

147. Shmuter, S., Nivi, H., " Computerized Identification of Gear Noise Related to Conjugate Errors and Nicks", Inter-Noise 84, pages 45-48, Dec. 1984.

148. Shugong, L., Seybert, A., "Acoustic Modal Analysis and Transmission Properties of a Prototype Induction System", SAE Paper 891170, 1989, 8 pages.

149. Soenarko, B., Seybert A., "On the Prediction of Sound Radiated by Engine Vibration", SAE Paper 852222, 1985, 7 pages.

150. Soroko, W., Chien, C-S., "Automotive Piston-Engine Noise And Its Reduction - a Literature Survey", SAE Paper 690452, 1969.

151. Starkman, E., Syts, W., "The Identification and Characterization of Rumble and Thud", SAE Transactions, Vol. 68, 1960, pages 93-100.

152. Stebar, R., Wiese, W., Everett, R., " Engine Rumble - A Barrier to Higher Compression Ratios ?", SAE Transactions, Vol. 68, 1960, pages 206 - 216.

153. Sung, S., Nefske, D., "Engine Vibration and Noise Reduction Using a Crank-Block System Model", SAE Paper 891129, 1989, 6 pages.

154. Sung, Y., Lalor, N., "The Prediction of Engine Noise Reduction by Using Shields and Partial Enclosures and the Optimization of Their Design", Proc. I. Mech. E., C29/88, 1988, 6 pages.

155. Takeyama, T., Nomura, K., "Combustion Noise of Two-Stroke Gasoline Engines and Its Reduction Techniques", SAE Paper 891125, 1989, 8 pages.

156. Takiguchi, M., Kikuchi, H., Furuhama, S., "Influence of Clearance Between Piston and Cylinder on Piston Friction", SAE Paper 881621, 1988, 9 pages.

157. Thien, G., "A Review of Basic Design Priciples for Low Noise Diesel Engines", SAE Paper 790506, 1979, 22 pages.

158. Thompson, J., Tree, D., "Finite Difference Approximation Errors in Acoustic Intensity Measurements", J of Sound And Vibration, 75(2), pages 229-238, 1981.

159. Thompson, R., Weichbrodt, B., "Gear Diagnostics and Wear Detection", ASME Paper 69-VIBR-10, 1969, 7 pages.

160. Thomson, W., "Fundamental of Automotive Engine Balance", Mechanical Engineering Publications Limited, London, 1978, 96 pages.

161. Tjong, J., Miller, W., Reif, Z., Gaspar, R., "Time Based Signal Analysis fot the Detection of Intermittent and Impact Noise and Vibration", Engineering Application of Mechanics 1990, Kingston, Canada, 1990.

162. Tjong, J., "Feasibility of Applying Vibration Monitoring Techniques to High Volume Multistation Transfer Machines", Masters Thesis, University of Windsor, Canada, 1984.

163. Tsangarides, M., Tobler, W., Heerman, C., "Interactive Computer Simulation of Drivetrain Dynamics", SAE Paper 850978, 1985, 26 pages.

164. Ufford, D., Berhard, R., Kohrman, G., Bolton, J., "Powertrain Sound Power Measurement Using a Two-Degree-of-Freedom Positioning Mechanism", SAE Paper 891164, 1989, 10 pages.

165. Volkswagenwerk, AG, Research Division, "Knocking of Combustion Engines", D-3180 Wolfsburg, Federal Republic of Germany, 1981.

166. Wallace, D., Darlow M., "Signal Processing of Transient Phenomena Using Fourier Transform Techniques", ASME Paper 85-DET-155, 1985, 6 pages.

167. Watanabe, Y., Rouverol, W., "Maximum - Conjugacy Gearing" SAE Paper 820508, 1982, 14 pages.

168. Watanabe, Y., Fujisaki, h., Tsuda, T., "DI Diesel Engine Becomes Noisier at Acceleration - The Transient Noise Characteristic of Diesel Engine", SAE Paper 790269, 1979, 12 pages.

169. Waters, P., "Recent Advances in Diesel Engine Research", SAE Paper 850971, 1985, 13 pages.

170. Warren, S., Handley, J., "Stochastic Combustion and Diesel Engine Noise", SAE Paper 770408, 1977, 12 pages.

171. Welbourn, D.B., "Fundamental Knowledge of Gear Noise - A Survey", I. Mech. E. conference Publication 1979-10, pages 9-14.

172. Windett, R., Johnson, R., "The Practical Reduction of Bare Engine Noise From a Conventional Diesel Engine", I. Mech. E. Conference Publication 1979-10, pages 111-118.

173. Winklhofer, E., Thien, G., "A Review of Parameters Affecting the Noise and Vibration in Diesel Powered Passenger Cars", SAE Paper 850966, 1985, 10 pages.

174. Wood, L., Vethecan, J., "Noise Cancellation Techniques in Motor Vehicles", Proc. I. Mech. E., C24/88, 1988, 8 pages.

175. Young, C., Renowden, P., "Measurements and Reduction of Spark Ignition Engine Fuel Injector Noise", Proc. I. Mech. E., C31/88, 1988, 8 pages.

APPENDICES

APPENDIX A

A. A SUMMARY CHART OF THE BIBLIOGRAPHY OF ENGINE NOISE AND VIBRATION

AUTHORS	DATE	REF. NO.	INSTRUMENTATION	MEASUREMENT TECHNIQUES	ACOUSTIC INTENSITY / SOUND POWER	DATA PROCESSING TECHNIQUES	FEA / MODAL ANALYSIS	GENERAL ENGINE NOISE	PISTON NOISE	GEAR NOISE	VALVETRAIN NOISE	TURBO / SUPERCHARGER NOISE	BEARING DRIVE	ACESSORIE DRIVE	USERS' EXPERIENCE
Abe, T.	1982	1	•	•	•			•							
Aibe, T.	1988	2									•				
Alfredson, R.	1977	3	•	•		•									
Alphei, A.	1980	4	•	•	•		•	•	•						
Anderton, D.	1980	5	•	•	•			•							
Anderton, D.	1979	6					•	•					•		
Anderton, D.	1979	7		•				•							
Astrew, S.	1979	8		•				•							
Aoyama, F.	1979	9	•	•		•	•	•							
Arrigoni, V.	1978	10	•	•											
Arrigoni, V.	1974	11				•		•							
Asphall, D.	1984	12	•	•	•	•	•	•	•	•	•	•	•	•	
Austen, A.	1965	13		•				•			•				
Barton, R.	1970	14	•	•				•							
Baxa, D.E	1982	15	•	•				•							
Bender, J.S.	1982	16				•									
Blanch, F.J.	1988	17	•	•		•		•							
Boch, R.	1984	18													
Boch, R.	1988	19													
Boesthlm, S.	1989	20					•								
Brandeis, J.	1982	21				•									
Brem, S.O.	1977	22		•		•									
Brem, S.G.	1980	23	•	•		•	•	•							
Bruel & Kjaer	ALL	24	•	•	•	•	•	•	•	•	•	•	•	•	
Burton, D.	1979	25					•	•							
Carr, J.E.	1988	26	•	•	•	•	•	•							
Cavaforum, A.	1979	27					•	•							
Chellm, R.	1982	28	•	•		•		•							
Chen, C.	1974	29	•	•		•		•							
Chamberd, H.	1979	30						•							

Author	DATE	REF. NO.	INSTRUMENTATION	MEASUREMENT TECHNIQUES	ACOUSTIC INTENSITY / SOUND POWER	DATA PROCESSING TECHNIQUES	FEA / MODAL ANALYSIS	GENERAL ENGINE NOISE	PISTON NOISE	GEAR NOISE	VALVETRAIN NOISE	TURBO / SUPERCHARGER NOISE	BEARING DRIVE / ACCESSORIE	USERS' EXPERIENCE
Chang, J.	1979	31		•	•	•		•						
Chang, J.Y.	1977	32		•		•		•						
Clerk, J.	1989	33												
Connell, G.	1975	34	•	•		•		•						
Cortea, E.	1970	35	•	•		•		•						
Cordosa, P.	1989	36												
Crocker, M.	1989	37												
Crocker, M.	1989	38												
Crocker, M.	1988	39		•	•	•		•						
Crocker, D.	1982	40		•	•	•		•						
Crocker, M.	1979	41		•		•								
Crocker, M.J.	1981	42		•	•	•								
Crocker, M.D.	1985	43					•	•						
Crocker, M.D.	1983	44					•	•						
Dejong, R.G.	1982	45		•		•	•		•					
Dejong, R.	1979	46		•		•	•	•						
Dixon, J.	1982	47		•		•		•						
Dourson, S.	1985	48		•				•						
Enodaon, L.	1977	49	•	•		•	•							
Fachbach, H.	1979	50		•				•						
Felanlmeyer, K.	1979	51		•				•						
Ferraro, C.V.	1978	52	•	•				•						
Fielthy, B.J.	1966	53		•		•					•			
Flower, W.	1985	54					•	•						
Ford, D.	1985	55					•	•						
Ford, D.	1979	56		•		•				•				
Fujimoto, T.	1987	57		•		•								
Fujimoto, Y.	1979	58		•		•			•					
Galena, C	1974	59				•								
General Motors		60		•										

226

AUTHORS	DATE	REF. NO.	INSTRUMENTATION	MEASUREMENT TECHNIQUES	ACOUSTIC INTENSITY / SOUND POWER TECHNIQUES	DATA PROCESSING TECHNIQUES	FEA / MODAL ANALYSIS	GENERAL ENGINE NOISE	PISTON NOISE	GEAR NOISE	VALVETRAIN NOISE	TURBO / SUPERCHARGER NOISE	BEARING NOISE	DRIVE ACCESSORIE NOISE	USERS' EXPERIENCE
Ozawa, K.		61													
Griffith, W.	1964	62		•		•		•							
Grover, E.	1979	63				•		•							
Haddad, S.	1974	64		•		•			•						
Hanada, M.	1973	65		•		•					•				
Hayes, P.	1982	66					•	•							
Hayes, P.	1979	67		•		•		•	•						
Hery, R.	1979	68	•	•											
Nikiforuk, R.	1982	69	•	•	•	•		•							
Hiraba, O.	1988	70	•	•		•		•			•				
Hodgetts, D.	1979	71	•	•		•	•		•						
Hoeg, G.	1988	72	•	•		•		•							
Honda, Y.	1989	73													
Jiang, J.	1989	74													
Kaizuma, K.	1989	75	•	•	•	•									
Kaiser, H.	1988	76		•					•						
Kamiya, T.	1988	77													
Kammer, U.	1987	78	•	•		•		•							
Klein, J.	1979	79	•	•	•			•							
Kobashi, M.	1989	80			•										
Kiriuya, S.	1988	81		•				•							
Kochanowski, H.	1979	82						•							
Kojima, N.	1989	83	•					•							
Kojima, N.	1982	84		•		•									
Kraus, R.	1985	85		•				•							
Krieger, G.	1979	86	•	•											
Kuroda, O.	1988	87		•		•	•	•			•		•		
Lalor, N.	1980	88		•		•	•		•						
Lalor, N.	1979	89	•	•	•	•	•	•	•	•	•		•	•	
Lynn, N.	1977	90						•	•			•	•	•	•

AUTHORS	DATE	REF. NO.	INSTRUMENTATION	MEASUREMENT TECHNIQUES	ACOUSTIC INTENSITY / SOUND POWER	DATA PROCESSING TECHNIQUES	FEA / MODAL ANALYSIS	GENERAL ENGINE NOISE	PISTON NOISE	GEAR NOISE	VALVETRAIN NOISE	TURBO / SUPERCHARGER NOISE	BEARING NOISE	DRIVE ACCESSORIE	USERS EXPERIENCE
McCandless, J.	1985	91						•							
McGinty, M.	1981	92	•	•		•		•							
McKinley, W.P.	1988	93						•							
Meier, R.C.	1985	94	•	•		•		•							
Meier, R.C.	1984	95	•	•		•		•							
Meier, R.C.	1984	96	•	•		•		•							
Meier, R.C.	1979	97	•	•		•		•							
Meier, R.C.	1981	98	•	•		•		•					•		
Meier, R.C.	1983	99	•	•	•	•			•						
Milenkovic, V.	1984	100	•		•	•		•		•					
Moneghan, M.L.	1985	101						•							
Morrison, D.	1979	102						•	•						
Munro, R.	1975	103		•							•				
Murphy, C.	1974	104									•				
Nivi, H.	1982	105		•		•		•		•					
Nivi, H.	1982	106						•							
Ochiai, K.	1979	107		•		•	•	•							
Oetting, H.	1979	108		•				•							
Ogorel, A.	1988	109			•				•						
Okamura, H.	1988	110				•	•	•							
Okuma, M.	1989	111													
Orzdneil, A.	1982	112		•		•		•							
Ota, D.	1988	113						•							
Padoan, R.	1979	114			•	•	•	•							
Pechtliller, A.	1979	115						•							
Parle, R.	1988	116		•		•		•							
Plechinger, F.	1979	117		•		•		•							
Pope, J.	1981	118		•	•	•		•							
Peter, R.	1989	119													
Priede, T.	1989	120													

228

AUTHORS	DATE	REF. NO.	INSTRUMENTATION	MEASUREMENT TECHNIQUES	ACOUSTIC INTENSITY / SOUND POWER	DATA PROCESSING TECHNIQUES	FEA / MODAL ANALYSIS	GENERAL ENGINE NOISE	PISTON NOISE	GEAR NOISE	VALVETRAIN NOISE	TURBO / SUPERCHARGER NOISE	BEARING NOISE	DRIVE ACENROLE	USERS' EXPERIENCE
Frick, T.	1985	121					•	•							
Frick, T.	1979	122		•		•		•							
Riemann, G.	1987	123			•										
Rhodes, D.	1983	124	•	•		•		•							
Richmond, J.	1987	125	•	•					•						
Ribe, E.	1983	126								•					
Ross, D.	1983	127		•		•			•						
Russell, M.	1983	128		•		•		•							
Russell, M.	1983	129		•		•		•							
Russell, M.	1982	130		•		•		•							
Russell, M.F.	1979	131		•		•		•							
Russell, M.	1979	132		•		•		•							
Russell, M.	1973	133		•		•		•							
Russell, M.	1972	134		•		•		•							
Sacha, M.	1989	135							•						
Sander, W.	1979	136		•		•		•							
Schmid Trettel	1983	137		•		•		•							
Schmidder, M.	1987	138		•		•		•							
Seth, B.B.	1984	139		•		•		•							
Seth, B.B.	1983	140		•		•		•							
Seth, B.B.	1983	141		•		•		•							
Seth, B.	1983	142		•		•		•							
Seth, B.	1983	143		•		•		•							
Sherrington, I.	1988	144		•		•		•	•						
Shahin, G.A.	1984	145		•		•		•		•					
Shenoy, S.L.	1984	146		•		•				•					
Shenoy, S.	1984	147		•		•									
Shenoy, L.	1989	148													
Somerin, B.	1983	149						•							
Sorokin, W.	1989	150	•	•		•		•							

229

DATE	REF. NO.	INSTRUMENTATION	MEASUREMENT TECHNIQUES	ACOUSTIC INTENSITY / SOUND POWER	DATA PROCESSING TECHNIQUES	FEA / MODAL ANALYSIS	GENERAL ENGINE NOISE	PISTON NOISE	GEAR NOISE	VALVETRAIN NOISE	TURBO / SUPERCHARGER NOISE	BEARING DRIVE / ACCESSORIE	USER EXPERIENCE
AUTHORS													
Sturhann, E. 1960	151		•		•		•						
Stuber, R. 1960	152		•		•		•						
Sung, S. 1989	153												
Sung, Y. 1988	154		•		•		•						
Takayama, T. 1989	155												
Takiguchi, M. 1988	156		•		•			•					
Thien, G. 1979	157		•		•		•						
Thompson, J. 1981	158			•									
Thompson, R. 1989	159								•				
Thomson, W. 1989	160												
Tjong, J.S.Y. 1990	161	•	•		•			•					
Tjong, J.S.Y. 1984	162	•	•		•				•				
Tengstdau, M. 1985	163				•		•						
Ufford, D. 1989	164												
Volkswagenwerk 1981	165												
Wallace, D. 1985	166		•		•								
Watanabe, Y 1982	167								•				
Watanabe, Y 1979	168		•		•		•						
Wanre, P. 1985	169		•		•		•						
Werner, S. 1977	170		•		•		•						
Welbourn, D.B. 1979	171								•				
Winkel, R. 1979	172		•		•	•	•						
Winklhofer, E. 1985	173		•		•		•						
Wood, L. 1988	174		•		•		•						
Young, C. 1988	175		•		•		•						

APPENDIX B

B. FLOW CHARTS OF THE COLD TEST STAND IN THE DEVELOPMENT STAGE AS WELL AS THE CURRENT OPERATING PRODUCTION TEST STAND

FLOW CHART OF DEVELOPMENT B-TEST STAND

WAIT FOR ACCEL COMMAND FROM PLC

INITIALIZE FOR ACCEL DATA COLLECTION

SYNCHRONIZE USING CRANK VRS PROBE

CRANK AND ENCODER SIGNALS O.K.? — NO / YES

START COLLECTION ON ENCODER EDGE AFTER NEXT CRANK INT.

COLLECTION PROCESS IS INTERRUPT DRIVEN (SEE NEXT PAGE)

ENABLE INTERRUPTS WAIT FOR DATA COLLECTION COMPLETE

SEND ERROR TO PLC

COLLECTION SUCCESSFUL? — NO / YES

A

B

C

233

```
  ┌───┐                    ┌───┐                                                    ┌───┐
  │ A │                    │ B │                                                    │ C │
  └───┘                    └───┘                                                    └───┘
    ▲                        │
    │                        │        NUMBER OF REVS TO COLLECT = 8
    │                        ▼        NUMBER OF SAMPLES PER REV = 1024
    │                 ┌─────────────┐
    │                 │  ORGANIZE   │ CHANNEL 1, REV 1, SAMPLES 1 -> 1024
    │                 │    DATA     │ CHANNEL 1, REV 2, SAMPLES 1 -> 1024
    │                 │    FOR      │
    │                 │ TRANSMISSION│ CHANNEL 1, REV 8, SAMPLES 1 -> 1024
    │                 │    TO PC    │ CHANNEL 2, REV 1, SAMPLES 1 -> 1024
    │                 └─────────────┘
    │                        │        CHANNEL 2, REV 8, SAMPLES 1 -> 1024
    │                        ▼
    │                 ╱─────────────╲
    │                ╱ SEND DATA VIA ╲
    │                ╲  XMODEM 128   ╱
    │                 ╲   TO PC     ╱
    │                  ╲───────────╱
    │                        │
    └────────────────────────┘
```

```
                         ┌──────────────┐
          ┌·············▶│     DATA     │
          ·              │  COLLECTION  │
          ·              │  INTERRUPT   │
          ·              └──────────────┘
          ·                      │
          ·                      ▼
          ·              ┌──────────────┐
          ·              │  STORE DATA  │
          ·              │  CHANNEL 1   │
          ·              └──────────────┘
          ·                      │
          ·                      ▼
          ·              ┌──────────────┐
          ·              │ TRIGGER NEXT │
          ·              │  CONVERSION  │
          ·              └──────────────┘
          ·                      │
          ·                      ▼
          ·              ┌──────────────┐
          ·              │  STORE DATA  │
          ·              │  CHANNEL 2   │
          ·              └──────────────┘
          ·                      │
          ·                      ▼
          ·              ┌──────────────┐
          ·              │ TOTAL SAMPLE │
          ·              │    COUNT     │
          ·              │     -1       │
          ·              └──────────────┘
          ·                      │
          ·                      ▼                      ┌──────────────────┐
          ·                   ╱─────╲                   │ DISABLE INTERRUPT │
          ·                  ╱       ╲                  │                   │ ·········▶
          ·                 ╱  = 0?   ╲···············▶│     INDICATE      │
          ·                 ╲         ╱                 │  DATA COLLECTION  │
          ·                  ╲       ╱                  │     COMPLETE      │
          ·                   ╲─────╱                   └──────────────────┘
          ·                      │ NO
          ·                      ▼
          ·              ┌──────────────┐
          ·              │     EXIT     │
          ···············│  INTERRUPT   │
                         │   ROUTINE    │
                         └──────────────┘
```

234   DEVELOPMENT   PAGE 2

FLOW CHART OF THE OPERATING PRODUCTION TEST STAND

WAIT FOR ACCEL COMMAND FROM PLC

INITIALIZE FOR ACCEL DATA COLLECTION

SYNCHRONIZE USING CRANK VRS PROBE

CRANK AND ENCODER SIGNALS O.K.?

START COLLECTION ON ENCODER EDGE AFTER NEXT CRANK INT.

COLLECTION PROCESS IS INTERRUPT DRIVEN (SEE NEXT PAGE)

ENABLE INTERRUPTS WAIT FOR DATA COLLECTION COMPLETE

SEND REJECT TO PLC

COLLECTION SUCCESSFUL?

A   B   C   D

236

BTS   PAGE 1

A

B

C

```
CALCULATE
VARIANCE FOR EACH
SAMPLE POINT
```

NUMBER OF REVOLUTIONS = 4
NUMBER OF SAMPLES PER REV = 1024

```
CHECK MAXIMUM
VARIANCE AGAINST
LIMITS
DETERMINE SAMPLE
POSITION OF MAX.
```

SEND RESULT VIA
SYTEK LINK
TO TANDEM HOST

RESULTS
O.K.?

NO

YES

SEND ACCEPT
TO PLC

```
DATA
COLLECTION
INTERRUPT
```

```
STORE DATA
CHANNEL 1
```

```
TRIGGER NEXT
CONVERSION
```

```
STORE DATA
CHANNEL 2
```

```
TOTAL SAMPLE
COUNT
-1
```

= 0?

DISABLE INTERRUPT
INDICATE
DATA COLLECTION
COMPLETE

NO

```
EXIT
INTERRUPT
ROUTINE
```

237

BTS   PAGE 2

APPENDIX C

C. COMPUTER PROGRAMS LISTING FOR SYSTEM NO. 1

The computer code listed below is the data acquistion program written for the HP300 workstation and the HP3561A analyzer. The code is very analyzer specific and therefore only a brief explanation of what each section of the code does will be of any value.

This first section of code intializes variables to a default condition and initializes communications between the analyzer and the computer. The variables which are defaulted in the section tell the analyzer how much data to sample, when to sample and where to store the resulting data.

```
1       CONTROL CRT,21;1
10      OPTION BASE 1
20      DEG
21      OUTPUT 2 USING "#,-K";CHR$(255),CHR$(75)
30      COM INTEGER Max_rec_size,Type_flag,Tinum
40      COM Mes$[80],Tiave$[1],A$[15],Answ$[1],Filthy$[1],Autosngl$[1],Asroot$[15]
50      COM REAL Rec_num,Span,Cutoff,Start,Rpm,Trv,Plug,Cal_fact,Fil_del
60      COM INTEGER Rge,Act,Autosngl_st,Autosngl_end
61      ON ERROR RECOVER Errr
70      ASSIGN @P1 TO "TRIGPARA"
80      ENTER
@P1,1;A$;Tiave$;Answ$;Rec_num;Span;Filthy$;Cutoff;Start;Rpm;Rge;Trv;Act;Plug;Cal_fact;Tinum;Fil_del
90      ASSIGN @P1 TO *
91      OFF ERROR
100     ASSIGN @Anz TO 711      !CREATE AN I/O PATH TO THE HP
101     Autosngl$="N"
102     Autosngl_st=1
103     Autosngl_end=1
104     Asroot$=""
```

The following is the main menu and controls the execution of the program. The menu allows access to subroutines to change default acquisition settings and also is the gateway to the actual acquisition portion of the program. After completion of any acquisitions or parameter change the program returns to this section and waits for any further actions.

```
110 Variable:  !
120     CONTROL 1,13;25
130     Menfl=1
140     ON KEY (1) LABEL "MENU1",12 GOSUB Menu1
150     ON KEY (2) LABEL "MENU2",12 GOSUB Menu2
160     ON KEY (3) LABEL "TESTMENU",12 GOSUB Mainmenu
170     ON KEY (4) LABEL "CHANGE PARAM",12 GOSUB Param
180     ON KEY (5) LABEL "SAVE PARAM",12 GOSUB Sapar
190     CONTROL 2,2;1
200     WHILE Wilber<>1
210     IF Menfl=1 THEN
220     GOSUB Menu1
230     Menfl=0
240     END IF
250     IF Menfl=2 THEN
260     GOSUB Menu2
270     Menfl=0
280     END IF
290     END WHILE
300 Param:  !
310     INPUT "NUMBER OF PARAMETER YOU WISH TO CHANGE",Sel$
320     SELECT Sel$
330     CASE "1"
340     INPUT "ENTER NEW MASS STORAGE SPECIFIER",A$
350     Mes$=""
360     CASE "2"
370     INPUT "DO YOU WANT A TIME AVERAGE",Tiave$
380     IF Tiave$="Y" THEN Start=0
390     Answ$="N"
400     Mes$=""
410     CASE "3"
420     INPUT "HOW MANY TIME AVERAGES",Tinum
430     Mes$=""
440     CASE "4"
450     INPUT "DO YOU WANT FREE RUN DATA",Answ$
460     Mes$=""
470     IF Tiave$="Y" AND Answ$<>"N" THEN
480     Answ$="N"
490     Mes$="CAN'T TIME AVERAGE AND FREE RUN AT THE SAME TIME"
500     END IF
510     CASE "5"
520     IF Answ$="N" THEN
530     Mes$="NOT AN ACTIVE VARIABLE (FREE RUN IS OFF)"
540     ELSE
550     INPUT "HOW MANY RECORDS PER FREE RUN",Rec_num
```

```
560    Mes$=""
570    END IF
580    CASE "6"
590    INPUT "ARE YOU USING A FILTER",Filthy$
600    Mes$=""
610    CASE "7"
620    INPUT "ENTER THE CUT OFF FREQUENCY FOR THE LOW PASS FILTER",Cutoff
630    Mes$=""
640    CASE "8"
650    INPUT "ENTER THE ANALYZER FREQUENCY SPAN",Span
660    Mes$=""
670    CASE "9"
680    IF Tiave$="Y" OR Answ$="N" THEN
690    Mes$="CAN NOT SET START FREQ UNLESS IN FREE RUN MODE"
700    ELSE
710    INPUT "WHAT IS THE STATING FREQUENCY",Start
720    Mes$=""
730    END IF
740    CASE "10"
750    INPUT "WHAT IS THE ENGINE RPM",Rpm
760    !es$=""
770    CASE "11"
780    INPUT "THE SETTLED ANALYZER RANGE",Rge
781    Act=(Trv/(10^,Rge/20))*100)
782    IF ABS(Act)>140 THEN
783    Act=SGN(Act)*140
786    END IF
787    Act INT(Act)
790    Mes$=""
800    CASE "12"
810    INPUT "THE TRIGGER VOLTAGE",Trv
812    Act=(Trv/(10^(Rge/20))*100)
813    IF ABS(Act)>140 THEN
814    Act=SGN(Act)*140
815    END IF
817    Act=INT(Act)
820    Mes$=""
830    CASE "13"
841    Act=(Trv/(10^(Rge/20))*100)
842    IF ABS(Act)>140 THEN
843    Act=SGN(Act)*140
844    END IF
846    Act=INT(Act)
850    PRINT TABXY(5,16);"*****  THEORETICALLY THE TRIGGER PERCENTAGE SHOULD BE";Act;
860    INPUT "WHAT PERCENTAGE TO TRIGGER ANALZER",Act
870    Mes$=""
880    CASE "14"
890    INPUT "WHAT IS THE ENGINE (BTDC) IN (DEGREES)",Plug
900    Mes$=""
910    CASE "15"
920    INPUT "WHAT ARE THE VOLTS PER UNIT OF THE TRANSDUCER",Cal_fact
930    Mes$=""
931    CASE "16"
932    INPUT "WHAT IS THE FILTER CAUSED DELAY",Fil_del
933    Mes$=""
934    CASE "17"
935    INPUT "DO YOU WANT AUTO_SINGLE FUNCTIONS",Autosngl$
936    IF Autosngl$="Y" THEN
937    Tiave$="N"
938    Answ$="N"
939    INPUT "WHAT IS THE ROOT NAME",Asroot$
941    INPUT "WHAT IS THE START NUMBER",Autosngl_st
942    INPUT "WHAT IS THE END NUMBER",Autosngl_end
943    END IF
945    Mes$=""
946    END SELECT
950    Sel=VAL(Sel$)
960    SELECT Sel
970    CASE 1 TO 10
980    Menfl=1
990    CASE 11 TO 17
1000   Menfl=2
1010   END SELECT
1020   RETURN
1030 Menu1:!
1040   OUTPUT 2 USING "#,-K";CHR$(255)&CHR$(75)
1050   FOR I=2 TO 11
1060   PRINT TABXY(1,I);"*";VAL$(I-1);
```

```
1070   NEXT I
1080   PRINT TABXY(5,2);"MASS STORAGE IS: ";A$;
1090   PRINT TABXY(5,3);"DO YOU WANT TO AVERAGE TIME DATA: ";Tiave$;
1100   PRINT TABXY(5,4);"HOW MANY TIME AVERAGES: ";Tinum;
1110   PRINT TABXY(5,5);"DO YOU WANT FREE-RUN DATA: ";Answ$;
1120   PRINT TABXY(5,6);"No. OF RECORDS OF FREE RUN: ";Rec_num;
1130   PRINT TABXY(5,7);"FILTER PRESENT: ";Filthy$;
1140   PRINT TABXY(5,8);"CUTOFF FREQUENCY (LP): ";Cutoff;
1150   PRINT TABXY(5,9);"FREQUENCY SPAN: ";Span;
1160   PRINT TABXY(5,10);"FREQUECNY START: ";Start;
1170   PRINT TABXY(5,11);"ENGINE RPM: ";Rpm;
1180   PRINT TABXY(5,17);Mes$;
1190   PRINT TABXY(5,18);"SELECT APPROPRIATE SOFTKEY";
1200   RETURN
1210 Menu2: !
1220   OUTPUT 2 USING "#,-K";CHR$(255)&CHR$(75)
1230   FOR I=12 TO 18
1240   PRINT TABXY(1,I-10);"*";VAL$(I-1)
1250   NEXT I
1260   PRINT TABXY(5,2);"SETTLED ANALYZER RANGE: ";Rge;
1270   PRINT TABXY(5,3);"TRIGGER VOLTAGE: ";Trv;
1280   PRINT TABXY(5,4);"PERCENTAGE OF RANGE TO TRIGGER: ";Act;
1290   PRINT TABXY(5,5);"BEFORE TOP DEAD CENTER (DEG): ";Plug;
1300   PRINT TABXY(5,6);"THE VOLTS PER UNIT ARE: ";Cal_fact;
1301   PRINT TABXY(5,7);"THE FILTER DELAY IS: ";Fil_del;
1310   PRINT TABXY(5,17);Mes$;
1320   PRINT TABXY(5,18);"SECLECT APPROPRIATE SOFTKEY";
1321   PRINT TABXY(5,8);"AUTOSINGLE ";Autosngl$;",";Autosngl_st;",";Autosngl_end;",";Asroot$
1330   RETURN
1340 Separ:!
1350   PURGE "TRIGPARA"
1360   CREATE BDAT "TRIGPARA",1,120
1370   ASSIGN @P1 TO "TRIGPARA"
1380   OUTPUT
@P1,1;A$;Tiave$;Answ$;Rec_num;Span;Filthy$;Cutoff;Start;Rpm;Rge;Trv;Act;Plug;Cal_fact;Tinum;Fil_del
1390   ASSIGN @P1 TO *
1400   RETURN
1410 Mainmenu:!
1420   !CONTROL 2,2;0  --- REMEMBER TO  INCLUDE THIS AFTER THE START
1430   CALL Measurement(@Anz)
1440   CONTROL 2,2;1
1450   GOSUB Menu1
1460   RETURN
1461 Errr:!
1462      IF ERRL(70)=1 OR ERRL(80)=1 THEN
1463      RESET 7
1466      GOTO 91
1468      END IF
1469      RETURN
1470   END
          This portion of the program is the actual data acquisition control code.  The analyzer is given
commands through this routine and acquires data under the restrictions imposed on it by the data acquisition
parameters.  Typical use is to trigger on some event and acquire 50 complete engine cycles of data.
1480   SUB Measurement(@Anz)
1490   !THIS PROGRAM READS DATA FROM THE -HP-3561A
1500   !THE HP MUST BE IN TIME CAPTURE MODE. UP TO 40
1510   !RECORDS ,OR 82910 BYTES (2048 BYTES PER RECORD-PLUS 350 BYTE HEADER)
1520   !CAN BE READ.
1530   !
1540   !ALL HP  DATA CONTAINS A DATA HEADER. IN TIME CAPTURE MODE, THE HEADER
1550   !IS SENT IN THE FIRST 350 BYTES OF THE TRANSFER. THIS PROGRAM REMOVES
1560   !THE HEADER AND RETURNS THE CALIBRATED TIME DATA.
1570   !
1580   OPTION BASE 1
1590   DEG
1600   ASSIGN @Fast TO BUFFER [82910];FORMAT OFF
1610   COM INTEGER Max_rec_size,Type_flag,Tinum
1620   COM Mes$[80],Tiave$[1],A$[15],Answ$[1],Filthy$[1],Autosngl$[1],Asroot$[15]
1630   COM REAL Rec_num,Span,Cutoff,Start,Rpm,Trv,Plug,Cal_fact,Fil_del
1640   COM INTEGER Rge,Act,Autosngl_st,Autosngl_end
1650   !CREATE AN I/O PATHE TO A 82270 BYTE BUFFER
1660   !350 DATA BYTE HEADER PLUS 2048 TIMES 40 RECORDS
1670   !TRANSFER IS IN BINARY FORM
1680   ON ERROR GOTO 1710
1690   IF A$=" " THEN GOTO 1750
1700   MASS STORAGE IS A$
1710   IF ERRN=52 THEN
1720   OFF ERROR
```

242

```
1730  GOTO 1660
1740  END IF
1750   PRINT ERRM$
1760  REAL Start_t,Stop_t,X,Rec_size
1770  INTEGER Tag_field(175)
1780  INTEGER Raw_data(101,2048)
1790  INTEGER Range,Rang(101)
1810  DIM Cal_fact$[15]
1820  ON KEY 1 LABEL "GET DATA",13 GOSUB Getit
1840  ON KEY 3 LABEL "RETURN",13 GOSUB Rtn
1850  OUTPUT 2 USING "#,-K";CHR$(255),CHR$(75)
1860  DISP "PICK APPROPRIATE SOFT KEY"
1870  CONTROL 2,2;1
1880  WHILE Bunk<>1
1890  END WHILE
1900  Getit:!
1910       Tiave$="Y"
1920       GOSUB Tiaverage
1922       Tiave$="N"
1923       Autosngl$="Y"
1925       GOSUB Auto_sngl
1930       Autosngl$="N"
1940       DISP "FINISHED COLLECTING DATA"
1941       GOSUB Store_data
1950       RETURN
2120  Rtn: !
2130   ASSIGN @Fast TO *
2131   GCLEAR
2140   SUBEXIT
2150   !-------------------------------------------------------------------
2160  How_many:      !DETERMINES HOW MANY RECORDS ARE TO BE TRANSFERRED
2170   !-------------------------------------------------------------------
2180   PRINT CHR$(12)
2190   INPUT "HOW MANY RECORDS TO TRANSFER?",Rec_size
2191   IF Tiave$="N" AND Answ$="N" THEN RESET @Fast
2220   RETURN
2230   !-------------------------------------------------------------------
2240  Read_data:      !READS DATA FROM HP TO BUFFER. TAKES 0.15 SECONDS
2250                  !PER RECORD PLUS .13 SECONDS
2260   !-------------------------------------------------------------------
2270   IF Tiflag=1 THEN
2280   CONTROL @Fast,5;1
2290   END IF
2300   OUTPUT @Anz;"DTBB"   !SEND DUMP-TIME-BUFFER-COMMAND
2310   TRANSFER @Anz TO @Fast;COUNT 350
2320   FOR I=1 TO Rec_size
2330     DISP "READING RECORD NUMBER:",I
2340     TRANSFER @Anz TO @Fast;COUNT 2048,WAIT
2350     NEXT I
2360   RETURN
2370   !-------------------------------------------------------------------
2380  Read_tag:      !GET RANGEA,SPAN,START AND STOP TIMES, BASEBAND DATA, AND
2390                 !BUFFER SIZE FROM DATA HEADER
2400  DISP "READING HEADER"
2410!
2420  CONTROL @Fast,5;1      !MOVE BUFFER POINT READER TO BYTE ONE OF HEADER
2430  ENTER @Fast;Tag_field(*)
2440  CONTROL @Fast,5;15      !MOVER BUFFER POINTER TO BYTE 15 AND READ SPAN
2450  ENTER @Fast;Span
2460  CONTROL @Fast,5;311
2470  ENTER @Fast;Start_t
2480  CONTROL @Fast,5;319
2490  ENTER @Fast;Stop_t
2500  CONTROL @Fast,5;31
2510  ENTER @Fast USING "#,B";Baseband !READS BASEBAND/ZOOM STATUS
2520  CONTROL @Fast,5;9
2530  ENTER @Fast;Max_rec_size      ! READS BUFFER SIZE
2540  CONTROL @Fast,5;35
2550  ENTER @Fast;Range              !READS RANGE
2560  RETURN
2570!-------------------------------------------------------------------
2580  Convert_data:      !READ INTEGERS FROM BUFFER CONVERT TO REAL VOLTS
2590!-------------------------------------------------------------------
2600  DISP "CONVERTING DATA"
2610  Factor=(4/3)*10.0^((Range+4.812)/20.0)/32768/Cal_fact
2620  Reg_5=351
2630  CONTROL @Fast,5;Reg_5
2640  ENTER @Fast;Slime(*)
```

```
2650 MAT Raw_data(Rn,*)= Slime
2656 Rang(Rn)=Range
2660 RETURN
2670 !---------------------------------------------------------------
2990 Anal_set: !
2991 !---------------------------------------------------------------
3000          IF Tiave$="Y" THEN GOTO 3070
3010          IF Answ$="Y" THEN
3020          G$=VAL$(Rec_num)
3030          Act$="0"
3040          Type_flag=1
3050          GOTO 3520
3060          END IF
3070          IF Filthy$="Y" THEN
3080          SELECT Cutoff
3090          CASE .01 TO 11.9
3100          M$="M0"
3110          F$=VAL$(INT(Cutoff*100))
3120          CASE .1 TO 119
3130          M$="M1"
3140          F$=VAL$(INT(Cutoff*10))
3150          CASE 100 TO 1190
3160          M$="M2"
3170          F$=VAL$(INT(Cutoff))
3180          CASE 1000 TO 11900
3190          M$="M3"
3200          F$=VAL$(INT(Cutoff/10))
3210          CASE 10000 TO 110000
3220          M$="M4"
3230          F$=VAL$(INT(Cutoff/100))
3240          END SELECT
3250          IF LEN(F$)<4 THEN
3260          Job=4-LEN(F$)
3270          FOR Fi=1 TO Rbb
3280          F$="0"&F$
3290          NEXT Fi
3300          END IF
3310          Filt$="F"&F$&M$
3320          SEND 7;MTA LISTEN 7 DATA "R",13
3330          Filt$="CB"&Filt$&"G8"&"IO"&"O6"
3340          SEND 7;MTA LISTEN 7 DATA Filt$,13
3350          SEND 7;MTA LISTEN 7 DATA "L",13
3360          END IF
3370          B$=VAL$(Span)
3380          IF Answ$<>"Y" THEN
3390          Start=0
3400          END IF
3410          B2$=VAL$(Start)
3420          B1$=VAL$(Span/2+Start)
3430          OUTPUT @Anz;"CF"&B1$&"HZ"
3440          OUTPUT @Anz;"SF"&B2$&"HZ"
3450          OUTPUT @Anz;"SP"&B$&"HZ"
3460          PRINT "THEREFORE THERE WILL BE";720*(2.56*Span/(6*Rpm));" SAMP/CYC"
3470          Total_time=120/Rpm
3480          Rec_num=INT(2.56*Span*Total_time/1024)+1
3490          G$=VAL$(Rec_num)
3500          Act$=VAL$(Act)
3510          Plug$=VAL$(Plug/(6*Rpm)+Fil_del)
3520          PRINT " AT THIS TIME CALIBRATE THE TRANSDUCER"
3530 LOCAL @Anz
3540          DISP "PRESS CONTINUE WHEN FINISHED"
3550          PAUSE
3560          IF Answ$="Y" THEN
3570          OUTPUT @Anz;"UDVU;"
3580          END IF
3590          OUTPUT @Anz;"TRIG"
3600          OUTPUT @Anz;"TRGR"
3610          OUTPUT @Anz;"EXT"
3620          IF Answ$="Y" THEN OUTPUT @Anz;"TRFR"
3630          IF Tiflag<>1 THEN OUTPUT @Anz;"TRMA"
3640          OUTPUT @Anz;"TLPR"&Act$&"PCT"
3650          OUTPUT @Anz;"DELY ON "
3660          OUTPUT @Anz;"DLY"&"+"&Plug$&"SEC"
3670          OUTPUT @Anz;"TBUF"
3680          OUTPUT @Anz;"TBST 0MSEC"
3690          OUTPUT @Anz;"TBPI100PCT"
3700          OUTPUT @Anz;"TBNR"&G$&"REC"
3710          IF Tiflag=1 THEN GOTO 3770
```

244

```
3720        PRINT " ARM TRIGGER (IF 2 CYCLE DATA) WHEN READY "
3730            OUTPUT @Anz;"SCAP"
3740 LOCAL @Anz
3750 PRINT "HIT CONTINUE WHEN FINISHED DATA COLLECTION"
3760 PAUSE
3770            RETURN
```

This portion of the program stores the data in a Standard Data Format is first stores header information in a header file which includes scaling factors for the raw data which is stored in binary format. It includes analyzer setting which are also used to help reconstruct the data into real numbers. It also stores the actual data in a 16 bit binary format engine cylce by engine cycle. It then stores in a third file text which describes the test and problems which may have occured.

```
3780 Store_data:!
3800            INPUT "WHAT NAME DO YOU WANT",Name$
3804            CREATE BDAT "HT"&Name$,1,512
3820            CREATE BDAT "H2"&Name$,Fn+1,Rec_num*2048
3830            CREATE BDAT "H1"&Name$,1,1024
3840            DIM Text$(1:5)[84]
3850            FOR I=1 TO 5
3860            PRINT "ENTER TEXT STRING NUMBER";I
3870            LINPUT Text$(I)
3871            Tlen=LEN(Text$(I))
3872            Text$(I)=Text$(I)&RPT$(" ",(84-Tlen))
3880            NEXT I
3883            ASSIGN @P3 TO "HT"&Name$;FORMAT OFF
3900            ASSIGN @P2 TO "H2"&Name$;FORMAT OFF
3910            ASSIGN @P1 TO "H1"&Name$;FORMAT OFF
3920            OUTPUT @P1,1;Tag_field(*);Total_time;Rpm;Span;Start;Rec_num;Type_flag,Cal_fact;Rang(*)
3921            FOR I=1 TO Fn+1
3930            MAT Slime= Raw_data(I,*)
3940            OUTPUT @P2,I;Slime(*)
3950            NEXT I
4090            OUTPUT @P3,1;Text$(*)
4110            ASSIGN @P3 TO *
4120            ASSIGN @P2 TO *
4130            ASSIGN @P1 TO *
4140            DISP "FINISHED STORING DATA"
4150            RETURN
4160 !---------------------------------------------------
4161 Tiaverage:!
4162 !---------------------------------------------------
4163 DIM Tiaverage(10240),Tempaver(10240),Tiaverage2(10240)
4164 INTEGER Tiaverage1(10240),Fn,Slime(10240)
4165 INPUT "HOW MANY FILES BESIDES THE AVG DO YOU WANT",Fn
4166 REDIM Rang(Fn+1)
4168 Tiflag=1
4169 Maxf=-10000
4170 GOSUB Anal_set
4171 Rec_size=Rec_num
4172 REDIM Slime(Rec_num*1024)
4174 REDIM Tiaverage(Rec_num*1024)
4175 REDIM Tiaverage1(Rec_num*1024)
4176 REDIM Tempaver(Rec_num*1024)
4177 REDIM Tiaverage2(Rec_num*1024)
4178 REDIM Raw_data(Fn+1,Rec_num*1024)
4180 OUTPUT @Anz;"CRCN OFF"
4181 OUTPUT @Anz;"PSRO ON "
4182 FOR Ijki=1 TO Tinum
4183 CONTROL @Fast,3;1
4184 OUTPUT @Anz;"TRMA"
4185 OUTPUT @Anz;"SCAP"
4186 OUTPUT @Anz;"MARM"
4187 B=0
4188 REPEAT
4189 A=SPOLL(@Anz)
4190 B=BIT(A,0)
4191 UNTIL B=1
4192 GOSUB Read_data
4193 GOSUB Read_tag
4194 IF Range>Maxf THEN Maxf=Range
4195 Factor=(4/3)*10^((Range+4.817)/20)/32768/Cal_fact
4196 Reg_5=351
4197 CONTROL @Fast,5;Reg_5
4198 ENTER @Fast;Tiaverage1(*)
4199 MAT Tempaver= Tiaverage
4200 MAT Tiaverage2= Tiaverage1*(Factor/Tinum)
4201 MAT Tiaverage= Tempaver+Tiaverage2
4202 !GOSUB Tim_plot
```

```
4203 PRINT Ijki
4204 NEXT Ijki
4205 OUTPUT aAnz;"CRCN ON"
4206 GOSUB Tim_plot
4207 PAUSE
4208 OUTPUT 2 USING "#,-K";CHR$(255),CHR$(75)
4209 Range=Maxf
4210 Factor=(4/3)*10^((Range+4.817)/20)/32768/Cal_fact
4211 MAT Tiaverage1= Tiaverage*(1/Factor)
4212 MAT Raw_data(1,*)= Tiaverag=1
4218 Rang(1)=Range
4219 RETURN
4650 Tim_plot:!
4660          DIM Maxv(200),Minv(200)
4670          Total_pts=2.56*Span*Total_time
4680          OUTPUT 2 USING "#,K";CHR$(255)&CHR$(75)
4690 GCLEAR
4700 GINIT
4710 ALPHA OFF
4720 GRAPHICS ON
4730 ALPHA ON
4740 VIEWPORT 25,125,28,98
4750 FRAME
4760 Y_max=MAX(Tiaverage(*))
4770 Y_min=MIN(Tiaverage(*))
4780 Maxv(Ijki)=Y_max
4790 Minv(Ijki)=Y_min
4800 WINDOW 0,Total_pts,Y_min,Y_max
4810 LINE TYPE 4
4820 GRID Total_pts/12,0,0,Y_min
4830 LINE TYPE 1
4840 MOVE 0,Y_min
4850 FOR Ijkl=1 TO Rec_num*1024
4860 IF Ijkl>Total_pts THEN GOTO 4890
4870 DRAW Ijkl,Tiaverage(Ijkl)
4880 NEXT Ijkl
4890 CSIZE 3,.6
4900 MOVE 0,Y_max
4910 CLIP OFF
4920 Lab$=VAL$(DROUND(Y_max,5))
4930 LORG 8
4940 LABEL Lab$
4950 MOVE 0,Y_min
4960 CLIP OFF
4970 Lab$=VAL$(DROUND(Y_min,5))
4980 LORG 8
4990 LABEL Lab$
5000 FOR I=0 TO 12
5010 Lab$=VAL$(60*I)
5020 MOVE I*Total_pts/12,Y_min
5030 LORG 6
5040 CLIP OFF
5050 LABEL USING "#,K";Lab$
5060 NEXT I
5070 RETURN
5080 Pltm:!
5090 GCLEAR
5100 GINIT
5110 ALPHA OFF
5120 GRAPHICS ON
5130 ALPHA ON
5140 VIEWPORT 20,133,28,98
5150 FRAME
5160 Y_max=MAX(Maxv(*))
5170 Y_min=MIN(Minv(*))
5180 WINDOW 0,Tinum,Y_min,Y_max
5190 LINE TYPE 1
5200 MOVE 0,0
5210 FOR Ijkl=1 TO Tinum
5220 DRAW Ijkl,Maxv(Ijkl)
5230 NEXT Ijkl
5240 MOVE 0,0
5250 FOR Ijkl=1 TO Tinum
5260 DRAW Ijkl,Minv(Ijkl)
5270 NEXT Ijkl
5280 MOVE 0,Y_max/2
5290 RETURN
5300 !-------------------------------------------------------------
```

```
5310 Auto_sngl:!
5320 !--------------------------------------------------------------
5331  OUTPUT 2 USING "#,K";CHR$(255),CHR$(75)
5332  INTEGER Asi,Rn
5342  Tiflag=1
5349 Rec_size=Rec_num
5355 OUTPUT @Anz;"PSRQ ON "
5356 FOR Asi=1 TO Fn
5357 Rn=Asi+1
5359 PRINT Asi
5360 CONTROL @Fast,3;1
5361 OUTPUT @Anz;"TRMA"
5362 OUTPUT @Anz;"SCAP"
5363 OUTPUT @Anz;"MARH"
5364 B=0
5365 REPEAT
5366 A=SPOLL(@Anz)
5367 B=BIT(A,0)
5368 UNTIL B=1
5369 GOSUB Read_data
5370 GOSUB Read_tag
5371 GOSUB Convert_data
5378 NEXT Asi
5380 CONTROL 2,2;1
5381 Tiflag=0
5387 RETURN
5397 SUBEND
```

DATA ANALYSIS PROGRAM FOR SYSTEM NO. 1

Data analysis techniques were developed by use of a user-interactive program on the HP300 workstation. The program code for this program is listed and commented below.

The following module is the main menu. Its functions are:

1) determine which type of analysis will be applied to acquired data

2) send control of the program to the subroutine which handles the type of analysis the user has requested

3) after analysis is completed regains control of the program to allow the user to enter another analysis technique or to plot results to a graphic device

```
10    ! DATA ANALYSIS PROGRAM
20    !
30    OPTION BASE 0
40    COM /A/ R(4095,1),T(4095,1),Rb(4095),File$[20],Span
50    COM /B/ INTEGER
Ra(4095),I,J,K,Rc,Tag_field(1:175),Type_flag,Slime(4095),Range,Nu,Tot_pts,Rn,Rang(1:26)!
60    COM /C/ INTEGER Raw(2047,100),REAL Fact(100),INTEGER Varflag,FnS
70    ON KEY 1 LABEL "FFT",10 GOSUB FftF
80    ON KEY 2 LABEL "VARIANCE",10 GOSUB VarianceI
90    ON KEY 3 LABEL "HILB",10 GOSUB HilbV
100   ON KEY 4 LABEL "PLOT",10 GOSUB Plt
110   ON KEY 5 LABEL "DUMPG",10 GOSUB Dumpgr
120   REPEAT
130   UNTIL Zzz=1.234"
140 Fft:  !
150       OUTPUT 2 USING "#,-K";CHR$(255),CHR$(75)
160       CALL Fft(0)
170       DISP "FINISHED FFT"
180       RETURN
190 Variance:!
200       OUTPUT 2 USING "#,-K";CHR$(255),CHR$(75)
210       CALL Variance
220       DISP "FINISHED VARIANCE"
230       RETURN I
240 Hilb:!
250       OUTPUT 2 USING "#,-K";CHR$(255),CHR$(75))
260       CALL Hilb
270       DISP "FINISHED HILB""
280       RETURN
290 Plt:!R
300       OUTPUT 2 USING "#,-K";CHR$(255),CHR$(75)
310       CALL Plt(1)I
320       DISP "FINISHED PLOT"
330       RETURN I
340 Dumpg:!U
350       CALL Dumpg
360       RETURN m
370 END
```

Subroutine COLLDATA is used by all data analysis subroutines to read data which has been stored in a standard format to disk. The subroutine can either read one time trace of data at a time or input many traces for variance analysis calculations.

```
380 !_____
390 SUB Colldata
400 !_____
410 OPTION BASE 0
420 ON ERROR RECOVER Err
430 COM /A/ R(4095,1),T(4095,1),Rb(4095),File$[20],Span
440 COM /B/ INTEGER Ra(4095),I,J,K,Rc,Tag_field(1:175),Type_flag,Slime(4095),Range,Nu,Tot_pts,Rn,Rang(1:26)
450 COM /C/ INTEGER Raw(2047,100),REAL Fact(100),INTEGER Varflag,Fn
460 DISP "COLLECTING DATA"
470 ASSIGN @P1 TO "H1"&File$
480 ASSIGN @P2 TO "H2"&File$
490 ENTER
@P1,1;Tag_field(*);Total_time;Rpm;Span;Start;Rec_num;Type_flag;Cal_fact,Rang(*)
500 Factor=(4/3)*10^((Rang(1)+4.812)/20)/32768/Cal_fact
510 Tot_pts=INT(Total_time*2.56*Span+.5)
520 N_int=INT(Tot_pts/1024)+15
530 Pow_2=INT(LOG(Tot_pts)/LOG(2))+1
540 Nu=INT(2^INT(Pow_2+.5)+.5)
550 IF Varflag=1 THEN GOSUB Varcol
551 INTEGER Lengh
553 STATUS @P2,4;Lengh
554 REDIM Slime(0:Lengh/2-1)
```

```
555 REDIM R(0:Lengh/2-1,1)
560 ENTER @P2,Rn;Slime(*))
570 MAT R(*,0)= Slime
580 MAT R= R*(Factor)
590 FOR I=Tot_pts TO Nu-1
600 R(I,0)=R(I-Tot_pts,0))
610 NEXT I
620 ASSIGN @P1 TO *
630 ASSIGN @P2 TO *
640 SUBEXIT
650 Varcol:!
660         FOR I=1 TO Fn
670 Fact(I-1)=(4/3)*10^((Rang(I)+4.812)/20)/32768/Cal_fact
680 ENTER @P2,I;Slime(*)
690 MAT Raw(*,I-1)= Slime
700 NEXT I
710 ASSIGN @P1 TO *
720 ASSIGN @P2 TO *
730 SUBEXIT
740 Err:!
750     PRINT ERRM$
760     IF ERRL(470)=1 OR ERRL(480)=1 THEN
770     DISP "ERROR:EITHER WRONG FILE NAME OR INSERT ANOTHER DISK"
780     PAUSE"
790     DISP ""
800     GOTO 460
810     END IF
820 SUBEND
```

        Subrountine REORDER is an element to conducting an FFT it reorders the time data such that the resulting frequency information from the Fast Fourier Transform is in proper order.

```
830 !_____
840 SUB Reordr
850 !_____
860 OPTION BASE 0
870 COM /A/ R(4095,1),T(4095,1),Rb(4095),File$[20],Span
880 COM /B/ INTEGER Ra(4095),I,J,K,Rc,Tag_field(1:175),Tyre_flag,Slime(4095),Range,Nu,Tot_pts,Rn,Rang(1:26)6
890 DISP "REORDERING DATA"
900 MAT Ra= Ra*(0)
910 Const=INT(LOG(Nu)/LOG(2)+.5)
920 FOR I=1 TO Const
930 Valu=2^I
940 Valu1=Nu/Valun
950 Va=2^(I-1)
960 FOR K=1 TO Valu/2/
970 IF K MOD 2=0 THEN
980 Inc=1M
990 ELSE
1000 Inc=0
1010 END IFD
1020 Aaa=(K-1)*Valu1
1030 Aaaa=Inc*Va
1040 FOR J=0 TO (Valu1-1)(
1050 Ra(Aaa+J)=Ra(Aaa+J)+Aaaa.
1060 NEXT J+
1070 NEXT K+
1080 NEXT I+
1090 Aa=Nu-1
1100 FOR I=0 TO Nu/2-1
1110 T(I,0)=R(Ra(I),0)
1120 T(Aa-I,0)=R(Aa-Ra(I),0)
1130 T(I,1)=R(Ra(I),1)
1140 T(Aa-I,1)=R(Aa-Ra(I),1)
1150 NEXT I
1160 SUBEND
```

        Subrountine Fort(Sign) is the Fast Fourier Transform. The Sign variable determines if the transform is to frequency or time domain.

VARIABLES
        Sign- INTEGER
                if equal to 1 transforms to frequency domain
                if equal to -1 fransfroms to time domain

```
1170!_____
1180 SUB Fort(Sign)
1190!_____
1200 OPTION BASE 0
1210 COM /A/ R(4095,1),T(4095,1),Rb(4095),File$[20],Span
1220 COM /B/ INTEGER Ra(4095),I,J,K,Rc,Tag_field(1:175),Type_flag,Slime(4095),Range,Nu,Tot_pts,Rn,Rang(1:26)
1230 DISP "TAKING FFT"
1240 Rc=INT(LOG(Nu)/LOG(2)+.5)
1250 P2=-Sign*2*PI/Nu0
1260 FOR K=1 TO Rc
1270 St=2^K1
1280 N1=2^(Rc-K)
1290 Wr=P2*N1-
1300 Wi=Nu/(2^(Rc+1-K))(
1310 FOR J=0 TO Nu/St-1(
1320 Ww=J*St
1330 Www=Ww+Wi
1340 FOR I=0 TO 2^(K-1)-1)
1350 Ang=Wr*IT
1360 N2=Ww+I
1370 N3=Www+IT
1380 E=T(N3,0)*COS(Ang)-T(N3,1)*SIN(Ang)
1390 F=T(N3,1)*COS(Ang)+T(N3,0)*SIN(Ang)
1400 T(N3,0)=T(N2,0)-E
1410 T(N3,1)=T(N2,1)-F
1420 T(N2,0)=T(N2,0)+E
1430 T(N2,1)=T(N2,1)+F
1440 NEXT I)
1450 NEXT J)
1460 NEXT K)
1470 IF Sign=1 THEN MAT T= T*(2/Nu)(
1480 SUBEND
```

Subrountime Timeweight is a windowing program designed for use with the Fast Fourier Transform. When this subrountine is called each element of a time trace is multiplied by a weighting factor. These weighting factors force the time data to appear periodic typically by forcing the first and last data point to be zero. This improves the accuracy of the Fast Fourier Transform.

```
1490 !_____
1500 SUB Timeweight(Arg)
1510 !_____
1520 COM /A/ R(4095,1),T(4095,1),Rb(4095),File$[20],Span
1530 COM /B/ INTEGER Ra(4095),I,J,K,Rc,Tag_field(1:175),Type_flag,Slime(4095),Range,Nu,Tot_pts,Rn,Rang(1:26)
1540 ! ARG IS SAVED LATER FOR SELECTION OF OTHER TIMEWEIGHTING METHODS
1550 DISP "DOING TIME WEIGHT"
1560 Rasio=2*PI/Tot_ptsE
1570 FOR I=0 TO Tot_pts-1G
1580 R(I,0)=R(I,0)*1.0012*(1-COS(Rasio*I))
1590 NEXT I=
1600 IF Nu<>Tot_pts THEN *
1610 Rasio=2*PI/(Nu-Tot_pts)
1620 FOR I=Tot_pts TO Nu-1
1630 R(I,0)=R(I,0)*1.0012*(1-COS(Rasio*(I-Tot_pts)))
1640 NEXT I
1650 END IF
1660 SUBEND
```

Subroutine Fft is the control program for conducting Fast Fourier Transforms. The Subroutine determines through variable <Auto> if the program will FFT all data or specific data. If a specific time trace is to be transformed then the subrountine asks for the filename and record position of the time trace.

```
1670 !_____
1680 SUB Fft(Auto)
1690 !_____
1700 COM /A/ R(4095,1),T(4095,1),Rb(4095),File$[20],Span
1710 COM /B/ INTEGER Ra(4095),I,J,K,Rc,Tag_field(1:175),Type_flag,Slime(4095),Range,Nu,Tot_pts,Rn,Rang(1:26)
1720 IF Auto<>1 THEN
1730 INPUT "WHICH FILE DO YOU WISH AN FFT OF? ",File$
1740 INPUT "WHICH RECORD DO YOU WANT ?",Rn
1750 END IF"
1760 CALL Colldata
1770 CALL Timeweight(1)
1780 CALL Reordr
1790 CALL Fort(1)
1800 SUBEND
```

The Hilb subrontine is an anlysis similar to the FFT except that is generates and energy envelope of the data.

```
1810 !_____
1820 SUB Hilb_
1830 !_____
1840 COM /A/ R(4095,1),T(4095,1),Rb(4095),File$[20],Span
1850 COM /B/ INTEGER Ra(4095),I,J,K,Rc,Tag_field(1:175),Type_flag,Slime(4095),Range,Nu,Tot_pts,Rn,Rang(1:26)
1855 DIM Var(1023,1),Avg(1023,1),Avg1(1023,1),Tmp(1023,1)y
1860 INPUT "WHAT FILE DO YOU WISH AN ENVELOPE STUDY OF",File$f
1870 INPUT "WHAT IS THE RECORD NUMBER",RnL
1874 REDIM R(1023,1)
1875 REDIM T(1023,1)
1876 CALL Colldata
1883 CALL Reordr
1884 CALL Fort(1)a
1890 MAT R= T*(2)a
1900 R(0,0)=R(0,0)/2
1910 FOR I=Nu/2 TO Nu-1
1920 R(I,0)=0/
1930 R(I,1)=0/
1940 NEXT I=
1950 CALL Reordr
1960 CALL Fort(-1)
1970 MAT R= R*(0))
1980 FOR I=1 TO Nu-1
1990 R(I,0)=SQR(T(I,0)*T(I,0)+T(I,1)*T(I,1))
2000 NEXT I=
2009  GOTO 2080 !--------
2010 CALL Plt(1)
2020 CALL Reordr
2030 CALL Fort(1)
2040 FOR I=0 TO 2
2050 T(I,0)=T
2060 T(I,1)=T
2070 NEXT I
2080 SUBEND
```

The variance subroutine calculates the variance from a stored data file. Each time trace from the data file is read into an array and variance is calculated from this technique.

```
2090 !_____
2100 SUB Variance
2110 !_____
2120 COM /A/ R(4095,1),T(4095,1),Rb(4095),File$[20],Span
2130 COM /B/ INTEGER Ra(4095),I,J,K,Rc,Tag_field(1:175),Type_flag,Slime(4095),Range,Nu,Tot_pts,Rn,Rang(1:26)
2140 DIM Var(4095),Avg(4095),Avg1(4095)
2150 COM /C/ INTEGER Raw(2047,100),REAL Fact(100),INTEGER Varflag,Fn
2160 Varflag=1
2170 INTEGER N,St,Ii,Lengh
2180 INPUT "WHAT IS THE FILENAME",File$
2190 ASSIGN @P1 TO "H2"&File$A
2200 STATUS @P1,3;Fn
2210 STATUS @P1,4;Lengh&
2220 ASSIGN @P1 TO *
2230 Lengh=INT(Lengh/2+.5)
2240 REDIM Slime(Lengh-1),Ra(Lengh-1)e
2250 REDIM R(Lengh-1,1),T(Lengh-1,1),Rb(Lengh-1),Var(Lengh-1),Avg(Lengh-1)
2260 REDIM Avg1(Lengh-1)
2270 REDIM Raw(Lengh-1,Fn-1)
2280 PRINT Lengh
2290 CALL Colldata
2300 DISP "CALCULATING VARIANCE"
2310 MAT Avg= Raw(*,0)
2320 MAT Avg= Avg*(Fact(0))A
2330 FOR Ii=0 TO Fn-2c
2340 MAT Var= Raw(*,Ii+1))
2341 MAT Var= Var*(Fact(Ii+1))
2342 MAT Var= Var-Avgc
2343 MAT Var= Var . Var(
2344 MAT Var= Var*(1/(Ii+1))
2345 MAT Avg1= Avg1*(Ii/(Ii+1))"
2346 MAT Avg1= Avg1+Var/
2400 NEXT Ii
2440 Varflag=0
2450 MAT R(*,0)= Avg1
2460 SUBEND
```

The plt subroutine will plot the results of the various analysis subroutines allowing the user if necessary to rescale the output.

```
2470 !_____
2480 SUB Plt(Sel)_
2490 !_____
2500 COM /A/ R(4095,1),T(4095,1),Rb(4095),File$[20],Span
2510 COM /B/ INTEGER Ra(4095),I,J,K,Rc,Tag_field(1:175),Type_flag,Slime(4095),Range,Nu,Tot_pts,Rn,Rang(1:26)
2520 DIM Plt(4095,1)
2530 INPUT "PLOT TIME SEQUENCE OR SPECTRUM (T/S)",Test$,
2540 N=NuT
2550 Summ=0"
2560 IF Test$="S" THEN E
2570 N=Nu/2-1=
2580 MAT Plt= Plt*(0)N
2590 FOR I=0 TO N*
2600 Plt(I,0)=SQR(T(I,0)*T(I,0)+T(I,1)*T(I,1))
2610 Summ=SQR(Summ^2+Plt(I,0)^2)
2620 NEXT IQ
2630 ELSE
2640 IF Sel=1 THEN N=Tot_pts
2650 MAT Plt= Plt*(0)T
2660 MAT Plt= Rl
2670 FOR I=0 TO N*
2680 Summ=SQR(Summ^2+Plt(I,0)^2)
2690 Linsum=Linsum+Plt(I,0)0
2700 NEXT I=
2710 END IF=
2720 Ymax=MAX(Plt(*))t
2730 Ymin=MIN(Plt(*))t
2740 INPUT "DO YOU WANT TO SCALE THE GRAPH",Sca$
2750 IF Sca$="Y" THEN
2760 INPUT "MAX VALUE",Ymax$
2770 INPUT "MIN VALUE",Ymin$
2780 END IF"
2790 OUTPUT 2 USING "#,-K";CHR$(255),CHR$(75)c
2800 GRAPHICS OFFN
2810 GCLEARC
2820 ALPHA OFF
2830 ALPHA ONF
2840 GRAPHICS ON
2850 VIEWPORT 20,125,38,90
2860 WINDOW 0,N,Ymin,Ymax0
2870 LINE TYPE 4
2880 IF Test$="T" THEN GRID N/12,(Ymax-Ymin)/10,0,Ymin
2890 IF Test$="S" THEN GRID N/10,(Ymax-Ymin)/10,0,Ymin
2900 LINE TYPE 6
2910 FRAME
2920 IF Ymin<0 THEN
2930 MOVE 0,00
2940 DRAW N,00
2950 END IF,
2960 MOVE 0,Plt(0,0)
2970 LINE TYPE 1
2980 FOR I=1 TO N,
2990 DRAW I,Plt(I,0)
3000 NEXT I,
3010 CSIZE 3,.6(
3020 IF Test$="S" THEN Cunt=10
3030 IF Test$="T" THEN Cunt=12
3040 FOR I=0 TO Cunt
3050 IF Test$="T" THEN Lab$=VAL$(60*I)
3060 IF Test$="S" AND I=0 THEN Lab$="0"Y
3070 IF Test$="S" AND I<>0 THEN Lab$=VAL$(INT(Span*I/10*1.28))
3080 IF Test$="T" THEN MOVE I*N/12,YminL
3090 IF Test$="S" THEN MOVE I*N/10,YminL
3100 LORG 6t
3110 CLIP OFF=
3120 LABEL USING "#,K";Lab$
3130 NEXT IU
3140 MOVE -.05*N,Ymin+ABS(Ymax-Ymin)/2
3150 LDIR PI/2
3160 LORG 5I
3170 LABEL "AMPLITUDE"
3180 LDIR 0"
3190 MOVE N/2,-.1*ABS(Ymax-Ymin)+Ymin2
3200 LORG 5/
3210 IF Test$="S" THEN LABEL "FREQUENCY (HZ)"
3220 IF Test$="T" THEN LABEL "ANGLE IN DEGREES"
3230 MOVE 0,Ymax
3240 Lab$=VAL$(DROUND(Ymax,4))
```

```
3250 LORG 8A
3260 CLIP OFFS
3270 LABEL Lab$0
3280 MOVE 0,Ymin
3290 LORG 8,
3300 Lab$=VAL$(DROUND(Ymin,4))
3310 CLIP OFFS
3320 LABEL Lab$
3330 IF Test$="S" THEN PRINT TABXY(2,25);Summ,Ymax,ABS(Ymax/Summ);
3340 IF Test$="T" THEN PRINT TABXY(2,25);"AVAR= ";(DROUND(Linsum/Tot_pts,5))
3350 IF Test$="T" THEN PRINT TABXY(32,25);"RMSVAR= ";Summ
3360 SUBEND
```

The Dumpg subroutines will send the graphics image displayed on the screen by using the Plt subroutine to a graphics device for a hardcopy.

```
3370 !_____
3380 SUB Dumpg
3390 !_____
3400 DIM Disp$[80]
3410 DUMP DEVICE IS 701_
3420 INPUT "ENTER GRAPH DESCRIPTOR",Disp$_
3430 DISP Disp$E
3440 CONTROL 1,12;1R
3450 DUMP GRAPHICS
3460 CONTROL 1,12;2R
3470 DISP ""
3480 SUBEND"
```

This programs allows visual inspection of the time data taken by the data acquisiton program.

```
10      ! THIS PROGRAM READS DATA AND DISPLAYS THE TIME HISTORY TAKEN OF
20      ! A SINGLE DATA FILE
30      INTEGER Tag_field(1:175),Range,Type_flag,Slime(1:5120),Alber,Register,Type_falg,Total_pts,Counter
40      INTEGER Rn,Fn,Reclen
50      INTEGER Rang(1:101)
60      ON ERROR GOSUB Err
70      INPUT "BETWEEN QUOTES WHAT IS THE MSUS? ",Msus$
80      IF Msus$="" THEN GOTO 100
90      MASS STORAGE IS Msus$
100     GRAPHICS ON
110     DIM Text$(1:5)[84]
120     DIM Real_data(1:5120)
130     GOSUB Read_data
140     GOSUB Convert_data
150     GOSUB Plot_data
160     INPUT "DO YOU WANT A PLOT",A$
170     IF A$="Y" THEN GOSUB Dump_g
180     DISP "HIT CONTINUE WHEN YOU WISH TO CONTINUE"
190     PAUSE
200     GOTO 130
210 Err:   !
220         IF ERRN=56 THEN
230         PRINT "NO SUCH FILE"
240         GOTO 130
250         END IF
260         IF ERRN=72 OR ERRN=52 THEN GOTO 70
270         PRINT ERRM$
280         PAUSE
290         RETURN
300     STOP
310 Read_data:   !
320             INPUT "WHAT FILE DO YOU WANT DISPLAYED",Name$
330             INPUT "WHAT RECORD NO",Rn
340     ASSIGN @P1 TO "H1"&Name$
350     ASSIGN @P2 TO "H2"&Name$
360     STATUS @P2,3;Fn
370     STATUS @P2,4;Reclen
380     REDIM Rang(1:Fn)
390     Reclen=INT(Reclen/2+.5)
400     REDIM Slime(1:Reclen)
410     REDIM Real_data(1:Reclen)
420     ASSIGN @P3 TO "HT"&Name$
430     ENTER @P1,1;Tag_field(*);Tot_   ime;Rpm;Freqspan;Freq_st;Rec_num;Type_falg;Cal_fact;Rang(*)
440     Total_pts=INT(Total_time*2.56  /eqspan)
450     ENTER @P2,Rn;Slime(*)
470     ENTER @P3,1;Text$(*)
490     RETURN
```

```
500 Convert_data:  !
510    Factor=(4/3)*10^((Rang(Rn)+4.812)/20)/32768/Cal_fact
520    MAT Real_data= Slime*(Factor)
530    RETURN
540 Plot_data:!
550 Ymax=Real_data(1)
560 Ymin=Real_data(1)
570 Counter=0
580    FOR I=1 TO Rec_num*1024
590    IF I>Total_pts THEN GOTO 630
600    IF Real_data(I)>Ymax THEN Ymax=Real_data(I)
610    IF Real_data(I)<Ymin THEN Ymin=Real_data(I)
620    NEXT I
630    OUTPUT 2 USING "#,K";CHR$(255)&CHR$(75)
640    GRAPHICS OFF
650    ALPHA OFF
660    ALPHA ON
670    GCLEAR
680    GRAPHICS ON
690    VIEWPORT 20,125,38,90
700    WINDOW 0,Total_pts,Ymin,Ymax
710    LINE TYPE 1
720    GRID Total_pts/12,(Ymax-Ymin)/10,0,Ymin
730    LINE TYPE 1
740    FRAME
750    IF Y_min<0 THEN
760    MOVE 1,0
770    DRAW Total_pts,0
780    END IF
790    Counter=0
800    MOVE 1,Real_data(1)
810    FOR I=1 TO Rec_num*1024
820    IF I>Total_pts THEN GOTO 850
830    DRAW I,Real_data(I)
840    NEXT I
850    CSIZE 3,.6
860    FOR I=0 TO 12
870    Lab$=VAL$(60*I)
880    MOVE I*Total_pts/12,Ymin
890    LORG 6
900    CLIP OFF
910    LABEL USING "#,K";Lab$
920    NEXT I
930    LDIR 0
940    LORG 8
950    Lab$=VAL$(DROUND(Ymax,5))
960    MOVE 0,Ymax
970    LABEL USING "#,K";Lab$
980    LDIR 0
990    LORG 8
1000   Lab$=VAL$(DROUND(Ymin,5))
1010   MOVE 0,Ymin
1020   LABEL USING "#,K";Lab$
1030   LDIR PI/2
1040   LORG 5
1050   MOVE -.05*Total_pts,Ymin+ABS(Ymax-Ymin)/2
1060   LABEL "AMPLITUDE"
1070   MOVE Total_pts/2,-.10*ABS(Ymax-Ymin)+Ymin
1080   LORG 5
1090   LDIR 0
1100   LABEL "ANGLE IN DEGREES"
1110   RETURN
1120 Dump_g:  !
1130        DIM Disp$[80]
1140        CONTROL 1,12;1
1150        INPUT "ENTER A DESCRIPTOR",Disp$
1160        DISP Disp$
1170        DUMP DEVICE IS 701
1180        DUMP GRAPHICS
1190        CONTROL 1,12;2
1200        RETURN
1210 END
```

The following source code will compute a variance of engine cycle time data. It will use a specific number of engine cycles to compute several variance results and then plot those in 3D format.

```
10      !PROGRAM -- 3 DIMENSIONAL PLOT OF VARIANCE
20      !******************************************
30      OPTION BASE 1
40      CONTROL CRT,21;1
50      DIM Cata$(100)[10],Drname$[20],Name$[10],Disp$[80]
60      INTEGER I,J,K,Inc
70      ON KEY 1 LABEL "CAT",11 GOSUB Cata
80      ON KEY 2 LABEL "3DPLOT",11 GOSUB Vari
90      ON KEY 3 LABEL "EXIT",11 GOSUB Exi
100     ON KEY 4 LABEL "DUMP",11 GOSUB Dump_g
110     LOOP
120     END LOOP
130 Cata:  !
140     CLEAR SCREEN
150     GCLEAR
160     INPUT "NEW DISK? (Y/N)",Drname$
170     IF Drname$="Y" THEN GOTO 190
180     IF Cata$(1)<>"" THEN GOTO 220
190     LINPUT "WHAT IS THE DRIVE",Drname$
200     IF Drname$<>"" THEN MASS STORAGE IS Drname$
210     CAT TO Cata$(*);NAMES,SELECT "H1"
220     FOR I=1 TO 5
230     FOR J=1 TO 20
240     Inc=Inc+1
250     IF Cata$(Inc)="" THEN
260     GOTO 310
270     END IF
280     PRINT TABXY(I*16-15,J);Inc;".";Cata$(Inc)[3,10];
290     NEXT J
300     NEXT I
310     Inc=0
320     RETURN
330 Vari:  !
340     INPUT "WHICH FILE DO YOU WANT TO WORK WITH",Name$
350     CALL Variance(Name$)
360     RETURN
370 Dump_g:  !
380       KEY LABELS OFF
390       ALPHA ON
400       INPUT "WHAT MESSAGE",Disp$
410       DISP Disp$
420       DUMP DEVICE IS 701
430       DUMP GRAPHICS
431       OUTPUT 701 USING "-,K";Disp$
440       KEY LABELS ON
450       RETURN
460 Exi:!
470     END
471     !_____
480     SUB Variance(Name$)
481     !-------------------------------------
490     OPTION BASE 1
500     DISP "<COLLECTING DATA>"
510     ON ERROR RECOVER Err
520     INTEGER Tag_field(1:175),I,J,K,Type_flag,Rang(1:100)
530     INTEGER Rn,Leng,Slime(4096),Inc
540     DIM Factor(1:100),Averg(4096),Averg1(4096)
541     ON KEY 1 LABEL "REPLOT",12 GOSUB Replot
542     ON KEY 2 LABEL "EXIT",12 GOSUB Exi
544     GOSUB Doit
545     LOOP
546     END LOOP
547     !
548 Doit:  !
550       ASSIGN @P1 TO "H1"&Name$
560       ASSIGN @P2 TO "H2"&Name$
570       ASSIGN @P3 TO "HT"&Name$
580       STATUS @P2,3;Rn
590       STATUS @P2,4;Leng
600       Leng=Leng/2
610       REDIM Rang(1:Rn)
620       REDIM Slime(Leng)
630       REDIM Averg(Leng)
640       REDIM Factor(1:Rn)
650       REDIM Averg1(Leng)
```

```
660    ALLOCATE Dat(Rn,Leng)
670    ENTER aP1,1;Tag_field(*);Total_time;Rpm;Span;Start;Rec_num;Type_flag;Cal_fact,Rang(*)
680    FOR I=1 TO Rn
690    Factor(I)=(4/3)*10^((Rang(I)+4.812)/20)/32768/Cal_fact
700    ENTER aP2,1;Slime(*)
710    MAT Averg= Slime*(Factor(I))
720    MAT Dat(I,*)= Averg
730    NEXT I
731    ASSIGN aP1 TO *
732    ASSIGN aP2 TO *
733    ASSIGN aP3 TO *
740    INPUT "FORM AVERAGE WITH CURRENT DATA",An$
750    IF An$="Y" THEN
760    MAT Averg= CSUM(Dat)
770    MAT Averg= Averg/(Rn)
780    MAT Dat(1,*)= Averg
790    END IF
830    !
840    !
850    ! FORMING THE VARIANCE IN PLACE WITH THE DATA
860    !
870    !
880    INTEGER Ntrace
890    INPUT "HOW MANY TRACES PER VARIANCE PLOT",Ntrace
900    DISP "<FORMING VARIANCE>"
910    Nloop=INT((Rn-1)/Ntrace+.5)
920    ALLOCATE Vari(Nloop,Leng)
930    Inc=1
940    FOR I=1 TO Nloop
950    MAT Averg= Averg*(0)
960    FOR J=1 TO Ntrace
970    Inc=Inc+1
980    MAT Averg1= Averg
990    MAT Averg= Dat(Inc,*)
1000   MAT Averg= Averg+Averg1
1010   NEXT J
1020   MAT Averg1= Dat(1,*)
1030   MAT Averg= Averg/(Ntrace)
1040   MAT Averg= Averg-Averg1
1050   MAT Averg= Averg . Averg
1060   MAT Vari(I,*)= Averg
1070   NEXT I
1080   !
1090   !
1100   !PLOTTING THE 3D GRAPH
1110   !
1120   !   (REARRANGING)
1130   !
1140   INTEGER Tot_pts,Ncol,Ncol1
1150   Tot_pts=INT(Total_time*2.56*Span+.5)
1160   Ncol=Tot_pts
1170   Loop1=Tot_pts/256
1180   IF Loop1>1 AND Tot_pts>300 THEN
1190   Loop2=0
1200   REPEAT
1210   Ncol1=Ncol1+1
1220   UNTIL Tot_pts/Ncol1<300
1230   Ncol=Tot_pts/Ncol1
1240   END IF
1250   ALLOCATE D3(Nloop,Ncol)
1260   ALLOCATE D5(Ncol1,Ncol)
1270   FOR I=1 TO Nloop
1280   Inc=0
1290   FOR J=1 TO Ncol
1300   FOR K=1 TO Ncol1
1310   Inc=Inc+1
1320   D5(K,J)=Vari(I,Inc)
1330   IF K=Tot_pts OR K=Leng/2 THEN GOTO 1270
1340   NEXT K
1350   NEXT J
1360   FOR K=1 TO Ncol
1370   MAT SEARCH D5(*,K),MAX;D3(I,K)
1380   NEXT K
1390   NEXT I
1400   DEALLOCATE D5(*)
1410   !
1420   !
1430   !   (PLOTTING)
```

```
1440  !
1441  ALLOCATE D4(Ncol)
1442  Scalx=.6
1443  Widthx=75
1444  Scaly=1.2
1445  Heighy=30
1446  Ang=30
1450 Plt: !
1460  CLEAR SCREEN
1470  GCLEAR
1480  GRAPHICS ON
1490  INTEGER Widthx,Heighy
1500  IF Max$<>"Y" THEN
1510  Z=MAX(D3(*))-MIN(D3(*))
1520  Y=TAN(-Ang*PI/180)*2
1530  W=Y*Z
1540  Minim=MIN(D3(*))+W
1541  Maxim=MAX(D3(*))
1551  ELSE
1552  Z=Maxim-Minim
1553  Y=TAN(-Ang*PI/180)*2
1554  W=Y*Z
1556  Minim=Minim+W
1557  END IF
1560  FOR I=Nloop TO 1 STEP -1
1610  VIEWPORT 20+(I-1)*Scalx,20+Widthx+(I-1)*Scalx,30+(I-1)*Scaly,30+Heighy+(I-1)*Scaly
1620  WINDOW 1,Ncol,Minim,Maxim
1630  MAT D4= D3(I,*)
1640  MOVE 1,D4(1)
1650  IF I=Nloop THEN GOTO 1730
1660  PEN -1
1670  FOR J=2 TO Ncol
1680  MOVE J,+W*J/Ncol
1690  DRAW J,D4(J)+W*J/Ncol
1700  NEXT J
1710  PEN 1
1720  MOVE 1,D4(1)
1730  FOR J=2 TO Ncol
1740  DRAW J,D4(J)+W*J/Ncol
1750  NEXT J
1760  NEXT I
1761  !
1762  !
1763  !          (AXES)
1765  !
1766  !
1769  MOVE 1,Minim-W
1770  DRAW 1,Maxim
1773  Label$=VAL$(DROUND(Z+Minim-W,5))
1774  CSIZE 3,.6
1775  LORG 8
1776  CLIP OFF
1777  Label$=Label$&" "
1779  LABEL Label$
1781  FOR I=1 TO 10
1782  MOVE -2,Z*I/10
1788  CLIP OFF
1789  DRAW 1,Z*I/10
1792  NEXT I
1793  FOR I=0 TO 12
1794  MOVE Ncol*I/12,Minim+W*I/12-.1*ABS(Z)-W
1795  CLIP OFF
1797  DRAW Ncol*I/12,Minim+W*I/12-W
1798  MOVE Ncol*I/12,Minim+W*I/12-.1*Z-W
1799  Label$=VAL$(I*60)
1800  LORG 6
1801  CSIZE 3,.6
1803  CLIP OFF
1804  LABEL Label$
1805  NEXT I
1806  RETURN
1807 Replot: !
1809          PRINT "CURRENT VALUE IS ";Scalx
1810          INPUT "WHAT IS SCALEX",Scalx$
1811          IF Scalx$<>"" THEN Scalx=VAL(Scalx$)
1812          PRINT "CURRENT VALUE IS ";Scaly
1813          INPUT "WHAT IS SCALEY",Scaly$
1815          IF Scaly$<>"" THEN Scaly=VAL(Scaly$)
```

```
1816        PRINT "CURRENT VALUE IS ";Widthx
1818        INPUT "WHAT IS WIDTHX",Widthx$
1819        IF Widthx$<>"" THEN Widthx=VAL(Widthx$)
1820        PRINT "CURRENT VALUE IS ";Heighy
1822        INPUT "WHAT IS HEIGHY",Heighy$
1823        IF Heighy$<>"" THEN Heighy=VAL(Heighy$)
1824        PRINT "CURRENT VALUE IS ";Ang
1826        INPUT "WHAT TILT ANGLE",Ang$
1827        IF Ang$<>"" THEN Ang=VAL(Ang$)
1828        INPUT "DO YOU WANT TO SET MIN & MAX",Max$
1829        IF Max$="Y" THEN
1830        PRINT "CURRENT VALUE IS ";Maxim
1832        INPUT "MAXIMUM VALUE",Maxim
1833        PRINT "CURRENT VALUE IS ";Minim+W
1835        INPUT "MINIMUM VALUE",Minim
1836        END IF
1837        GOSUB Plt
1838        RETURN
1839 Err: !
1840        PRINT ERRM$
1841        IF ERRM$="" THEN PRINT "TERMINATED WITH NO ERRORS"
1842        PAUSE
1843 Exi: !
1844  SUBEND
```

APPENDIX D

D. FLOW CHARTS OF 8 - CHANNEL DATA ACQUISITION SYSTEM

(SYSTEM No.3).

.

START

NUMBER OF
SAMPLES PER REV

DEFAULT=512
256, 128, 64

VALID ENTRY?
512, 256, 128, 64 — NO

YES

NUMBER OF REVS

DEFAULT=16
64, 1

VALID ENTRY?
1 THROUGH 64 — NO

YES

SEND COMMAND
TO DAC UNIT

WAIT FOR
RESPONSE
FROM DAC

RESPONSE FROM DAC? — NO - TIMEOUT

OUTPUT MESSAGE

TRANSMISSION
PROBLEM OR DAC
NOT RESPOND.

A

B

C

D

262

DYNO PC   PAGE 1

```
         ┌─┐              ┌─┐              ┌─┐                              ┌─┐
         │A│              │B│              │C│                              │D│
         └─┘              └─┘              └─┘                              └─┘
                                            │
                                            ▼
                                    ╱───────────╲        ╱───╲        ╱───╲
                               YES ╱ ERROR        ╲ YES ╱ 1 ? ╲  NO  ╱ 2 ? ╲  NO
                          ┌────────┤ RESPONSE?     ├─────┤     ├──────┤     ├──────────┐
                          │         ╲             ╱      ╲   ╱        ╲   ╱             │
                          │          ╲───────────╱        ╲─╱          ╲─╱             │
                          │               │NO             │YES         │YES            │
                          │               ▼               ▼            ▼               │
                          │        ┌────────────┐  ┌────────────┐ ┌─────────────┐      │
                          │        │ WAIT FOR   │  │ OUTPUT     │ │ OUTPUT      │      │
                          │        │ DATA       │  │ MESSAGE    │ │ MESSAGE     │      │
                          │        │ FROM DAC VIA│ │ PIP SIGNAL │ │ DI-MAG SIGNAL│     │
                          │        │ XMODEM 1024│  │ ERROR      │ │ ERROR       │      │
                          │        └────────────┘  └────────────┘ └─────────────┘      │
                          │               │               │            │               │
                          │               ▼               │            │               │
                          │        ┌────────────┐         │            │               │
                          │        │ CREATE FILE│         │            │               │
                          │        │ ACCELDAT.???│        │            │               │
                          │        │ ON PC      │         │            │               │
                          │        └────────────┘         │            │               │
                          │               │               │            │               │
                          │               ▼               │            │               │
                          │          ╱─────────╲          │            │               │
                          │       N ╱ CHANGE    ╲  ESC   ┌──────┐      │               │
                          │    ┌────┤ COLLECTION ├───────│ EXIT │      │               │
                          │    │     ╲ PARAMETERS?╱      └──────┘      │               │
                          │    │      ╲─────────╱                      │               │
                          │    │          │Y                           │               │
                          │    │          └───────────────────────────────────────────┘
                          └────┘
```

```
                    ┌─────────────┐
                    │  WAIT FOR   │
              ┌────▶│  COMMAND    │
              │     │  FROM PC    │
              │     └─────────────┘
              │            │
              │     ┌─────────────┐
              │     │     SET     │
              │     │ SAMPLES PER REV │
              │     │   SELECTOR  │
              │     └─────────────┘
              │            │
              │     ┌─────────────┐
              │     │     SET     │        ┌─ = SAMPLES_PER_REV•NUMBER_OF_REVS
              │     │ TOTAL SAMPLE│◀───────┤
              │     │    COUNT    │
              │     └─────────────┘
              │            │
              │     ┌─────────────┐
   NO PIP SIGNAL    │ SYNCHRONIZE │
              │ ◀───│ PIP/DI-MAG/CID │
              │     └─────────────┘
              │            │
              │          ◇─────◇                ┌─────────────┐
              │         ╱  CID   ╲      NO       │   USE PIP   │
              │        ◇  SIGNAL   ◇────────────▶│ SIGNATURE TOOTH │   TFI ENGINES
              │         ╲ PRESENT? ╱             │   TO SET    │
              │          ◇─────◇                 │   TRIGGER   │
              │            │                     └─────────────┘
              │           YES                          │
              │     ┌─────────────┐                    │
              │     │   USE CID   │  DIS OR EDIS        │
              │     │   TO SET    │  ENGINES            │
              │     │   TRIGGER   │                     │
              │     └─────────────┘                     │
              │            │                            │
              │            └──────────────◀─────────────┘
              │            │
              │     ┌─────────────┐
              │     │    START    │      ┌─ SHOULD BE CYLINDER #1 PIP
              │     │ COLLECTION ON │◀────┤
              │     │ DI-MAG AFTER │
              │     │ NEXT RISING │
              │     │  PIP EDGE   │
              │     └─────────────┘      ┌─ COLLECTION PROCESS IS INTERRUPT DRIVEN (SEE NEXT PAGE)
              │            │             │
              │     ┌─────────────┐◀─────┘
              │     │ ENABLE INTERRUPTS │
              │     │  WAIT FOR   │◀·················· C
              │     │ DATA COLLECTION │
              │     │  COMPLETE   │
              │     └─────────────┘
              │            │
              │          ◇─────◇
    ┌─────────────┐ NO   ╱COLLECTION╲
    │ SEND ERROR  │◀────◇ SUCCESSFUL? ◇
    │   TO PC     │      ╲           ╱
    └─────────────┘       ◇─────◇
              │            │
              │           YES
              A            B                              C
```

265   DYNO DAC020   PAGE 1

A

B

C

ORGANIZE
DATA
FOR
TRANSMISSION
TO PC

SEND DATA VIA
XMODEM 1024
TO PC

NOR   = NUMBER OF REVS TO COLLECT
NOSPR = NUMBER OF SAMPLES PER REV

CHANNEL 1, REV 1,   SAMPLES 1 -> NOSPR
CHANNEL 1, REV 2,   SAMPLES 1 -> NOSPR

CHANNEL 1, REV NOR, SAMPLES 1 -> NOSPR
CHANNEL 2, REV 1,   SAMPLES 1 -> NOSPR

CHANNEL 4, REV NOR, SAMPLES 1 -> NOSPR

DATA
COLLECTION
INTERRUPT

NUMBER OF
READS PER SET
-1

= 0?   NO   TRIGGER NEXT
CONVERSION

STORE DATA
2 CHANNELS

YES

STORE DATA
LAST
2 CHANNELS

TOTAL SAMPLE
COUNT
-1

= 0?   DISABLE INTERRUPT

INDICATE
DATA COLLECTION
COMPLETE

NO

EXIT
INTERRUPT
ROUTINE

266

APPENDIX E

E. ADDITIONAL COLD TEST DATA.
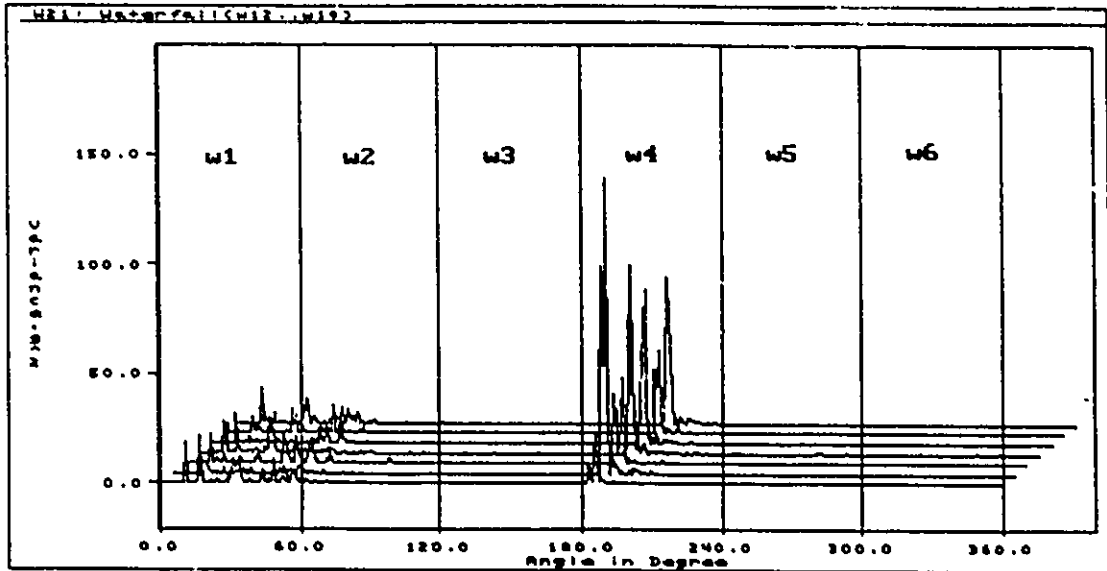
Figure E.1 : Accelerometer #1 Vibration Running Variance for
#1 Rod Cap Bearing Missing
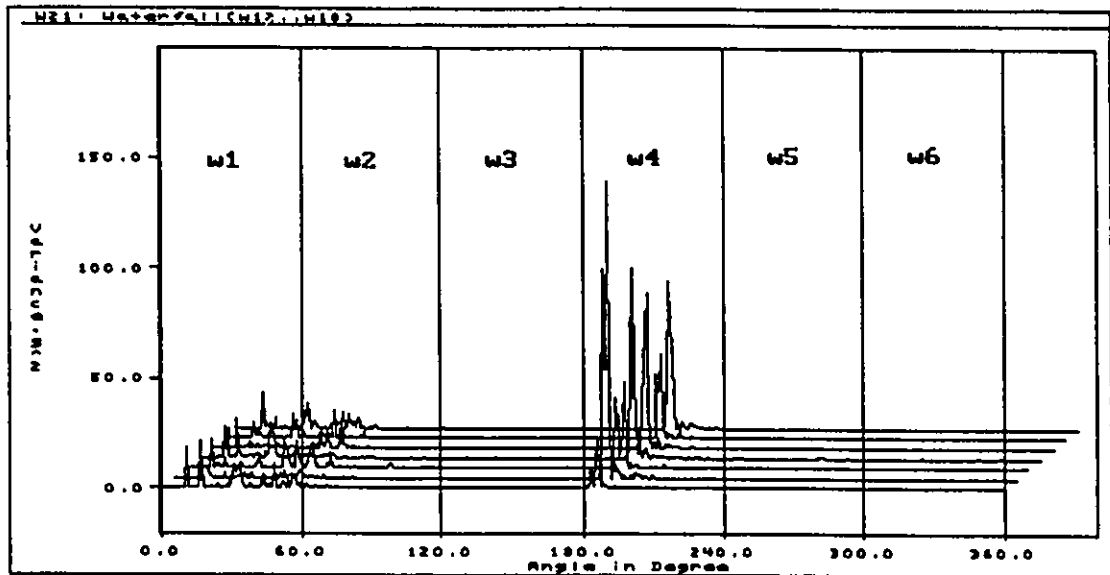
Figure E.2 : Accelerometer #2 Vibration Running Variance for
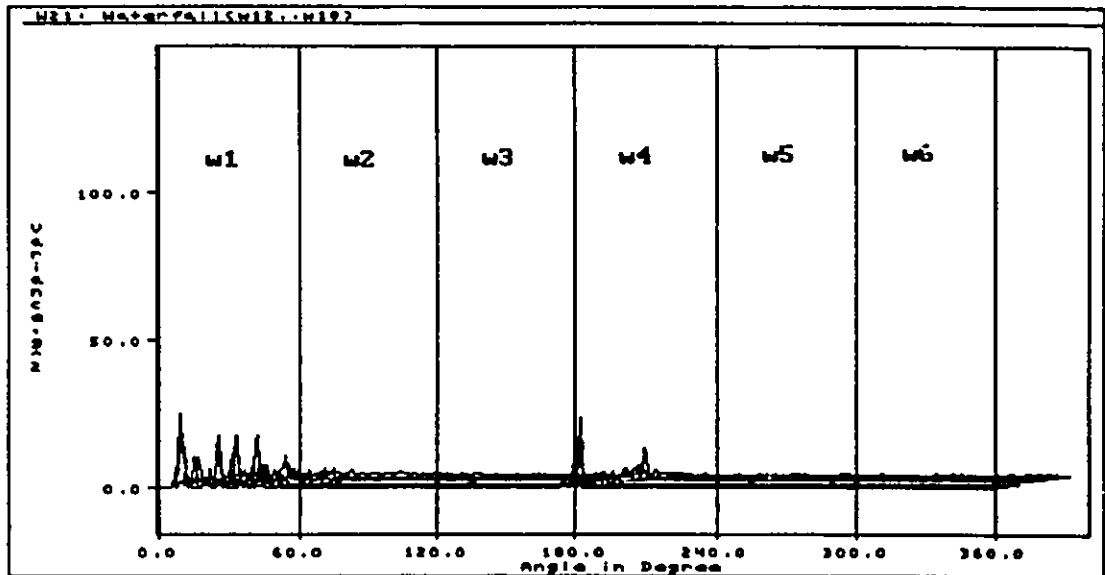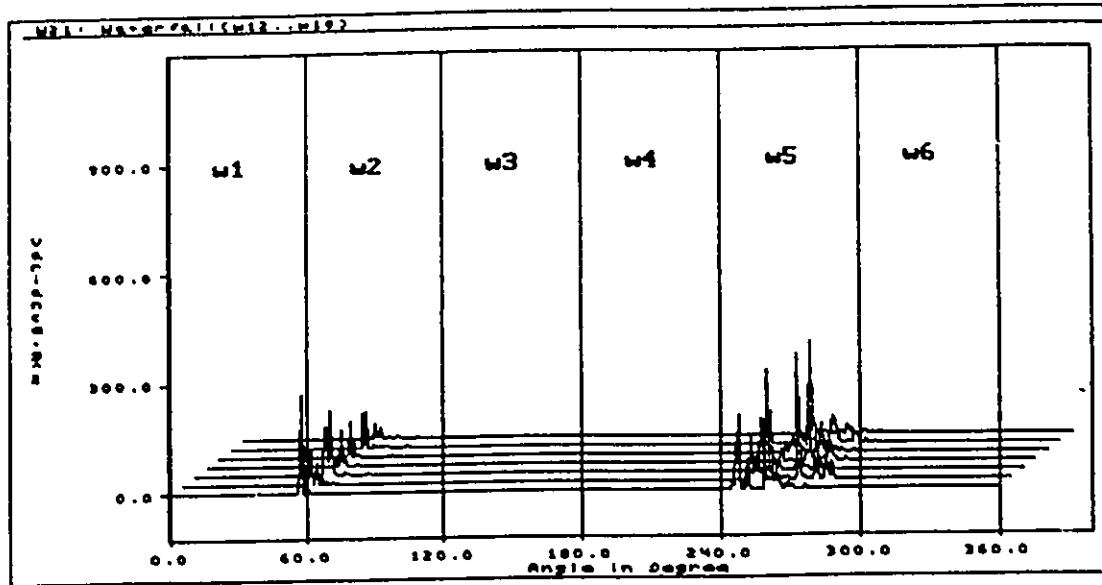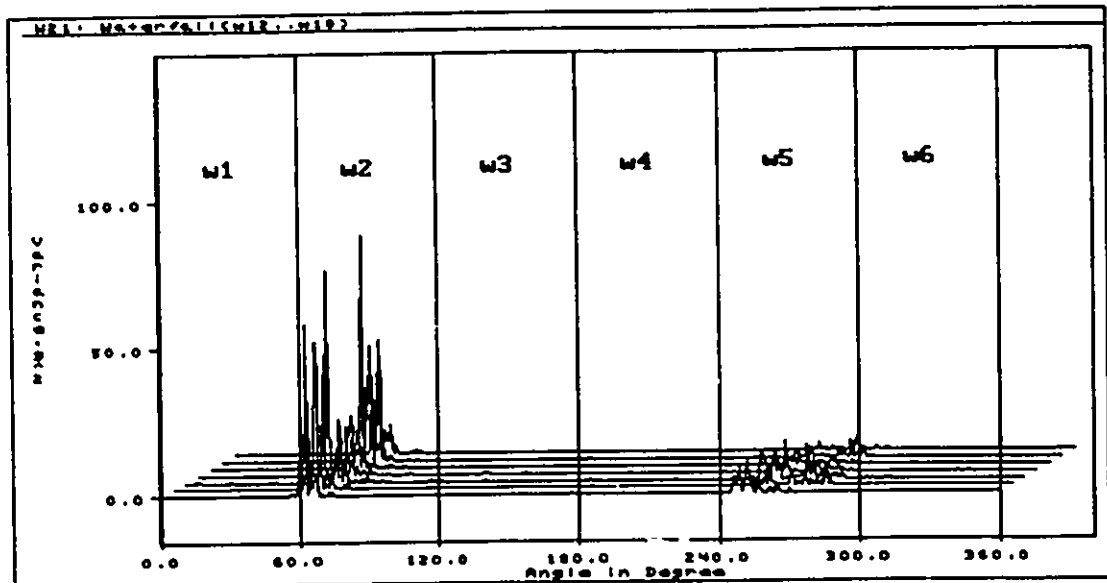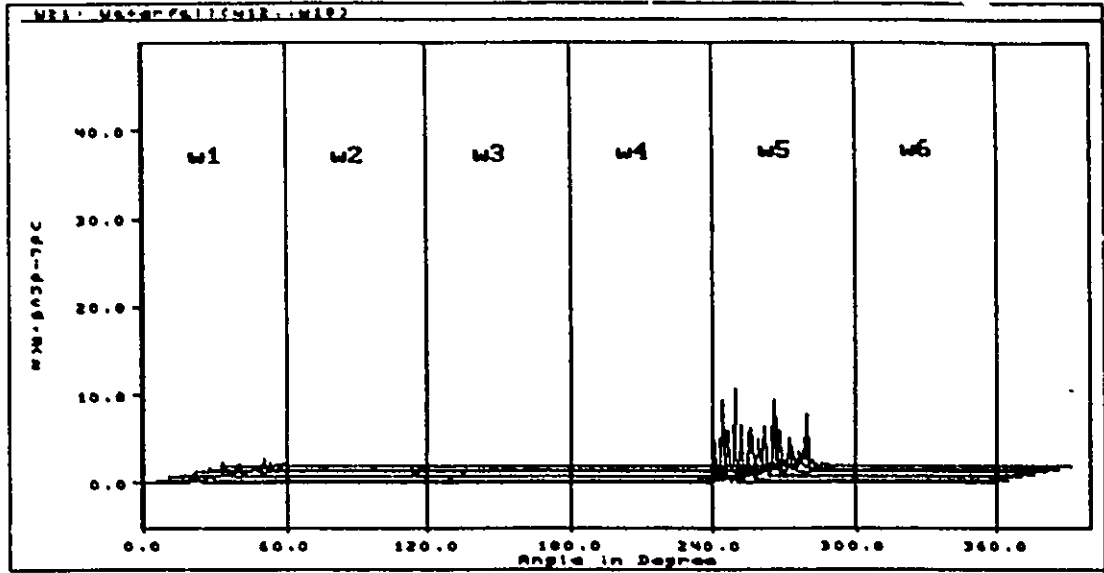#1 Rod Cap Bearing Missing

268
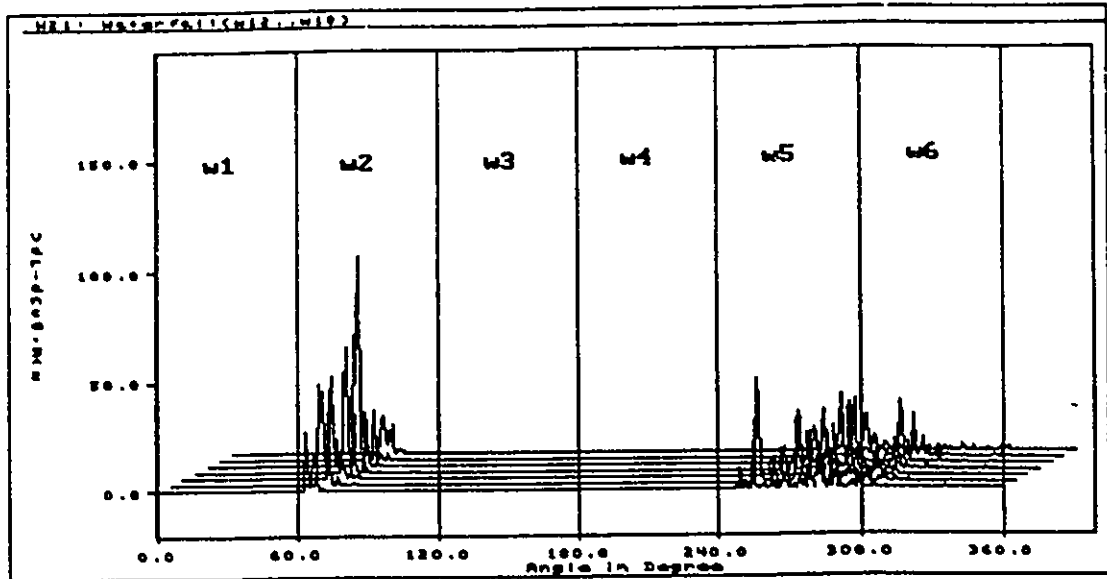
Figure E.3 : Accelerometer #1 Vibration Running Variance for
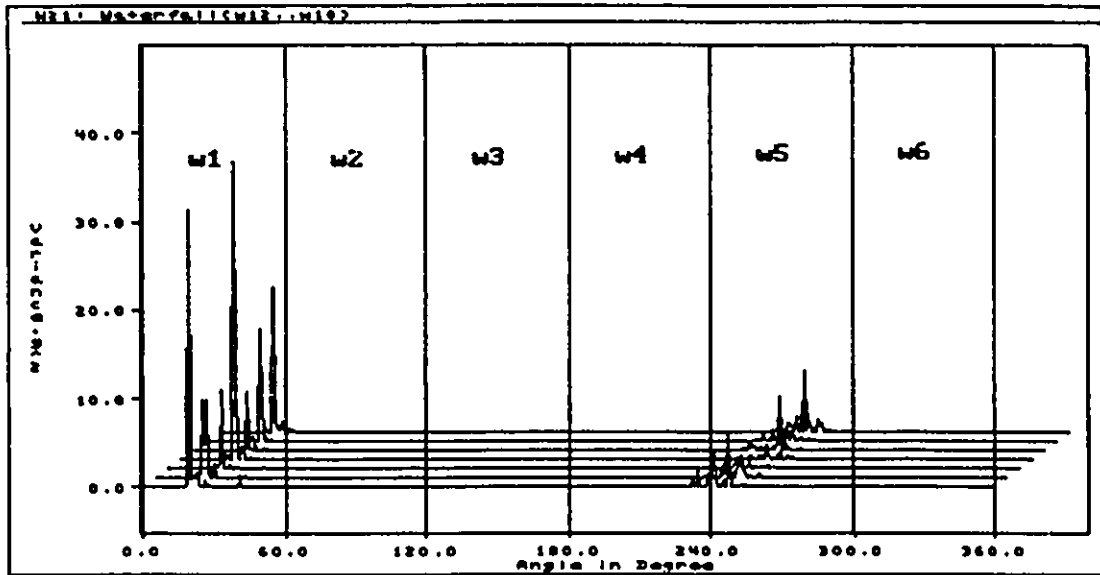#2 Rod Cap Bearing Missing
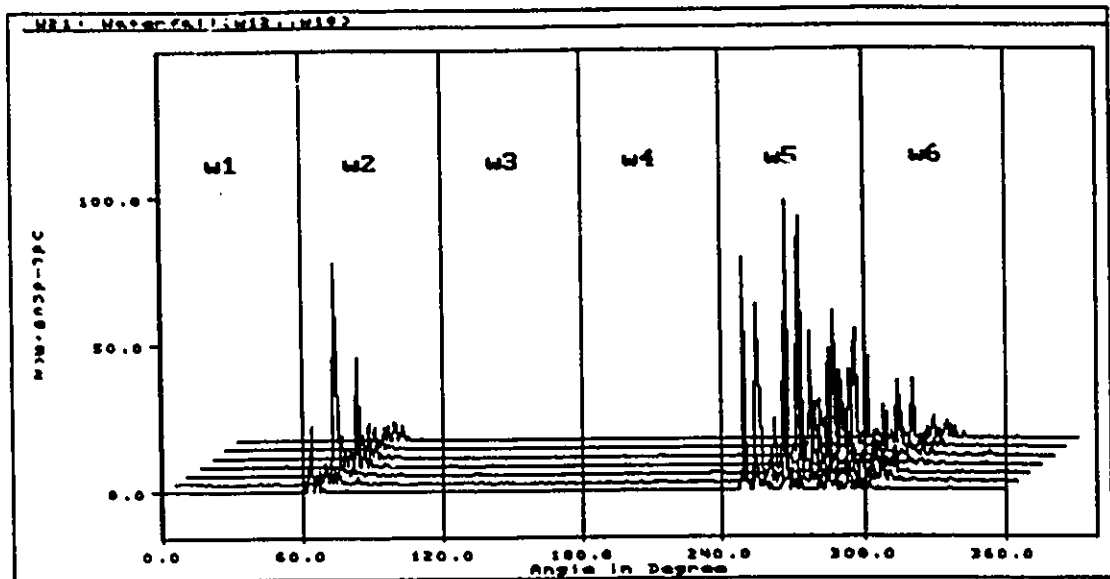
Figure E.4 : Accelerometer #2 Vibration Running Variance for
#2 Rod Cap Bearing Missing
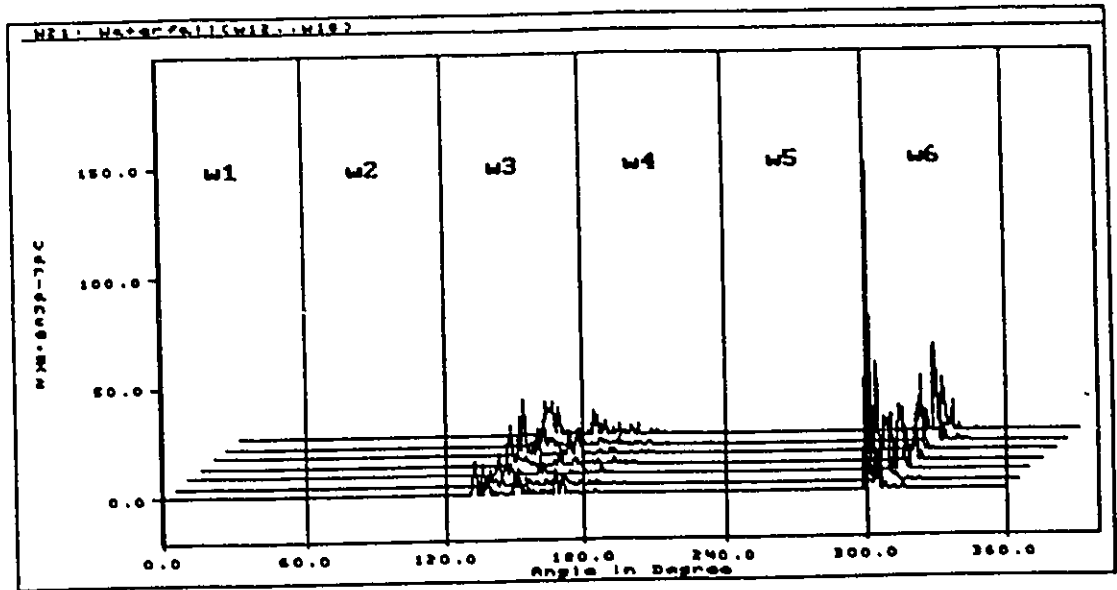
Figure E.5 : Accelerometer #1 Vibration Running Variance for
#3 Rod Cap Bearing Missing
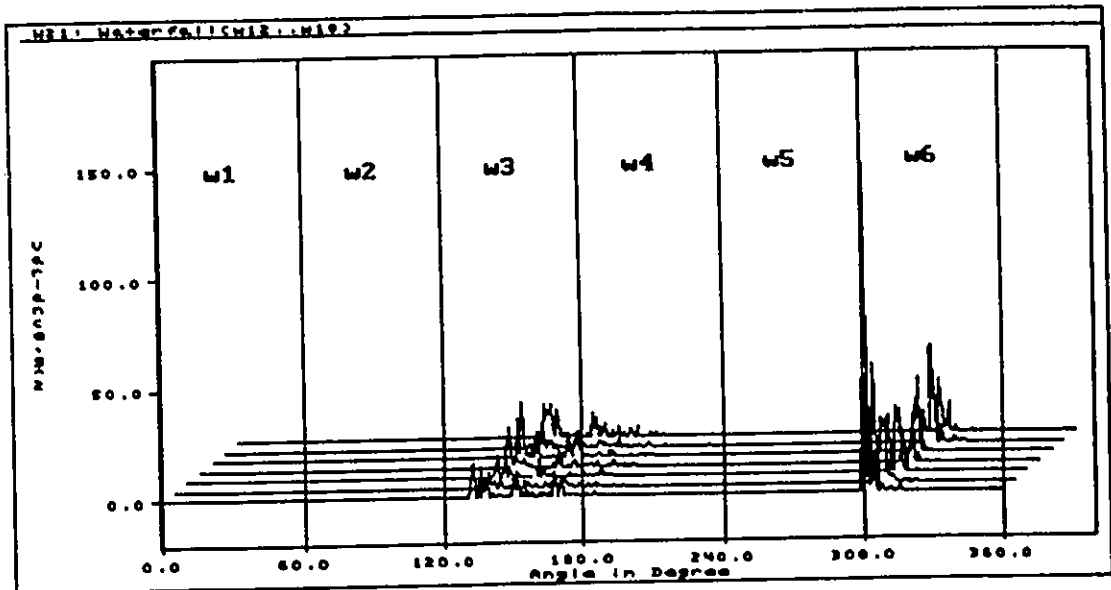
Figure E.6 : Accelerometer #2 Vibration Running Variance for
#3 Rod Cap Bearing Missing
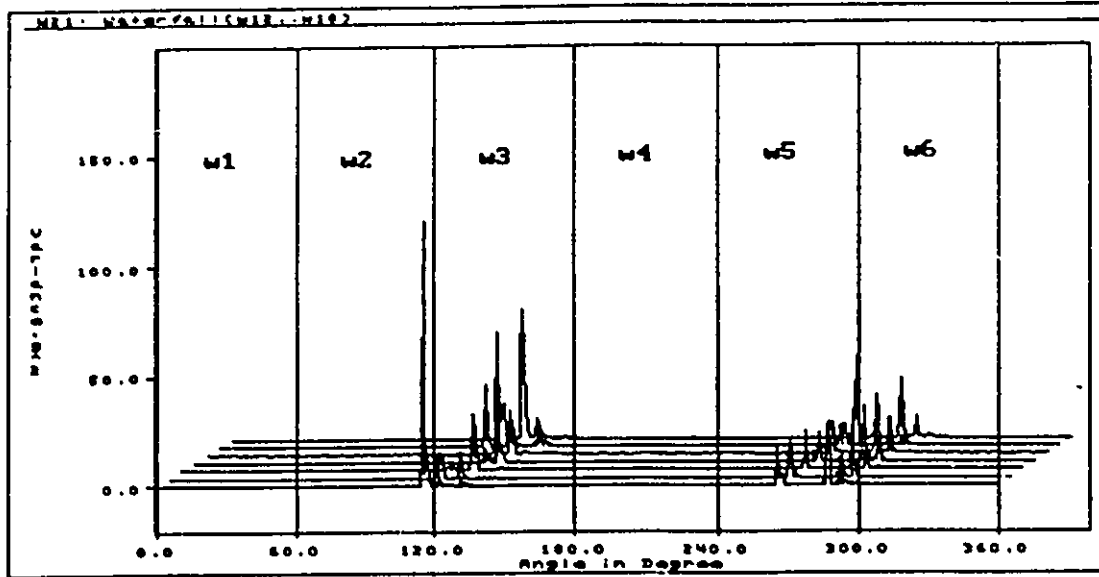
270
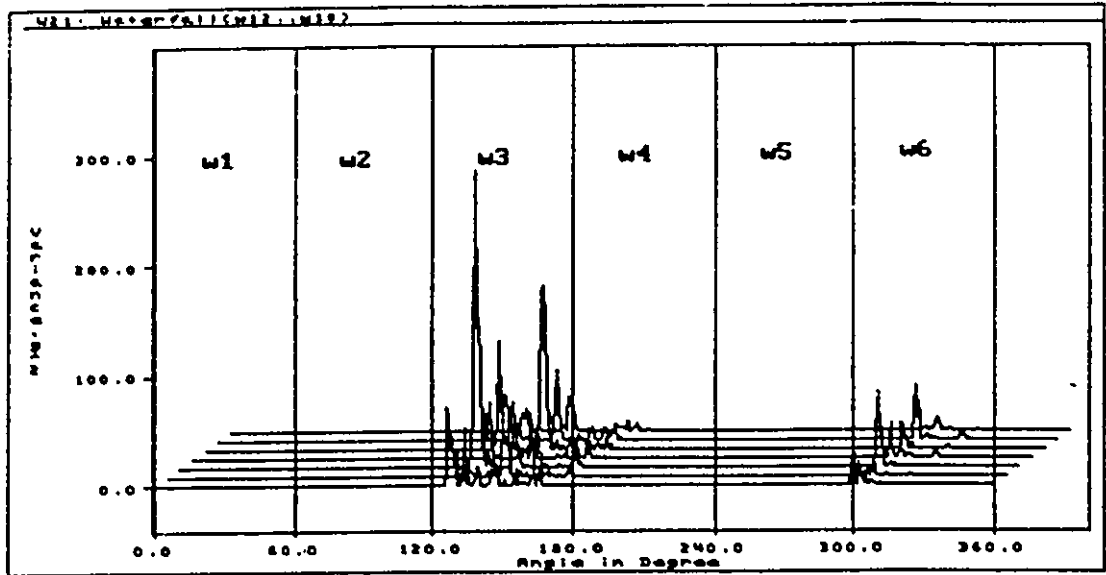
Figure E.7 : Accelerometer #1 Vibration Running Variance for
#4 Rod Cap Bearing Missing
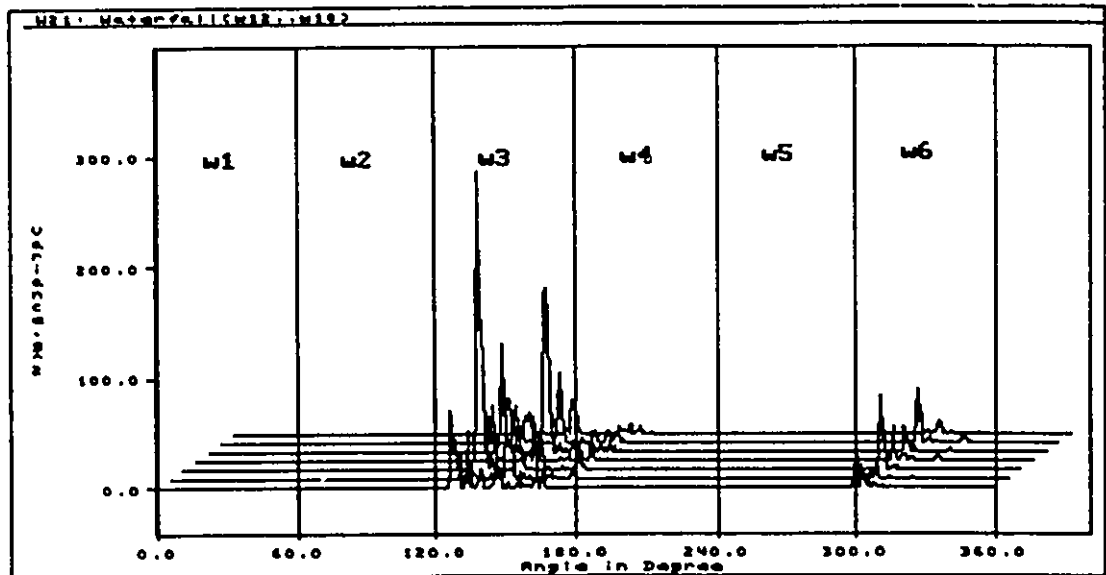
Figure E.8 : Accelerometer #2 Vibration Running Variance for
#4 Rod Cap Bearing Missing
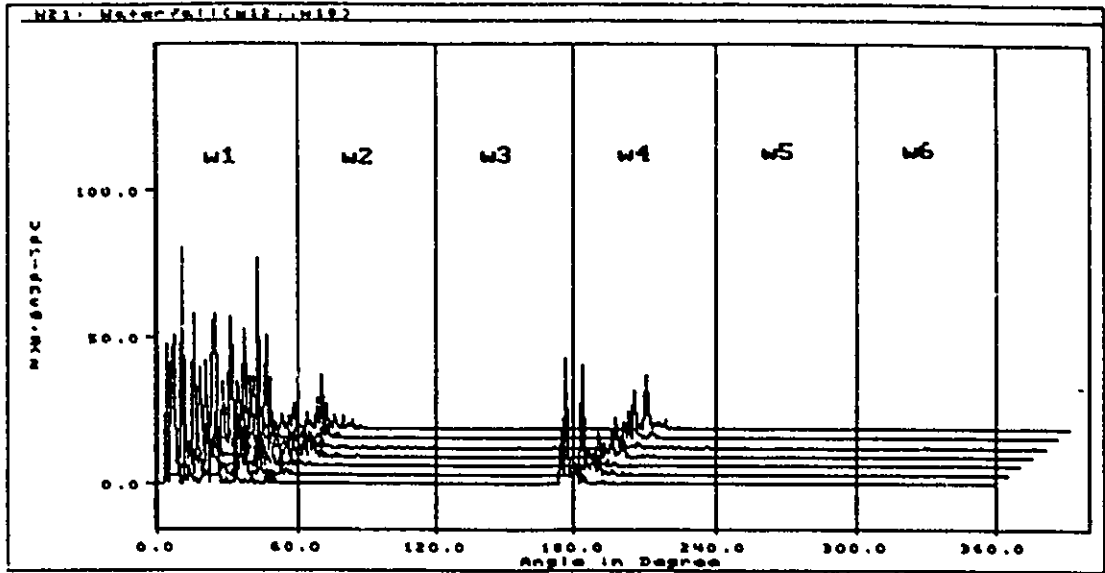
Figure E.9 : Accelerometer #1 Vibration Running Variance for
#5 Rod Cap Bearing Missing

Figure E.10 : Accelerometer #2 Vibration Running Variance for
#5 Rod Cap Bearing Missing

Figure E.11 : Accelerometer #1 Vibration Running Variance for #6 Rod Cap Bearing Missing

Figure E.12 : Accelerometer #2 Vibration Running Variance for #6 Rod Cap Bearing Missing

Figure E.13 : Accelerometer #1 Vibration Running Variance for #1 Rod Bearing Missing

Figure E.14 : Accelerometer #2 Vibration Running Variance for #1 Rod Bearing Missing

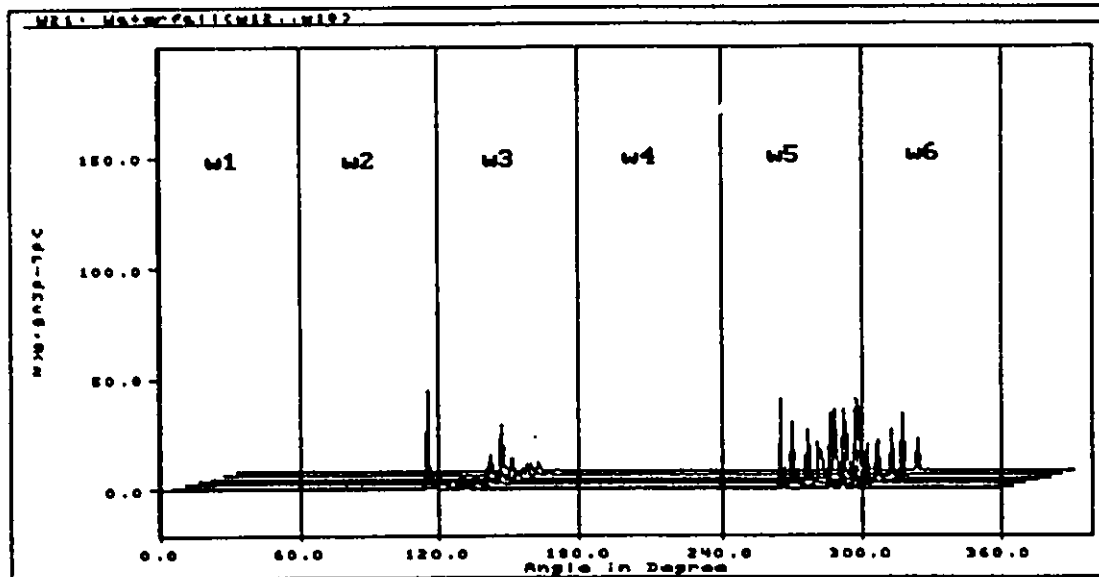Figure E.15 : Accelerometer #1 Vibration Running Variance for #2 Rod Bearing Missing

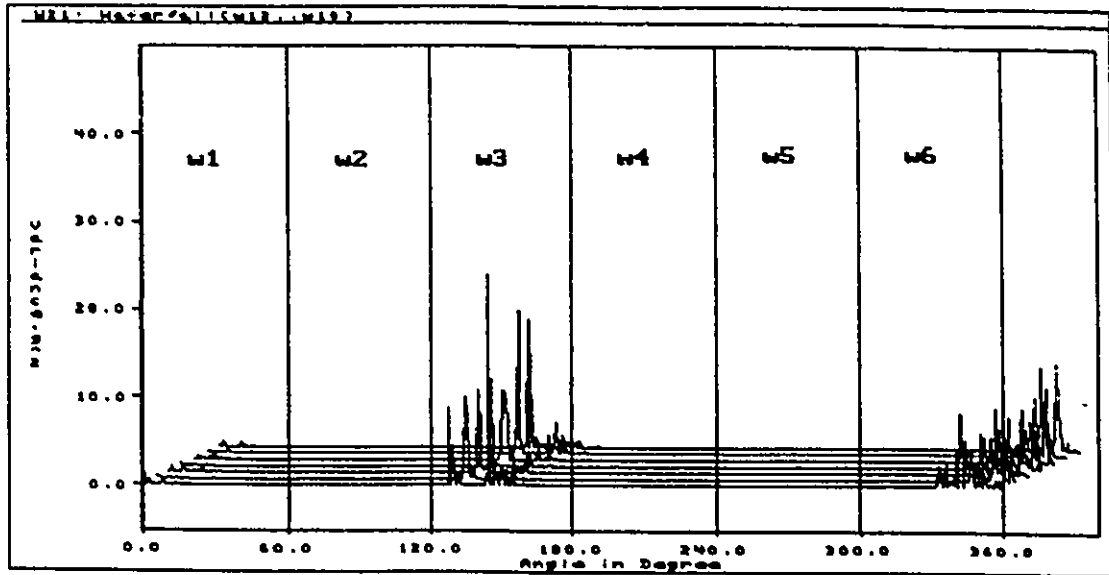Figure E.16 : Accelerometer #2 Vibration Running Variance for #2 Rod Bearing Missing

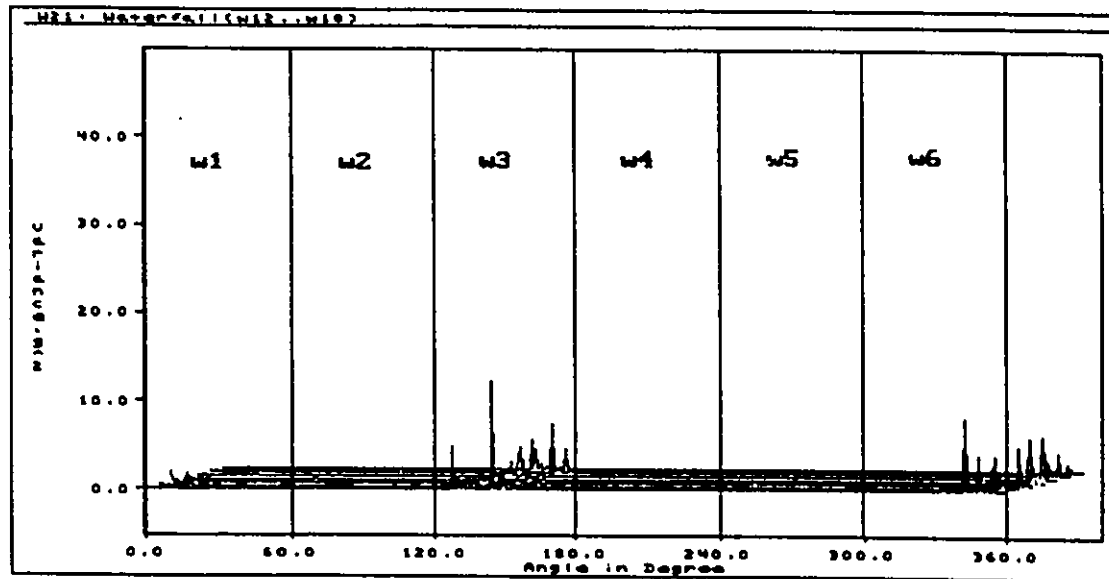Figure E.17 : Accelerometer #1 Vibration Running Variance for
#3 Rod Bearing Missing

Figure E.18 : Accelerometer #2 Vibration Running Variance for
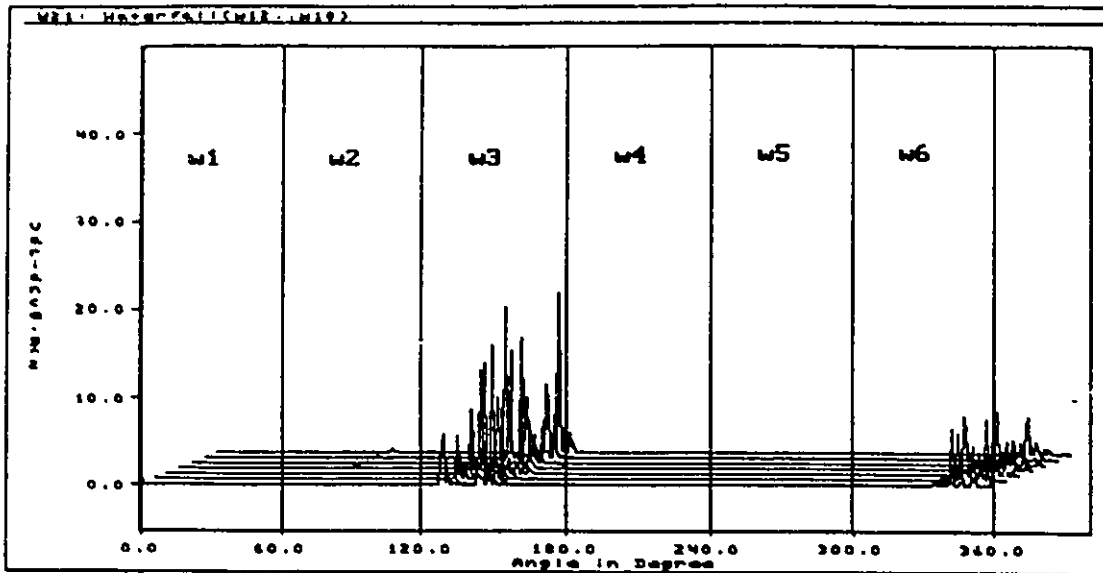#3 Rod Bearing Missing

276

Figure E.19 : Accelerometer #1 Vibration Running Variance for #4 Rod Bearing Missing
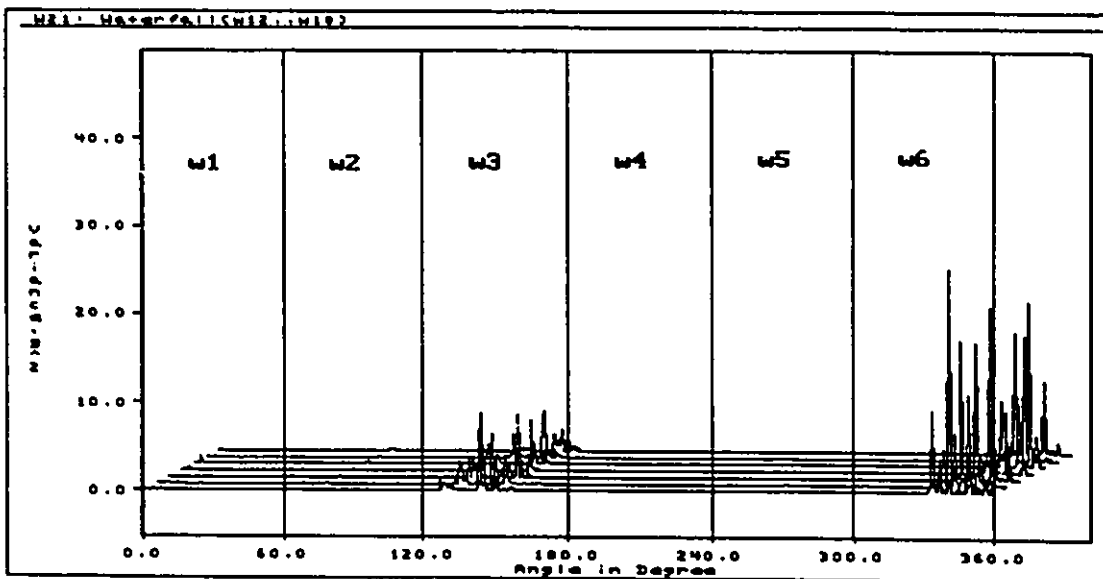

Figure E.20 : Accelerometer #2 Vibration Running Variance for #4 Rod Bearing Missing

Figure E.21 : Accelerometer #1 Vibration Running Variance for #5 Rod Bearing Missing

Figure E.22 : Accelerometer #2 Vibration Running Variance for #5 Rod Bearing Missing
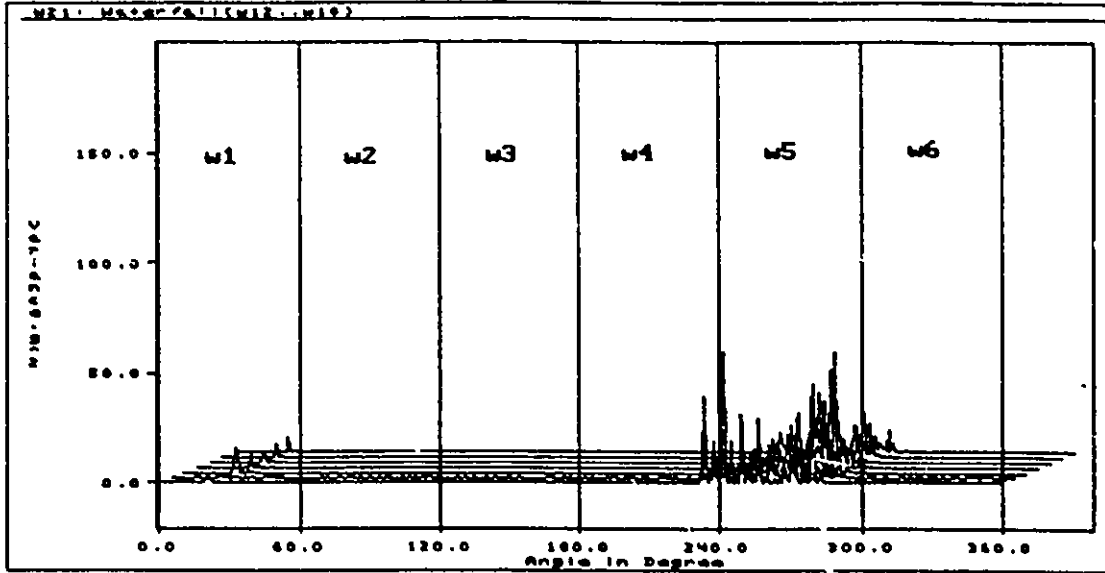
Figure E.23 : Accelerometer #1 Vibration Running Variance for #6 Rod Bearing Missing
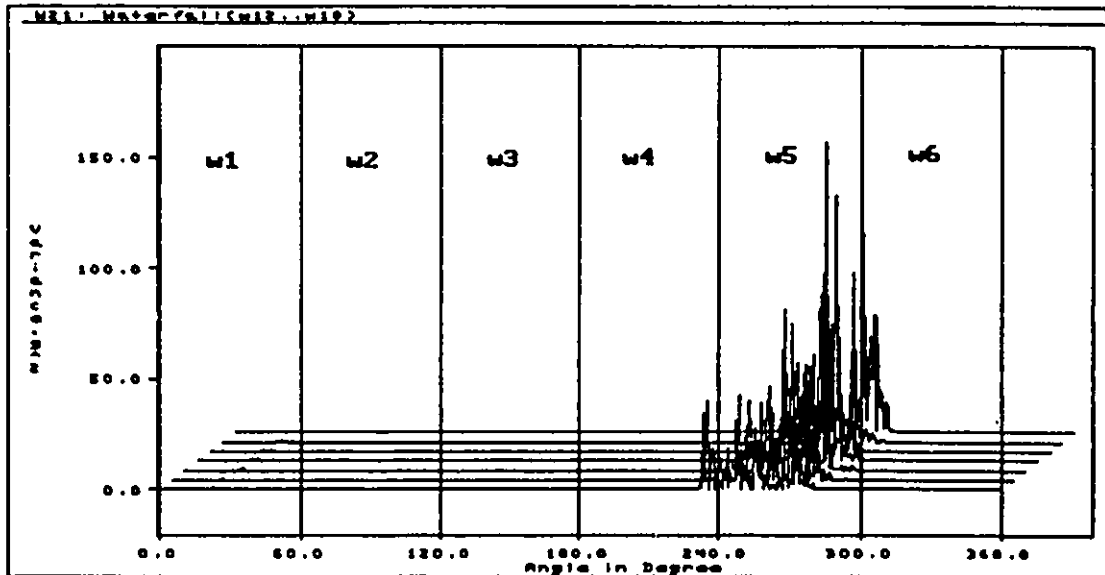

Figure E.24 : Accelerometer #2 Vibration Running Variance for #6 Rod Bearing Missing

Figure E.25 : Accelerometer #1 Vibration Running Variance for #1 Loose Connecting Rod Nuts.

Figure E.26 : Accelerometer #2 Vibration Running Variance for #1 Loose Connecting Rod Nuts.

280

Figure E.27 : Accelerometer #1 Vibration Running Variance for
#2 Loose Connecting Rod Nuts.
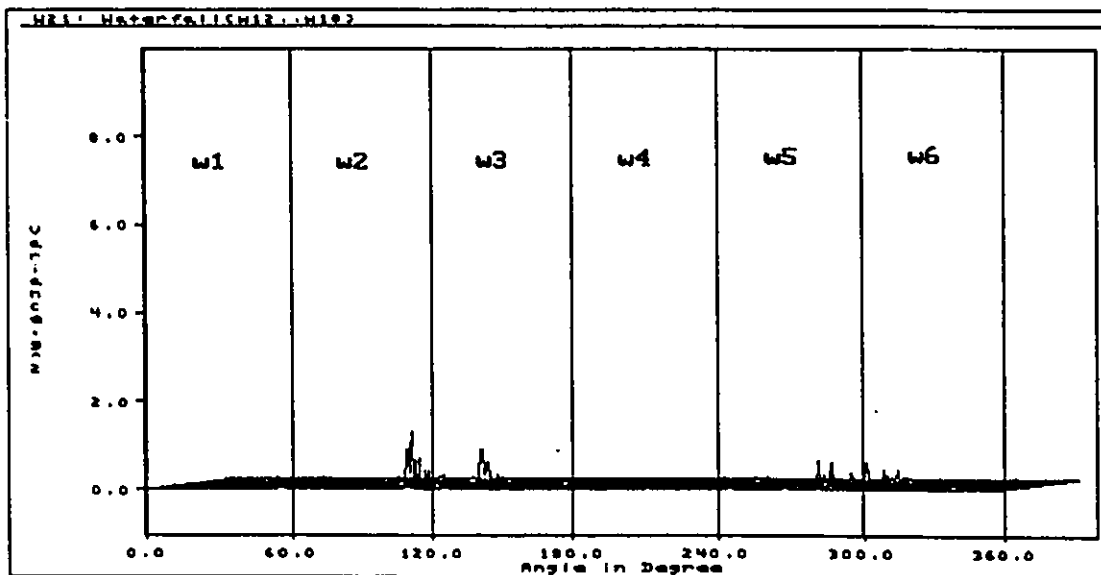
Figure E.28 : Accelerometer #2 Vibration Running Variance for
#2 Loose Connecting Rod Nuts.

281

Figure E.29 : Accelerometer #1 Vibration Running Variance for
#3 Loose Connecting Rod Nuts.

Figure E.30 : Accelerometer #2 Vibration Running Variance for
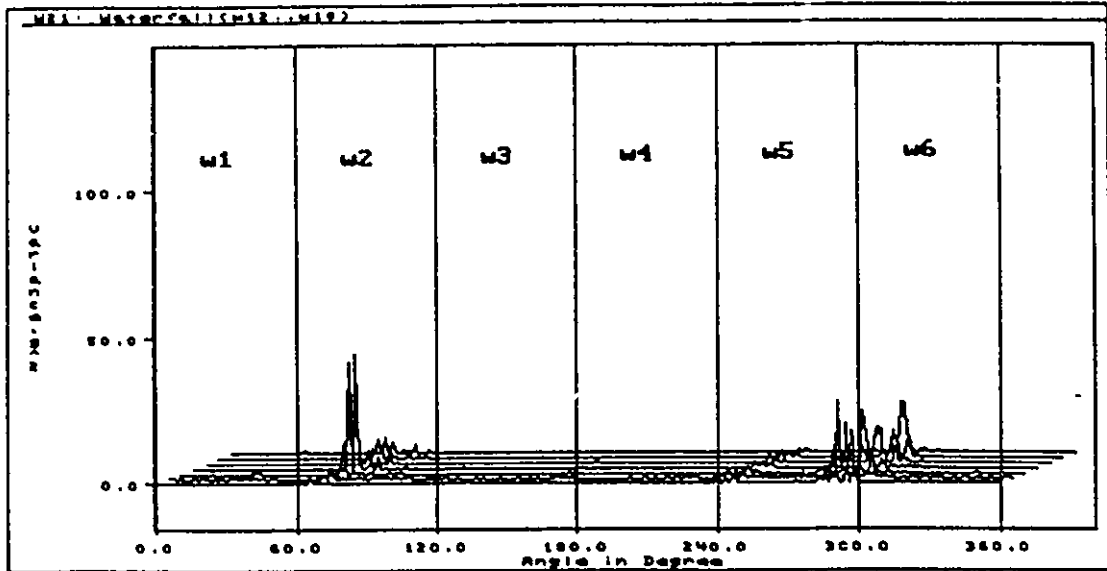#3 Loose Connecting Rod Nuts.

Figure E.31 : Accelerometer #1 Vibration Running Variance for
#4 Loose Connecting Rod Nuts.

Figure E.32 : Accelerometer #2 Vibration Running Variance for
#4 Loose Connecting Rod Nuts.

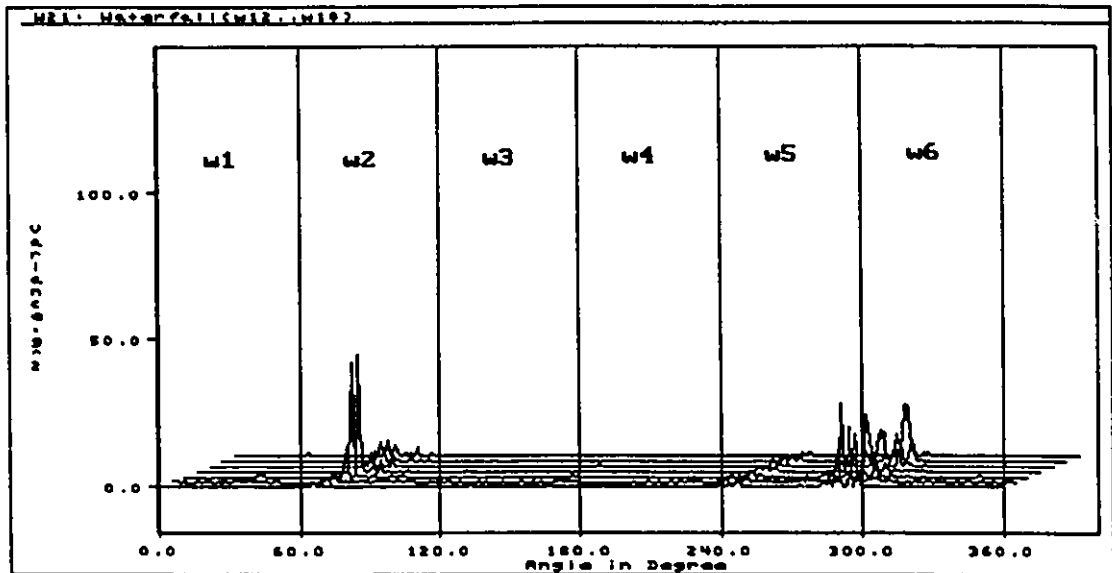Figure E.33 : Accelerometer #1 Vibration Running Variance for #5 Loose Connecting Rod Nuts.
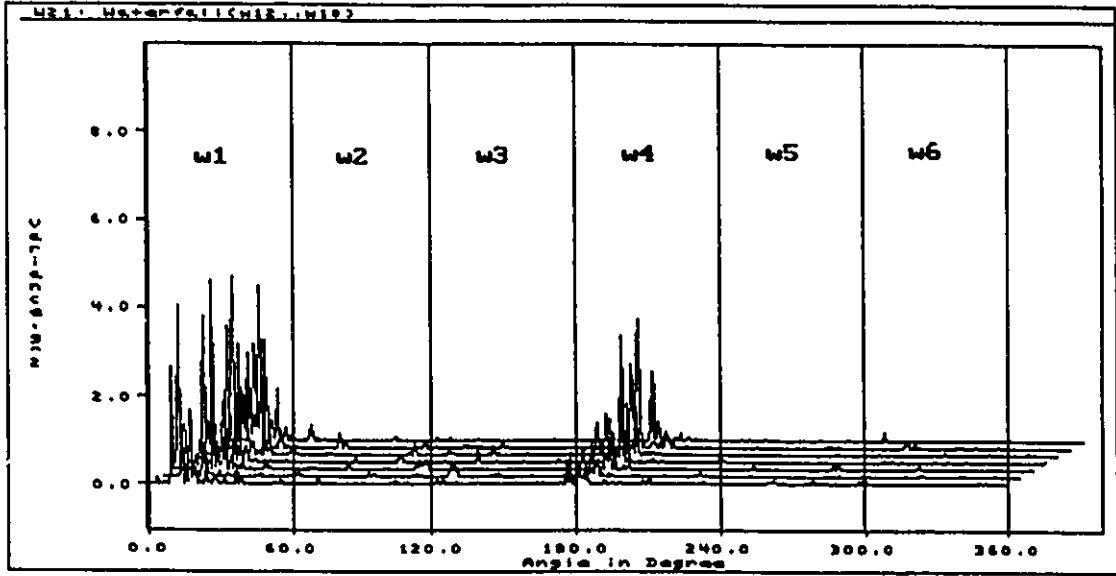
Figure E.34 : Accelerometer #2 Vibration Running Variance for #5 Loose Connecting Rod Nuts.
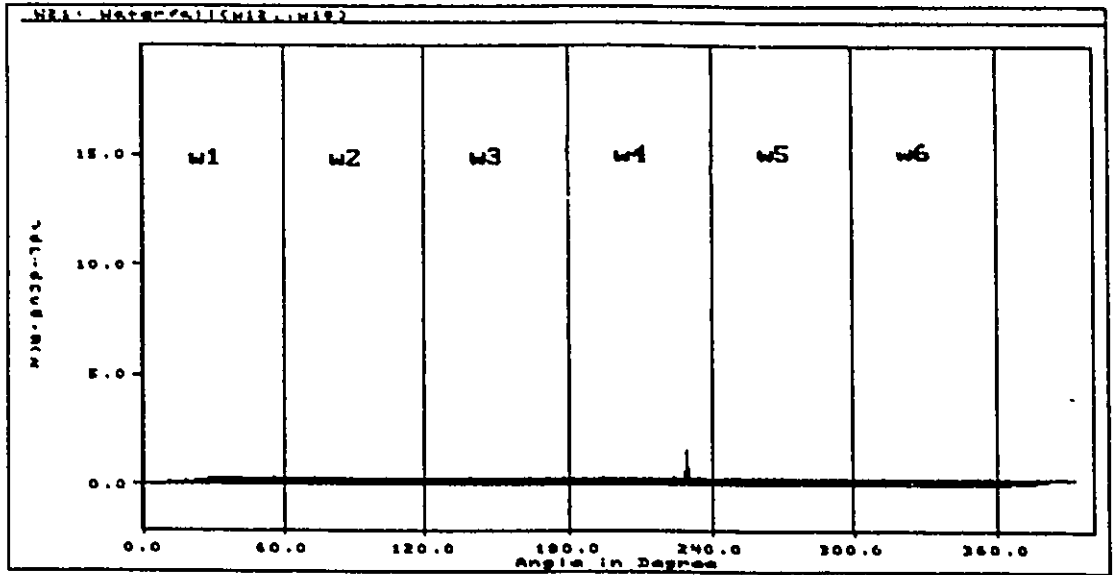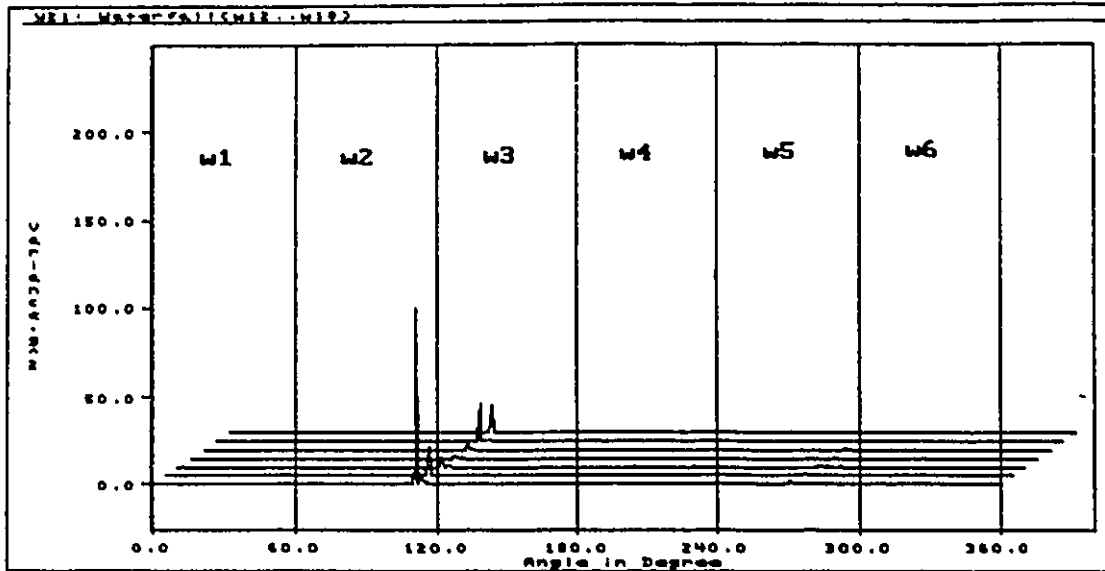
Figure E.35 : Accelerometer #1 Vibration Running Variance for
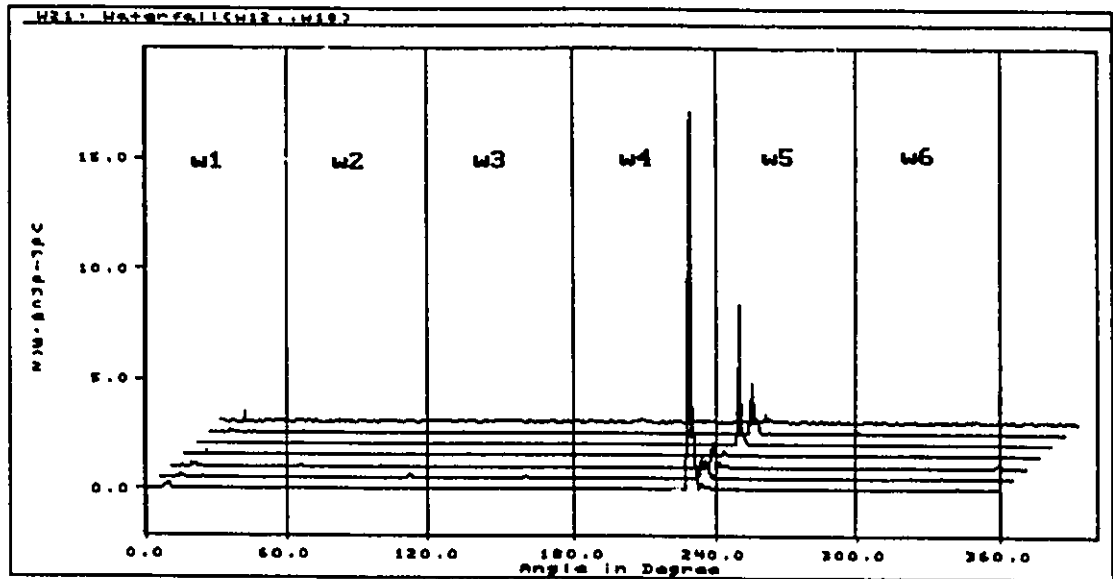#6 Loose Connecting Rod Nuts.
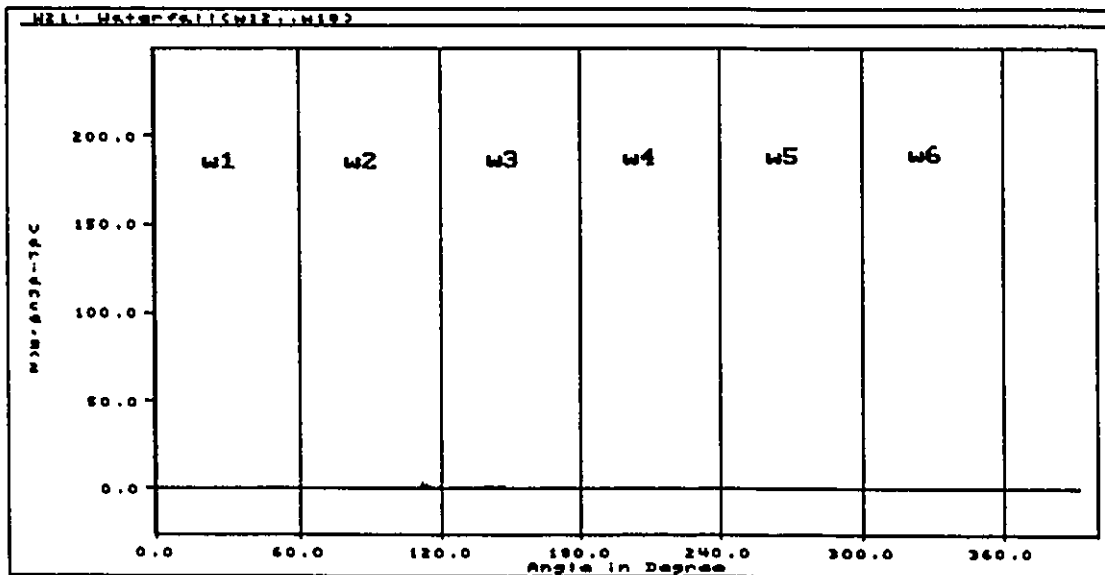
Figure E.36 : Accelerometer #2 Vibration Running Variance for
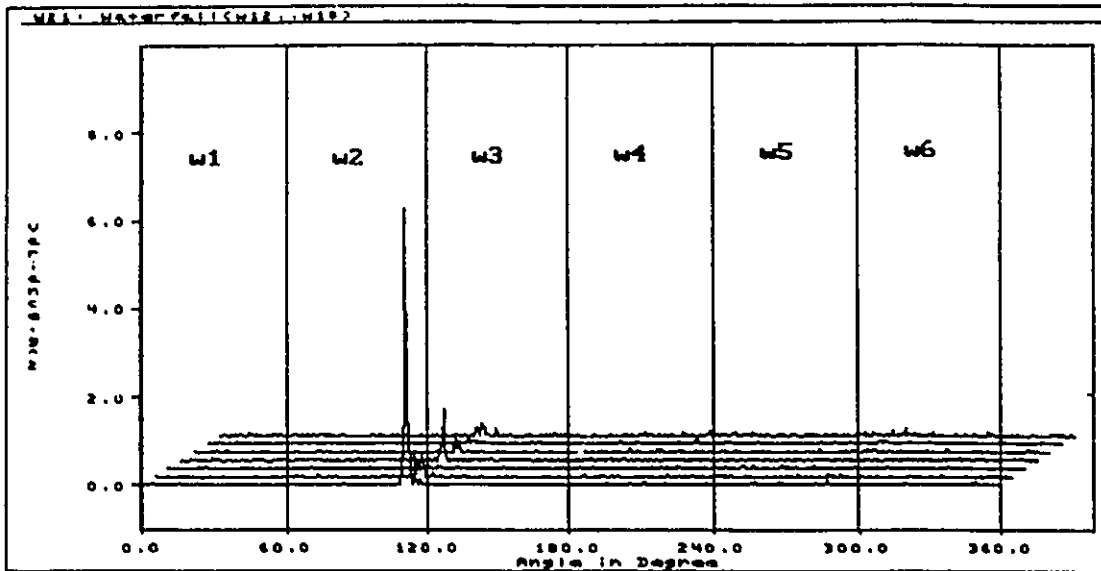#6 Loose Connecting Rod Nuts.

285
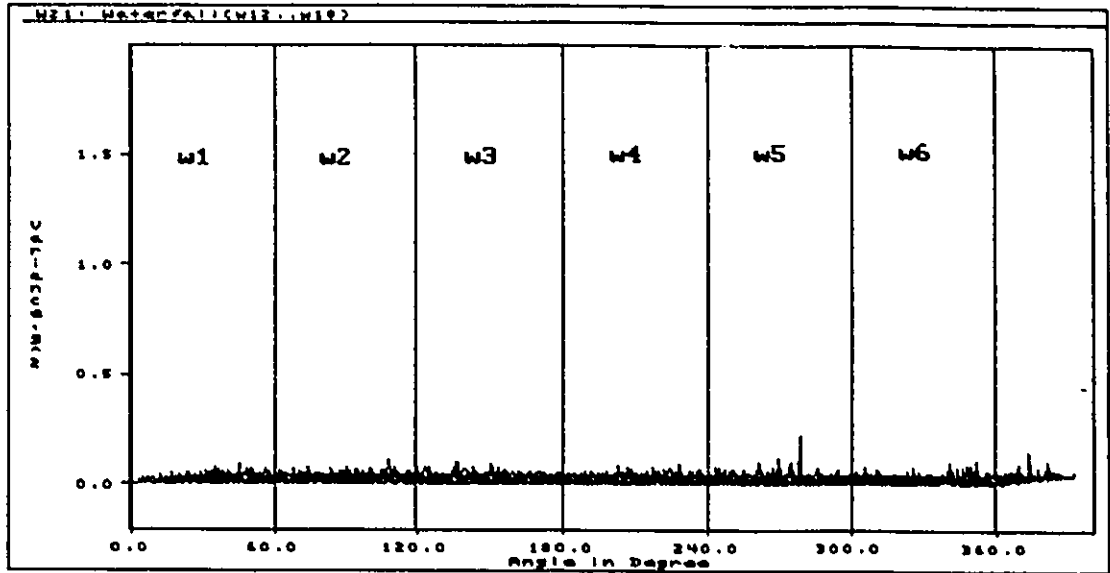
Figure E.37 : Accelerometer #1 Vibration Running Variance for
#1 Reversed Bearing Cap.
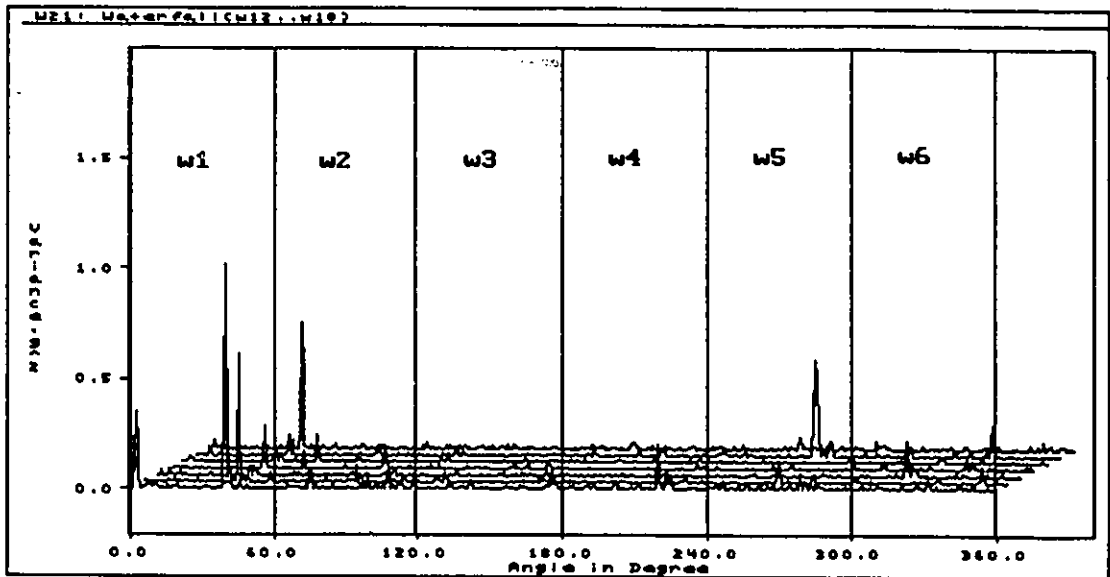
Figure E.38 : Accelerometer #2 Vibration Running Variance for
#1 Reversed Bearing Cap.
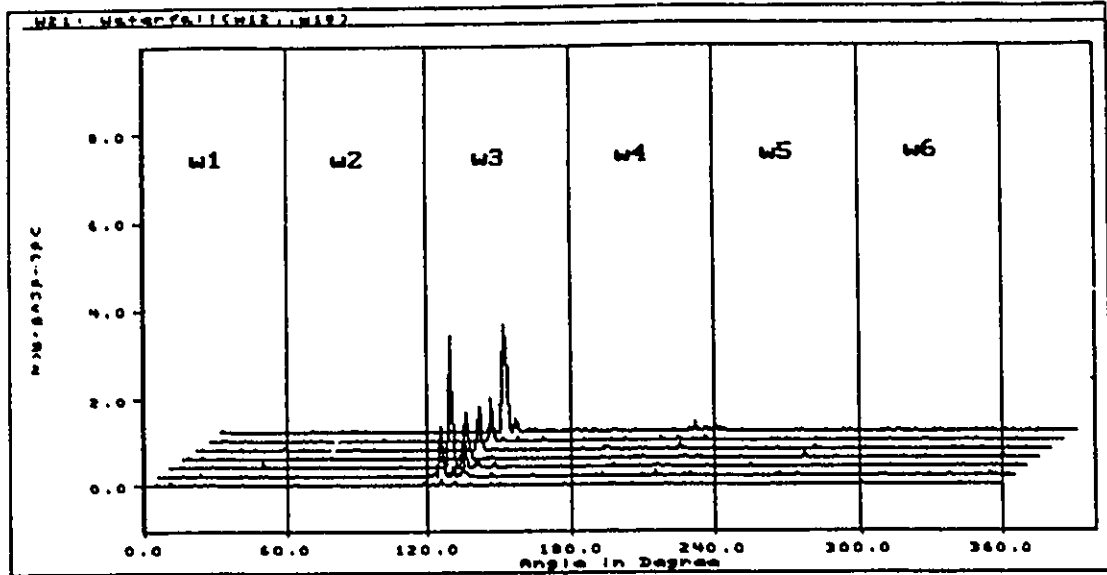
Figure E.39 : Accelerometer #1 Vibration Running Variance for
#4 Loose Rod Nuts (Engine A).
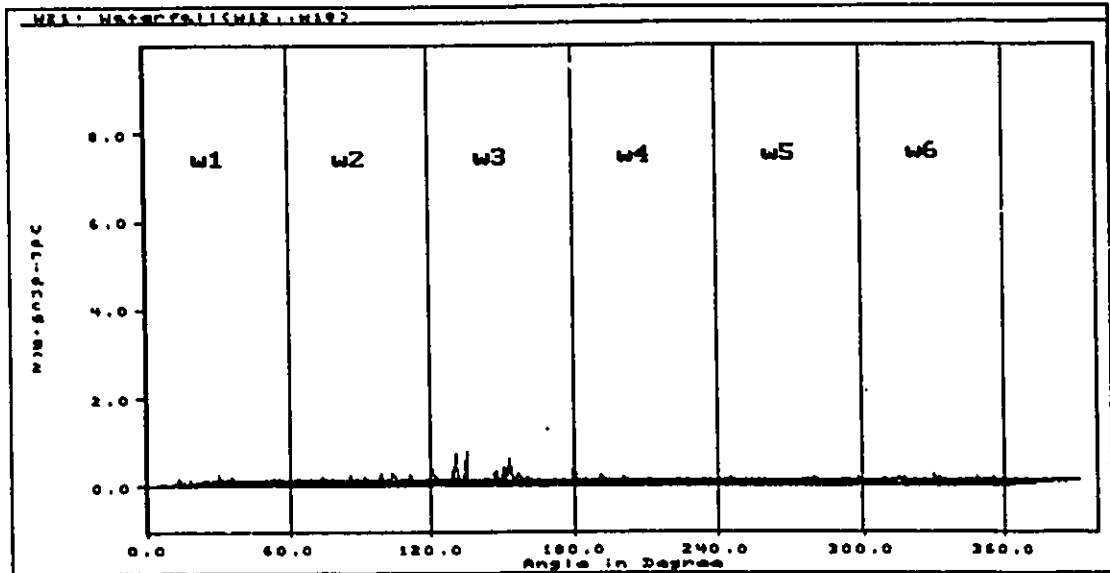
Figure E.40 : Accelerometer #2 Vibration Running Variance for
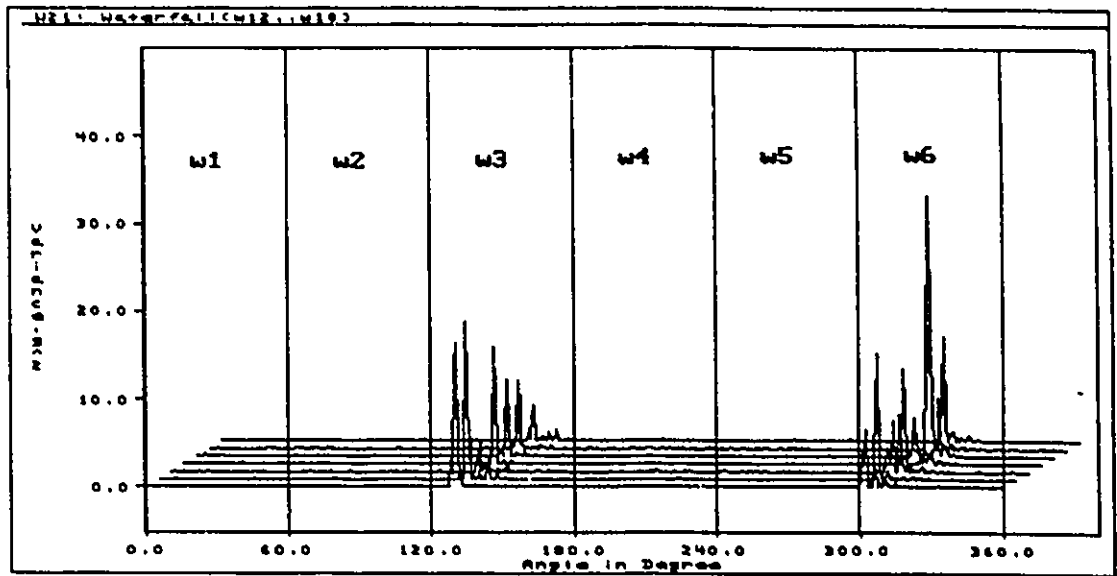#4 Loose Rod Nuts (Engine A).

287
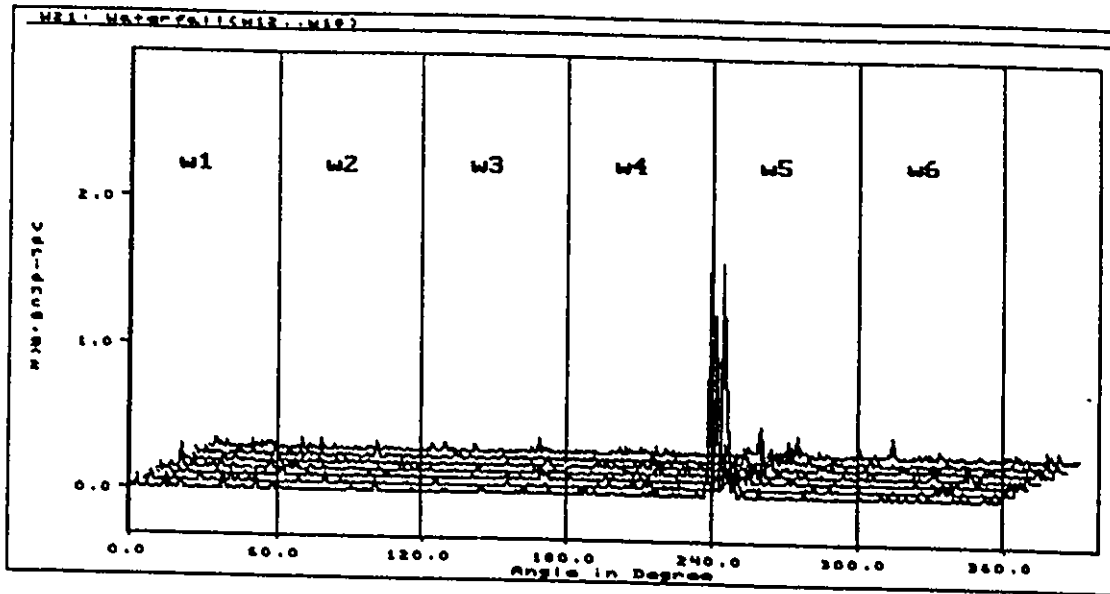
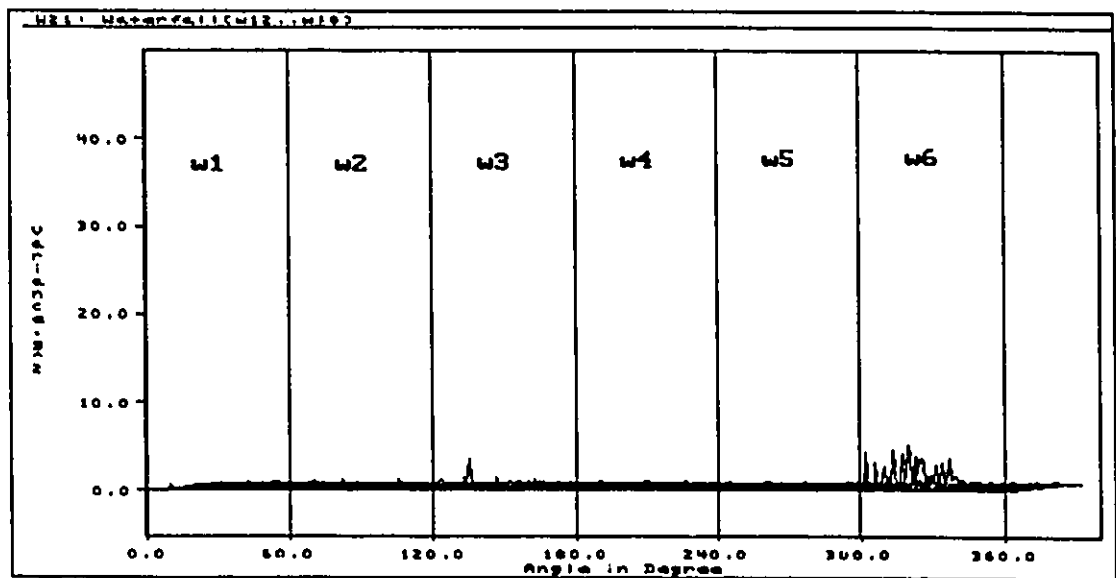Figure E.41 : Accelerometer #1 Vibration Running Variance for #6 Loose Rod Nuts (Engine B).

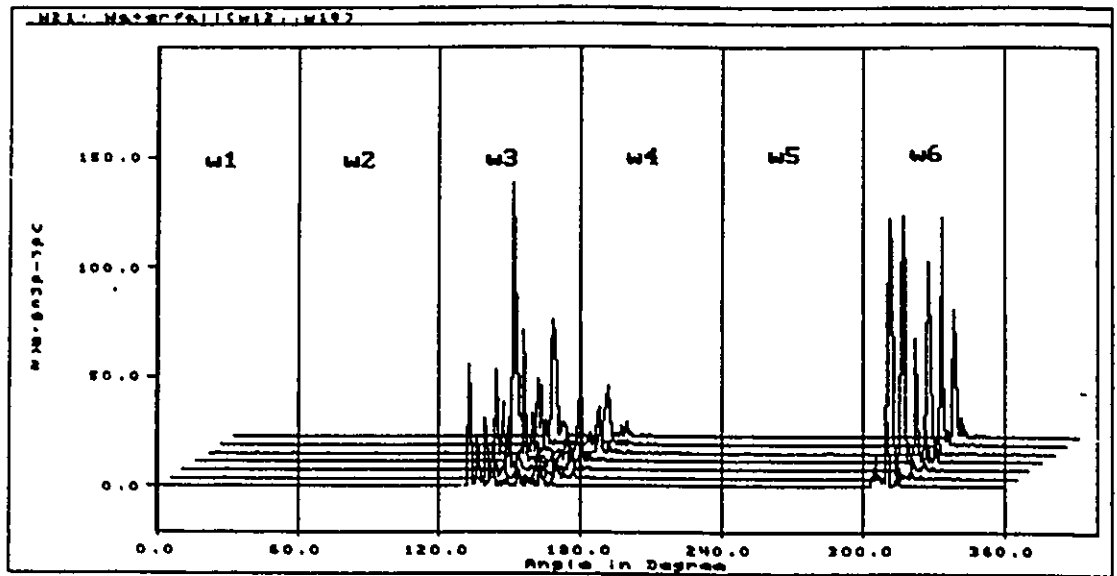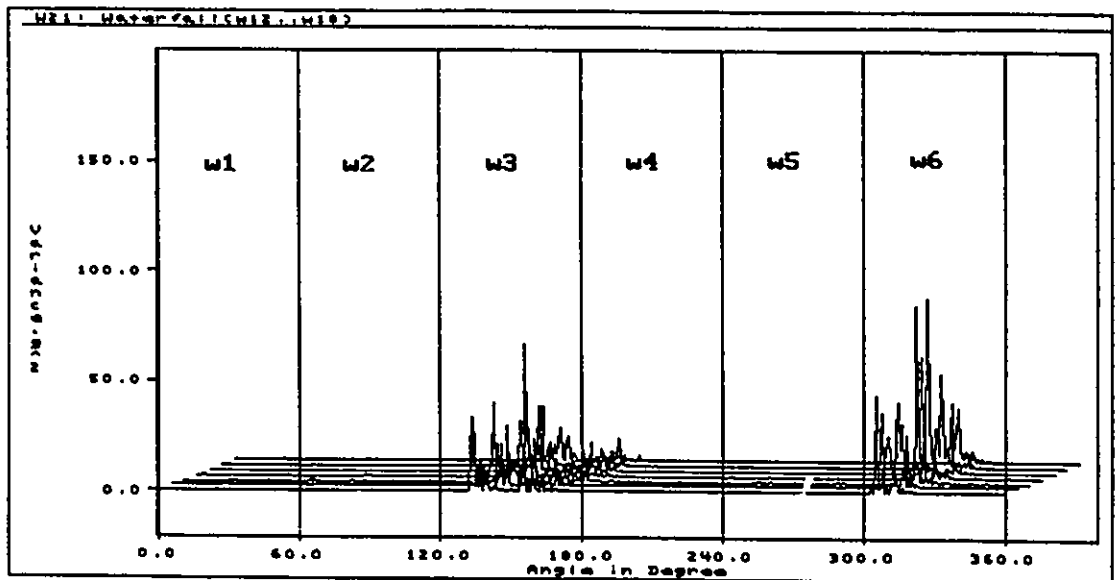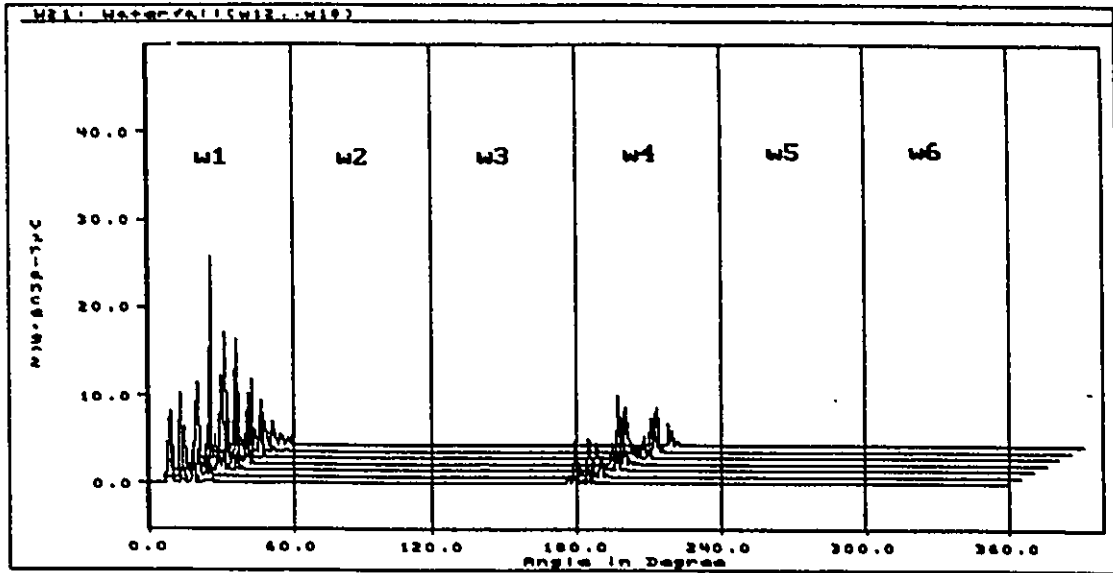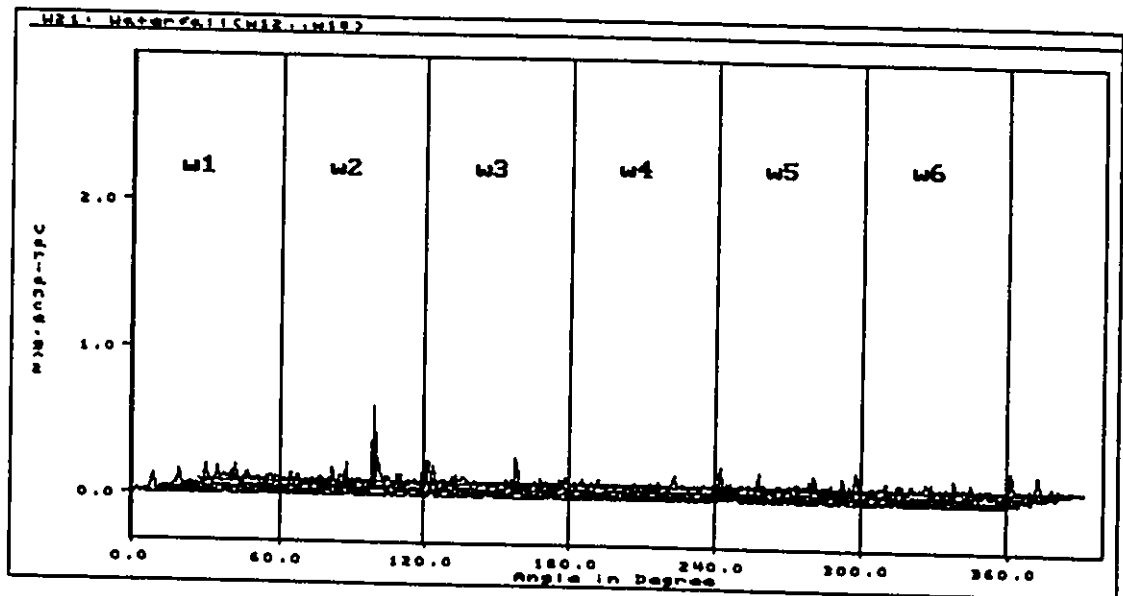Figure E.42 : Accelerometer #2 Vibration Running Variance for #6 Loose Rod Nuts (Engine B).

288
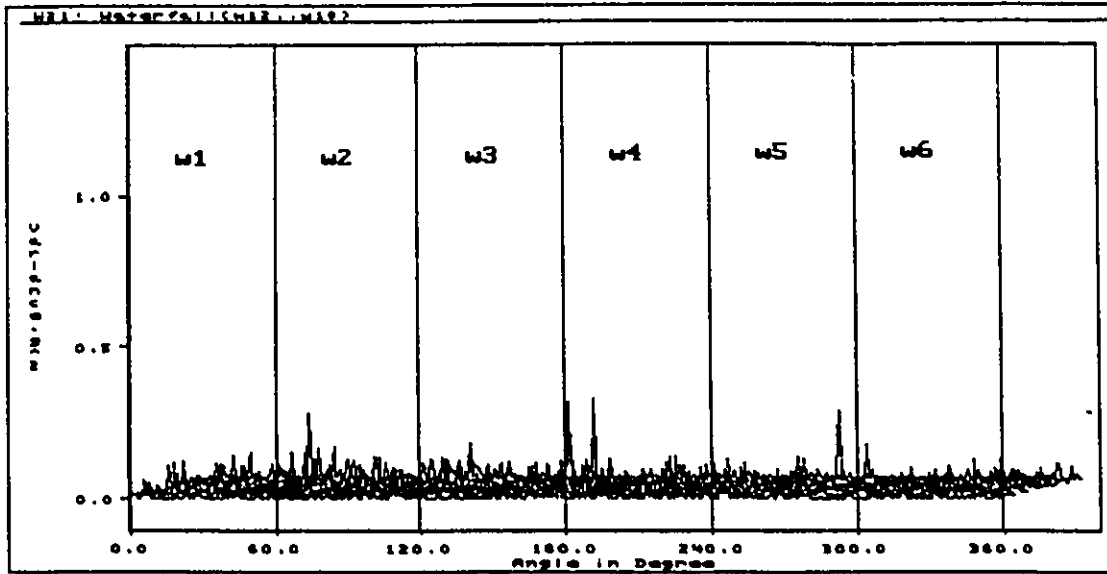
**Figure E.43 : Accelerometer #1 Vibration Running Variance
for #1 Piston Ring Missing.**
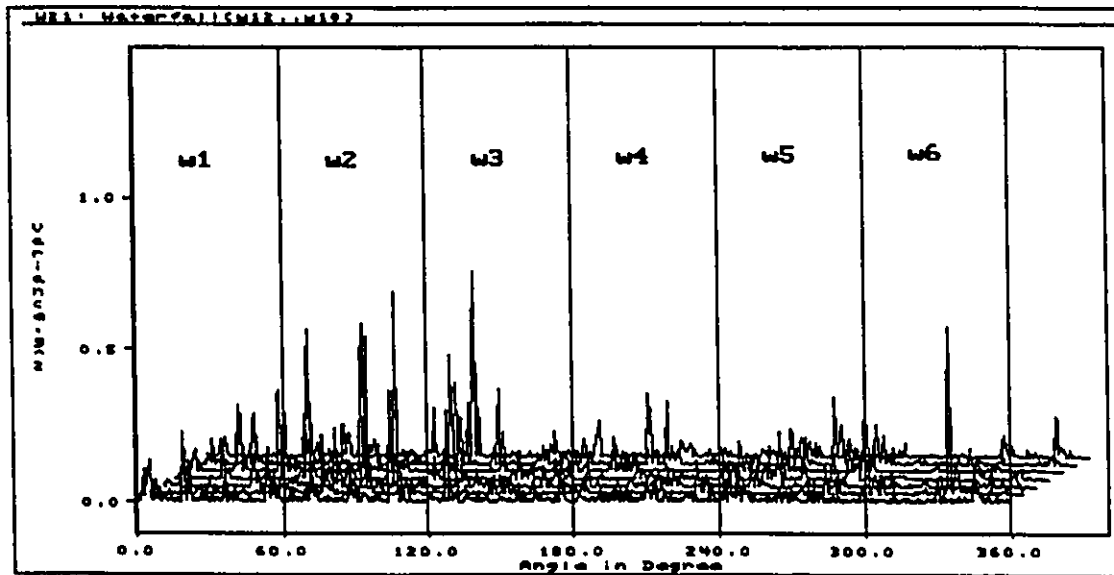
**Figure E.44 : Accelerometer #2 Vibration Running Variance
for #1 Piston Ring Missing.**

APPENDIX F

F. MEASUREMENT EQUIPMENT SPECIFICATIONS

Accelerometer B&K Type		4384
Weight	grams	11
Charge Sensitivity	pC/ms^{-2}	$1 \pm 2\%$
Voltage Sensitivity	mV/ms^{-2}	≈ 0.8
Mounted Resonance	kHz	42
Frequency Range	5% Hz	0.2 ~ 9100
Capacitance	pF	1200
Max. Transverse Sensitivity	%	<4
Transverse Resonance	kHz	15
Piezoelectric Material		PZ23
Construction		Delta Shear
Typical Base Strain Sensitivity (in base plane at 250μϵ)	$ms^{-2}/\mu\epsilon$	0.02
Typical Temperature Transient Sensitivity (3 Hz LLF, 20 dB/decade)	$ms^{-2}/°C$	0.4
Typical Magnetic Sensitivity (50 Hz - 0,03T)	ms^{-2}/T	4
Typical Acoustic Sensitivity Equiv. Acc. at 154 dB SPL (2-100Hz)	ms^{-2}	0.01
Min. Leakage Resistance at a/20°C	$G\Omega$	20
Ambient Temperature Range	°C	-74 to 250
Max. Operational Shock (±Peak)	kms^{-2}	200
Maximum Operational Continuous Sinusoidal Acceleration (Peak)	kms^{-2}	60
Max. Acceleration (Peak) with Mounting Magnet	kms^{-2}	1.5
Base Material		Titanium ASTM Gr.2

Figure F.1 : Specification for Type 4384 Bruel and Kjaer
Accelerometer

Charge Input:	Inherent Noise (2 Hz to 22 kHz):
10^5 pC max. input rating	5×10^{-3} pC referred to input with maximum sensitivity and capacitance of 1nF
Transducer Sensitivity Conditioning: 3 digit dial-in of transducer sensitivity from 0.1 to 10.99 pC/ms^{-2}	**Test Oscillator:** Generates 160 Hz sinusoid, level factory preset Level adjustable internally
Amplifier Sensitivity: 0.1mV to 10 V/pC corresponding to -40 to +80 dB with transducer capacitance of 1nF	**Rise Time:** Typically 2.5 V/µs
Calibrated Output Ratings: Selectable in 10 dB steps Acceleration: 0.1 mV to 1V/ms^{-2} Velocity: 10 mV to 100 V/ms^{-1} Displacement: 0.1 mV to 10 V/mm	**Overload Indicator:** Light emitting diode
Maximum Output: 8 V(8 mA) peak	**Max. Offset at Output:** 50 mV DC
Output Impedance: ≤ 1Ω	**Power Supply:** Internal battery, 3 x 1.5 V IEC Type R 20 or External DC supply, +6 V to +28 V, nominally 55 mA or External DC supply, ±14 V nominally 7mA
Frequency Range: -10% limits Acceleration: Switchable 0.2 Hz or 2 Hz to 100 kHz Velocity: Switchable 1 Hz or 10 Hz to 10 kHz Displacement: Switchable 1 Hz or 10 Hz to 1 kHz	**Dimensions:** (excl. feet, knobs, etc.) Height: 132.6 mm (5.22 in) Width: 69.5 mm (2.74 in) Depth: 200 mm (7.87 in) B & K module cassette KK 0022, 2/12 of 19'' rack module
Low-Pass Filters: Filter Slope 40 dB/decade (12 dB/octave) -10% limits quoted 6 position: 100 kHz, 1 kHz, 3 kHz, 10 kHz, 30 kHz and ≥ 100 kHz	**Weight:** 1.45 kg (3.21b) with batteries

Figure F.2 : Specification for Type 2635 Bruel and Kjaer Charge Amplifier

SPECIFICATIONS: Model Number		302A21
Range (±2.5V output)	±g pk	160
Resolution	g pk	0.007
Useful Overrange	g pk	200
Sensitivity (nominal)	mV pk/g pk	15
Resonant Frequency (mounted)	kHz	45
Frequency Range (±5%)	Hz	5-3000
Frequency Range (±10%)	Hz	3-6000
Discharge Time Constant	s	≥0.1
Amplitude Linearity	%	≤1.0
Polarity (accel into base)		positive
Output Impedance	ohm	≤1000
Output Bias	+V	4-8
Overload recovery	μs	10
Transverse Sensitivity	%	≤5.0
Strain Sensitivity	g/μin/in	0.01
Temperature Range	°F	-100 to +400
Temperature (max operational)	°F	+600
Temperature Coefficient	%/°F	0.01
Structure		quartz
Size (hex x height)	inch	0.50 X 1.78
Sealing	hermetic	welded
Case Material		
Weight	gm	35
Connector	coaxial	10-32
Excitation (constant current)	mA	2
Voltage to Current Regulator	+VDC	18 to 28

Figure F.3 :   Specification for Model 302A21 PCB Piezoelectric
Incorporated Accelerometer

SPECIFICATIONS: Model Number		308M86
Range (/ or ±5V output)	g	±50
Resolution	g	0.001
Sensitivity (±2%)	mV/g	100
Resonant Frequency (mounted)	Hz	25000
Frequency Range (±5%)	Hz	1 to 3000
Frequency Range (±10%)	Hz	0.7 to 6000
Linearity	% F S	1
Output Impedance	ohm	<100
Output Bias (nominal)	V	11
Overload Recovery	μs	10
Transverse Sensitivity (max.)	%	5
Strain Sensitivity	g/μin/in	0.05
Temperature Coefficient	%/°F	0.03
Temperature Range	°F	-100 to +250
Size (dia. x height)	in	0.75 X 1.32
Weight	gm	27
Excitation	VDC	+18 to +28
Constant Current	mA	2 to 20

Figure F.4 :   Specification for Model 308M86 PCB Piezoelectric
Incorporated Accelerometer

SPECIFICATIONS: Model Number		480D06
Transducer Excitation	VDC	+27
Excitation Current	mA	2
Voltage Gain (selectable)	x	1, 10, 100
Coupling Capacitor	μF	22
Frequency Range (±5%)	Hz	0.15 to 100 000
Output Signal	V	+10, -5
Noise Output (pk to pk) x 1	mV	0.2
x 10	mV	2
x 100	mV	20
DC Offset (into megohm)	mV	30
Connectors	micro	10-32
Meter	V F S	27
Size (lxwxh)	in	1.5 x 2.9 x 4
Weight	oz	12
Batteries	V	27
Battery Life	hr	40

Figure F.5 :   Specification for Model 480D06 PCB Piezoelectric Incorporated Power Supply

---

VIBRATION SYSTEM:
Electromagnetic exciter with internal built-in piezoelectric accelerometer (shear type) for servo regulation of vibration amplitude.

Frequency: 159.2 Hz ±1% (1000 $rads^{-1}$)
Acceleration: 10 ms^{-2} (RMS) ± 3%
Velocity: 10 mms^{-1} (RMS) ± 4%
Displacement: 10 μm (RMS) ± 5%
Transverse amplitude: less than 5% of main axis amplitude
Distortion: less than 5% for 10 to 70 gram load and less than 3% for 20 to 60 gram load
ACCELEROMETER MOUNTING:
Maximum Load: 70 grammes
TEMPERATURE RANGE:
+ 10 to + 40 °C (50 to 104 °F) for 10 ms^{-2} reference within ± 3%
− 10 to + 55 °C (14 to 131 °F) for 10 ms^{-2} reference within ± 5%
HUMIDITY: Up to 90% RH (non-condensing)
POWER REQUIREMENTS:
Built-in Battery: One 9 V alkaline Battery

Figure F.6 :   Specification for Type 4249 Bruel and Kjaer Calibration Exciter

OFFSET VOLTAGE: Velocity: for 1 m/s range, ±50 mV for 0.2 m/s range, ±30 mv Displacement: ± 20 mV DIMENSIONS (in carrying case): Height: 550mm Width: 670 mm Depth: 250 mm WEIGHT (in carrying case with batteries): 21 kg RETREFLECTIVE TAPE DU 0164: Weight: 17mg/cm^2 Thickness: 0.1 mm	ACCESSORIES INCLUDED WITH 3544: Transducer Power supply.........2815 Laser Velocity Tranducer........8323 Carrying case..................KE0276 Battery pack...................QB0040 Battery charger for QB0040....ZG0166 Angle mirror adaptor..........UA0965 Tripod........................UA0989 Connecting cable..............AO0308 7-pin pluf....................JP0703 One BNC-to-BNC cable, 1.2m....AO0087 One BNC Plug..................JP0035 Two 2.5 A fast blow fuses.....VF0029 5 lots of reflective tape.....DU0164 Instruction Manual

Figure F.7 : Specification for Type 3544 Bruel and Kjaer Laser
              Velocity Transducer Set

TIP HAMMER CONFIGURATION EXTENDER	PLASTIC/VINYL NONE OR STEEL	LG. SUPER SOFT STEEL	LG. SUPER SOFT NONE
HAMMMER SENSITIVITY (S_t) (mV/N)	0.21	0.21	0.19

Figure F.8 : Sensitivity of PCB Model 086B05 Impulse Force Hammer

SPECIFICATIONS: Model Number		303A02
Range (*for ±5V output*)	g	±500
Resolution	g	0.01
Sensitivity (nominal)	mV/g	10
Resonant Frequency (mounted)	kHz	70
Frequency Range (±5%)	Hz	1 to 10000
Discharge Time Constant	sec	1
Linearity	%	1
Output Impedance	ohm	100
Output Bias (nominal)	V	11
Overload Recovery	μs	10
Transverse Sensitivity (max.)	%	5
Strain Sensitivity	g/μin/in	0.05
Temperature Coefficient	%/°F	0.03
Temperature Range		
(operational to +250°F)	°F	-40 to +200
Vibration	g	±1000
Shock (protected)	g	2000
Size (hex. x height)	in	0.28 X 0.48
Weight (approx.)	gm	2
Connector (solder terminals)		2
Case Material		s.s.
Seal		Epoxy
Excitation Voltage	V	+18 to +24
Excitation Current	mA	2 to 20

Figure F.9 :   PCB Model 303A02 Accelerometer

SPECIFICATIONS: Model Number		112A
Range	psi	3000
Maximum Pressure	psi	10000
Resolution	psi	0.004
Sensitivity (nominal)	pC/psi	1.0
Resonant Frequency (nominal)	kHz	250
Rise Time	μs	2
Linearity (zero based BSL)	%	1
Polarity		Negative
Insulation Resistance	ohm	1×10^{12}
(room temp.)		
Capacitance	pF	18
Acceleration Sensitivity	psi/g	0.002
Temperature Coefficient	%/°F	0.01
Temperature Range	°F	±400
Flash Temperature	°F	3000
Vibration	g peak	2000
Shock	g peak	20000

Figure F.10 :   PCB Model 112A Pressure Transducer

FREQUENCY WEIGHTING: A, C weighting to IEC 651 Type1 (Type 0) Linear (10 Hz - 20kHz) All-pass (2 Hz - 70 kHz) **DETECTOR:** Characteristics: RMS, peak Linearity range: 70 dB Pulse range: 73 dB Crest factor capability: 13 dB at FSD **THE WEIGHTING CHARACTERISTICS:** "I": to IEC 651 Type 1 (Type 0) "F": to IEC 651 Type 1 (Type 0) "S": to IEC 651 Type 1 (Type 0) "Peak": rise time < 50 μs Max. Hold decay rate: 0 dB/s (digital) L_{eq} **RESPONSE TIME FOR CONSTANT INPUT SIGNAL:** 1 s after reset **CONVERTIBILITY:** Loading: Enabled by module section: module removed after loading into internal memory. Every application module has its own face plate. Capacity: 4 kbyte ROM for general routines, tables etc. 16 kbyte RAM for application software and data storage. Interface: Via optional Bruel Kjaer Serial Interface Module 219101. **DISPLAY:** Digital: 4 digits 14 segments, liquid crystal, 8mm high, resolution 0.1 dB Quasi-ananlogue: 60 dB scale, 2 dB resolution for monitoring current SPL (RMS or Peak) **AC OUTPUT:** 1V RMS for full scale (3.16 V RMS for full range), output impedance 120 Ω, short circuit protected, mini-jack socket. **DC OUTPUT:** 3 V for full scale (3.5 V for full range), 0 V bottom scale, 50 mV/dB, output impedance <100 Ω, short circuit protected mini-jack socket.	**MICROPHONE:** Type: 1/2 inch B & K Prepolarized Condenser Microphone Type 4155 Sensitivity: 50 mV/Pa Capacitance: 15 pF Windscreen effect: <0.9 dB up to 10 kHz Polarization Voltage: Selectable-0V, 28V, 200V. Allows use of almost any microphone in the Bruel Kjaer range. **CALIBRATION:** Acoustical: With Sound Level Calibrator Type 4230, Pistonphone Type 4220 or Multifunction Acoustic Calibrator Type 4226 by potentiometer adjustment Electrical: With internal reference source by potentiometer adjustment **REFERENCE CONDITON FOR ACOUSTICAL CALIBRATION WITH TYPE 4230:** Type of Sound Field: Free Reference Incidence Direction: Perpendicular to microphone diaphragm Reference SPL: 94 dB (re 20 μPa) Reference Frequency: 1 kHz Reference Temperature: 20°C Reference Measuring Range: 110 dB FSD **EFFECT OF HUMIDITY (AT 40 °C AND 1000 Hz):** <0.5 dB for 30% <RH<90% **EFFECT OF TEMPERATURE:** Microphone: -0.006 dB/°Ctypically Complete instrument: <0.5 dB -10 to +50 °C Operating range: -10 to +50 °C (+14 to 122 °F) Storage without batteries: -20 to 70 °C (-4 to 158 °F)

Figure 7.11 : Specification for Type 2231 Bruel and Kjaer Sound Level
             Meter

TRANSFER FUNCTION Filter characterstic	8-pole/8-zero Elliptic, one high-pass channel, one low pass channel; band-pass when channels cascaded; band reject when channels paralleled
PASSBAND RESPONSE Low Pass Response High Pass Response Passband Gain	0.1 dB ripple, DC to F, 0.1 dB ripple, F, to upper 3 dB point approximately 400 kHz 0 dB, $\pm 0.1 dB$
STEP RESPONSE Peak Overshoot, Low Pass	17%

CUTOFF FREQUENCY

Range	0.1 Hz to 110 kHz
with option -01	0.01 Hz to 110 kHz

Resolution	RANGE	RESOLUTION
	0.1 Hz to 110 Hz	0.1 Hz
	1.00 Hz to 1.10 KHz	1 Hz
	1.00 KHz to 11.0 KHz	10 Hz
	10.0 KHz to 110 KHz	100 Hz
with option -01	0.01 Hz to 11.0 Hz	0.01 Hz

Attenuation	0.1 dB
Accuracy	$\pm 2\%$
Stability	220 ppm/$^\circ C$
Channel-to-channel match	± 0.2 dB amplitude, $\pm 2^\circ$ phase

STOPBAND RESPONSE Attenuation Rate Stopband Attenuation Max Attenuation	140 dB/octave Low pass: 90 dB at 1.56 X F, high pass: 90 dB at 0.64 X F, 90 dB
INPUT CHARACTERISTICS Configuration Common mode Rejection Input Impedance Input Coupling Input Range Input Range Accuracy Input Noise Absolute maximum Input	Differential (floating), or single ended (grounded) >80 dB, 50-60 Hz, > 60 dB, DC to 1 kHz 1 Megohm in parallel with 50 pF, each side to ground DC or AC with 0.3 Hz cutoff 1mV RMS (-60dBV) to 31.6 V RMS (+30 dBV) full-scale in 10 dB steps $\pm$ 0.1 dB 10 nanovolts/$\sqrt{Hz}$, typical for f>1 kHz $\pm$ 100 Volts peak

OUTPUT CHARACTERISTICS

Impedance		50 ohms, Single-ended
Full-Scale Signal	Bipolar:	$\pm 10 Volts, \pm 5 Volts$
	Unipolar:	0 to +10 V, 0 to +5 V
		0 to -10 V, 0 to -5 V
Output Noise		

Figure F.12 :   Specification for Model 2783 Rockland Signal Processing Filter

INPUT CHARACTERISTICS:	ANALYSIS PARAMETERS:
Two identical channels (Channel A & B) Inputs: Indpendent selection of 3 inputs on both channels Preamp. Input: Via standard B & K 7 pin "Pre-amplifier Input" 0 + 28 of 200 V Microphone Polarization Voltage can be selected Accelerometer Input: Line Drive via TNC connector. Coupling: AC 3 dB down at 0.2 Hz or 3 Hz nominal Direct Input: Via BNC connector. Impedance: $1M\Omega//100$ pF. Coupling: AC down 3dB at 3 Hz nominal. DC with automatic DC-offset compensation Maximum Peak Input Voltage: 28 ranges from 15 mV to 100 V in a 1.5, 2, 3, 4, 6, 8, 10 sequence. Nominal or Inverted Input Autorange: Selects optimum peak input voltage on both channels Maximum Input Voltage: 100 V RMS. 2032 is designed to be operated with its signal and chassis ground at each potential. Analog Anialiasing Filters: 2 matched low-pass filters with 25.6 kHz cut-off frequency. Max. ±0.3 dB ripple in the passband. Provide at least 75 dB attenuation of those input frequencies which can cause aliasing. Max. gain difference: 0.3 dB. Max. phase difference: 3° up to 20 kHz, 5° up to 25.6 kHz. The filters can be bypassed Low Pass Filters: 2 matched low-pass filters with 6,4 kHz cut-off frequency. Max. fain difference: 0.1 dB. Max phase difference: 1° up to 6.4 kHz. The filters can be bypassed Input Sampling: Internal: 65.536 kHz. External: Max. 67 kHz. A/D-conversion: 12 bit. Quantization error: Max. ±1/2 LSB Calibration: User-defined in engineering units U, or in volts Calibration Annotation: V/V, V/unit, V/Pa, V/m/s^2, V/ m/s, V/m, V/N, V/g, V/in/s, V/mil, unit/V ANALYSIS CHARACTERISTICS Frequency Rannge: 0 to 25.6 kHz. 15 Frequency spans from 1.56 Hz to 25.6 kHz. Digital zoom giving resolution from 1.95 mHz to 32 Hz anywhere in the frequency range, corresponding to zoom factorsfrom 2 to 16 384 in a binary sequence	Resolution: Samples in time functions: 2048 for each channel. Resolution elements in frequency functions: 801. Amplitude classes in probability: 512 Weighting: Rectangular, Hanning, Transient or Exponential selectable on each channel. Transient and Exponential window with selectable position and length Real Time Frequency Range: > 5 kHz in dual spectrum averaging mode > 10 kHz in single spectrum averaging mode TRIGGER: Trigger Input: Free run, internal on channel A or B before or after digital low-pass filtering, external, synchronous with pseudo random noise sequence, or manual Trigger Slope: Posetive or negative Trigger Level: Adjustable in 199 steps across the input voltage range Delay: Trig → A or Trig → B: delay between trigger and start of channel A ot B set in seconds from -T to 9999s. Resolution: Δ T Ch. A → B: Delay between start of channel A and channel set in seconds from 0 to 9999 s. Resolution: Δ T AVERAGING: Exponential: The number of averages indicated in the measurement setup determines the effective averaging time Linear: Equal weighting. Stops in reaching the selected number of averages. A true average is always displayed and the number of averages is indicated on the display Peak: (Single channel only), the maximum level occuring in each channel is held SYSTEM ACCURACY: Frequency Response: ±0.4 dB at filter centres with DC coupling Amplitude Linearity: ±0.1 dB or ±0.01 % of maximum input voltage, whichever is greater, measured in Autospectrum with at least 32 independent averages, in the presence of another in-band signal not less than 20 dB below max. input Dynamic Range: >75 dB, for Autospectrum with at least 32 independent averages. Noise, distortion, and spurious signals at least 75 dB below max. input voltage

Figure F.13 : Specification for Type 2032 Bruel and Kjaer Dual Channel Signal Analyzer

FREQUENCY AND TIME
MEASUREMENT MODES:
Narrowband: 125 µHz to 100,000 Hz
frequency range. Resolution is
frequency span/400. All window,
trigger and averaging types are
available.
Phase: Phase spectrum is available
with or without triggering. When
triggered, phase can be referenced to
the trigger.
1/3 Octave: 0.8 Hz to 80 kHz
Full Octave: 1 Hz to 63 kHz
Time Capture: Time record can be
extended from 1k to 40k samples of
continuous input data. Up to 40X zoom
expansion factor can be applied to
this data with variable center
frequency.
External Sampling: Input sample rate
can be externally controlled up to
256 kHz. TTL compatible sample rate
input on rear panel. (Note: Some
specs may be degraded in external
sample mode).
FREQUENCY SECTION:
0 to 100 kHz: Measurement is made
over the full frequency range of the
analyzer with 250 Hz resolution.
Define Start or Center: Measurement
is made over the selected frequency
span. Start or center frequency can
be set anywhere in the 0 to 100 kHz
range with resolution of 0.25 Hz.
Define Span: Measurement frequency
spans are provided in a 1, 2, 2.5, 5,
10 sequence. (Other spans exist
between these intervals, but are too
numerous to list in the space
available.)
Define Time Length: Measurement time
can be set from 0.004 seconds to 651
minutes per time record. Time setting
is rounded up to agree with next
available span.
ACCURACY:
Frequency Accuracy: ±0.003% of
frequency reading
RESOLUTION:
Frequency Resolution: Span/400
MEASUREMENT WINDOWS: Windows are
weighting functions which are applied
to input data to reduce errors caused
by leakage.
Flat Top:
Hanning:

Uniform:
Exponential:

AMPLITUDE AND INPUT
AMPLITUDE:
Input Range: The calibrated input
range is 27 dBV (+22.4 V) to -51 dB
(3 mV) maximum input level (single
tone RMS). Range is adjustable in 1
dB (10%) increments.
Dynamic Range: Distortion, spurious
and alias products ≥80 dB below input
range
Amplitude Accuracy: Full Scale
Accuracy at calculated frequency
points. Overall accuracy is the sum
of absolute accuracy, window flatness
and noise level
Absolute Accuracy:
±0.15 dB ±0.015% of input range: +27
dBV to -40 dBV
±0.25 dB ±0.025% of input range: -41
dBV to 51 dBV
Window flatness:
Flat top: +0- 0.01 dB
Hanning: +0-1.5 dB
Uniform: +0-4.0 dB
INPUT
Input Impedance: 1 MΩ ±5% shunted by
95 pF maximum.
Floating Ground to Case Capacitance:
< 0.25 µF
DC Isolation: Input low may be
connected to chassis ground or
floated up to 30 volts RMS (42 Vpk).
Input Coupling: The input signal may
be ac or dc coupled. Low frequency 3
dB roll off < 1.0 Hz for ac.
Anti-Alias Filter Roll-Off: Analog
and digital anti-aliasing filters
roll off at a nominal rate of 130
dB/Octave with a cut-off frequency at
105 kHz nominally.
TRIGGER
TRIGGER MODES:
Free Run:
External: TTL signal.
Internal:
Input:
HP-IB:

Figure F.14 : Specifications for Model HP3561A Hewlett Packard Dynamic Signal
Analyzer.

INPUTS:	Differential
a. Coupling:	AC, DC, GND (AC -3dB = 1.5 Hz ±10%)
b. Ranges (Full Scale):	30 mV to 120 V, 12 steps
c. Impeadance:	1 Mwgohm ±2%, 50 pF
d. Zero Position Range:	0 to 100% Full Scale
VERITCAL RESOLUTION:	12-bits (0,025%)
TIME BASE ACCURACY:	±0,01%
DIGITIZING RATE:	10 MegaSamples/second (100 ns/point) .
a. Maximum	0.1 Sample/second (10 s/point)
b. Minimum	64K Samples per channel (256K Optional)
RECORD LENGTH:	±0.25 % Full Scale
MAXIMUM STATIC ERROR	
RMS NOISE (open inputs)	
a. 30 mV to 120 mV:	±0.15% Full Scale
b: 300 mV to 120 V:	±0.13% Full Scale
COMMON MODE REJECTION	
a. DC	-72 dB
b. 1 kHz	-60 dB
c. 1 MHz	-40 dB
COMMON MODE VOLTAGE RANGE	(DC + Peak AC)
a. 30 mV to 1.2 V	±5 Volts
b. 3 V to 12 V	±50 Volts
c. 30 V to 120 V	±100 Volts
FILTER (Swithable)	100 kHz ± 10%
EXTERNAL TRIGGER RANGE	12 Volts Full Scale
EXTERNAL TRIGGER SENSITIVITY:	200 mV p-p to 12 V Full Scale
EXTERNAL TRIGGER LAVEL ACCURACY	±2%

Figure F.15 : Specification for Nicolet 440 Benchtop Waveform Acquisition System.

APPENDIX G

G. GATED SOUND INTENSITY TECHNIQUE

The gated sound intensity technique is used for analyzing repetitive non-stationary signals. The sound intensity from a source is measured using a two-microphone sound intensity probe. The signals from the microphones are fed into the sound intensity analyzer where the sound intensity, $\vec{I}$, is calculated. The calculated sound intensity goes to the averager which is started and stopped synchronously with the source.

The signal to be analyzed using the gating technique is assumed to be repetitive with a cycle of T , i.e.

$$\vec{I}(t) = \vec{I}(t+T)$$ $(G.1)$

The variation within one cycle is analyzed in time windows with the length of t_w by averaging the signal within that window:

$$\vec{I}_w = \frac{1}{t_w}\int_0^{t_w} \vec{I}(\tau)d\tau$$ $(G.2)$

The time window can be offset relative to the trigger point by introducing the time

delay t_d:

$$I_w(t_d) = \frac{1}{t_w} \int_{t_d}^{t_w + t_d} \bar{I}(\tau)d\tau \qquad (G.3)$$

In order to minimize the statistical uncertainty each window is averaged for a number
of cycles, N:

$$I_w(t_d) = \frac{1}{N} \sum_{n=1}^{N} \left[\frac{1}{t_w} \int_{t_d}^{t_d + t_w} \bar{I}(\tau + (n-1) \cdot T)d\tau \right] \qquad (G.4)$$

using the assumption in (1), that the time signal is repetitive with the period, T. By using
a real time analyzer, I(t_d) may be presented as a power spectrum.

The synchronization is done by the desktop calculator, using the service request line
of the Hewlett Packard Interface Bus (HPIB) for triggering.

A tachometer signal is generated once per cam revolution of the noise source, by
using an inductive pickup attached to the spark plug number 1 wire. This trigger is
delayed a time t_d, after which a time window with length t_w is opened. Within this time
window, the sound intensity is averaged. After time t_w the averager is stopped. In the
next revolution, the averager proceeds with the averaging in the period t_w. This
process is repeated for a number of revolutions, N, after which the averaged sound
intensity is transferred from the analyzer to the computer. The averager is reset, a new
delay, t_d, is selected and the process is repeated.

By measuring with a number of different time delays, t_d, the noise coming from the
various parts of the rotational cycle of the engine can be analyzed.

VITA AUCTORIS

1956	Born in Jakarta, Indonesia on February 20
1980	Received the Degree of Bachelor of Applied Science in Mechanical Engineering from the University of Windsor, Windsor, Ontario, Canada.
1980 to 1981	Full Time Graduate Student at the University of Windsor, Windsor, Ontario, Canada.
Summer 1981	Employed as Mechanical Engineer by Timberjack Inc., Woodstock, Ontario, Canada.
1981 to 1984	Employed as Research Engineer by F. Jos. Lamb Co. (Canada) Ltd.
1984	Received the Degree of Master of Applied Science in Mechanical Engineering from the University of Windsor, Windsor, Ontario, Canada.
1984 to Present	Employed as Section Supervisor of the Quality Office at the Ford Motor Co., Windsor, Ontario, Canada and a Candidate for the Degree of Doctor of Philosophy in Mechanical Engineering from the University of Windsor.

TECHNICAL PUBLICATIONS

1. Tjong J., Chang D., Lau T., Reif Z.,
   "Monitor Engine Condition with Vibration Signal",
   11th International Modal Analysis Conference, Kissimmee, Florida, February 1-4, 1993.

2. Tjong J., Reif Z., and Chang D.,
   "Detection of Engine Manufacturing Defects Using Signature Analysis", 12th Machinery Dynamics Seminar, Edmonton, Aberta, Canada, Oct., 1992.

3. Tjong J., Lau T., Chang D. and Reif Z.,
   "Monitoring Drill Condition Via Time Domain Vibration Signal", 12th Machinery Dynamics Seminar, Edmonton, Alberta, Canada, Oct., 1992.

4. Tjong J., Miller H. and Reif Z.,
   "Time based signal analysis for the detection of intermittent and impact noise and vibration ", Engineering Application of Mechanics 1990, Kingston, Canada, May, 1990.

5. Tjong J., Miller H. and Gaspar R.,
   "Determination and verification of optimum operating conditions of high speed machining station using modal and finite element analysis", 7th international Modal Analysis Conference, Las Vegas, U.S.A., Jan 1989.

6. Tjong J., Ngo T., and Reif Z.,
   "Early detection and diagnosis of alternating current motor problems", 10th Machinery dynamics Seminar, Calgary, Canada, Sept., 1988.

7. Tyler C., Verdonck B., Gaspar R., and Tjong J.,
   "Establishment of criteria and procedures for the development of a machine health monitoring database for automotive production machinery", 10th Machinery Dynamics Seminar, Calgary, Canada, Sept., 1988.

8. Tjong J., Gardner A., and Reif Z.,
   "Application of vibration monitoring techniques to rotating machinery at an automotive engine plant", 9th Machinery Dynamics Seminar, Montreal, Canada, Sept., 1986.

9. Moore, T., Tjong J. and Reif Z.,
   "Using frequency response function measurements to predict workpiece noise radiation during face milling", 4th International Modal Analysis Conference, Los Angeles, U.S.A., Feb., 1986.

10. Tjong J., Moore T. and Reif Z.,
    "The reduction of structural-borne noise through the combined application of modal and signature analysis techniques", 3rd International Modal Analysis Conference, Orlando, U.S.A., Jan., 1985.

11. Tjong J., and Reif Z.,
    "Application of vibration monitoring to high volume, multistation transfer machines", 3rd International Modal Analysis Conference, Orlando, U.S.A., Jan., 1985.

12. Tjong J., and Reif Z.,
     "Feasibility of applying vibration monitoring to high volume, multistation transfer
     machines", 8th Machinery Dynamics Seminar, Ottawa, Canada, Oct., 1984.

13. Tjong J.,
     "Feasibility of applying vibration monitoring techniques to high volume,
     multistation transfer machines", Master of Applied Science Thesis,
     University of Windsor, Canada, Apr. ,1984.